On the non-microbial sources and sinks of dissolved metabolites in seawater

by

Noah Paul Germolus

B.Env.E.
University of Minnesota Twin Cities, 2018

Submitted to the Department of Civil and Environmental Engineering in partial fulfillment of the requirements for the degree of

Doctor of Philosophy

at the

MASSACHUSETTS INSTITUTE OF TECHNOLOGY

and the

WOODS HOLE OCEANOGRAPHIC INSTITUTION

September 2024

Authored by: Noah Germolus
Department of Civil and Environmental Engineering
June 11, 2024

Certified by: Dr. Elizabeth B. Kujawinski
Senior Scientist
Woods Hole Oceanographic Institution
Thesis Supervisor

Accepted by: Dr. Edward Boyle
Chair, Joint Committee for Chemical Oceanography
Massachusetts Institute of Technology

Accepted by: Dr. Heidi Nepf
Donald and Martha Harleman Professor of Civil and Environmental Engineering
Chair, Graduate Program Committee
Massachusetts Institute of Technology

On the non-microbial sources and sinks of dissolved metabolites in seawater

By

Noah P. Germolus

Submitted to the Department of Civil and Environmental Engineering on June 11, 2024,
in partial fulfillment of the requirements for the degree of
Doctor of Philosophy

Abstract

Dissolved marine metabolites are small (<1000 Da) organic chemicals that remain in seawater when passed through a filter (typically <0.2 μm pore size). Their name implies their biological function: to be produced and consumed by cellular metabolism. These chemicals are the flows of the "microbial loop"—the principle that most of the photosynthesized matter in the ocean is exchanged, respired, and restructured by single-celled organisms. Metabolites have critical biological utility, so they are considered extremely labile; estimates of the time each spends outside cells range from hours to days. Their concentrations are drawn down by their consumers to nanomolar and picomolar levels, making measurement difficult. However, improved techniques to measure metabolites simultaneously and at extremely low concentrations avail the question of what happens to metabolites outside the cell membrane. Conventionally, representations of labile DOM exchange networks avoid that question—metabolites' short lifetimes imply their flows lead from one organism to the next. This thesis begins to interrogate that assumption, asking if there are other processes that could change the seawater exometabolome on time scales that are relevant to microbial life. In Chapter 1 I discuss the ways ambient metabolite pools could be affected by animals, chemistry, and physics. In Chapter 2 I investigate the photolysis of metabolites and examine metabolomic techniques' suitability for such experiments. In simulated sunlight, 11 of 57 metabolites decayed to some extent in artificial or natural seawater, and tryptophan and kynurenine may decay rapidly in the mixed layer of an oligotrophic ocean. For Chapter 3, I captured five species of migratory zooplankton and measured metabolites in their dissolved excreta. Four species survived the experiment and produced 43 metabolites, many at a rate that should be measurable in field samples. Chapter 4 harnesses the previous two chapters, plus a model for physical mixing, to probe a field dataset comprising 60 metabolites from Hydrostation S (south of Bermuda). Based on eight profiles over the course of two days, I posit: (1) copepods alone can supply the entire demand of >20 compounds to the mixed layer; (2) mixing is rapid enough to erase input signatures in the mixed layer; and (3) photochemistry is a slow leak of metabolites to forms whose lability is yet unknown. Chapter 5 reflects on how metabolites break the microbial loop—and suture it together with more ecological richness than with elemental fluxes alone.
Thesis supervisor: *Dr. Elizabeth B. Kujawinski*
Title: *Senior Scientist with Tenure, Woods Hole Oceanographic Institution*

Acknowledgments

The research documented here was funded by Simons Foundation International through the BIOS-SCOPE collaboration and WHOI's Academic Programs Office, as well as the MIT BIOS Fund and the WHOI Ocean Ventures Fund. In some sense, this sterile acknowledgement is all that is required, but anyone reading this should take a moment to note how bonkers that is: Due to my advisor asking in a very nice and scientific way, Jim Simons, who is now dead, effectively paid me to work on a small set of incredibly niche chemistry problems for six years, and WHOI paid me to take classes, rent a house, and buy groceries. Anyway, science funding is wild.

I have acknowledged those whose authorship and collaboration enabled this thesis within the chapters relevant to their contributions, and would like to take this section to be a little more personal, because if I have to write it as stiffly as the rest of the document my eyes will cramp. Buckle in. I will spare no words. The experience of getting a PhD was a dynamic chunk of my life containing some of its most affirming and most depressed parts, the latter only bearable because I managed to meet some of the people who inhabit the idealized world of my dreams. These pages are the only place I will have to make a true and lasting account of those feelings.

I thank my advisor, Elizabeth Kujawinski. I'm grateful for you pulling me into this program, but even more so for your commitment to seeing me through as a student. I was not an easy student, and I know that. You treated me with a kind of understanding that I did not always appreciate, and allowed me to live my life, to take care of myself, and perhaps most critically as a PhD advisor, made space for me to find my own interests. To anyone who's not Liz: this means that I had a lot of wacky and intractable

ideas and several abject failures during the course of my research. I have had dead cultures, dried-up fungi, a poster that will never again see the light of day, a modeling chapter that didn't happen, and pages on pages of notes outlining experiments I was never able to try. Liz handled this all with equanimity, only sometimes getting truly exasperated. I relied on her for my executive function regarding what, of all of that, ended up being part of this thesis. The part about Liz as an advisor that really hit the hardest, though, was beyond the research itself. Occasionally, we got to a point where I could do nothing but bear my soul to her: my doubts about my research, my insecurity about the future, and my uncertainty about my place in the world. When those times came, she usually had a surprisingly relatable anecdote from her own life, which has had some pretty harrowing periods. Her capacity for empathy towards her own graduate students may not be directly reflected in her professional achievements as a scientist, but: Liz, you have been good to me, and I know it. Not every grad student can say that about their advisor. I've been fortunate, and even if I do not follow your footsteps, I will remember what I learned from you about being a mentor.

My committee, to some extent, endured the same things that Liz did, except since they only saw me about once every six months, many of the meetings were…difficult. They forced me to explain more than I thought I had to—to take a step out of my own head for a while—not out of malice but out of a desire to understand and to help. Phil Gschwend and Collin Ward kept me honest about the chemistry and what it means; Heather Kim made me feel like the math I was using wasn't necessarily insane gobbledegook; Desirée Plata stepped in to mediate and, with Liz, take a bit of a broader view of the situation; and Hilary Close would add some ecological insights I hadn't

known were possible. More personally, though: Phil, it has been an honor to learn from you, to teach under you, and to have you witness my clumsiness on the softball field. The reason I've done most of the research I've done is because the things I learned from you felt so empowering. Collin, you're the coolest cucumber, and I'm glad you've been willing to be real with me about the photochemistry. We never talked much about music, but I feel like that'd be fun. Heather, your teaching that inspired me to harness numerical tools, and to be creative in ways that play to my unique strengths as someone studying metabolites. Desirée, you took me on as a student despite me not joining your lab, and even treated me like a part of it whenever I was around. Also, sometimes I distracted Eric, which made Parsons feel homier even though I rarely appeared there. Hilary, even from afar, and even after I had steered away from co-sampling with you and your group, you stayed on and were willing to discuss my projects one-on-one when we met in Bermuda. Frankly, that meant a lot, and some day soon I will watch Hereditary and let you know how it goes.

To the others of the Kuj Lab: thank you for your guidance, your patience, and your spirits. Craig took me in during my first ever visit to Cambridge, and he and a few other JP students took me to a small jazz bar where some Berklee students were ripping it onstage. I will remember that forever, as I will remember the rest of you: Alex for calling me at 9pm on a Saturday asking where a particular piece of glassware had gone (I had no idea); Brittany for giving her all to an exhausting and careful development of the tools that enabled my entire thesis, and for her calm self-determination; Erin for the cheer and kindness that she radiated like a star, and the trust she put in me when asking me to help solve problems; Yuting for being both someone

I'd gladly take a road-trip with again and a whip-smart chemist with expertise that came exactly when I needed it most; Brianna for being a proactive torch-bearer of our new method and a beast of an organizational mind; Gretchen for her tireless contributions to teaching and enabling almost everything I've ever done in this lab and for my love of Back to the Future; Krista for being my rock on the BIOS-SCOPE cruises, among her manifold other contributions to my work conceptually and materially; Melissa for her role as the veteran F1 driver of mass spectrometry and her golden sense of humor; Herman for being a friend full of delightful surprises and many talents; Natalie for being her frank and fascinating self 100% of the time.

I lived most of these six years in a small house near downtown Falmouth, first with Lauren and Beckett and, upon Lauren's departure, Glenn. Functionally, this worked like a big domestic partnership. You don't live with and share food with people for this long without it being a little like a marriage. I love you all, and am going to miss living at 52 Amvets dearly. You all brought me a loving environment where I could be both a lazy sloth and the grill/lawnmower dad all at once. I hope you all still make coffee for each other in the morning when I leave. Beckett, I'm sorry you didn't finish Tears of the Kingdom.

To the folks I played music with over the years: it has been an honor to gig with all of you: the CEE band, Crabs With Guns, Nivalis, Paradise Rock, the Moonlighters, and, most frequently, Dickie Nolan. You were my community; you gave me the chance to make other people happy with the thing that makes me feel most like a human being: playing saxophone and—when required—singing. It is legitimately devastating to leave all of you; not only do I consider many of you my friends, but music is best when you

understand each other. It's a rush to lock eyes with Craigo or Dickie and see the slight nod that means, "*improvise NOW*" or decide exactly when to end "1612" after an extended jam and stick the landing. Nothing else is quite like it, and it only gets better when you play with the same folks for hundreds of hours.

Graduate school is weird in a number of ways, but one of them is that if you make friends with other students, they tend to form a rotating cast over the years. Eric Johnson and Anna Walsh helped me feel less like a lonely ghost when I arrived up at MIT. By the time I moved down to Falmouth, Katie Halloran and I had figured out that we were going to make the Trailer the coolest trash heap of an office there's ever been, and we'd started playing Dungeons and Dragons with a group that was more concerned with funny character nicknames than advancing the plot. I mean that adoringly. The year 2020 attacked, and Katie and I started shellfishing. Bethany and Scotty Stevens bought a house and took on my brother-in-Halloween Cory Berger as a squatter, and they were like a second home for me. Somehow, Jen Kenyon entered the chat and has been a pillar of emotional support for years now. Annaliese Meyer entered the Joint Program with gusto and brightens my day every time I get to see her—even if she's just dropping by to do laundry in my basement. I had the privilege of partaking in the absolutely stellar climbing/pho eating/drinking/life support group with Brynn Hamilton, Jonas Kaare-Rasmussen, and Margot Debyser.

Much of the science that I did was through BIOS-SCOPE, and I made friendships there that astounded me. Michelle, Fabian, Lillian, and Chance: I've said this before, but while we didn't have to be friends just because we were grad students on a cruise, my life is better because we are. You're a group of people with whom I was immediately

comfortable and uncomplicated. Our stints together were to me like little checkpoints in the motion and trials of graduate school; places outside of time where we were more people than scientists.

Outside even science and musical connections, I owe my start in climbing and many good reads to Ryon Merrick, who, whenever he was in town, made it a priority to spend time with me. While I do appreciate my therapist, these visits were like a hot shower for my soiled, embittered brain. Austen Tallman didn't just drink beer and shoot the bull with me; he made beer and astutely analyzed history while his and Shavonna Bent's dog tried to lick my pyloric sphincter. Elsie Stickler, Connor O'Brien, and Kirstine Grab grew from trauma-bonded band geeks to a loving group of ride-or-dies facing the world of adulthood in many ways. Even the friends from my hometown—Brenden Jacobson, Marcie Woehl, Christian Weber, Sydney Munns, Dawson Abel, Kayleigh and Nick Perrin—the moments I've gotten to share with you have always been peppered with the excitement of watching each other grow and feel out our lives. It's not so lonely.

Here we see the folly of trying to write something special for every person who mattered in just six years of life. We're going to jump to my family now, but if I have not added your name, it's only because this is longer than any Acknowledgments section I have ever seen, I'm t-47 hours to submission, and I'm worried I will be told to cut it. To the friends, new and old: I love you all. I will see you around.

Logan, I love you too. I wouldn't move to Hawaii for most people, but you're perhaps the most devoted partner I could ask for. You've seen every ugly thing I can be, and you work on our relationship like it's the most important project you've ever taken

on. Beneath the “pure theatre” of which you’re capable onstage, you bring an ocean of genuineness and choose to share it with me.

To my family: to Mom, Benjamin, Isaiah, and my uncles, aunts, cousins, and every other member of the family that comes together in the best way whenever anyone gets married or dies, thank you for bearing with the prodigal son. Dad won’t ever read this, and I’m not sure I would have wanted him to. If we had more time, the things I’d want to do with him would have nothing to do with the chemistry of metabolites. That list will only grow now, and I’d trade this degree in to be able to work on it. Alas, here we are, and now on with the science.

Contents

List of Figures

List of Tables

List of Supplementary Material

Supplementary material is provided in the file

Germolus_germolus_PhD_CEE_2024_tables_supplemental.xlsx

Contents:

- Identifiers_withInChI: Metabolite names, identifiers, and abbreviations.
- Chapter2_Metabolites: Processed metabolite data for Chapter 2 with concentrations, limits of detection.
- Chapter2_VSWRates: Regressed photochemical rate parameters and statistics for metabolites in Chapter 2 evaluated in Vineyard Sound Water.
- Chapter2_ASWRates: Regressed photochemical rate parameters and statistics for metabolites in Chapter 2 evaluated in artificial seawater.
- Chapter2_FilteredMolarExt: Processed molar extinction coefficients from 250-800 nm for glutamine, glutamate, histidine, tryptophan, and kynurenine.
- Chapter3_Metabolites: Processed metabolite data for Chapter 3, with concentrations and limits of detection.
- Chapter3_IncubationMetadata: Extended metadata for animal incubations.
- Chapter4_Metabolites: Processed metabolite data for Chapter 4, with date and time, sample information, sampling depth, and cast-niskin IDs for matching with other BIOS-SCOPE data.

"Each species, be it a form of bacteria or deer, is knitted together in a network of interdependence, however indirect the links may be."[1]

Chapter 1: Introduction

1.1 Background and Motivation

At the micron scale of single cells, organisms interact with the environment through chemical exchanges, and in aquatic environments dissolved organic matter (DOM) is the yarn from which the web between them is knit. Photosynthetic organisms reduce CO_2 into biomolecules, which may be respired, recycled, or released, whether through death or excretion as DOM, and the organisms around them may import these molecules and use them for energy and raw materials, perhaps wasting CO_2 to then be taken up by the phytoplankton and fixed again.[2] This is the microbial loop; it is the stable base for the higher trophic levels of the marine ecosystem. Roughly one quarter of the carbon atoms fixed by phytoplankton pass between producer and consumer at least once before their mineralization back to CO_2.[3] In this cycle a molecule exists briefly as DOM—dissolved in the liminal space between cells—on the scale of hours, resulting in a closed, invisible current of carbon 3-4 times as large (33-39 Gt C y^{-1}) as human CO_2 emissions (10.2 Gt C) in 2023.[3–5]

DOM is neither monolithic in its structure nor its ecological function. The nature of DOM released by organisms (and what organisms are present to release it) depends on their local environment: seasonality,[6] diel periodicity,[6,7] and more nuanced factors like photosynthetic overflow, nutrient availability, and signal response.[8–10] If an organism dies, its mode of annihilation (predation, viral infection, senescence) produces different chemical mixtures.[11] The individual biomolecules within DOM released through any of these sources can be termed metabolites, although "metabolite" is imprecise when

applied to DOM: dissolved metabolites are more like the collective metabolism of the entire community, rather than the more conventional denotation in monoculture or organismal tissue.[12] Kujawinski's "superorganism" metaphor helps for dissolved metabolites,[13] although the carbon in metabolites and the broader "labile DOM" are only a small fraction (< 0.1%) of the total pool of dissolved organic carbon (DOC).[14] The less-labile DOM is produced and consumed at rates orders of magnitude slower than the metabolites that are the focus of this thesis,[4,15] and while both groups are diverse, many of the labile DOM compounds are structurally well-defined biomolecules that can be quantified, like amino acids and B-vitamins.[16,17] Both within and outside the labile subclass exist thousands of yet-unidentified compounds, and deconstructing their diversity is the domain of untargeted (semi-quantitative and often discovery-focused) metabolomics.[8,18,19]

DOM diversity is critical, because the microorganisms within the loop are also diverse—each only has a small subset of all possible metabolic genes and some enzymes are specific to or prefer one isomer, analog, or protonation state.[20,21] Many organisms have metabolic deficiencies requiring an external source of at least one metabolite (auxotrophy), and metabolites excreted by living cells have functions ranging from the specific (metallophores, quorum sensing signals) to the bewildering (prochlorosins).[8,22–24]

Despite its intractability to determinism, comprehending the microbial loop remains a pillar of oceanography with good reason: the ecosystem so far described, or variants of it, covers 70% of the Earth's surface. It exudes roughly half the atmospheric oxygen and absorbs most of the CO_2 that humans produce.[25] A system this critical to

the functioning of the biosphere must be—and has been—incorporated into various models of the climate, and more focused numerical models of the microbial loop appear regularly, most recently leveraging the genomes of cells themselves to capture the specifics of metabolite exchange.[26–28]

The capability to model individual microbes as actors with complex sets of genetic instructions has firmly implanted bioinformatics in the toolbox of quantitative ecological analysis, but the majority of modeling approaches scalable to even a one-dimensional water column share an often-unspoken assumption: if microbes are the primary source of labile metabolites and these metabolites have short residence times in the dissolved phase, microbes are the only factor that controls their fate. This thesis was meant to test that assumption, and in so doing demonstrate the capabilities of metabolomics techniques to evaluate many chemicals simultaneously for well-known reactions and transport processes. This includes some conceptual redundancy for the benefit of molecular specificity: among those building models of DOC, the idea that organic molecules may be mixed around, altered by sunlight, or excreted by animals is not new.[4,15] Closely examining individual DOM compounds, however, raises new questions. This thesis investigates three factors relevant to labile DOM fluxes—photochemistry, zooplankton excretion, and mixing—in the context of a novel set of metabolite field data. What this Introduction intends is to introduce not only the factors I did evaluate, but review evidence and literature gaps for what is left to check.

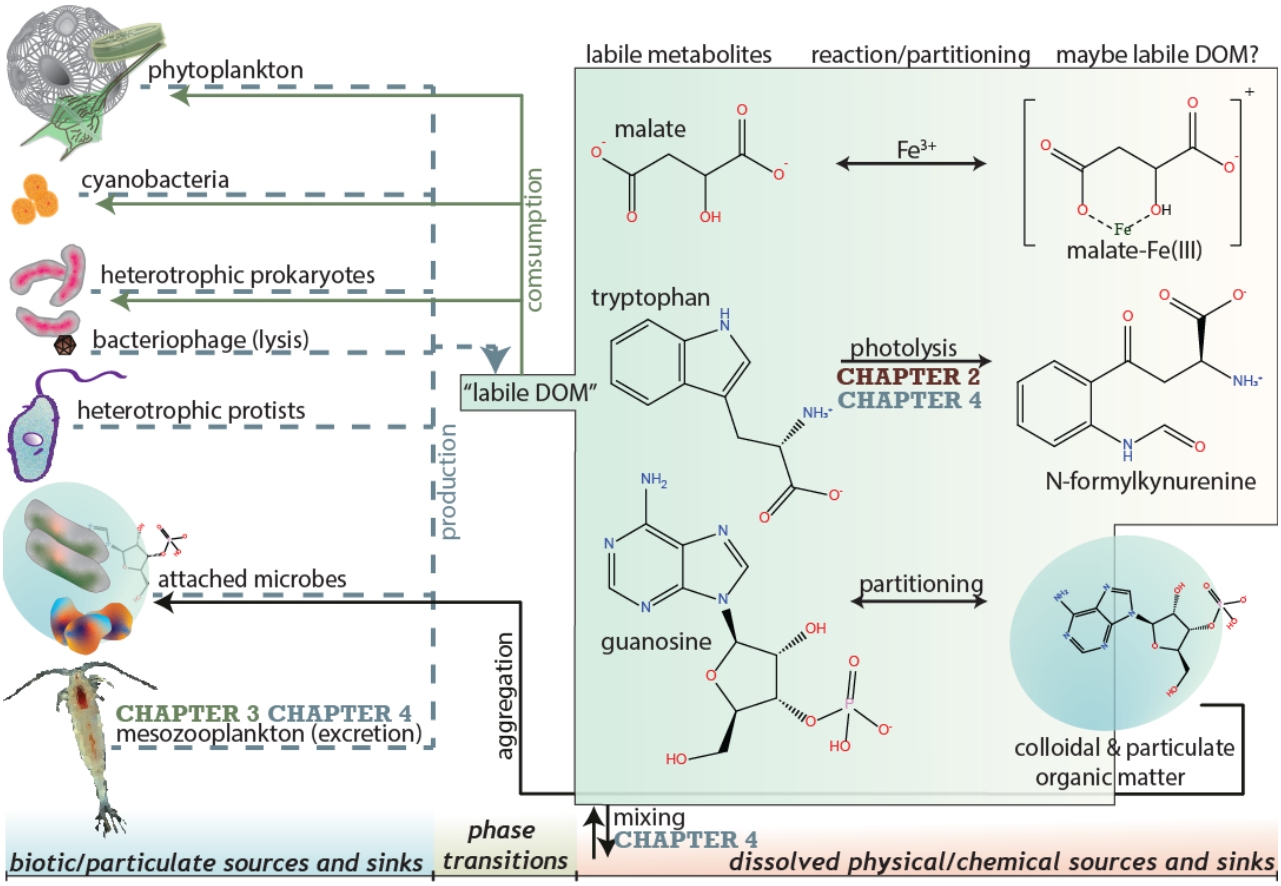

Figure 1-1: Diagram of some of the possible alternative sources and sinks of metabolites. Protonation state is shown as the dominant form at pH 8.1, and trophic relationships are omitted for simplicity. Factors investigated in this thesis are shown explicitly.

The broad strokes I have outlined are, in their holistic sense, not a single investigation or thesis but a new framework (Figure 1-1) that advocates bringing together the new tools (metabolomics) and old concepts (ex. modeling a kinetic rate) to fill a gap in an otherwise nuanced picture of the microbial ocean. At most, I examined 64 different chemicals, and in a way that does not account for stereochemistry (frighteningly, this may matter, as one bacterioplankton apparently can inhibit its neighbors by exuding the D-stereoisomer of arginine).[29] Aside from the analytical techniques used for the metabolites themselves, the chemistry is not new. The techniques—high-resolution liquid chromatography-mass spectrometry methods capable of trace metabolite measurements—are featured as a promising development

that makes this expansive web of chemical/biological/physical interactions (Figure 1-1) more accessible, with the ability to measure tens to hundreds of compounds in one sample.

1.2 Notation and Kinetic Constraints

A primary assumption that I will use is a similar one to much of the environmental contaminant literature: unless otherwise known, if metabolite i becomes "not i", that is, a bond is broken, an isomerization occurs, or i is complexed or sorbed into a particulate or colloidal phase, we consider it (putatively) unavailable. This assumption is intended to bring thermodynamic and kinetic expressions of metabolite activity to bear on the discussion. While many compounds produced in abiotic reactions are labile, many are not, or are of unknown biochemical utility.

Metabolites are generally present in ocean water at concentrations seldom exceeding 10 nanomolar (nM or 10^{-9} moles L^{-1}), and often in or below the picomolar (pM or 10^{-12}) range. At the level of the individual metabolite species, this is one reason for the assumption of microbial dominance. Any conventional rate law of the first or second order depends on concentration, so any chemical reaction that changes the concentration (C_i) of a metabolite appreciably in the hours-to-days time scale must satisfy one of three conditions: (1) a rate constant (k_{rxn}) at or near the limit of molecular diffusion ($10^{9.87}$ s^{-1} for seawater at 35 ppt salinity, first-order), (2) condition (1) and/or a bimolecular reaction with a much more concentrated reactant, or (3) a process not empirically governed by a conventional rate law.

Condition 3 applies to several of the processes that follow: some equilibrium processes (like acid-base) satisfy 1 and 2 *a priori*; animal excretion is governed by

feeding behavior, diet, temperature, and the bioenergetics of motility;[30] enzymes are usually modeled by Michaelis-Menten kinetics (but are derived from first and second-order kinetics).

Attributing patterns in field data to any of these factors requires a knowledge of which reactions would be observable at all under ideal conditions: one reaction operating on one metabolite. With current techniques, it is possible to measure a difference of 10 pM between two replicate sets for many metabolites, and if we assume that the time between samples is a constant value of 6 h (sampling interval in Chapter 4), we can ask what reactions could be detected if they took place in isolation.

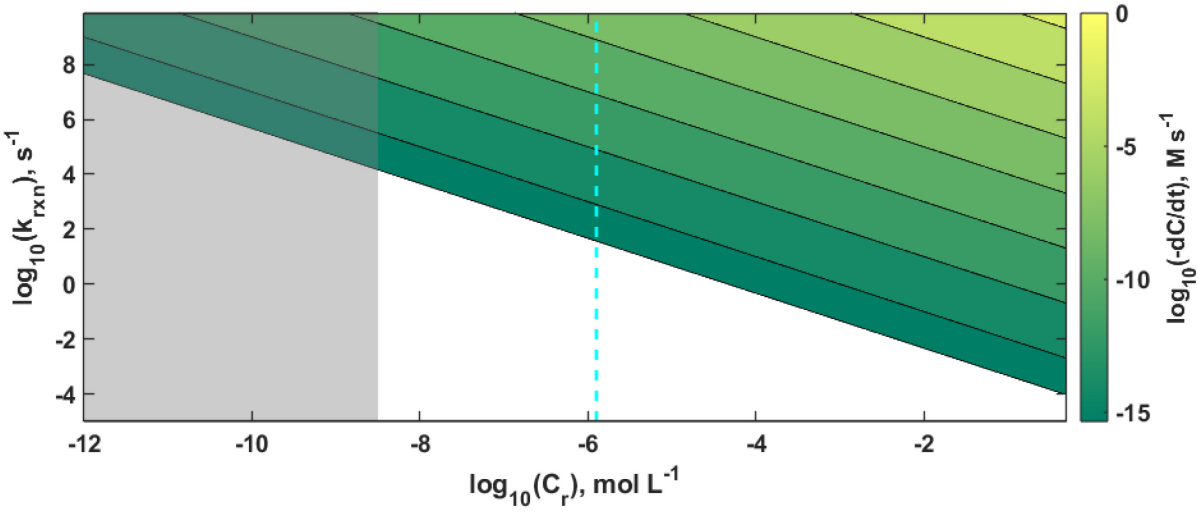

Figure 1-2: Competitive bimolecular reactions of a metabolite present at 10 pM. The y-axis is a hypothetical bimolecular reaction coefficient multiplied by 10 pM to yield a pseudo-first order constant; it is bounded on top by the diffusion limit of $10^{9.87}$ s^{-1}, while the x-axis is the range of secondary reactant concentrations from 1 pM to 1 M. The green shaded region contains reaction rates above the detectability threshold: greater than 10 pM change in 6 hours. The gray shaded region covers the range of metabolite concentrations in this thesis, and the dotted cyan line is the approximate [OH^-] in pH 8.1 seawater.

Figure 1-2 shows how the reaction rate and concentration interact for a hypothetical metabolite undergoing a bimolecular reaction. For most metabolite concentrations (gray box), reactions with other species, whether transient oxidants or other metabolites, requires a reaction rate constant that even most enzymes do not

achieve.[31] This requirement means that reactions between metabolites, such as dimerization, can be discounted. Reactive oxygen species can react with some compounds at rates near the diffusive limit, but their own steady-state concentrations are often so low that the difference would still be undetectable in environmental samples during a field campaign.[32] Base-catalyzed hydrolytic reactions are much more likely, as [OH^-] is much more abundant, and require pseudo-first order coefficients above ~10^2 s^{-1} to be observable at ambient concentrations.

1.3 Equilibrium Processes

This subsection will discuss some factors that may influence both a metabolite's reactivity and microbial lability: protonation and ionic state, complexation, and partitioning. They are not investigated in detail in this thesis but have bearing on both the experimental conditions (making artificial seawater) and potential influences on the results (see Chapter 2) in some cases.

1.3.1 Acid-Base and Ionic Equilibrium

Seawater has a pH of ~8.1, which means that most metabolites I will discuss are either anions or zwitterions in solution. Amino acids are notable here, because most are zwitterionic at this pH, having $pK_{a,1}$ values around 2.2 and $pK_{a,2}$ values of around 9.4, although many have ionic side chains that are either anionic (aspartate, glutamate) or cationic (arginine, lysine) at pH 8.1, while tyrosine and histidine's side chains are uncharged and cysteine is 33% ionized to its thiolate form.[33]

Many important marine metabolites such as glycine betaine, ectoine, homoserine betaine, dimethylsulfoniopropionate, and thiamine bear permanent positive charges because of quaternary amines (or sulfonium) groups; however, other ionic species

actively donate or accept protons. Many non-amino acid species are negatively charged (2,3-dihydroxypropane-1-sulfonate, ciliatine, malate, nucleic acid phosphates) due to the carbonate, phosph(on)ate, or sulf(on)ate groups having pK_a < 7, while amine-containing metabolites like spermidine may have one or more N atoms with pK_a > 9, and are thus protonated in seawater.[34]

1.3.2 Metal-Organic Ligands

Negatively-charged metabolites, especially those with two or more ionic sites, can chelate major ions (Ca^{2+}) and trace metals (Fe^{2+} or Fe^{3+}) in seawater, and whether or not this influences the liganded metabolite's lability to microbes is an open question. The same principle applies to lone pairs on amino and thiol groups, which is how many enzymes coordinate their metal cofactors.[35,36] Glutamate is a mono- or bidentate ligand that can bind Ca^{2+} with formation constants of 4.77 M^{-1} (*alpha*-NH_2) and 23.05 M^{-1} (*alpha*-NH_2 and *epsilon*-COO^-), and the analogous constants for aspartate are even higher (9.74 M^{-1} and 62.40 M^{-1}).[37] Using the second formation constants for both (more relevant for the ambient pH of 8.1), the pK_a values for the amino group that must be deprotonated for the bidentate form (9.7 for glutamate, 9.6 for aspartate), and a Ca^{2+} concentration of 10 mM, the fraction of each bound to calcium in seawater can be (crudely) estimated:

$$\frac{[CaL]}{L_{Tot}} = \frac{[Ca^{2+}]K}{[Ca^{2+}]K + 1 + 10^{pK_a}10^{-pH}}$$

Equation 1-1: Glutamate and aspartate complexation by calcium

For glutamate, this represents 0.6% bound to calcium and for aspartate, 1.9% bound, even though the majority of these two metabolites' amino groups are protonated at ambient pH. These results may not have any impact on bioavailability, but the binding

of any metabolite to a major and conservative seawater component would be a functionally universal property within the dissolved phase.

Iron siderophores, and metallophores in general, have been a topic of interest for trace metal chemists for some time, especially after the discovery that most (>99%) of dissolved Fe in seawater is bound in organic complexes.[38,39] Trace metals like iron, zinc, and copper can be complexed by relatively simple metabolites such as malate, and unlike calcium, the stability coefficients tend to be higher ($10^{12.66}$ for malate-Fe(III)) but apply to free metal ion concentrations in the sub-picomolar range.[40,41] Notably, the strength of the malate-Fe(III) complex (and to lesser extents, those with Ni^{2+}, Cu^{2+}, and Co^{2+}) is similar to that of L_1 ("strong") ligands thought to be a method by which many bacteria regulate available iron—in some cases possessing transporter genes for wholesale complex uptake.[42,43]

Future considerations of this topic might yield interesting results, but part of the reason that very small (as opposed to a bacteriocin or ferrioxamine) ligands may not have appeared in the literature of seawater is methodological.[23,44] Tools for identifying these compounds are genomic or extraction-based chemical methods that would either assume (correctly) that malate has a different metabolic use (thereby ignoring it as a siderophore) or fail entirely to capture it.[43,44] Strictly speaking, the derivatization-based method used in this thesis is the only known way to accurately measure malate (and many other metabolites) at pM concentrations in seawater. Considering the breadth of central carbon metabolites that have amino, thiol, and carboxylic acid groups, this seems ripe for further work.[33,45]

1.3.3 Colloidal/Particulate Partitioning

Polymeric DOM produced by marine organisms dynamically organizes into nano- and microgels, up to 10% of the ambient DOC at equilibrium.[46] Assuming this gel phase acts like a suspended solid, it may have an affinity (relative to seawater) for some metabolites. The tangled polymers that make microgels are “polyanionic polysaccharides, proteins, nucleic acids, and other amphiphilic hydrophobic moieties” generally nucleated around Ca^{2+} ions.[47] We do not know what, at equilibrium, the concentrations of metabolites in the nano- and microgel phase are, but assuming standard partitioning behavior in a dilute two-phase solid-water system, the fraction in the gel (“solid”) phase can be approximated:

$$f_{gel} \cong C_{gel} K_{i,gel}$$

Equation 1-2: Fractional partitioning of a metabolite into a suspended gel/solid[48]

Where f_{gel} is the fraction of the metabolite dissolved in the gel phase, C_{gel} is the concentration of gel in the bulk water phase and $K_{i,gel}$ is the equilibrium partition coefficient $K_{i,gel} = C_{i,gel}/C_{i,w}$, where $C_{i,gel}$ is the concentration of metabolite in the gel phase (pmol μmol^{-1}) and $C_{i,w}$ is the concentration of metabolite in the water phase (pmol L^{-1}). $K_{i,gel}$ essentially represents the relative free energy change for a metabolite dissolving into the gel, but unlike other partition coefficients is empirical and combines information about surface area and different bonding processes.[48] Using a molar basis of carbon for the gel allows us to make a direct approximation: assuming a relatively normal Sargasso Sea sample with 65 μM DOC, there is about 6.5 μmol L^{-1} of gel.[49–51] Subsequently, any $K_{i,gel}$ greater than 0.0015 L μmol^{-1} is sufficient to scrub >1% of a metabolite from the water.

Here, the convenient framing breaks down, as most known values similar to $K_{i,gel}$ are analogues: values for anthropogenic contaminants in either soil organic matter or freshwater DOM with a high degree of aromaticity, which are substantially different from the acetylated saccharides making up much of marine DOM.[52,53] The closest analog might be the $K_{i,oc}$ values for ketones, carboxylic acid esters, and aliphatic amines with Suwanee River fulvic acid reported by Schwarzenbach et al. (2016) using polyparameter linear free-energy relationships, which range from 10^{-5} to 0.1 L μmol^{-1}. That latter value is extreme, estimating f_{gel} as 65%, but frames a gulf of possibility with respect to partitioning to suspended solids/gels. The process might matter where metabolites are concerned, and could also work in reverse—proteins are components of marine microgels, and some of those proteins are hydrolytic enzymes.[54] The process of gel formation could create transient sources of cleaved mono- and oligomeric metabolites such as peptides (amino acids) and saccharides (sugars), but whether the condensed gel phase of marine DOM and colloids is a source or a sink of metabolites is unknown and depends on the metabolite in question, the ambient DOC, and UV irradiance.[47]

1.3.4 Nonequilibrium Processes

The previous section considered some equilibrium processes that determine metabolite speciation in the water column. Assuming most of them are thermodynamically controlled, their contributions are reasonably approximated with the right coefficients and a few basic assumptions. The following factors are more dynamic. Not all are chemical reactions, but each controls the time-varying abundance of each metabolite

through a mechanism that is largely independent of the microbial loop itself but influences the overall labile DOM landscape with which microbes contend.

1.3.5 Photochemistry

The photolytic loss of recalcitrant DOM may be critically important for the millennial-scale cycling of fixed carbon.[4,14,55] "Loss," however, is a term that covers more than one step in the mineralization of DOM to CO_2: photolysis of recalcitrant DOM may be largely sensitized by colloidal matter, and leads to the production of specific compounds that are labile to microbes.[55–57] This production flux is a significant source of labile metabolites in the ocean relative to, for example, phytoplankton exudates, with production rates in the nM h^{-1} range in the Sargasso Sea for several labile aldehydes and carboxylic acids.[55,58]

The menu of labile compounds produced from recalcitrant DOM is, however, limited in diversity, and some of the products can subsequently be lost to air-water exchange processes and photolysis.[58] Compounds like pyruvate and acetaldehyde are small (≤ C_3) and are biochemically useful more as raw substrates rather than as preconstructed cofactors and monomers. For compounds like amino acids and vitamin cofactors, their larger, heteroatom-rich structures seem more likely to be destroyed by the action of sunlight rather than produced by it (although if fresher, richer riverine DOM is irradiated, amino acids can be produced).[59]

As an example, dissolved riboflavin (vitamin B_2) is anticorrelated with sunlight in seawater and can be degraded in minutes to lumichrome and other compounds using visible (405 and 435 nm) light at photon fluences (1.9 μE s^{-1} L^{-1}) about two orders of magnitude higher than those of the subtropical ocean at solar noon at the same

wavelengths.[6,60] This concept has ecological implications: if some metabolites thought to be currencies of the microbial ecosystem are also highly photolabile, the compounds encountered by microbes are a different set than those initially released. After photolysis, either the photoproducts are ultimately used by the microbes, or the photoproducts represent leakage from the microbial loop—places in the biochemical pathway map of the ocean where the labile DOM transitions to a less-labile state. Evidence for whether photochemistry makes DOM more or less labile to microbes is mixed, as it depends on the original structure of the organic matter.[61–64]

Not only might this process matter for some metabolites in their assumed ambient speciations; complexes formed with metals also affect photolability, most often increasing it through the creation of a larger molecular orbital system involving the *d*-orbitals of transition metals.[65,66] Whether this affects only the photoreactivity of the metal, which can be reduced, released and recycled,[67,68] or whether the chimeric chromophore is actually degraded is another place where the compound in question is important. Iron and DOM interact to produce color, but exactly what happens to the relevant DOM species is still a question involving too many parallel moieties to definitively answer.[69]

1.3.6 Animal Sources

Zooplankton and larger animals excrete DOM, and because many are mobile, they can eat a biochemical sample of the microbial ecosystem, digest it, and jettison the waste products hundreds of meters away from their initial dining location. This phenomenon, specifically for migratory zooplankton, has been studied as a way to move carbon and nitrogen to the mesopelagic zone,[70–72] but Chapter 3 (and Chapter 4) applies the latter

framework to individual metabolites across four species of zooplankton. High excretion rates of taurine and other amino acids have been measured by others,[73,74] but with a new benzoylation method, we have greatly expanded metabolite analysis in zooplankton excreta by increasing the number of metabolites and dramatically decreasing the sample requirements to a single animal per sample (as opposed to ~50).[17,75]

Excretion rates of individual metabolites can be paired with other types of data to draw useful conclusions. Because zooplankton do not subsist on DOM, measuring dissolved organic carbon and nitrogen in the same incubation experiments allows us to estimate how much of the excreta has been captured by the metabolite targets:

$$\Delta[DOC] = \sum n_{C,i} \Delta C_i$$

Equation 1-3: Summation of DOC excretion as a function individual molecular formulae

In words: the change ($\Delta[DOC]$) in dissolved organic carbon (or nitrogen) during an incubation is equal to the sum of each metabolite's concentration change (ΔC_i) times the number of carbon (or nitrogen) atoms in the metabolite ($n_{C,i}$).

In addition to gaining a metric for what portion of dissolved excretions can be accounted for by metabolite measurements, the data can be applied to the field. Pairing measured excretion rates—usually normalized by dry biomass—with zooplankton abundance data involves assumptions about residence times, species composition, and feeding behavior, but it has been done for bulk elemental contributions.[71] Doing so in Chapter 4 allowed us to both pinpoint the source of a transient metabolite anomaly and

to estimate residence times for metabolites from the side of supply, and therefore independent from prior methods dependent on bacterial uptake rate.[a]

1.3.7 Physical Mixing

Mixing is unlike anything discussed so far in that it is agnostic to the identity of the metabolite, instead acting on gradients which depend on the metabolite's profile. Determining how this affects local metabolite concentrations requires K_z, the vertical eddy diffusivity coefficient—as well as some estimate of metabolite-depth gradient steepness. Fortunately, the measurement and estimation techniques for K_z as a function of depth have greatly improved over the last decade, allowing either CTD-level resolution (~1 m) estimates when combined with wind speed data and density gradients or direct measurements from glider-attached sensors.[76,77] Both of these produce $K_z(z)$ profiles that vary across several orders of magnitude, and allow for numerical gradient calculations of greater accuracy and resolution than metabolite measurements.

The advancement of K_z data begs for its application to dissolved chemicals, and metabolites make a great test case, given their transience and locality.[78] Metabolites are sampled from Niskin bottles, precluding the direct pairing of K_z at the same depth resolution; however, with eddy diffusivity profiles we can ask what kinds of metabolite gradients would be observable at all, and at what times of the year as the depth of the mixed layer varies seasonally (by >100 m near Bermuda) and is an important process for the ecology of the area.[79,80] What bearing does fine-scale mixing have on metabolite profiles within the mixed layer? Are inputs below the mixed layer primarily consumed within the few meters they might appear? Without any new metabolite measurements,

[a] This is enormously promising, as it is much more difficult to determine "what microbes in a complex community produce or consume metabolites at a given rate" than it is to "get trapped crustaceans to pee in a bottle."

we can simulate answers to these questions—but their application was triggered by anomalies in the data in Chapter 4.

1.3.8 Other Factors

Two details that will not be explored in this thesis in detail are hydrolytic reactions and air-water exchange processes. Some metabolites, produced both biotically and abiotically, are volatile and escape the water column at the air-water interface.[58,81] Generally, the compounds to which this applies are nonionic, with only 1-3 carbon atoms, and are not captured by the methods I have used here.

Hydrolysis is unlikely to be a rapid sink for most metabolites; however, the exceptions may be important. For example, vitamin B_1, or thiamine, is an auxophore. There are many planktonic organisms that lack the capability for its endogenous synthesis, and some that tend to reconstruct it from its component parts, namely AmMP (the pyrimidine group).[82,83] AmMP has been measured in seawater, both by myself and by others.[84] Thiamine is susceptible to spontaneous hydrolysis, with a base-catalyzed hydrolysis half-life of 6.1 h at pH 8.1 (hydration of the thiazole ring),[85] and while producing AmMP would require additional steps, recent work has shown that some eukaryotes and prokaryotes can utilize a formylated AmMP, which is one C-N bond away from Herrmann et al.'s hydrolysis end-product.[86] While this is an example of a process I have not investigated, it is also an example of the sort of work that benefits from the parallel measurements made available by quantitative LC-MS and through identification-focused untargeted metabolomics.[87]

1.4 Thesis Outline

This thesis has three chapters brought together by a common theme of interpreting metabolite data through the lens of a new method: pre-extraction benzoyl chloride derivatization with stable-isotope labeled internal standards.[17] Chapter 2 features a photochemistry experiment that yielded rate parameters for a handful of metabolites with photodegradation potential. We exposed a suite of metabolites to simulated sunlight in both natural and artificial seawater at pM to nM concentrations. In concord with the idea of this thesis, the objective was to evaluate potential metabolite fluxes for many compounds in parallel. Because the 111 metabolites in the experiment were individually present at pM-nM concentrations, I focused primarily on direct, rather than indirect, photochemistry. Figure 1-2 demonstrates this reasoning: a metabolite present at ambient concentrations (~10^{-11} M) in seawater may be capable of reacting with excited chromophoric DOM (^{3}CDOM) or reactive oxygen species (ROS), but for this to happen at a competitive rate, the reaction between the two must have a near-maximal rate coefficient *and* concentrations of the excited reactant that are on the order >10^{-11} M. The first condition is actually not uncommon; the latter is unlikely.[32]

Chapter 2 considers indirect photochemistry to some extent; hence, the use of natural seawater as a comparison just in case the DOM did affect reaction rates. Most of the metabolites were not expected to react at all. Direct absorption of light in the visible and near-UV range is generally not a property of the set of analytes we used: only kynurenine has a faint yellow hue when dissolved in pure water.

Chapter 3 examines metabolites excreted by four (five, counting a dead euphausiid) zooplankton species in terms of their composition and rates. Our explicit

objective was a table of excretion rates to be used in conjunction with field data to calculate zooplankton metabolite contributions to the water column, but we also looked at how much of the total DOC and total dissolved N excreted could be explained solely by the compounds we measured and evaluated differences between the animals.

Chapter 4 was the first dataset of this thesis chronologically—a large set of field samples collected in November 2021—but became the reason for conducting the experiments in Chapters 2 and 3. Over two days, I collected metabolite profiles every 6 hours, and once I had done so, I needed a framework to interpret the data. The patterns present could have been loosely associated to several different water column parameters or microbial actions, but some features made me wonder whether the photochemistry, zooplankton excreta, and mixing described above may be responsible for some of it. For many of the chemicals in question, there was simply nothing to which to compare the data, and so this project began with the objective of determining the non-microbial factors that alter the metabolite landscape. This was, as may already be apparent, potently hubristic.

1.5 A Note on Data and Names

In this thesis, I have linked the text to repositories in each chapter where the raw data and processing codes can be found online. There are two reasons for this: (1) it is good practice to share, and (2) both of these things have attributes (sheer length, lack of interpretability in print) that make it unreasonable for them to be printed in this thesis. While they are accessible, I have also provided the processed data and metadata for each chapter (ex. QA/QC-screened metabolite concentrations, sampling depth, extinction coefficients) in an Excel file,

Germolus_germolus_PhD_CEE_2024_tables_supplemental.xlsx as per the MIT Specifications for Thesis Preparation. These data are more easily reckoned with, but nonetheless do not fit neatly onto published pages.[b] The first sheet in that Excel workbook is a list of different chemical identifiers. The reason for including these is clarity. I refer to metabolites by their "trivial names," shortened versions of a chemical name that may be ambiguous (to stereoisometry, protonation state, etc.), which is an inevitable problem in metabolomics. Given a recent set of guidelines, I formatted the identifier sheet such that it contains identifiers (International Chemical Identifier or InChI) that are easy to look up and contain exactly as much structural information as I reasonably could know, and nothing else.[88] For example, our chromatography is not stereoselective, and *in situ* ionic state must be inferred.

[b] I did not choose to put my last name twice in the file name, but that is the inevitable result of MIT's specified naming scheme.

Chapter 2: The photochemical decay rates of marine metabolites

Co-authors[c]: Collin P. Ward, Melissa C. Kido Soule, Elizabeth B. Kujawinski

Abstract

Dissolved organic matter (DOM) in the ocean comprises tens of thousands of unique chemical species. Metabolites are the small, biogenic products making up much of the most labile DOM. Targeted analyses like quantitative LC-MS probe ocean endo- and exometabolomes, but they do more than just capture the products of metabolism; they capture the abiotic chemistry of the ecosystem as well. Here, we have turned the scope of dissolved metabolomics outward, from microbial sources and sinks to photochemistry. We evaluated photolysis as a sink for labile metabolites at environmentally relevant (pM-nM) concentrations. Of 57 quantified metabolites, 11 decayed significantly under simulated sunlight. Of these, seven decayed in seawater with pseudo first-order rates and had half-lives ranging from 1.5-63 h. Rates for tryptophan and kynurenine were higher in the presence of natural organic matter. These results, though bearing on a small subset of marine organic matter, indicate that the sun participates in the elemental flows of the surface ocean to an underappreciated degree, changing labile organic matter into secondary products on hourly-to-daily timescales that compete with microbial uptake.

2.1 Introduction

Ocean microorganisms and dissolved organic matter (DOM) interact with molecular specificity, producing and consuming the biochemical blocks with which the ecosystem constructs itself.[45,89,90] About half of the carbon fixed during primary production is thought to cycle through this microbial loop, the "labile DOM".[3,14] From the perspective of single-celled life, labile DOM does not exist; rather, DOM is a molecular menu from which each organism may prefer some fraction according to its genetic dictates. This creates a rich picture of the microbial loop, with an enormous number (>10^5) of organic biological products, or metabolites, each passing rapidly in parallel and unique sets of enzymatic pathways on the way to export or mineralization.

[c]Department of Marine Chemistry and Geochemistry; Woods Hole Oceanographic Institution, Woods Hole, MA, USA

The metabolite exchange network is typically packaged with the assumption that due to the short residence times (hours to days) of metabolites in the water column, microbiological activity is responsible for most—if not all—additions, removals, and transformations of metabolites. Trace organic chemistry in seawater is analytically challenging, so investigators typically zoom in on one or a few molecules at a time. Cases such as dimethylsulfoniopropionate (DMSP)'s photochemical-bacterial collaborative mineralization or photochemical production of acetaldehyde or pyruvate might be seen as exceptions.[57,58,91] An expanding list of labile organic compounds produced (or consumed) by photochemistry alone hints that for metabolites, sunlight may affect the biochemical menu available to the ecosystem.[92,93]

It is essential to examine the photochemical influence on individual compounds within labile DOM, and not solely for the purpose of making elemental flux models more complicated. These abiotic factors are critical for ecology, as they are that to which the ecosystem must be adapted. Photochemical cleavage of recalcitrant DOM can be a source for labile matter,[92] but photolysis of labile metabolites implies that what is produced and what is consumed in the microbial loop are not the same sets of compounds. Gaps in an organism's metabolic oeuvre and genes that remain unannotated may be sated by compounds formed through non-biological pathways. Giving up genes to produce a metabolite, and thus requiring an exogenous source (i.e., auxotrophy) may be more or less advantageous depending on whether a dissolved metabolite photolyzes to a useful precursor or becomes an inaccessible degradation product.[94–96]

Metabolomics as a field of study uses chemistry to examine the products of biochemistry, but at its core is a science of massively parallel chemical quantification. When applied to dissolved organic matter, it sees more than the pathways inside of cells (canonically a very effective use[90,97]) and presents an opportunity to add a granular chemical perspective that models of chemical exchange currently lack. Quantitative liquid chromatography-mass spectrometry (LC-MS) also has the unique benefit of simultaneously measuring many small (<1000 Da) chemical species at levels (10^{-9}-10^{-12} M) that are both similar to the oligotrophic ocean and dilute enough to avoid interactive effects when testing tens or hundreds of compounds simultaneously.[16,17]

We paired simulated sunlight and quantitative LC-MS to evaluate 111 metabolites for their potential to photochemically react in the dissolved phase. We tested the hypotheses: (1) that most metabolites would not show a net change over the course of irradiation owing to the lack of chromophore groups and sensitizers; (2) that our chosen metabolites would not be photoproduced from natural DOM; and finally, (3) that some metabolites would react faster in the presence of natural DOM owing to the material's photosensitization potential.

2.2 Methods

2.2.1 Preparation of Water

We used three different aqueous solvents: MilliQ water (MQ, for blanks), artificial seawater (ASW, seawater lacking natural chromophores), and Vineyard Sound water (VSW, a natural coastal seawater with a complex mixture of natural DOM). We prepared artificial seawater (ASW) following the recipe for the Aquil* culture medium without the nutrients and trace metals.[98] To reduce organic contamination, we

combusted the sodium chloride in a muffle furnace (450 °C, 6 h) before making the ASW. We collected Vineyard Sound seawater (VSW) in an acid-washed polycarbonate bottle at high tide and brought it to the lab for immediate filtration (0.2 μm PTFE membrane). We adjusted the pH of the ASW to that of the VSW (8.13) using dropwise addition of 8 M NaOH, then gravity-filtered 2 L each of VSW and ASW using a 142 mm Georig with a 0.2 μm Omnipore PTFE membrane.

2.2.2 Metabolite Additions

Following Widner et al. (2021), we made six stock mixes of metabolites at 10 μg mL^{-1} and diluted each stock 1:100 into ASW for a secondary (2º) stock of 111 metabolites at 100 ng mL^{-1}. We diluted the latter to a tertiary (3º) stock at 500 pg mL^{-1} and sterilized both the 2º and 3º stocks using a syringe filter (0.2 μm PTFE). We split aliquots of ASW, VSW, and MQ water and, using the 2º stock, spiked bottles of ASW, VSW, and MQ to a metabolite concentration of 700 pg mL^{-1}. These spiked matrices are referred to as sASW, sVSW, and sMQ for the remainder of the Methods, whereas the “s” will be dropped in the Results and Discussion, which focuses on the spiked matrices.

2.2.3 Simulated Solar Irradiation

We cleaned 12 mL quartz tubes (14 mm inside diameter, 85 mm exposed length, with flat bottom and Viton septum) using triple-rinses of water, methanol, acetone, and dichloromethane and dried them in a fume hood under a foil dust shield for several days before use. We filled each clean tube with water (no headspace).

We placed 14 tubes on a black aluminum plate in the Suntest XLS+ solar simulator with an optical filter to screen wavelengths <280 nm. We irradiated five vials each of sASW and sVSW for metabolite analysis and flow cytometry, and one each of

sASW, sVSW, ASW, and VSW for UV-Vis spectrophotometry at the completion of irradiation. We ran chilled water through the aluminum plate, keeping the temperature of the vials at 22 ± 3 °C. We left four control tubes (sASW, sVSW, ASW, and VSW) in a dark drawer (20 °C), wrapped in foil, for the duration of the incubation, and another four, sampled immediately, served as matrix blanks (ASW, VSW) and zero-hour time points (sASW, sVSW).

At each time point (0, 1, 2, 4, 6, and 12 h), we removed the corresponding tubes from the Suntest and/or retrieved the dark controls (12 h) or blanks (0 h). We split the water in each tube into three 3.25 mL sample replicates in 8 mL combusted amber glass vials (for metabolites) and one 500 µL sample in a 1.5 mL cryovial (for flow cytometry).

We drew upon the data collected by Freeman et al. (2023)—where the authors measured downwelling irradiance at twelve locations in the same solar simulator used in this work—using a StellarNet Black Comet Spectral Radiometer, which measured the lamp output (W m^{-2}) in 1 nm intervals from 280-699 nm.[99]

2.2.4 Dissolved Organic Carbon

We allocated 3x40 mL of all six possible matrices (MQ, sMQ, ASW, sASW, VSW, and sVSW) and acidified each to pH < 2 with 40 µL HCl (12 M) for analysis of dissolved organic carbon (DOC) and total dissolved nitrogen (TDN) on a Shimadzu TOC-L using high-temperature catalytic oxidation. Each sample's linear calibration curve included at least four potassium hydrogen phthalate reference standards, and we determined final DOC and TDN by subtracting the instrument blank signal from the average sample peak area and dividing by the calibration slope.[100]

2.2.5 UV-Vis Spectrophotometry

We collected UV-Vis absorption spectra with a PerkinElmer Lambda 650 S spectrophotometer, scanning the wavelengths between 250 and 800 nm at 1 nm intervals using a 100 mm quartz cuvette (Starna Cells, Inc.). We collected triplicate spectra with the pre-incubation matrices, using a new aliquot of water for each measurement and rinsing between matrices with MQ. Each matrix was analyzed three times. After incubation, we collected analytical replicates only for the irradiated matrices (ASW, VSW, sASW, sVSW) due to sample volume limitations.

We used the equations of Fichot and Benner (2012) to approximate terrigenous DOC in our natural seawater (VSW) as total dissolved lignin phenols using the spectral slope coefficient $S_{275-295}$ after converting to a Napierian absorption coefficient $a_g(\lambda)$ and regressing $\ln(a_g(\lambda))$ on λ.[101,102]

2.2.6 Metabolite Quantification

We measured metabolites using a previously-published method.[17] Briefly, we benzoylated amine and alcohol groups within the samples to improve chromatography and to add ^{13}C-labeled internal standards matched to each metabolite. We then concentrated each sample and standard using BondElut PPL solid-phase extraction resin. The only notable modification from the method as published is that our samples were 3.25 mL rather than 1 mL or 25 mL. This presented no difficulty, and the procedural steps and UHPLC-Orbitrap MS conditions used to quantify metabolites based on isotopic label pairs are in the Supplemental Information spreadsheet.

2.2.7 Data Processing

We integrated UHPLC peak areas using Skyline,[103] manually checking each compound for the presence of its benzoylated derivative, its $^{13}C_6$ isotopologue (SIL-IS), and one to two characteristic MS2 fragments for each. Where Skyline was unable to find these fragments, we manually checked the corresponding retention time in mzMine3 to confirm their presence.[104]

In MATLAB R2022a, we used a calibration routine that performed a linear regression of light-to-heavy peak area ratios on added standard concentrations. The script also calculated limit of quantification (LOQ) for each compound as $LOQ = \frac{3.3\sigma_b}{m_{std}}$ where σ_b and m_{std} are the uncertainty in the y-intercept and the slope of the standard curve, respectively. Since all concentrations were initially calculated in pg mL^{-1}, we converted each to molar units (pM or nM) using a table of molecular weights for each metabolite stock. For a metabolite to be quantified, we deigned that it must be present in at least five points of the standard curve, along with its SIL-IS counterpart. The resulting calibration line must also have $R^2 > 0.85$.

All scripts used in this analysis can be found on GitHub (https://github.com/germo006/metabolitephotochem).

2.2.8 Reaction Rates

We used mean metabolite concentrations at 0 h (C_0), 12 h (C_{12}), and in the 12 h dark control ($C_{control}$) as overall indicators of photoreactivity through two difference tests: a t-test between C_0 and C_{12}; and a t-test between C_{12} and $C_{control}$. Where the p<0.2 for both tests, we calculated $\Delta C = C_{12} - C_{control}$, the concentration difference attributable to

irradiation. A positive ΔC indicates photoproduction; a negative value indicates photodegradation.

For all metabolites $\Delta C < 0$, we attempted to fit an exponential rate law to the data. This involved finding two coefficients, C_0 and k_p, the initial concentration and decay rate coefficient. Because the ASW and VSW cannot be assumed to have metabolite concentrations below our detection limits, we fixed C_0 not at the 0.7 ng mL^{-1} spike, but at the concentration (pM) measured at 0 h and then set an arbitrary initial guess of 0.1 d^{-1} for k_p and defined the parameters μ_i and σ_i, the sample mean and standard deviation, for each time point. Assuming a normal distribution for measurement error, we simulated 10^5 datapoints from each distribution, treating them as mean values ($\mu_i{}'$) and assigning each a modified variance $\sigma_i' = \sigma_i + |\mu_i - \mu_i{}'|$ which penalizes the randomly assigned $\mu_i{}'$ if it lies further from the experimental mean.

We fit each simulated dataset to a first-order rate law by minimizing the chi-squared value of the rate equation with MATLAB's *fminunc* function.

$$\chi^2 = \sum_{i=1}^{6} \frac{\left(\mu_i' - C_0 e^{-k_p t_i}\right)^2}{\sigma'^2_i}$$

Equation 2-1: Chi-squared function for a fitted exponential rate law.

Using the optimized values for C_0 and k_p, we constructed probability distributions for C_0 (normal) and k_p (lognormal) and calculated the expected values (coefficient estimates) and their 90% confidence regions (coefficient uncertainties). At this point we eliminated any metabolites whose 90% confidence region for k_p eclipsed zero and calculated R^2 for the optimized regression. We calculated half-lives in the experimental apparatus as $t_{1/2} = \ln(2)/k_p$.

2.2.9 Extinction Spectra and Quantum Yields

We collected the extinction spectra of five compounds (histidine, glutamine, glutamic acid, tryptophan, and kynurenine) in near-saturated MQ water solutions in a 10 cm quartz cuvette on the Lambda 650 spectrophotometer (250-800 nm). Several diluted solutions of tryptophan and kynurenine were needed to provide absorbance data within the limits of the spectrophotometer for near-UV and UV ranges, and we combined the spectra after they were concentration-normalized and corrected for the MQ blank.

After noticing that there was some (5-15%, depending on wavelength) variance in irradiance depending on position in the SunTest, we developed a method for leveraging this to calculate apparent quantum yields for some compounds. This method relies on the fact that each time-point in the experiment received a slightly different irradiance profile, and therefore would have had a different degradation rate. For histidine, glutamine, tryptophan, and kynurenine, we combined the matrix solution absorbance $\alpha_{matrix}(\lambda)$, the extinction coefficient $\varepsilon_i(\lambda)$, incoming photon flux at each sample's position in the SunTest $E_\lambda(x, y)$, the measured metabolite concentrations at each time point $C_i(x, y, t)$, and the measured dimensions of the quartz tubes (85 mm length, 7 mm inside radius). Using equation 2-2, we calculated the the compound's photolytic quantum yield (Φ_i).

$$C_i(t_0) - C_i(t) = \Phi_i \bar{C} \int_{\lambda_{min}}^{\lambda_{max}} \frac{E(\lambda)\varepsilon_i(\lambda)}{\alpha_{matrix}(\lambda)} d\lambda$$

Equation 2-2: Fitting apparent quantum yield based on measured parameters.

For one specific location (x, y) within the solar simulator, $C_i(t_0)$ and $C_i(t)$ are the concentrations of metabolite i at the beginning of the test and at time t, where the difference between them is the total amount of consumed metabolite. The integral on

the right side contains the previously discussed variables relating to the sample in one location, as well as the apparent (broadband) quantum yield term Φ_i. $E(\lambda)$ is itself an integral of the light absorbed by the pronate cylinder of sample (see 2.5 Appendix: Supplemental Methods). The other terms in the integral account for the fraction of absorbed light contributed by metabolite i directly, if the product $\varepsilon_i(\lambda)C_i(t)$ is small compared to $\alpha_{matrix}(\lambda)$, which is a valid assumption in this study (~nM metabolite concentrations). $\overline{C}$ is the vertical centroid of the degradation curve bounded by t_0, and t with a two-point reaction coefficient $k_{pt} = -\ln(C_0/C_t)$. Rather than using fitted overall first-order data to estimate concentration over time, our approach results in a quantity representing the time-weighted average of molecules available for light, while the integral in (2) is the number of photons absorbed by metabolite i on a molar basis (2.5 Appendix: Supplemental Methods).

We used a spectral band of 280-699 nm for all calculations, although the value of Φ_i is effectively for wavelengths where $\varepsilon_i(\lambda) > 0$, which differs by metabolite (see Supplemental Information).[99] We set $\varepsilon_i(\lambda)$ to zero at all wavelengths for which the original compound-specific absorbance measurements were not significantly different from zero (t-test, $p > 0.05$). Finally, we used MATLAB's *fminunc* function to find the value of Φ_i that minimized the difference between right and left sides of Eq. 2 simultaneously for all five time points after 0 h.

2.3 Results and Discussion

We quantified time-courses of 57 metabolites over 12 hours, of which 11 decayed significantly relative to the controls. Of these, 7 had pseudo-first order reaction constants significantly different from zero, and three exhibited half-lives <2 d. The latter

three (tryptophan, kynurenine, and tryptamine) decayed faster in the presence of natural DOM (Table 2-1). We will describe a summary of all metabolites and move from photoreactive (those with significant degradation at 12 h and/or fitted rate parameters to photostable and anomalous metabolites. We will then discuss how the latter categories may influence metabolite speciation and abundance in the open ocean.

2.3.1 Measured Metabolites

Literature evaluating reaction rates and quantum yields for compounds of biological importance generally involve 1-5 analytes and/or concentrations in the nM-mM range.[40,93,105–110] Dissolved metabolites are frequently in the pM range,[45,111] which is far lower than the 100 nM threshold where at least one compound (acrylate) is thought to be quenched from its excited state faster than it can photolyze.[106] If the photolytic transformation of metabolites is halted (or enhanced) by different sets of variables at trace concentrations than at the concentrations previously studied, LC-MS methods capable of measuring such concentrations in a seawater matrix are an attractive analytical option.

Of the 111 metabolites analyzed in this experiment, we quantified 57 within the samples; the remaining 54 had one or more issues preventing a full time-course analysis: poor chromatographic peaks, undetectable SIL-IS peaks, or poor standard curve linearity. The full table of quantified metabolites can be found in the Supplemental Information. Notably, the limits of detection for the 57 quantified metabolites were often subpicomolar, representing a significant advance in both the parallelism and realism of evaluating metabolite chemistry.

Table 2-1: Photoreactive and photosensitive metabolites. Columns k, k^-, and k^+ are the pseudo-first-order rate constants for photodegradation, with lower and upper bounds. Bounds on k_p are not symmetrical because the parameter is lognormally distributed. C_0 is the measured initial concentration. SSR is the sum of squared residuals on the fitted rate curve. The column p is the probability that $C_{12}<C_{control}$ (t-test). - ΔC is the mean difference in concentration at 12 h relative to the control samples, and $t_{1/2}$ is the estimated half-life given the rate constant. Blank boxes indicate nonsignificant rate parameters. *indicates unreliable quantification (cystine). †indicates that while $C_{12} < C_{control}$, C_{12} and C_0 are not significantly different.

Metabolite	Matrix	*k*	*k*$^+$	*k*$^-$	*C*$_0$	*SSR*	*p*	*-ΔC*	*t*$_{1/2}$
		h^{-1}	h^{-1}	h^{-1}	nM	nM^2		nM	h
tryptophan	ASW	0.19	0.19	0.18	3.154	0.432	0.008	2.542	3.7
kynurenine	ASW	0.11	0.13	0.10	2.976	0.219	0.000	1.523	6.0
tryptamine	ASW	0.09	0.11	0.07	2.455	1.609	0.100	3.078	7.8
cystine*	ASW	0.04	0.05	0.04	6.074	1.623	0.094	1.159	15.5
asparagine	ASW	0.04	0.05	0.04	3.381	0.449	0.017	1.473	15.5
glutamine	ASW	0.04	0.05	0.03	4.523	1.535	0.000	0.871	16.0
S-(1,2-dicarboxyethyl) glutathione	ASW	0.03	0.03	0.03	1.527	0.112	0.037	0.199	23.2
histidine	ASW	0.03	0.03	0.03	4.709	0.181	0.082	0.526	24.0
chitotriose	ASW	0.02	0.02	0.02	1.119	0.035	0.010	0.118	30.9
malic acid†	ASW						0.081	3.033	
tryptophan	VSW	0.46	0.52	0.41	3.119	1.362	0.001	2.976	1.5
tryptamine	VSW	0.15	0.16	0.14	3.332	0.708	0.001	2.557	4.6
kynurenine	VSW	0.14	0.16	0.11	2.733	0.632	0.006	1.819	5.1
cystine*	VSW	0.02	0.03	0.02	4.831	0.349	0.000	0.705	28.8
amMP	VSW	0.01	0.01	0.01	5.286	0.898	0.087	1.479	63.3
histidine†	VSW						0.033	1.199	
arginine†	VSW						0.100	0.399	

Well-quantified analytes included proteinogenic amino acids, compatible solutes, nucleotides and their derivatives, acetylated saccharides, and B-vitamins or their metabolic products/precursors. We also measured a time-course of cystine, a dimer of cysteine; however, cystine is not present in our metabolite stocks except as an oxidative product of cysteine degradation. Therefore, the quantifications of both cysteinic species are relative.

We measured extinction spectra for five compounds (glutamate, glutamine, histidine, tryptophan, and kynurenine) because this information was either not accessible or because the existing references were limited in the waveband used, typically not extending into the visual range prominent in natural sunlight.[112,113] While glutamate was not included in the quantum yield calculations, it and the other metabolites' extinction spectra are included in the Supplemental Information in tabulated format.

While we will broadly discuss three groups of metabolites (photodegraded, photosensitive, and photostable), many resisted these classifications. Some exhibit different patterns in the presence of natural organic matter (ASW vs. VSW); some clearly reacted but with broad variance in control behavior (cysteine/cystine), and a few (glutamate, asparagine, and *gamma*-aminobutyric acid) seemed to be transiently photoproduced.

2.3.2 Photodegraded Metabolites

Irradiation decreased concentrations of seven metabolites consistently enough to fit non-zero rate parameters: kynurenine, tryptamine, tryptophan, *N,N',N''*-triacetylchitotriose (chitotriose), glutamine, cystine, and histidine in ASW; and kynurenine, tryptamine, tryptophan, and cystine in VSW. The latter four (plus histidine) have either aromatic groups or, in the case of cystine, a disulfide bridge that make them more prone to direct photochemistry than many of the other metabolites.[114–117] Glutamine and chitotriose, on the other hand, do not contain chromophores, and while no UV-visible spectrum is available for chitotriose, our spectrum for the aliphatic glutamine was the least absorbant among the five compounds we tested.

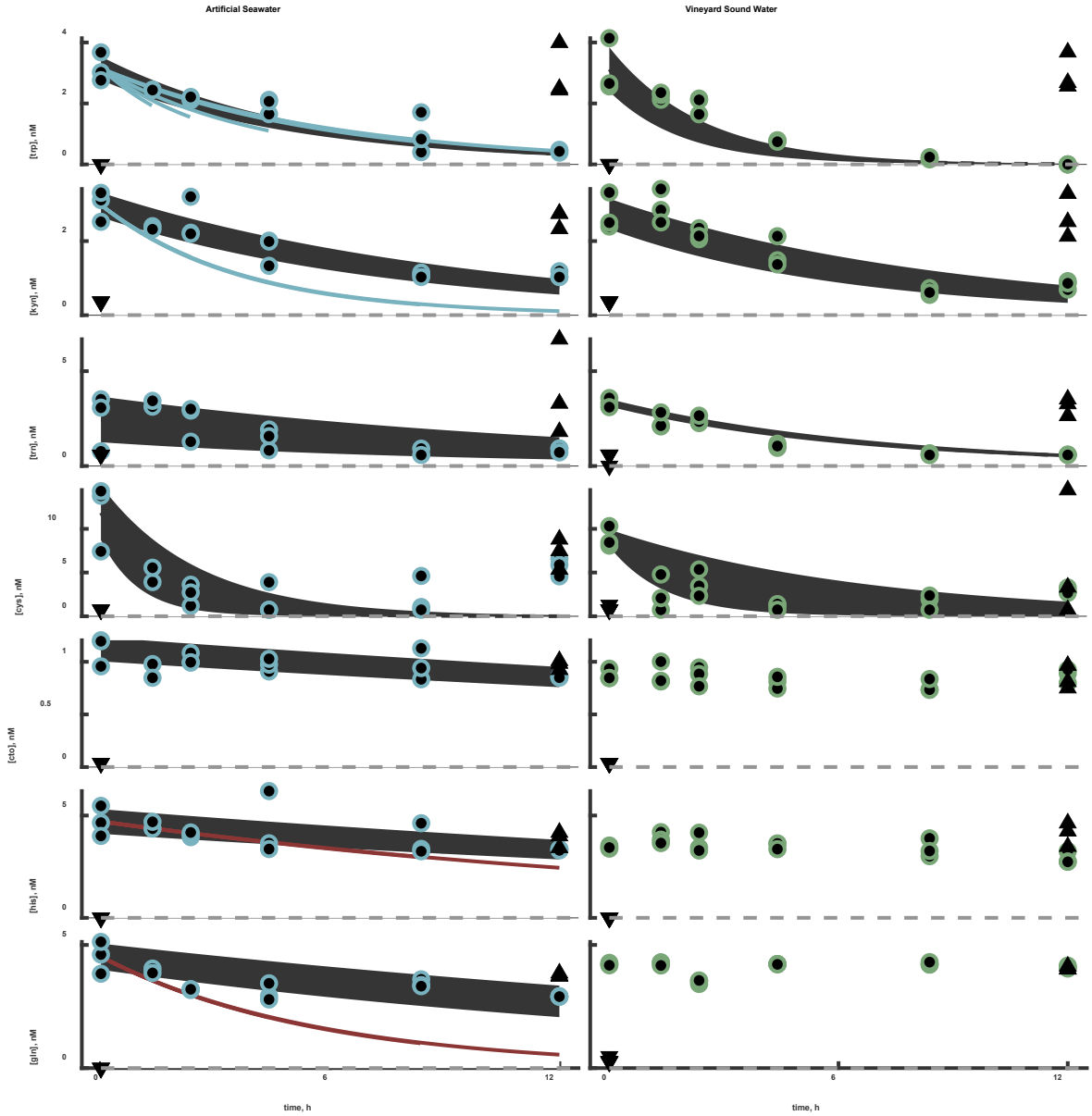

Figure 2-1: Metabolite time-courses and fitted rate estimates for tryptophan (trp), kynurenine (kyn), tryptamine (trn), cysteine (cys), N,N,N'''-triacetylchitobiose (cto), histidine (his), and glutamine (gln) in two different matrices: artificial seawater (ASW; left) and Vineyard Sound water (VSW; right). LOQ (grey dotted line) is 3.3 * the standard deviation of the standard curve's y-intercept, divided by the standard curve slope. Lower and upper bounds for the confidence intervals (grey areas) are derived from the 90% CI estimates on reaction coefficients: the upper bound uses the upper lower k_p CI value, whereas the lower bound is the opposite. Black dotted lines are the fitted pseudo-first-order decay curves; circles are the irradiated samples; triangles are the dark controls (upward triangles at 12 h) and matrix blanks (downward triangles at 0 h). Solid lines use the estimated AQY and photon fluence to estimate decay where possible (blue, AQY<1; red, AQY>1).

Tryptophan is well-studied enough that its photochemical decay was expected:[93,115,118] it can react with excited triplet-state chromophores in heterogeneous

organic matter or reactive oxygen species, in addition to undergoing direct photolysis under UV light.[93] Its half-life in artificial seawater was 4.4 hours and in natural seawater (VSW) only 1.5 hours. In the dark controls for both matrices, concentrations decreased by 4.5-5.7%, less than the error on the measurements. In an ocean surface layer, tryptophan would break down with a substantially (>2x) longer half-life on average based on the fact that the SunTest irradiance was similar (±29%) to simulated subtropical solar noon (in the 297-310 nm range), but the daily averaged irradiance for 40 °N in the same range is 33.6±4.2% of the value for solar noon.[48,119,120] Tryptophan's decay product *N*-formyl-kynurenine (NFK) can further photosensitize tryptophan degradation, but again, the concentrations of each compound were ≤ nM range, decreasing NFK's ability to form hydroxyl radical or perform much intermolecular chemistry in its excited state.

We did not measure NFK or other downstream products of tryptophan and kynurenine *sensu stricto*. The irradiated samples did include several chromatographic peaks with masses identical to various photoproducts (NFK, dioxyindolylalanine, aspartylurea, hydroxytryptophan, thiochrome) observed by others.[116,118] However, our targeted method relied on having standards for retention time comparison and only collected fragmentation spectra for analyte targets, precluding an exact diagnosis of which products appeared—as there were usually four or more isomers detected for each mass. We may have observed photodegradation products, but their exact identities and concentrations remain unknown.

Kynurenine degraded with half-lives of 5.1 h (VSW) and 7.3 h (ASW), which we thought initially to be underestimates. Whereas most of our measured metabolites are

not related to each other as direct photoproducts, kynurenine is formed when the tryptophan photoproduct NFK is deformylated. While we were concerned that the photoproduction of kynurenine from tryptophan may have influenced the concentration of kynurenine, this is unlikely in abiotic conditions. Kynurenine deformylation is common in cells through enzymatic reactions such as Photosystem II repair; therefore it is unlikely to dominate here, although it is worth considering the fate of NFK under sunlight in case this is incorrect.[121,122] The structure of NFK is not locked into the two-ring indole system but may be a better chromophore with a larger conjugated π-system (14 e^- vs. 10 e^-). It is not conformationally locked to a planar structure but has a resonance allowing for proton exchange between the formamido and ketone groups. Its absorbance spectrum shows a peak in the UVA range at 322 nm and shows peak fluorescence at 434 nm when excited at 325 nm. The shift between absorbance and fluorescence here corresponds to an energy change of 14.7 kJ mol^{-1}, which is within reason for an excited-state intramolecular proton transfer for a conformationally-favored hydrogen-bonded -RNH group donating to an enol tautomerization.[123,124] The kinetics of such a reaction and its consequences are beyond the scope of this paper; however, the analysis above as well as the evidence reviewed extensively elsewhere indicates that NFK and subsequent products (such as N-formylanthranilic acid) would dominate in our experimental regime.[118]

Tryptamine degraded in both types of seawater, although the control samples created a wide enough distribution that the dark control was not significantly different from the irradiated 12 h sample; one ASW sample in particular appeared to be quite depleted but its chromatographic signal was poor. The same was true for histidine in

both matrices, but its reactive potential under irradiation has been well-documented by others as a $^1O_2$-dependent reaction.[93,109,116,125]

Cystine, though only quantified relative to itself, can be fit with a first-order half-life (15.5 h in ASW; 28.8 h in VSW)–substantially slower than kynurenine or the indole derivatives, but still deserving of consideration considering its higher stability in oxic habitats and potential usefulness as a sulfur source.[126] Its absorption spectrum extends further than its monomer (cysteine) into the near-UV,[112] and its simplest analogue, dimethyldisulfide, can form both thiyl and perthiyl radicals through homolysis of the disulfide bridge.[127]

The metabolites (*N,N',N''*)-triacetylchitotriose (chitotriose), asparagine, S-(1,2-dicarboxyethyl)-glutathione, and glutamine passed the significance criteria for non-zero rate constants in ASW, and their half-lives ranged from 15.5-30.9 h. All are abiotically labile, although there is no clear photochemical pathway and their disappearance is slower (half-life > 1 d) than anticipated microbial diel cycling.[6,7,128] Whatever the reaction, both decay somewhat in the dark controls; the different kinetics between the irradiated samples and the controls in these two cases could be due to the difference in temperature (up to 7 °C) inside and outside the solar simulator. Using glutamine's initial and final concentrations and the Arrhenius equation, a reaction that could explain the difference between decay in the controls and the irradiated sample would have an activation energy of about 94 kJ mol^{-1}, which is high relative to some known hydrolytic reactions (generally <50 kJ/mol for esters and ethers, <35 for amides like glutamine).[129,130] The same calculation performed for chitotriose corresponds to a reaction with activation energy of 68 kJ mol^{-1}. We find it unlikely that hydrolysis was

responsible for the degradation we observed, even if no known photochemical pathway is yet known for these compounds (see section 2.3.5).

2.3.3 Quantum Yields

Apart from fitting a first-order reaction rate, we estimated apparent quantum yields (AQY) for the photolysis of four metabolites (histidine, glutamine, tryptophan, and kynurenine) in ASW. Tryptophan's AQY Φ_{trp}, using wavelengths of 280-699 nm, was 0.084, and kynurenine, for wavelengths 280-507 nm, was 2.38×10^{-4}. The result of applying these numbers to the concentration and irradiance data can be seen in Figure 2-1, where Φ_{trp} and Φ_{kyn} produce results close to the simple first-order fit.

Evaluating uncertainty in the case of these AQYs is not a matter of error propagation; the measurement errors were inherent to the fitting routine, but their accuracy can be evaluated through a chi-squared goodness-of-fit test ($\nu = 4$). Predicted concentrations using Φ_{trp} have a χ^2 of 0.90 ($p = 0.07$) versus the observations, while the same values for kynurenine are $\chi^2 = 86$ and $p = 1.0$. The fit of Φ_{trp}, then, is a somewhat-reasonable approximation that can reproduce observations when paired with the appropriate irradiance and concentration data, while Φ_{kyn} is certainly an overestimate. The latter was inevitable, as the pseudo-first order degradation scheme (both fitted by k_p and mechanistically implied in Equation 2-2) did not apply to kynurenine as neatly as to tryptophan (see the apparent asymptotic behavior of kynurenine as opposed to tryptophan in Figure 2-1). It could be possible that an as-yet undocumented deformylation reaction could have been producing kynurenine downstream from tryptophan, but the measurement variance of kynurenine was also

high enough (up to 18% in ASW and 20% in VSW) that an alternative mechanism is not necessary.

Histidine ($\Phi_{his} = 3.04$) and glutamine ($\Phi_{gln} = 165$) required unreasonably high AQY values to fit their degradative profiles (red lines in Figure 2-1), owing to their very low absorption. For these compounds, trying to fit AQYs makes apparent that other factors are likely at play, and the contrast between their low but significant k_p values (Table 2-1) and the mechanistically constrained fitting of quantum yields serves to illustrate this.

Our objective was a set of numbers relevant to the simplest distinction relevant for a biological entity: transformation to something other than the original molecule in fully oxygenated waters. In that context, fluorescence is irrelevant, and modes of ionization and intersystem crossing are only relevant insofar as they enable intra- or intermolecular transformation rather than relaxation. This may be why tryptophan and kynurenine quantum yields for non-radiative processes such as electron ejection or photoionization appear to be higher (0.012-0.28) than our measurements (10^{-2}-10^{-4}), although that may be partly due to the often much narrower and higher-energy wavelength ranges used to excite the molecules in other studies.[131,132] One study measured wavelength-dependent quantum yields for tryptophan photolysis, but used a single value of ε_λ across the entire spectrum, resulting in a $\Phi_{trp}(\lambda)$ that looks suspiciously like the molecule's extinction spectrum.[133] We feel comfortable dismissing this comparison to extant literature.

Having a way to calculate usable AQY values for future estimations of field-based decay rates was important for this work, but the limitations of our experiment will

allow in most cases only for the calculation of an apparent rate k_{p-obs}, which depends on incoming radiation over an integrated wavelength band. We have provided these (280-699 nm) for compounds with a significant first-order fit, using a modification of Zhu et al. (2019)'s equation in the Supplemental Information.[58]

$$k_{p-obs} = \ln\left(\frac{C_0}{C_{12}}\right)/E$$

Equation 2-3: Irradiance-normalized reaction rate coefficient.

In Equation 2-3 for irradiance-normalized reaction rate coefficient., C_0 and C_{12} are the starting and ending concentrations of a metabolite and E is the average integrated photon dose over the time-course (mol photons cm^{-2}). Multiplied by a waveband-integrated photon fluence, k_{p-obs} becomes another estimate for k_p (s^{-1}), with the benefit of being scalable for evaluating field data; something that may be done for future measurements. For those compounds with k_{p-obs} estimates in both ASW and VSW (tryptophan, tryptamine, kynurenine, and cystine), the two values can be seen as a range encompassing a natural coastal water type (VSW) and something closer to the open ocean (ASW) with respect to the implicit water characteristics of DOM qualities and the fractional absorption of the metabolite in question.

2.3.4 Photostable Metabolites and Non-Photolytic Decay

The strict criterion for rate fitting—where the 12 h control must be significantly different from the 12 h irradiated sample—obscured a much broader pattern. If we relaxed this criterion, we found non-zero first-order decay rate constants fitting 35 metabolites in at least one of the two matrices, with average half-lives of 20.1 h in ASW (n = 30) and 41.3 h in VSW (n = 20). Parameters for the complete set of nonlinear regressions can be

found in the Supplemental Information, but something else aside from direct photochemistry was eliminating metabolites from solution.

Replicate metabolite measurements often varied substantially, with a 15.8% mean relative standard deviation across measured metabolites. This relatively wide range disqualified many metabolites from consideration as photoreactive; some (such as adenosine, cysteine, chitobiose, and others) appear to undergo degradation, but the t-test between the final time points and the control samples cannot distinguish the effects of photodegradation from any other potential effects, such as hydrolysis or simple analytical variance. Still, there are reactions that may quickly degrade metabolites in the environment but are not captured mechanistically in this experiment. What follows is an assessment of those metabolites that do not clearly fit into the regime of photostability, but also do not show the exclusive photoreactive properties examined later.

The data for cysteine are not strictly quantitative (see *Measured Metabolites*), but still show a decay half-life of less than 2.5 h in both ASW and VSW. Cysteine degraded quickly but was classified as “putatively photostable” based on concurrent decay in the dark controls. Cysteine is notorious for reacting with hydrogen peroxide to form the sulfenic acid intermediate, then condensing with a second thiol residue (in a protein, another cysteinyl residue to form cystine). While photochemical H_2O_2 production would not occur in our dark controls, this is not necessary to explain the degradation in the controls *and* the irradiated samples: unlike the other ROS we dismissed earlier, H_2O_2 is naturally formed in surface ocean water at steady state concentrations sometimes exceeding 10^{-7} M, and with a half-life of up to 120 hours, especially in the absence of

metals or catalase enzymes.[134,135] In retrospect, H_2O_2 may have present in the matrix water at the beginning of the experiment—more than enough to react with the ~10^{-9} M concentrations of cysteine in the samples.[59] While solar simulation would allow for more H_2O_2 production, it was not necessary to transform the added cysteine.

We did not see the generation of cystine via dimerization, but this too is unsurprising, as bimolecular reactions between cysteine (~10^{-9} M) and its activated sulfenic acid counterpart (<< 10^{-9} M) would be slow even for a diffusion-limited reaction (k_D ~ 7.42x10^9 M^{-1} s^{-1}, based on the Stokes-Einstein relationship and adjusting for the viscosity of seawater at 35 ppt). For cysteine in surface seawater, the oxidative products of photochemistry almost certainly render it a different species within hours of its release into the dissolved phase.

2.3.5 Transient Photoproduction and Alternative Pathways

Both artificial and natural seawater were unable to sustain the production of any one metabolite over twelve hours. In VSW, glutathione, 4-aminobenzoic acid, and uridine had 12-hour concentrations greater than those at 0 h ($p < 0.1$) but indistinguishable from the controls, evincing a mechanism independent of irradiation such as the dissociation from colloids, hydrolytic production, or in the case of glutathione, possible reduction of its oxidized dimer, which, like cystine, can be an impurity in the stock. Glutathione also appears to have been produced in ASW, which fits the latter hypothesis.

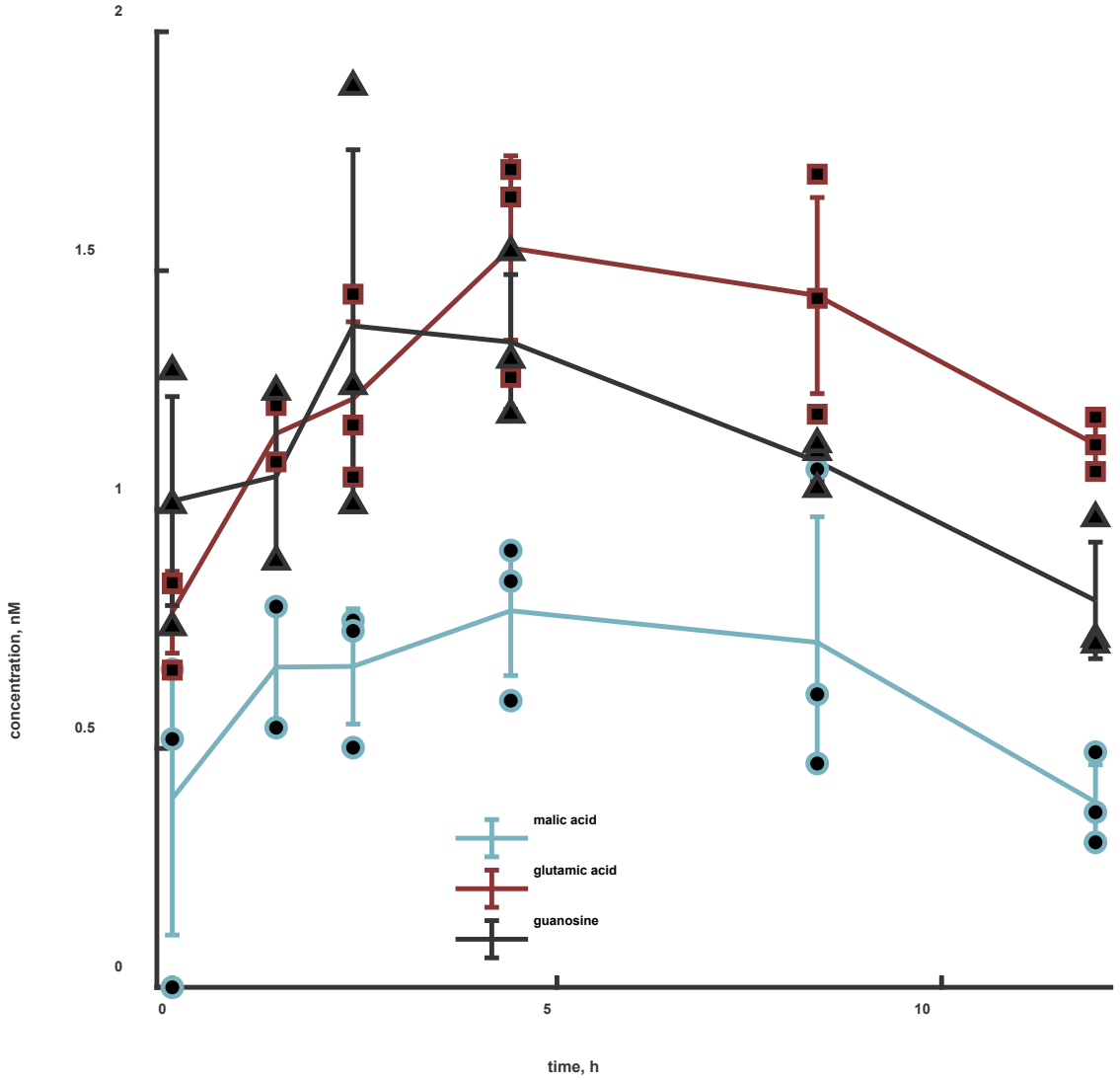

Figure 2-2: Transiently photoproduced metabolites. The time course for each is represented as lines connecting the means of triplicate measurements with ±σ as error bars. Individual data points are displayed on top with colors corresponding to the metabolites.

The major outlier among these marginally or incidentally photoproduced metabolites was glutamic acid, which increased in concentration in ASW by 2.4 nM. When examined more closely, glutamic acid was among a small group of compounds that smoothly increased over the first 2-4 hours of irradiation, and then fell again, as if at least two competing processes were operating within the 12-h experiment. These metabolites—glutamic acid, guanosine, and malic acid being the most prominent

examples (Figure 2-2)—shared no obvious chemical features. We entertained the idea that there was some bacterial interference, but the ~10^5 cells mL^{-1} we measured could not have measurably affected concentrations of these metabolites even if we treated them as spheres entirely comprising a relevant degradatory enzyme (see 2.6 Appendix: Supplemental Results and references therein).

There is a solid record of molecules that are both microbial metabolites/ substrates and products of organic matter photolysis. As of 1997, fourteen organic compounds entirely comprising small aldehydes, ketones, and carboxylic acids including the important substrate pyruvate were detected as products of photochemical processes applied to natural DOM.[57,92] These compounds, as well as subsequent discoveries such as the photooxidation of dimethylsulfide to dimethylsulfoxide still contained a motif of molecular simplicity: when heterogeneous natural organic matter is irradiated, larger molecules tend to break down into smaller, more aliphatic, and/or volatile forms, rather than the more reduced, heteroatom-rich, and highly bioavailable structures we tracked.[58,92]

The work of Tarr et al. (2001) seemed to contradict the general trends we observed—they irradiated organic matter in a solar simulator, and measured increases in some nitrogen-bearing compounds; specifically histidine, norvaline, serine, glutamic acid, alanine, asparagine, and citrulline.[59] Their paper is similar in many ways to this work; however, it dealt with a fundamentally different set of organic matter (humic and fulvic acids; bayou colloids) at much higher concentrations (~30 mg L^{-1}). Their use of colloidal (>1000 Da) matter also positions the work as more of a complement than an opposition, as the properties of this colloidal matter may allow for different kinds of

release than posited by the authors, such as the UV-inhibition of sorptive matrix such as micro- and nanogels.[47] Such a release would work like a reversal of the process by which enzymatic material concentrates in hydrophobic regions to create steep, multiphasic diffusion gradients.[136]

In addition to the possibility of consolidation in aggregates, it is worth considering singlet oxygen. One of the benefits of being able to work at field-relevant concentrations is that ROS like $^1O_2$ were thought to be of little influence at such low concentrations, but this may not have been the case. Producing a change of 100 pM (a general threshold for observability) over the course of the experiment for a compound like histidine (~5000 pM initial concentration) using steady-state $^1O_2$ in a solution with virtually no chromophoricity (Figure 2-6) requires a simple rate law:

$$\frac{dC_i}{dt} = k_{1O_2}\left[\ {}^1O_2\right]_{ss} C_i = k' C_i$$

The bimolecular reaction rate constant k_{1O_2} from Boreen et al. (2008) is 8.3 ± 1.1 x 10^7 M^{-1} s^{-1}, and treating its product and the steady-state $^1O_2$ as the pseudo-first order k', the time-scales and minimal concentration change above yield $k' = 4.6\ x\ 10^{-7}\ s^{-1}$. The dividend of k'/k_{1O_2} yields 5.7 ± 0.7 x 10^{-15} M $^1O_2$. This is entirely possible, as even oligotrophic seawater can have singlet oxygen in this range and the ~5 μM total DOC in these samples could have provided sufficient sensitization.[32,137] This deserves further investigation, because the other side of having analytical sensitivity is being able to see such minute changes. Consideration of organic colloids is also relevant here: if partitioning does occur rapidly enough to assembled DOC, the concentration of chromophores and metabolites may significantly elevate ROS formation and activity on

a local scale.[138] We did not anticipate this at the outset, but it at least serves to explain the unreasonable AQY value for histidine.

Our work was not trace-metal clean, and many metabolites (such as glutamic acid, cysteine, glutathione, and malic acid) are capable of forming transition metal-ion complexes with high stability coefficients and their own unique light absorption properties.[40,65,66] We do not know whether our derivatization method frees metabolites from such complexes, but it is likely case-dependent. For example, malic acid forms Fe(III) and Fe(II) complexes in seawater that are stable for at least a year, one of which is stronger at high pH and involves the same hydroxyl oxygen that our method depends on for derivatization.[40] Utilizing coefficients for two malic acid-iron(III) complexes ($\log_{10} K_1 = 12.66 \pm 0.33$ for Fe(mal) and $\log_{10} \beta_2 = 15.21 \pm 0.25$ for $Fe(mal)_2$) and assuming that malic acid concentrations represent free malic acid (4-6 nM), a free [Fe^{3+}] of 0.2 pM would be sufficient to bind half of the malic acid to iron. Seeing as surface ocean waters have ~0.03-3 nM of total iron and this is mostly (>99%) complexed, this specific example may be one of many metal-mediated linkages between metabolite photochemistry and metabolite cycling.[39,139,140] We would require further investigation to know whether this was at play in the SunTest, but offer it as a hypothesis. In searching for photoproduction, we may have stumbled across a dual mechanism where iron (or copper, or another transition metal) are freed during irradiation and complex with metabolites, reducing the metabolites' availability to our measurements.

In addition, the apparent production of some metabolites (glutamate, malic acid) may have been the result of reactions involving metal-mediated conversions of a single functional group unaided by a traditional chromophore (glutamine to glutamate by

deamination, aspartate to malic acid by deamidation). For glutamine, this could explain the observed degradation, as it did not absorb much light on its own and required an unreasonable AQY to meet the assumption of direct photolysis. For guanosine, its closest relative in the metabolite mix was xanthosine, but production of guanosine would require the addition of nitrogen to replace a resonance-stabilized ketone group with an amino group; in biological systems this is supplied by glutamine and mediated by guanosine monophosphate synthetase,[141] but the form of this enzyme is known from eukaryotes and biological interference has already been dismissed in this case (see 2.6.2).[142]

Guanosine presents issues for the assumption that it is a product of abiotic xanthosine conversion. Assuming the 1.3 μM total nitrogen in the ASW before the metabolite spike is entirely NH_3/NH_4^+, the solution pH (8.1) dictates that 100 nM would be available as the ammonia nucleophile at any given time. A bimolecular rate constant of 2.7 M^{-1} s^{-1} would be sufficient to produce the excess guanosine (~300 pM) present at 2 h; however, there are two problems. The first is that if such a reaction were occurring, it would depend on an excited complex or transient species such as the amino radical. The former is of unknown likelihood, and the amino radical is more likely to simply tear electrons off the aromatic group than it would be to initiate a substitution.[143] The second, more sound dismissal of the interconversion hypothesis is that xanthosine did not decrease in concentration over the first two time points: it increased in both VSW ($\Delta[xanthosine]_{2h} = 0.69 \pm 0.64\ nM$) and ASW ($\Delta[xanthosine]_{2h} = 0.41 \pm 1.5\ nM$), although with enough variance to yield t-test p-values of 0.54 and 0.08 respectively.

2.3.6 Photochemistry Opens the Microbial Loop

If tryptophan and kynurenine both undergo photolysis but are not part of a single chain of degradative reactions following familiar biochemical pathways, they—along with any of the other photoreactive metabolites studied here—deserve attention. Photochemistry does not necessarily transform metabolites in the same ways that cellular enzymes do, and the impact of this piece of physical chemistry on the ecology of the open ocean is hard to constrain with existing data. Microbial life in the upper ocean relies upon systems of nutritive interdependence down to the level of specific molecules.[94] The manufacture and exchange of those molecules may drive co-evolution, and we may now hypothesize that for some metabolites, becoming an auxotroph may be disadvantageous simply due to dissolved-phase chemistry. Evolving a high-affinity tryptophan transporter may not help a cell when, by the time tryptophan reaches a cell's membrane, it is instead N-formylanthranilic acid. One question underlying the reality of auxotrophic interdependence is why specific molecules are auxophores at all: what advantage does SAR11 gain by giving up the ability to make simple and frequently-consumed amino acids while retaining the capability to manufacture the less-used and more energy-intensive tryptophan?[95,96,144] Part of the answer may just be that tryptophan is present at lower ambient concentrations, but that reasoning does not usually include the idea that non-biological forces are at work in the ecosystem. To rely in whole or in part on exogenous sources of a substantial fraction of the metabolomic oeuvre, organisms must compete with the sun.

This ecological perspective requires more knowledge of the microbes that can import each metabolite, as well as those with specific requirements. There is data on

what auxophores have been verified experimentally or inferred genetically (see references in Johnson et al. (2020)),[94] but the complexity extends beyond those molecules typically thought of as “complete” metabolites, as different degradation and alteration products can be just as (if not more important) for some auxotrophs, as in the case of thiamine.[84,86]

If photochemistry controls the resources microbes have at their disposal, several complicating factors need to be acknowledged. First, this effect depends on the incoming light (wavelength/intensity),[145,146] contents of the water (screening/ sensitization),[93] depth, and the metabolite in question. We can only make the roughest estimations here: for aromatic and reduced-sulfur compounds, the reaction rates on sunny days in the upper water column may rival those at which microbes produce and consume these molecules. Expanding these estimates would involve likely applying the AQY values to both measurements of the metabolites themselves and solar spectra attenuated down the water column, and even this requires caution, as the AQY values here were estimated in artificial seawater without the presence of natural organic matter. Only Φ_{trp} had a reasonably explanatory fit, and histidine demonstrated the possibility that even picomolar changes can be attributed to reactive oxygen species.

Several chemical suspects already show interesting dynamics in the dissolved phase: in the Sargasso Sea’s euphotic zone, tryptophan increases in the day and decreases at night, while riboflavin (known for its photochemical decay to lumichrome) does the opposite.[6] Even then, at the shallowest points (<50 m) tryptophan concentrations tend to stay close to zero. Correlations and anticorrelations with sunlight occur frequently, although this should be unsurprising in a microbial environment

dominated by diel periodicity.[7,128] Neither the reactions mediated by cellular enzymes nor physical factors operate in isolation. Each chemical is multifaceted, not just in its interactions with biological agents, but in how the aquatic environment transports and transforms it. Measuring dissolved metabolites—and their various sources and sinks—is essential for considering the fullness of chemical ecology in the ocean.

2.4 Conclusion

The compounds we evaluated were intended to provide an overview of photochemical potential. The derivatization and LC-MS pipeline we used is not the only way to measure many of the metabolites shown, and there are some (such as riboflavin mentioned above) for which better methods exist. However, metabolites are so diverse in their structures and sizes that just as no one reaction mechanism applies to all of them *in situ*, no way of quantifying them captures every moiety. Of the 57 metabolites we quantified, six (5%) met our criteria for measurable photodegradation in seawater, and of those only three might be the object of competition between microbial uptake and photodegradation in the euphotic zone. However, if we imagine that this number scales with any accuracy to the collection of “tens of thousands” of distinct molecules that ocean microbes can release, it is not unreasonable to imagine the spiraling diversification brought on by abiotic reactions contributing to the “hundreds of thousands of distinct organic features in marine DOC” reviewed in Moran et al. (2022).[45,116]

Importantly, when we looked for direct photolysis, we found many patterns that were not simple, but indicative of interacting chemical networks, both inorganic and organic, but not biological. This idea, too, pushes up against the limits of how we define “metabolite,” as it may well be the case that many of the dissolved organics we find,

even if they are biogenic in their origin, are not what was originally manufactured: to the question of “who makes and eats which chemicals?” the answer, sometimes, is light.

Acknowledgments

The contributions of several individuals were needed to make this experiment possible: Gretchen Swarr for preparing more than one hundred individual metabolite stocks; Chloe Smith, Katie Halloran, and Dr. Krista Longnecker for their assistance in using the flow cytometer; Dr. Anna Walsh in advising proper use of the Suntest; and Dr. Yuting Zhu for her willingness to discuss the experimental setup. The colors used in the figures here came from the cover of the Friday Pilots Club album *Nowhere* (2024). The authors thank Danielle Haas Freeman (MIT-WHOI) for maintaining the solar simulator and providing processed radiometry data for the irradiation experiments.

2.5 Appendix A: Supplemental Methods

2.5.1 Flow Cytometry

We added 20 µL of paraformaldehyde (10% w/v) to each sample taken for flow cytometry and let them sit in a dark drawer for 10-20 min. We froze the fixed samples (-80 ºC) until analysis. On the day of analysis, we plated 200 µL of each fixed sample along with three aliquots of fresh MQ in a 96-well plate. We stained each well using SYBR Green I, working in low light and covering the plate with foil for 30 min afterwards. We measured cell-like objects with a Guava EasyCyte HT with high-gain settings and monitoring forward scatter and green fluorescent channels.

Using the CytoFlow package in Python,[147] we set a gate to count "cell-like" objects as those outside the main range of false positives in the MQ replicates, then subtracted the average remaining "noise," or the non-excluded hits in the MQ.

2.5.2 Benzoyl Chloride Derivatization and Workup

We prepared a standard curve using dilutions of the 2º and 3º stocks in ASW, ranging from 0 pg mL^{-1} to 1500 pg mL^{-1} with the lowest nonzero standard (70 pg mL^{-1}) prepared in triplicate. We also created a stable isotope-labeled internal standard (SIL-IS) by benzoylating a 1:5 dilution of 2º stock (20 ng mL^{-1}) with $^{13}C_6$-BzCl. This resulted in a mixture of SIL-IS corresponding exactly to our analytes.

We derivatized each sample and standard through benzoylation, modifying reagent proportions from Widner et al.'s original method for our sample volumes.[17] Briefly: we basified the samples with 97.5 µL of 8 M NaOH, then added 650 µL of 5% (v/v) benzoyl chloride (BzCl) in acetone and mixed the solution by inversion for five minutes. We quenched the reaction by adding 48.8 µL concentrated H_3PO_4 and then

added 100 µL of SIL-IS solution. We stored samples at 4 ºC until workup (<12 h). During sample workup, we dried acetone from the samples using a Vacufuge until they lost the mass of acetone added (0.488 ± 0.024 g).

Next, we concentrated analytes using solid-phase extraction by 1 g BondElut PPL cartridges. A Vacufuge dried the resulting methanolic extract completely, and we partially redissolved the analytes in 100 µL 5% (v/v) acetonitrile in MQ. The liquid contained benzoic acid precipitate, so we centrifuged it at 20,000 x g for 15 minutes before transferring the supernatant to chromatography vials and adding 5 µL acetonitrile to prevent additional precipitation.

2.5.3 UHPLC-Orbitrap MS Conditions

Using an autosampler set to 4 °C, we injected samples (5 µL per ion mode) onto a reversed phase Waters Acquity HSS T3 column (2.1 × 100 mm, 1.8 µm) equipped with a Vanguard pre-column (Waters) held at 40 °C. We used mobile phases (A) 0.1% (v/v) formic acid in water and (B) 0.1% (v/v) formic acid in acetonitrile. The gradient, at 0.5 mL min^{-1}, was: 0-0.5 min (1% B), 2 min (10% B), 2-5 min (10% B), 7 min (25% B), 7-9 min (25% B), 12.5 min (50% B), 13 min (95% B), 13-14.5 min (95% B) and re-equilibration with 1% B (total run time = 16 min). Other instrument parameters were: ESI voltages = 3600 V (positive) and 2600 V (negative); source gases = 55 (sheath), 20 (auxillary), and 1 (sweep); capillary temperature = 350 °C; vaporizer temperature = 400 °C. We collected MS data from 170-1000 m/z at resolution 60,000 fwhm (at m/z 200), automatic gain control (AGC) at 4e5, and max injection time 50 msec.

Upon detection of a target compound's mass, we isolated the parent ion in the quadrupole at a width of 1 m/z, and collected MS/MS data at resolution 7,500 fwhm,

AGC at 5e4, and max injection time 22 msec using higher energy collisional dissociation (HCD) with 35% collision energy and intensity threshold at 2e4.

2.5.4 Integration of Light Over a Cylinder

In general, placing the reaction vessels pronate on the aluminum plate probably kept them cooler due to higher surface contact, but meant that each cross-sectional profile absorbed a slightly different amount of radiation. We solved this problem geometrically.

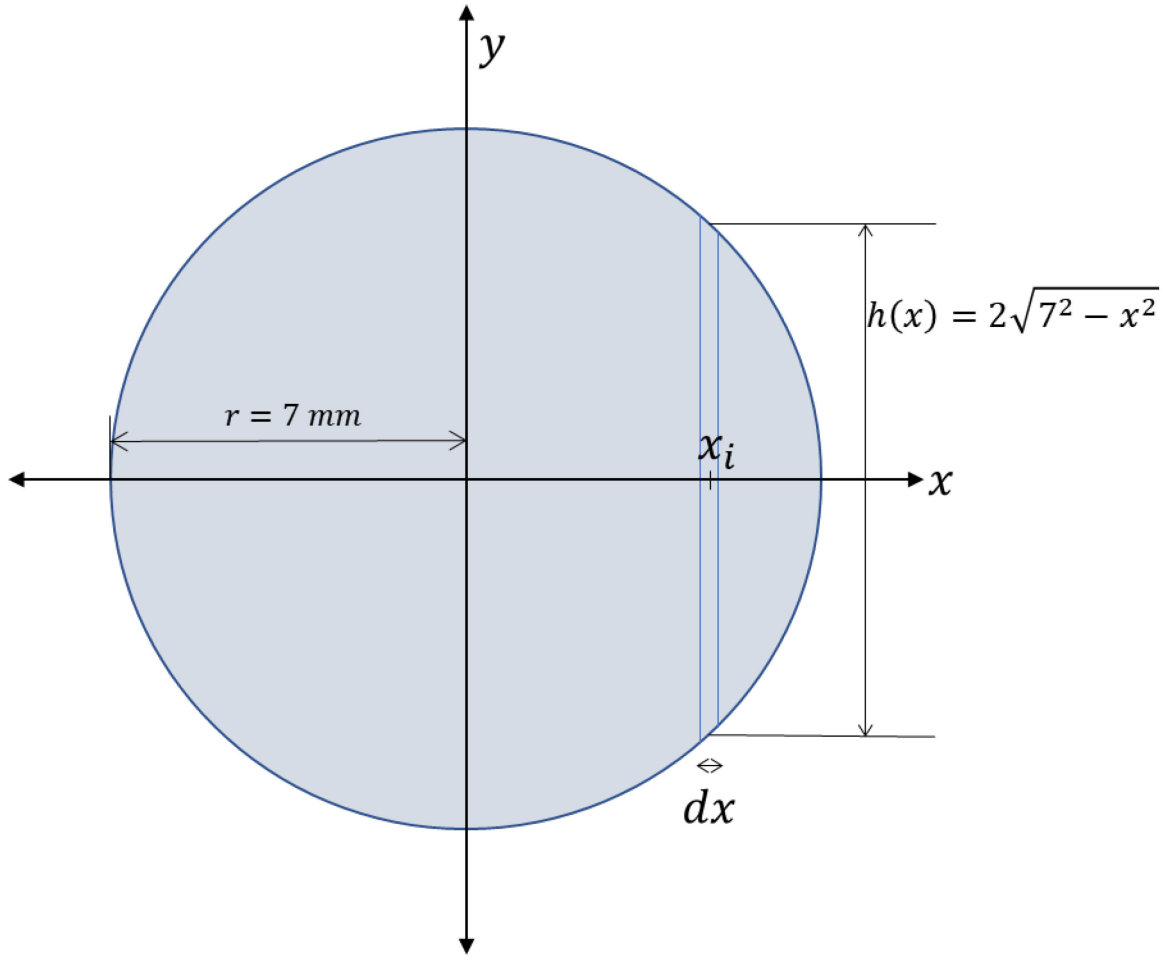

Figure 2-3: Diagram of circular tube cross-section with calculated pathlength h(x).

Using symmetry along x and y in Figure 2-3 and given the Napierian absorbance coefficients α_λ for the water, the radius r of the tube (7 mm), the incoming irradiance I_λ, we get the following.

$$W_\lambda = \frac{4}{\pi r^2}\int_0^r 1 - 10^{-2\alpha_\lambda\sqrt{r^2-x^2}}dx$$

Equation 2-1: Absorption of light over a prone cylinder

Where the quantity $4/\pi r^2$ comes from a factor of 2 (integrating from 0 to r and not -r to r) and from converting an areal (cm^{-2}) irradiance over the rectangular top view of the vials to a volumetric photon absorbance by a factor of $A/V = 2lr/\pi r^2 l = 2/\pi r$.

2.6 Appendix B: Supplemental Results

2.6.1 Description of Additional Files

The datasets involved in this work were large, and unfit for display in their entirety. In addition to the repositories for processing code and smaller metadata (https://github.com/germo006/metabolitephotochem) and the raw metabolite data (www.ebi.ac.uk/metabolights/MTBLS7513), we have provided supplements as a spreadsheet. Sheet 1 is the five compound-specific absorption datasets (histidine, glutamate, glutamine, tryptophan, and kynurenine) and the sequence of steps which combined them into molar extinction coefficients. Sheet 2 contains all metabolite measurements used in the final analysis, alongside useful metadata such as quantification bounds, ion mode, and an InChI key for each analyte containing the highest level of identification possible according to Koistinen et al. (2023) (single structural isomer but no implied stereochemistry).[88] Sheet 3 contains the radiometry data cited in the main text alongside a comparison to the SMARTS simulation of downwelling irradiance in the Atlantic Ocean on July 11.[99,148]

What follows is an additional series of figures and tables that were not included in the main text, and discussion of their relevance or why they were excluded from the main text.

2.6.2 Metabolite Measurements

While the Supplementary Information contains more workable data, I have included the following table of all measurements from this experiment.

Table 2-2: Metabolite measurements for Chapter 2. This sheet contains "raw preprocessed data": In other words, the concentrations have been calculated, but I have not removed metabolites that I consider suspect. All values in picomol L^{-1}, and sample names correspond to their matrix (ASW/VSW), type (sample/control/blank), and ordered time-point (t0, t1, etc.). Each group of three with the same identifiers represent a technical triplicate set. LOQ denotes the limit of quantification and the Max Std. is the highest concentration in the standard curve. Abbreviations: HMP (4-amino-5-hydroxymethyl-2-methylpyrimidine); amMP (4-amino-5-aminomethyl-2-methylpyrimidine)

Trivial Name	LOQ (pM)	Max Std. (pM)	ASW_t0_1_sample	ASW_t0_2_sample	ASW_t0_3_sample	VSW_t0_1_blank	VSW_t0_2_blank
xanthosine	1.2	4683.7	1694.8	3075.7	1932.9	0.0	0.0
valine	2.1	12804.1	7934.9	10854.3	5646.6	0.0	0.0
uridine	1.2	6142.5	4349.1	4593.2	3466.1	0.0	0.0
tryptophan	0.9	7344.7	3023.6	3677.5	2761.5	0.0	0.0
tryptamine	2.3	9362.1	773.1	3517.5	3075.8		582.4
thymidine	2.2	6192.5	1777.0	1750.0	4256.0	719.7	0.0
threonine	1.8	12592.3	4731.3	6620.6	3267.5	0.0	0.0
taurine	2.0	11985.6	11198.5	12176.5	6224.4	1759.8	3107.8
glycerol 3-phosphate	0.5	4049.5	2074.8	1873.3	1629.5	2225.2	3814.7
serine	3.8	14273.5	8861.7	2671.5	1581.8	0.0	0.0
sarcosine	2.2	16836.9	6903.2	9479.1	5725.6	458.6	524.9
putrescine	2.2	9312.7	5325.3	5050.9	3436.5	2025.4	2234.2
proline	1.1	13028.8	7980.9	7258.7	6416.3	0.0	349.7
phenylalanine	0.5	9080.5	3189.9	3912.5	3296.3	0.0	68.7
pantothenic acid	0.4	6295.4	3139.9	3013.7	2751.5	68.8	121.5
ornithine	2.0	8879.9	2078.2	2798.9	2244.4	0.0	0.0
muramic acid	1.0	5970.6	3366.1	3963.9	2748.4	0.0	220.3
malic acid	2.8	11186.5	3875.3	4963.5	0.0	0.0	0.0
leucine	3.7	11435.5	3722.7	4282.1	2635.4	0.0	0.0
kynurenine	2.7	7204.3	3106.7	3301.7	2520.1	361.9	361.9
isoleucine	2.7	11435.5	3588.7	4004.5	2519.7	0.0	0.0
isethionate	1.7	10127.6	4017.2	3210.9	3666.1	686.7	1039.1
inosine	0.8	5592.2	5578.7	7728.7	2489.3	0.0	0.0
indole-3-acetic acid	1.2	8562.6	3600.2	4745.6	3028.6	258.8	258.8
homoserine	2.3	12592.3	7134.3	8218.8	4128.2	470.1	696.6
homoserine betaine	1.2	9316.8	4236.5	4576.4	3510.9	544.0	718.8
histidine	1.4	9668.1	4652.6	5471.7	4002.3	0.0	0.0
guanosine	1.1	5296.6	3565.4	4553.4	2662.4	0.0	0.0
glyphosate	1.0	8872.1	4340.7	4660.7	3597.5	220.5	220.5
glutathione	0.7	4881.2	4936.6	6000.4	2783.0	0.0	0.0
glutamine	1.3	10264.1	4612.4	5124.9	3832.2	268.4	473.9
glutamic acid	1.7	10195.1	5740.8	5754.3	4512.5	0.0	1194.3
glucose 6-phosphate	1.4	4932.6	1738.4	1855.8	241.7	514.6	613.6
glucosamine-6-phosphate	0.5	5790.4	2812.3	2986.5	1935.7	107.6	107.6
ectoine	2.2	10551.5	3814.8	4806.8	4278.2	493.6	536.9
cysteine	3.0	12380.3	13780.5	14312.3	7415.8	740.9	740.9
cystine	1.0	12380.3	6171.0	6703.9	5346.5	165.9	182.5
cysteate	1.6	8867.9	7660.6	6529.2	6458.7	513.0	955.9
citrulline	1.5	8562.1	3764.8	5513.5	3116.6	0.0	0.0
cilatine	1.5	11994.2	5905.0	4628.4	3585.1	514.8	667.2
chitotriose	0.2	2391.2	1204.4	1195.0	956.6	36.9	36.9
chitobiose	1.0	3534.4	1671.4	1967.5	2259.5	264.1	264.1
aspartate	2.4	11269.7	3029.7	3282.7	2926.5	0.0	0.0
asparagine	2.6	11353.3	3707.3	3928.9	2507.5	0.0	337.8
arginine	1.8	8610.8	2997.2	2677.7	2636.7	0.0	0.0
amMP*	1.8	10935.3	5704.4	6172.6	5224.8	0.0	0.0
alanine	3.3	16836.9	7498.2	6880.2	4950.0	0.0	0.0
adenosine	1.0	5612.9	2332.0	2881.6	1736.8	0.0	0.0
(1,2-dicarboxyethyl) glutathione	0.5	3542.7	1536.9	1756.3	1286.7	97.0	97.0
N-acetyl-muramic acid	1.3	7929.4	3917.1	4692.7	3920.9	0.0	295.6
HMP	2.4	10779.0	3421.2	5694.5	4377.3	1324.5	1371.6
gamma-aminobutryic acid	1.1	14546.2	6873.2	7598.4	6606.2	0.0	230.9
2,3-dihydroxypropane-1-sulfonate	2.0	9605.5	3712.3	4405.3	2895.3	2503.8	3965.6
uridine 5′ -monophosphate	0.4	4074.4	1888.9	1826.2	1465.0	137.0	129.4
4-aminobenzoic acid	1.5	10937.7	5918.3	6456.2	4552.5	0.0	0.0
adesnosine 3′ -monophosphate	0.4	4320.0	2011.8	2021.6	2033.4	94.6	94.6
2′deoxyguanosine	0.7	5612.9	2093.6	2413.1	2229.5	167.6	167.6

Trivial Name	LOQ (pM)	Max Std. (pM)	VSW_t0_3_blank	VSW_t0_1_sample	VSW_t0_2_sample	VSW_t0_3_sample	ASW_t1_1_sample	ASW_t1_3_sample	VSW_t1_1_sample	VSW_t1_2_sample	VSW_t1_3_sample	ASW_t2_1_sample
xanthosine	1.2	4683.7	0.0	1130.8	1916.3	1284.8	2696.0	1986.0	2330.1	1924.3	2812.0	1916.7
valine	2.1	12804.1	0.0	7149.3	5751.3	6787.1	4289.1	6508.6	5758.3	5899.8	4073.5	6467.9
uridine	1.2	6142.5	0.0	2546.0	2625.5	2298.2	1410.9	2186.3	1874.9	1672.1	1577.3	2864.1
tryptophan	0.9	7344.7	0.0	4141.5	2559.3	2656.1	2452.3	2439.7	2120.4	2277.1	2353.9	2099.6
tryptamine	2.3	9362.1	582.4	3312.0	3582.5	3102.4	3128.3	3436.0	2085.9	2124.4	2825.9	1281.9
thymidine	2.2	6192.5	0.0	3264.6	3289.4	1217.5	4644.1	1650.4	1360.2	1582.3	1415.9	1596.8
threonine	1.8	12592.3	0.0	3888.6	3847.6	4790.8	5018.5	4781.5	3600.0	4613.4	4087.5	4805.3
taurine	2.0	11985.6	1643.2	11616.8	10972.0	11301.9	4985.1	9557.7	8210.8	11131.8	5891.8	9229.2
glycerol 3-phosphate	0.5	4049.5	1824.0	3394.8	4371.7	3590.9	1725.0	1706.2	3390.2	3645.1	3643.7	1633.9
serine	3.8	14273.5	0.0	4324.0	1641.9	1258.9	1868.3	7000.5	5806.2	3638.2	4500.7	5437.9
sarcosine	2.2	16836.9	441.6	6324.1	5688.9	8786.5	5946.8	5803.7	6239.9	9248.6	5732.4	6052.4
putrescine	2.2	9312.7	1259.9	6650.4	7090.2	6008.4	5326.9	6741.9	5255.7	4463.0	6690.0	10501.0
proline	1.1	13028.8	0.0	5722.2	5513.4	5373.8	6987.3	6639.9	5514.8	6726.5	6443.0	6096.9
phenylalanine	0.5	9080.5	0.0	3837.0	3924.1	2737.0	3640.2	3589.4	3078.2	3424.2	3318.1	4006.0
pantothenic acid	0.4	6295.4	96.3	2846.6	2906.9	2174.7	2780.0	2955.1	3043.7	2999.6	2964.4	2136.2
ornithine	2.0	8879.9	0.0	1706.6	1652.4	1761.5	2532.6	1683.2	2393.8	1835.7	2490.8	1686.7
muramic acid	1.0	5970.6	0.0	2590.0	2952.0	2865.6	2478.3	2241.4	2589.1	2318.1	2323.4	2402.5
malic acid	2.8	11186.5	0.0	1551.3	618.9	641.3	5942.1	4053.0	1140.2	1829.2	2324.2	3741.3
leucine	3.7	11435.5	0.0	3302.0	3283.2	3255.6	4410.6	3339.5	2683.8	3266.7	4255.5	3279.4
kynurenine	2.7	7204.3	361.9	2391.2	2497.3	3311.1	2402.0	2319.5	2838.5	3405.4	2503.6	3196.9
isoleucine	2.7	11435.5	0.0	3061.5	3028.8	3012.4	4150.1	3166.1	2572.5	3078.8	3964.2	3103.4
isethionate	1.7	10127.6	774.2	4032.9	4441.4	4196.0	4335.6	3905.6	4897.8	4634.6	5447.3	3096.6
inosine	0.8	5592.2	0.0	4089.9	5021.5	3881.8	2604.2	6216.9	4691.6	6673.9	3735.8	6461.3
indole-3-acetic acid	1.2	8562.6	258.8	2974.6	3261.3	3100.3	3195.8	3250.7	3387.5	2994.1	3268.4	3253.9
homoserine	2.3	12592.3	514.4	5198.4	6338.2	5125.1	4873.6	4847.7	3527.9	5114.6	5510.1	4435.1
homoserine betaine	1.2	9316.8	432.5	4529.4	4521.6	4128.6	3934.0	3707.6	4735.4	4913.0	4866.0	3586.4
histidine	1.4	9668.1	0.0	3533.5	3381.5	3434.2	4359.7	4692.1	4186.9	3821.7	3653.0	3942.3
guanosine	1.1	5296.6	0.0	2073.1	3047.1	2289.1	3148.1	4403.5	3676.3	4188.0	3662.7	3564.0
glyphosate	1.0	8872.1	220.5	3831.1	3788.1	3484.7	3904.1	4259.9	3813.6	3992.8	3836.1	3796.6
glutathione	0.7	4881.2	0.0	3661.4	3363.2	3626.5	6715.9	11265.6	3508.8	5580.7	3132.8	10729.8
glutamine	1.3	10264.1	264.4	4272.6	4206.8	4174.8	4040.8	3863.1	4281.6	4294.0	4167.7	3169.4
glutamic acid	1.7	10195.1	417.2	5877.6	6623.9	5070.3	8277.4	7474.9	6159.8	5369.7	5372.6	7999.4
glucose 6-phosphate	1.4	4932.6	308.8	1749.2		1928.9	2274.1	1949.3	2145.3	1899.9	3081.6	1929.4
glucosamine-6-phosphate	0.5	5790.4	107.6	2003.6	2332.4	2113.7	1746.0	1425.2	1298.5	1498.5	1501.9	1862.6
ectoine	2.2	10551.5	0.0	3921.3	5252.4	5033.6	4817.0	3156.1	1711.3	2378.3	1853.1	3138.5
cysteine	3.0	12380.3	740.9	8077.4	8445.2	10311.9	3912.1	5551.5	740.9	4775.1	2074.3	3609.9
cystine	1.0	12380.3	175.2	4919.4	4861.0	4711.5	5281.5	5156.2	4814.6	4586.9	4782.6	4981.4
cysteate	1.6	8867.9	437.3	5799.4	5987.8	5582.5	3810.1	5750.2	8116.7	6043.6	4183.3	5494.2
citrulline	1.5	8562.1	0.0	3029.0	3387.7	3554.0	3490.0	3643.3	3314.3	3371.5	3350.8	3259.8
ciliatine	1.5	11994.2	503.3	5249.9	3709.1	3712.9	3821.7	4894.1	5319.5	5128.4	5129.8	4311.7
chitotriose	0.2	2391.2	36.9	934.3	843.8	847.0	978.4	847.9	813.0	820.0	1001.5	1084.0
chitobiose	1.0	3534.4	264.1	1466.4	1890.2	1681.1	661.8	1524.2	951.3	1604.4	963.4	508.0
aspartate	2.4	11269.7	0.0	2390.7	2441.1	2419.9	3182.2	2770.2	3678.6	2610.2	2640.0	2875.3
asparagine	2.6	11353.3	0.0	3260.1	3156.2	3176.5	3769.6	2835.4	2423.7	3311.8	3244.6	2280.5
arginine	1.8	8610.8	0.0	1932.1	2504.8	2471.0	3433.7	2762.0	2742.2	2414.7	3458.6	2483.5
amMP*	1.8	10935.3	0.0	5175.8	5237.3	5444.8	4578.8	4559.4	5129.5	5103.1	5184.2	6559.7
alanine	3.3	16836.9	0.0	6232.9	6947.0	9333.8	7623.3	6968.7	5543.3	6849.6	5908.5	5209.7
adenosine	1.0	5612.9	0.0	2119.3	2075.2	1863.6	2051.8	1906.3	1496.6	1688.1	1798.3	2079.6
(1,2-dicarboxyethyl) glutathione	0.5	3542.7	97.0	1316.6	1145.5	1273.8	1353.5	1194.3	1140.4	1336.1	1334.8	1266.7
N-acetyl-muramic acid	1.3	7929.4	308.9	3381.9	6636.5	3758.2	2162.4	2428.3	4151.3	3227.1	3012.2	2517.8
HMP	2.4	10779.0	595.2	3136.1	3967.2	4527.9	3586.8	3106.3	4573.6	3180.0	3268.0	3378.0
gamma-aminobutryic acid	1.1	14546.2	0.0	6671.4	7485.8	7162.8	6016.5	5918.3	6989.2	5929.7	7010.8	6410.5
2,3-dihydroxypropane-1-sulfonate	2.0	9605.5	2204.1	5908.1	5312.7	5223.5	4418.5	2932.4	6070.4	6729.3	7997.4	2900.1
uridine 5’ -monophosphate	0.4	4074.4	129.4	1404.1	1350.7	1162.0	2022.6	1806.3	1191.1	1162.9	1528.5	1924.7
4-aminobenzoic acid	1.5	10937.7	0.0	5473.9	4634.6	4745.3	5052.3	6902.1	5331.7	4894.5	4722.0	5906.9
adesnosine 3’ -monophosphate	0.4	4320.0	94.6	1946.3	2023.6	1572.2	2079.4	1966.9	2107.3	1846.3	1992.1	2045.3
2'deoxyguanosine	0.7	5612.9	167.6	1935.4	1626.0	1662.6	2368.7	2460.2	2512.4	2315.9	1769.0	1838.7

Trivial Name	LOQ (pM)	Max Std. (pM)	ASW_t2_2_sample	ASW_t2_3_sample	VSW_t2_1_sample	VSW_t2_2_sample	VSW_t2_3_sample	ASW_t3_1_sample	ASW_t3_2_sample	ASW_t3_3_sample	VSW_t3_1_sample	VSW_t3_2_sample
xanthosine	1.2	4683.7	2523.3	3503.6	2032.4	1999.0	2398.3	2911.6	2326.9	2680.0	2513.5	1915.3
valine	2.1	12804.1	5841.5	4188.1	8273.1	6007.9	5871.8	4659.8	7044.6	8022.3	6818.9	5729.3
uridine	1.2	6142.5	3013.9	2223.4	2393.9	2856.7	2568.9	2270.0	3148.2	2975.9	2316.2	2567.4
tryptophan	0.9	7344.7	2128.0	2212.5	2160.0	1644.3	2117.3	2118.1	1649.8	2067.7	780.0	792.2
tryptamine	2.3	9362.1	2922.7	3002.9	2261.4	2342.6	2653.7	1924.1	825.7	1573.1	957.0	1177.4
thymidine	2.2	6192.5	1488.0	2746.6	1253.3	2195.2	1285.4	3204.8	1830.7	1515.7	1310.4	1243.7
threonine	1.8	12592.3	4911.5	3399.5	5100.8	4138.0	3540.8	3363.0	4052.5	6835.0	4816.1	4640.1
taurine	2.0	11985.6	8824.0	4883.0	11259.2	11434.6	9956.7	5001.0	9391.9	6852.7	11432.5	11092.7
glycerol 3-phosphate	0.5	4049.5	1513.4	1527.7	3730.2	3518.7	3982.8	1962.2	2022.4	2250.6	2941.6	3505.1
serine	3.8	14273.5	5087.0	6101.7	5425.8	4778.2	4996.8	5984.3	6402.4	24540.8	2050.1	3879.7
sarcosine	2.2	16836.9	9195.8	6307.5	5933.8	6028.2	5720.6	5767.8	5848.9	5636.2	6107.4	7501.7
putrescine	2.2	9312.7	5942.6	6498.7	7705.6	6841.7	4198.9	7325.4	10098.0	5375.0	4560.4	3739.8
proline	1.1	13028.8	6265.3	6547.1	5732.9	5835.0	5895.5	6512.6	6173.3	7971.0	6225.3	6206.5
phenylalanine	0.5	9080.5	2411.4	3764.4	3724.9	2753.0	3601.3	3615.3	3569.8	3500.0	3229.8	3225.5
pantothenic acid	0.4	6295.4	2482.6	2821.4	2832.4	2824.6	1763.9	2911.2	2631.0	2582.6	2774.8	2860.0
ornithine	2.0	8879.9	1830.9	2706.1	1797.8	1736.2	1873.3	2916.6	1816.9	3963.8	1711.5	1701.3
muramic acid	1.0	5970.6	2580.8	2427.2	2251.9	2564.8	2369.6	2382.1	2347.4	2232.2	2241.5	1980.8
malic acid	2.8	11186.5	5723.6	5563.2	2838.8	2708.6	0.0	6339.5	6818.3	4475.0	3391.2	3647.2
leucine	3.7	11435.5	3244.5	4518.3	3298.0	3262.5	3089.7	4680.0	3191.1	2777.8	3192.8	3015.8
kynurenine	2.7	7204.3	2225.2	2196.5	2345.8	2049.5	2137.8	2011.6	1332.6	1987.7	1482.1	2130.7
isoleucine	2.7	11435.5	2966.5	4335.3	3100.7	3086.7	2641.6	4477.4	3093.7	2833.9	2993.6	2414.8
isethionate	1.7	10127.6	3227.1	4359.6	3554.8	4098.0	4161.0	4400.6	3112.7	2935.7	3923.4	4459.4
inosine	0.8	5592.2	8279.8	4537.1	6068.9	7524.4	6160.4	3879.4	5329.3	7233.7	11770.1	9922.0
indole-3-acetic acid	1.2	8562.6	2936.5	3229.8	3219.1	3468.4	3058.4	3568.1	3144.2	4754.6	3346.8	3384.8
homoserine	2.3	12592.3	5685.7	5377.6	5218.2	4814.0	5893.3	4470.0	4796.8	5934.4	5782.4	6237.6
homoserine betaine	1.2	9316.8	3178.8	3543.0	3814.0	4087.2	4303.5	4136.5	3665.1	2991.6	3933.5	4118.4
histidine	1.4	9668.1	4070.9	4172.3	3431.6	4162.0	3290.5	3645.1	3361.5	6194.2	3625.5	3633.6
guanosine	1.1	5296.6	6657.4	4444.7	4141.4	5222.4	5023.5	4233.4	4639.5	5434.4	4184.0	6399.2
glyphosate	1.0	8872.1	3526.2	3956.1	3697.0	3725.7	4083.8	3748.2	4046.3	3954.6	3474.3	3804.5
glutathione	0.7	4881.2	10167.2	5261.6	10639.4	10451.1	11555.7	6580.6	14865.8	13405.5	6549.9	5839.7
glutamine	1.3	10264.1	3200.6	3200.8	3415.5	3544.0	3558.7	2929.3	2786.6	3442.4	4223.0	4225.3
glutamic acid	1.7	10195.1	7258.7	9861.0	8832.5	9989.8	9046.2	11242.1	8676.9	11634.2	4485.5	5146.1
glucose 6-phosphate	1.4	4932.6	1662.0	2401.8	1857.8	2059.4	1592.4	2765.8	1695.6	1589.4	1555.5	1547.8
glucosamine-6-phosphate	0.5	5790.4	1254.0	1334.8	1654.9	1491.1	1706.8	1421.2	1445.8	1363.0	1461.5	1199.3
ectoine	2.2	10551.5	1846.7	3162.8	2010.0	6969.2	3590.3	1700.6	3061.1	1124.4	1117.4	3858.2
cysteine	3.0	12380.3	1191.0	2720.3	5352.1	3464.9	2333.7	3898.9	740.9	740.9	1186.2	1391.7
cystine	1.0	12380.3	4207.9	4815.9	3781.1	4582.3	4045.3	4585.5	4429.9	4043.4	4226.4	3620.2
cysteate	1.6	8867.9	5848.3	3797.8	5878.5	6029.3	7601.4	3984.0	5274.3	7327.3	6249.4	6872.4
citrulline	1.5	8562.1	3807.9	3365.1	3327.4	3322.6	3487.5	3567.7	3240.6	7840.3	3637.9	3706.9
ciliatine	1.5	11994.2	3658.4	5240.5	3551.1	4998.0	3714.6	5146.1	4900.8	4758.9	3645.4	4588.6
chitotriose	0.2	2391.2	992.3	995.6	946.0	884.1	767.4	908.1	973.2	1027.7	812.5	746.0
chitobiose	1.0	3534.4	732.6	762.0	764.5	924.7	1053.5	816.8	886.8	408.8	854.4	1036.1
aspartate	2.4	11269.7	2826.1	2784.3	3090.5	2731.4	2884.9	3282.6	3038.2	5018.3	2279.5	2974.5
asparagine	2.6	11353.3	2270.5	2823.8	2572.0	2505.1	2543.0	2894.9	2022.5	2751.7	3148.5	3234.2
arginine	1.8	8610.8	2627.4	3321.8	2700.5	2651.7	2717.1	3675.4	2383.7	5005.8	2593.7	2764.9
amMP*	1.8	10935.3	5417.5	5322.3	5342.4	5549.8	4893.5	4955.5	9474.8	5362.3	5121.2	5150.2
alanine	3.3	16836.9	7509.6	5193.0	8079.3	5785.9	7955.9	6794.4	5394.5	10678.1	5709.2	4836.5
adenosine	1.0	5612.9	1932.3	1889.5	1693.7	1930.6	1882.0	1901.5	2014.5	2005.1	2006.6	1791.7
(1,2-dicarboxyethyl) glutathione	0.5	3542.7	1112.2	1290.8	1267.0	1193.0	1029.5	1318.5	1256.9	940.3	1224.7	1085.9
N-acetyl-muramic acid	1.3	7929.4	2359.3	2229.1	2948.8	3575.7	3517.5	2619.8	1976.3	1887.6	3135.4	3559.2
HMP	2.4	10779.0	2196.1	2441.5	3580.4	2794.1	4036.5	2526.1	3205.6	2235.0	3416.4	2959.7
gamma-aminobutryic acid	1.1	14546.2	6155.8	6677.4	7798.3	6091.5	6639.2	7622.9	6378.2	6571.6	5745.9	5915.3
2,3-dihydroxypropane-1-sulfonate	2.0	9605.5	2907.6	5028.3	6164.6	5315.9	5051.4	4756.8	3012.7	2375.2	5919.9	4959.2
uridine 5’ -monophosphate	0.4	4074.4	1854.1	2169.5	1728.8	1454.6	1498.3	2010.9	1707.2	1751.5	1116.4	1184.8
4-aminobenzoic acid	1.5	10937.7	5131.9	4808.3	4766.9	4840.9	4806.5	4870.1	6420.8	7090.7	5536.6	6718.1
adesnosine 3’ -monophosphate	0.4	4320.0	1527.5	1801.4	1590.4	1687.1	1708.2	1895.3	2043.7	1686.2	1507.9	1604.5
2'deoxyguanosine	0.7	5612.9	2417.9	2755.7	2633.9	2313.0	1979.0	2336.6	2560.7	1875.4	2093.4	2207.4

Trivial Name	LOQ (pM)	Max Std. (pM)	VSW_t3_3_sample	ASW_t4_1_sample	ASW_t4_2_sample	ASW_t4_3_sample	VSW_t4_1_sample	VSW_t4_2_sample	VSW_t4_3_sample	ASW_t5_1_sample	ASW_t5_2_sample	ASW_t5_3_sample
xanthosine	1.2	4683.7	1936.7	1458.8	2786.9	2477.2	1677.0	2188.2	1654.9	1805.6	1178.9	1210.0
valine	2.1	12804.1	6167.2	6917.4	4771.7	4292.8	5784.5	6825.8	5825.4	6292.8	6641.1	7033.9
uridine	1.2	6142.5	2612.8	2535.6	2231.9	5577.7	2092.5	2044.3	2157.8	2145.0	2163.3	2761.4
tryptophan	0.9	7344.7	743.1	403.0	830.0	1710.1	164.5	195.6	238.8	386.0	478.8	428.0
tryptamine	2.3	9362.1	1052.6	916.2	582.4		582.4	672.5	582.4	916.2	926.5	717.8
thymidine	2.2	6192.5	1670.3	2921.7	5823.6	611.0	1787.9	1305.9	1540.5	1835.1	1620.2	2081.4
threonine	1.8	12592.3	5008.4	4789.4	3768.5	2929.8	4616.0	4526.8	4190.7	5243.3	5217.5	4875.2
taurine	2.0	11985.6	9755.2	9516.7	5989.3	5969.3	11383.0	11492.1	11672.4	6965.6	9266.1	9354.2
glycerol 3-phosphate	0.5	4049.5	3150.0	1538.9	1772.3	1650.4	3418.7	3671.4	3193.2	2051.7	1556.3	1799.2
serine	3.8	14273.5	4740.3	6219.6	8557.7	4370.1	1002.3	3585.0	5185.4	1804.6	5691.9	4412.6
sarcosine	2.2	16836.9	6023.3	6366.1	5567.0	7056.1	6504.5	6223.6	6172.8	6132.0	5578.8	6847.2
putrescine	2.2	9312.7	5094.2	4960.3	4348.1	6623.1	3980.4	3499.8	6477.5	3525.3	4740.1	5564.3
proline	1.1	13028.8	5919.4	5936.8	5768.1	6626.4	6051.2	6042.1	5991.6	6351.5	5970.4	5201.9
phenylalanine	0.5	9080.5	2954.3	3797.8	3687.4	2783.2	3627.8	3860.2	3797.1	3754.9	3551.4	3148.9
pantothenic acid	0.4	6295.4	2836.7	2838.6	2851.1	2819.6	2843.6	2900.1	2895.4	2560.2	2151.4	2722.1
ornithine	2.0	8879.9	1570.7	1964.7	2426.5	2635.9	1657.5	1654.0	1758.8	1779.4	1800.0	1670.9
muramic acid	1.0	5970.6	2704.8	2563.6	2448.1	1363.3	2051.2	2097.1	2297.4	2068.3	2180.8	2627.2
malic acid	2.8	11186.5	1450.7	4574.0	3493.6	8085.1	3394.3	3474.0	3518.4	2263.4	3670.5	2733.2
leucine	3.7	11435.5	3261.9	3347.1	3033.3	3910.5	3225.0	3285.1	3250.1	2556.6	3293.3	3261.4
kynurenine	2.7	7204.3	1368.6	1094.1	1149.6	1029.7	548.5	731.6	613.7	1187.2	1037.2	1028.5
isoleucine	2.7	11435.5	2918.4	3388.7	3086.3	3943.8	3046.5	3125.8	3058.9	2666.8	3304.6	3345.0
isethionate	1.7	10127.6	4233.5	2891.1	4810.2	4737.3	4310.1	4052.9	4202.6	4011.9	3649.8	3428.4
inosine	0.8	5592.2	10182.5	5171.1	4022.3	3829.8	7609.1	9548.0	4835.5	4756.8	5254.3	4111.3
indole-3-acetic acid	1.2	8562.6	3828.4	3666.9	3247.4	3251.7	2910.8	3574.4	3235.1	3592.4	3441.8	3121.9
homoserine	2.3	12592.3	5174.2	5617.2	3784.8	1855.7	5666.9	5545.6	5170.1	5331.3	5094.7	5924.2
homoserine betaine	1.2	9316.8	4753.9	3567.6	4136.5	4148.8	4700.0	4511.0	4596.8	4289.3	3727.9	3483.9
histidine	1.4	9668.1	3357.8	3370.4	4623.4	3252.7	3013.9	3884.8	3267.5	3360.3	3363.6	3298.5
guanosine	1.1	5296.6	5035.1	3957.4	3684.7	4014.7	4802.4	4091.6	4170.6	3468.0	2576.1	2534.1
glyphosate	1.0	8872.1	3764.4	3623.1	3569.9	3596.3	3680.9	3713.3	3724.2	3739.0	3475.8	4031.0
glutathione	0.7	4881.2	5502.2	11274.4	4614.6	5433.5	5080.9	5014.4	5313.9	6786.2	7678.4	8262.6
glutamine	1.3	10264.1	4212.6	3603.6	3370.7	3326.2	4209.9	4202.2	4303.4	2922.5	2895.9	2903.1
glutamic acid	1.7	10195.1	5360.2	8152.9	9801.5	11568.7	5504.0	4557.0	4917.3	8111.2	7338.1	7717.9
glucose 6-phosphate	1.4	4932.6	1185.4	1602.7	2057.3	2338.1	1491.6	1633.0	1436.2	1618.1	1666.2	1551.0
glucosamine-6-phosphate	0.5	5790.4	1715.3	1554.5	1338.2	1203.2	1053.8	1286.6	1193.1	2050.1	1892.6	2199.5
ectoine	2.2	10551.5	4362.6	2546.6	2788.5	5577.2	1615.5	539.8	2567.4	4425.8	3784.5	3597.7
cysteine	3.0	12380.3	740.9	1062.2	4613.8	740.9	1928.7	2367.4	740.9	6595.0	5888.6	4565.9
cystine	1.0	12380.3	4309.3	4536.4	5084.7	4618.3	3589.5	3428.6	4056.6	3630.3	3549.9	3573.3
cysteate	1.6	8867.9	5875.6	5693.3	6893.0	6744.4	5881.9	5946.6	6011.0	7654.4	5353.6	5441.8
citrulline	1.5	8562.1	3946.6	3683.0	3161.1	3078.0	2885.2	3083.8	3038.0	3431.3	3647.7	3628.9
ciliatine	1.5	11994.2	3959.3	5061.7	3633.4	5746.7	3619.5	4586.3	5229.0	3543.3	5047.7	3641.5
chitotriose	0.2	2391.2	856.9	1128.1	833.7	940.5	733.2	735.4	836.3	861.8	854.2	849.1
chitobiose	1.0	3534.4	820.8	264.1	1322.2	264.1	1215.2	962.0	848.2	1290.2	1206.2	1087.5
aspartate	2.4	11269.7	2510.8	2866.2	3729.6	3353.1	2609.4	2665.0	2435.4	3213.0	3203.9	3228.2
asparagine	2.6	11353.3	3234.9	2660.4	2323.0	2541.8	3236.5	3316.9	3317.4	1677.9	1989.7	1984.4
arginine	1.8	8610.8	2250.9	2853.8	2790.9	2974.5	2496.3	2393.8	2386.3	2833.5	2791.9	2735.2
amMP*	1.8	10935.3	4969.2	5096.0	4336.8	4781.2	4824.9	4458.6	7998.2	4927.3	4523.3	9426.0
alanine	3.3	16836.9	6659.8	7142.0	8407.0	5885.0	5667.4	5247.7	5550.2	6554.9	8448.5	7648.6
adenosine	1.0	5612.9	1841.6	2229.7	1701.7	1732.8	1655.9	1858.0	1893.2	1927.5	1875.1	1996.5
(1,2-dicarboxyethyl) glutathione	0.5	3542.7	1124.9	1238.9	1184.3	1254.6	1148.6	1200.4	1250.4	922.4	1002.8	1100.2
N-acetyl-muramic acid	1.3	7929.4	3778.7	2253.1	2317.9	289.2	2937.2	3483.5	3190.1	2907.5	2942.8	3116.6
HMP	2.4	10779.0	4624.9	3016.6	3783.3	5677.5	2367.8	1716.0	2770.5	3004.3	3234.4	1809.4
gamma-aminobutryic acid	1.1	14546.2	6104.0	8113.0	8351.7	7097.8	6593.9	6227.9	7188.8	6353.2	5755.4	5786.6
2,3-dihydroxypropane-1-sulfonate	2.0	9605.5	5908.7	3341.4	3988.7	4492.1	6462.1	6722.5	6223.7	2532.1	2753.1	4074.6
uridine 5’ -monophosphate	0.4	4074.4	1206.6	1734.5	1699.1	2247.3	1269.2	1217.7	1308.7	1790.7	1732.5	1695.1
4-aminobenzoic acid	1.5	10937.7	5660.8	5546.3	4936.4	5842.4	4840.0	4975.7	4613.1	6682.5	5804.6	5213.1
adesnosine 3’ -monophosphate	0.4	4320.0	1808.8	1798.8	2095.0	2101.4	1635.8	1829.2	1986.9	1870.5	1800.7	1543.0
2'deoxyguanosine	0.7	5612.9	1902.3	2237.8	1942.0	3055.8	1991.4	2270.8	2668.9	1740.9	1999.5	1631.3

Trivial Name	LOQ (pM)	Max Std. (pM)	VSW_t5_1_sample	VSW_t5_2_sample	VSW_t5_3_sample	ASW_t5_1_ctrl	ASW_t5_2_ctrl	ASW_t5_3_ctrl	VSW_t5_1_ctrl	VSW_t5_2_ctrl	VSW_t5_3_ctrl	ASW_t5_1_blank
xanthosine	1.2	4683.7	1566.3	1795.8	1384.5	2378.2	1692.2	1210.1	2184.2	6134.7	2042.1	0.0
valine	2.1	12804.1	7942.5	8137.8	6812.1	3869.3	5841.9	5926.8	6203.4	7370.2	6861.6	0.0
uridine	1.2	6142.5	3168.1	2696.4	2898.8	2777.0	2670.4	2532.6	2191.0	4481.4	3826.7	0.0
tryptophan	0.9	7344.7	0.0	0.0	0.0	3993.2	2490.6	2435.5	2564.7	3680.8	2683.6	0.0
tryptamine	2.3	9362.1	604.6	582.4	582.4	6684.1	1809.2	3301.2	2645.7	3271.5	3523.8	582.4
thymidine	2.2	6192.5	1367.5	1349.1	2001.5	2325.3	3112.3	1429.0	1846.5	586.8	939.6	0.0
threonine	1.8	12592.3	4940.5	5434.9	3703.8	3397.3	4901.9	4289.6	5019.5	4721.8	4530.0	316.7
taurine	2.0	11985.6	11068.9	11311.3	11266.1	4730.2	8818.9	9480.5	8111.2	10716.4	10997.6	0.0
glycerol 3-phosphate	0.5	4049.5	2935.4	3391.1	3128.3	1245.4	1331.1	1539.2	4103.6	226.7	2751.3	317.4
serine	3.8	14273.5	4137.5	3679.3	5685.6	5559.4	3877.2	3020.8	5218.7	8498.3	6636.6	0.0
sarcosine	2.2	16836.9	6087.1	6451.4	6183.3	5844.2	5664.8	6347.5	5918.4	5969.6	5776.9	467.8
putrescine	2.2	9312.7	4919.8	2960.6	2782.8	3742.6	3164.0	3331.1	5113.7	2737.6	4477.4	0.0
proline	1.1	13028.8	5486.7	5951.8	6239.9	4538.2	6494.0	5780.4	6606.8	5975.4	4541.4	0.0
phenylalanine	0.5	9080.5	3025.6	3601.0	3242.4	3510.5	3099.5	2634.1	3312.8	3420.6	3179.1	0.0
pantothenic acid	0.4	6295.4	2144.6	2861.7	2520.9	2725.8	2688.6	1626.0	2879.3	229.9	2531.3	64.0
ornithine	2.0	8879.9	1984.4	2137.3	1662.7	3206.5	1585.7	1705.3	2361.0	1786.3	1630.8	0.0
muramic acid	1.0	5970.6	2551.2	2299.6	3515.1	2316.9	2454.4	2217.7	2446.0	9987.7	3305.1	0.0
malic acid	2.8	11186.5	1139.6	2520.8	1816.3	8341.1	5167.2	4256.8	2598.5	0.0	1499.5	0.0
leucine	3.7	11435.5	3202.3	3235.5	3191.7	4411.2	3137.2	3116.4	2548.3	3244.0	3213.1	0.0
kynurenine	2.7	7204.3	919.4	691.2	860.6	2746.6	2331.4	2742.8	3281.3	2126.1	2520.0	361.9
isoleucine	2.7	11435.5	2969.3	3071.6	2730.0	4182.3	2990.3	2821.8	2363.1	2999.7	2975.1	0.0
isethionate	1.7	10127.6	2728.3	3367.2	3687.9	4156.6	3169.0	3681.1	4314.2	562.0	2759.1	391.5
inosine	0.8	5592.2	4869.4	5155.8	5325.9	2679.4	5625.8	4662.8	6056.7	59465.0	8146.2	0.0
indole-3-acetic acid	1.2	8562.6	3231.4	3202.7	2994.0	3448.6	2822.6	3435.4	3406.5	2984.4	3367.0	361.5
homoserine	2.3	12592.3	5759.4	5669.8	4648.9	5181.9	5399.8	6166.9	6138.7	6015.9	5434.2	0.0
homoserine betaine	1.2	9316.8	3464.7	4424.1	4296.0	3612.9	3319.3	3400.9	4644.8	466.3	3084.4	209.1
histidine	1.4	9668.1	3257.0	2752.9	2737.4	3999.2	3425.5	4174.1	4233.8	3483.4	4627.3	0.0
guanosine	1.1	5296.6	2739.6	3161.8	3196.8	2840.1	2830.1	2774.9	4406.5	13500.0	4188.3	0.0
glyphosate	1.0	8872.1	3491.0	3810.9	3579.4	4293.0	3863.6	3364.7	3564.7	3758.4	3884.6	220.5
glutathione	0.7	4881.2	4586.6	4381.7	4649.2	2474.6	4406.2	4007.0	2390.6	1704.5	5509.2	0.0
glutamine	1.3	10264.1	4158.0	4095.6	4041.3	3853.3	3758.0	3722.2	4133.4	4033.0	4011.1	0.0
glutamic acid	1.7	10195.1	4927.6	5343.5	5935.5	5299.1	4018.0	4014.0	5540.5	4457.2	4934.4	0.0
glucose 6-phosphate	1.4	4932.6	1338.0	1547.6	1381.1	1700.2	1201.3	1357.5	1864.6	933.8	1186.7	241.7
glucosamine-6-phosphate	0.5	5790.4	2107.4	2384.5	1549.0	1697.6	2144.4	1751.4	1683.0	3724.5	2599.9	107.6
ectoine	2.2	10551.5	2994.9	4359.0	5835.2	4381.9	4654.5	2564.5	5468.2	1207.2	2127.2	0.0
cysteine	3.0	12380.3	2835.9	3284.3	2671.2	5355.3	8805.0	7492.0	14439.3	740.9	3310.9	740.9
cystine	1.0	12380.3	3537.4	3744.9	3722.9	5194.4	5346.8	3690.7	4345.6	4387.1	4388.2	165.9
cysteate	1.6	8867.9	5808.4	6124.6	5908.0	3694.4	5203.4	5337.6	7997.4	5239.6	5562.1	0.0
citrulline	1.5	8562.1	3179.3	3501.8	3023.4	3103.6	3373.2	3644.2	3546.0	3209.0	2736.3	0.0
cliatine	1.5	11994.2	5255.1	5145.0	3588.5	5078.6	3694.7	6482.0	5020.8	4446.2	5045.6	396.2
chitotriose	0.2	2391.2	888.9	798.9	925.1	1009.9	984.1	924.5	810.6	749.9	964.7	36.9
chitobiose	1.0	3534.4	1541.7	648.7		807.8	1800.0	2133.8	1128.3	264.1	1154.2	264.1
aspartate	2.4	11269.7	2401.7	2627.6	2414.8	2687.4	2303.4	2289.4	2922.3	2319.4	2391.6	409.8
asparagine	2.6	11353.3	3160.1	3319.2	3205.5	4075.6	2975.6	3019.9	2987.5	3206.5	3083.6	0.0
arginine	1.8	8610.8	1966.8	2433.5	2249.5	3088.8	2497.2	2532.2	2858.4	2568.4	2419.6	0.0
amMP*	1.8	10935.3	4689.3	4612.8	4623.8	5095.9	5473.6	4642.9	5244.3	7402.7	5716.0	0.0
alanine	3.3	16836.9	5240.5	7871.2	5369.9	6224.5	6362.1	7008.0	8010.8	5780.2	6651.6	1164.8
adenosine	1.0	5612.9	2002.6	1915.4	1987.8	1914.7	2017.1	1914.4	1976.8	1258.3	2260.8	0.0
(1,2-dicarboxyethyl) glutathione	0.5	3542.7	1196.0	1215.3	1168.0	1253.1	1129.6	1241.1	967.3	1213.8	1263.0	97.0
N-acetyl-muramic acid	1.3	7929.4	3822.5	3346.5	3717.6	2710.3	3441.4	3769.0	3564.9	558.5	4335.2	0.0
HMP	2.4	10779.0	3110.1	2988.7	3021.5	3338.2	2060.4	2624.9	3172.1	1211.5	1739.7	497.3
gamma-aminobutryic acid	1.1	14546.2	6288.8	5864.9	6705.1	7366.4	5896.6	5747.6	5841.5	5785.3	5918.5	224.4
2,3-dihydroxypropane-1-sulfonate	2.0	9605.5	5320.8	6628.7	5768.3	4427.2	2710.5	3665.9	4442.2	431.3	4203.5	0.0
uridine 5' -monophosphate	0.4	4074.4	1289.4	1444.6	1285.9	1608.6	1548.4	1401.6	1351.2	1140.6	1261.6	129.4
4-aminobenzoic acid	1.5	10937.7	5415.4	6039.3	6896.8	4533.6	8594.2	6779.3	5633.9	4964.0	4829.1	0.0
adesnosine 3' -monophosphate	0.4	4320.0	1491.0	1830.5	1831.9	1971.9	1556.8	1474.5	1816.7	852.3	1731.4	94.6
2'deoxyguanosine	0.7	5612.9	1804.9	1982.2	2317.6	1873.8	2465.1	1722.7	1919.4	797.1	2348.8	167.6

Trivial Name	LOQ (pM)	Max Std. (pM)	ASW_t5_2_blank	ASW_t5_3_blank	VSW_t5_1_blank	VSW_t5_2_blank	VSW_t5_3_blank
xanthosine	1.2	4683.7	0.0	0.0	0.0	0.0	0.0
valine	2.1	12804.1	0.0	0.0	0.0	0.0	0.0
uridine	1.2	6142.5	0.0	0.0	0.0	0.0	0.0
tryptophan	0.9	7344.7	0.0	0.0	0.0	0.0	0.0
tryptamine	2.3	9362.1	582.4	582.4	582.4	582.4	582.4
thymidine	2.2	6192.5	0.0	0.0	0.0	0.0	0.0
threonine	1.8	12592.3	297.6	0.0	0.0	0.0	298.2
taurine	2.0	11985.6	0.0	0.0	1678.9	1660.7	1663.8
glycerol 3-phosphate	0.5	4049.5	256.8	173.3	2111.1	2103.0	2017.6
serine	3.8	14273.5	0.0	0.0	0.0	0.0	0.0
sarcosine	2.2	16836.9	452.3	445.0	496.0	513.2	588.6
putrescine	2.2	9312.7	0.0	706.2	1894.3	2049.1	883.8
proline	1.1	13028.8	0.0	0.0	0.0	0.0	0.0
phenylalanine	0.5	9080.5	0.0	0.0	255.6	144.9	161.8
pantothenic acid	0.4	6295.4	63.6	63.8	92.8	90.1	94.1
ornithine	2.0	8879.9	0.0	0.0	0.0	0.0	0.0
muramic acid	1.0	5970.6	0.0	0.0	0.0	0.0	0.0
malic acid	2.8	11186.5	1220.3	2425.1	0.0	0.0	0.0
leucine	3.7	11435.5	0.0	0.0	0.0	0.0	0.0
kynurenine	2.7	7204.3	361.9	361.9	361.9	361.9	361.9
isoleucine	2.7	11435.5	0.0	0.0	312.9	0.0	311.0
isethionate	1.7	10127.6	351.8	347.6	811.4	809.4	613.2
inosine	0.8	5592.2	0.0	0.0	0.0	0.0	0.0
indole-3-acetic acid	1.2	8562.6	326.8	314.8	363.4	443.0	373.3
homoserine	2.3	12592.3	0.0	0.0	0.0	0.0	504.3
homoserine betaine	1.2	9316.8	200.3	208.5	487.6	444.1	382.5
histidine	1.4	9668.1	0.0	0.0	0.0	0.0	0.0
guanosine	1.1	5296.6	0.0	0.0	0.0	0.0	0.0
glyphosate	1.0	8872.1	220.5	220.5	220.5	220.5	220.5
glutathione	0.7	4881.2	0.0	0.0	0.0	0.0	0.0
glutamine	1.3	10264.1	0.0	0.0	273.4	245.3	269.2
glutamic acid	1.7	10195.1	0.0	0.0	657.2	392.4	793.2
glucose 6-phosphate	1.4	4932.6	241.7	241.7	371.4	360.1	366.7
glucosamine-6-phosphate	0.5	5790.4	107.6	107.6	107.6	107.6	107.6
ectoine	2.2	10551.5	0.0	0.0	428.1	800.6	0.0
cysteine	3.0	12380.3	740.9	740.9	1278.9	740.9	740.9
cystine	1.0	12380.3	165.9	168.0	177.3	175.0	174.2
cysteate	1.6	8867.9	0.0	0.0	667.5	656.5	561.3
citrulline	1.5	8562.1	0.0	0.0	0.0	0.0	0.0
cliatine	1.5	11994.2	399.8	399.6	562.1	570.8	555.2
chitotriose	0.2	2391.2	36.9	36.9	36.9	36.9	36.9
chitobiose	1.0	3534.4	264.1	264.1	264.1	264.1	264.1
aspartate	2.4	11269.7	400.6	464.9	0.0	0.0	0.0
asparagine	2.6	11353.3	0.0	0.0	292.3	0.0	0.0
arginine	1.8	8610.8	0.0	0.0	0.0	0.0	0.0
amMP*	1.8	10935.3	0.0	0.0	0.0	0.0	0.0
alanine	3.3	16836.9	633.0	1044.4	715.5	1976.1	623.5
adenosine	1.0	5612.9	0.0	0.0	0.0	0.0	0.0
(1,2-dicarboxyethyl) glutathione	0.5	3542.7	97.0	97.0	97.0	97.0	97.0
N-acetyl-muramic acid	1.3	7929.4	0.0	0.0	461.4	0.0	281.5
HMP	2.4	10779.0	481.6	0.0	990.1	1012.3	832.8
gamma-aminobutryic acid	1.1	14546.2	204.8	219.1	238.1	210.7	180.4
2,3-dihydroxypropane-1-sulfonate	2.0	9605.5	0.0	0.0	2140.8	1927.8	2097.8
uridine 5' -monophosphate	0.4	4074.4	129.4	129.4	151.3	163.3	129.4
4-aminobenzoic acid	1.5	10937.7	0.0	0.0	0.0	0.0	0.0
adesnosine 3' -monophosphate	0.4	4320.0	94.6	125.3	109.5	173.8	158.5
2'deoxyguanosine	0.7	5612.9	167.6	167.6	167.6	167.6	167.6

2.6.3 Flow Cytometry

Figure 2-4 displays the results of our flow cytometry analysis. There is actually growth following a typical logistic shape in the samples (open circles) incubated in the SunTest, though the numbers even in the dark controls never reach 10^5 cells mL^{-1}.

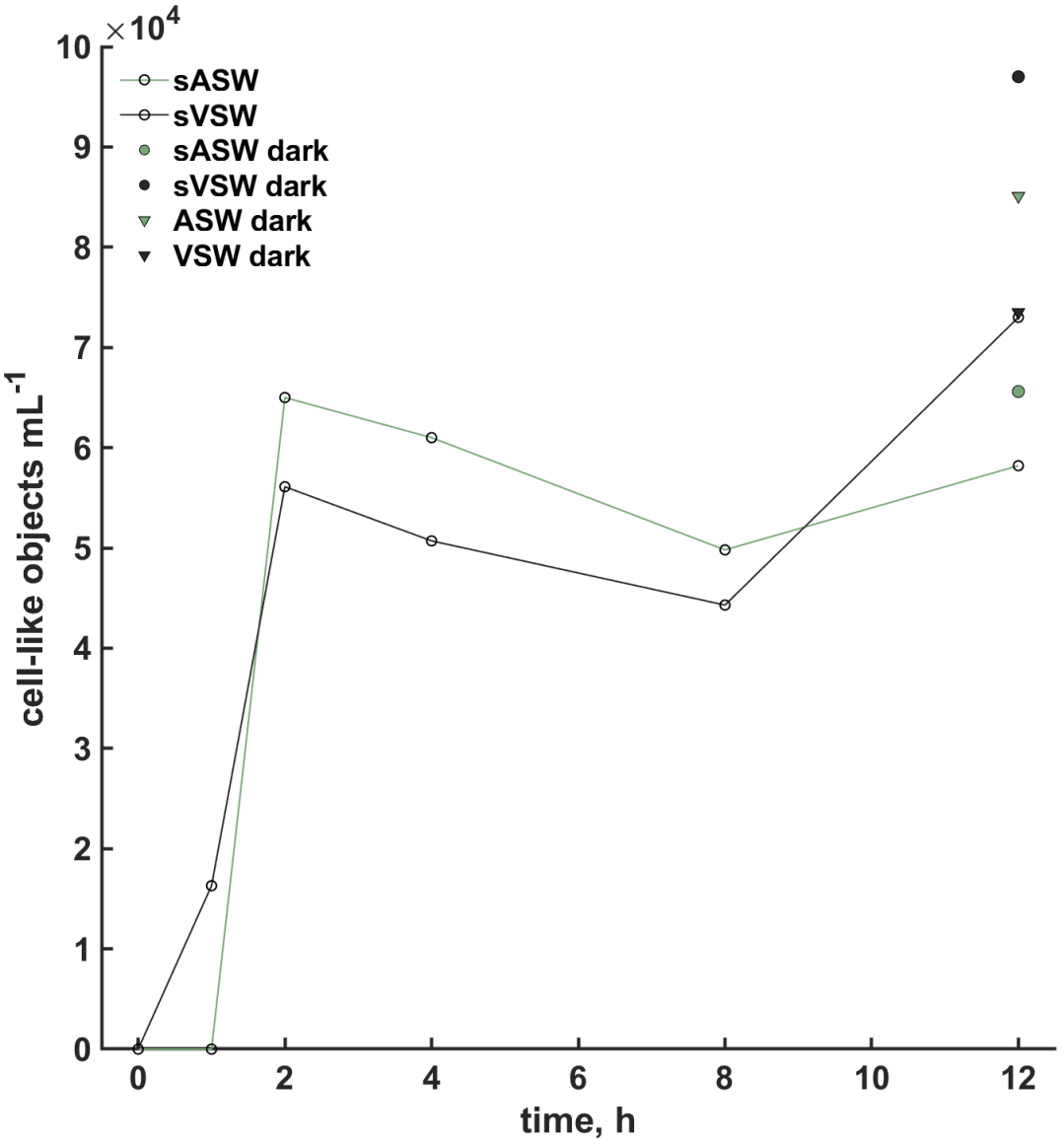

Figure 2-4: Flow cytometry-based cell counts tracking the irradiated samples and dark-control endpoints. ASW (black) and VSW (orange) are artificial seawater and Vineyard Sound water, and a lowercase “s”

denotes a metabolite spike, notated as circles. Samples were irradiated (hollow symbols) unless noted "dark" (filled symbols).

Importantly, we can show that for one odd example case (the pathway which converts glutamine to glutamate and then to GABA, or *gamma*-aminobutyric acid) the cell growth that we observed would not have made a difference. These three compounds showed complementary patterns: decreasing glutamine, increasing then decreasing glutamate, then increasing GABA. This was one case where we thought the microbial growth may have changed the composition of organic metabolites in the samples. The deamidation of glutamine to glutamate takes place in cells through the glutaminase enzyme and continues to GABA by way of glutamate decarboxylase. If these enzymes had been at play in the experiment, we would expect to see an increase in GABA following the uptick in glutamate—and we did, peaking at about eight hours.

Given that we could not entirely prevent cell growth in these samples, we may evaluate whether this growth accounts for the behavior of glutamine, glutamate, and GABA. With an average $6x10^4$ cells/mL (measured, Figure 2-4), a conservative set of assumptions would be that these cells each contain 20 fg C; that they contain a similar glutaminase to Bacillus subtilis YlaM with a mass of 74.57 kDa; that 50% of the enzyme is made of carbon by mass; and that every cell is exclusively made of the enzyme.[149,150] Using Michaelis-Menten kinetics with measured values for Km and kcat, a constant glutamine concentration equal to the initial (~4.5 nM), we calculate a ν for glutamine of 2.6 pM h-1: in other words, the microbial influence on this short reaction pathway would be undetectable within our error margins.

2.6.4 Irradiance

Irradiance in the SunTest was qualitatively higher than a simulated solar noon downwelling irradiance at the ocean surface near Bermuda on a midsummer day (July 11). Figure 2-5 shows that the experimental irradiance in the 300-700 nm range contrasted to the values estimated by the Simple Model of the Atmospheric Radiative Transfer of Sunshine (SMARTS).

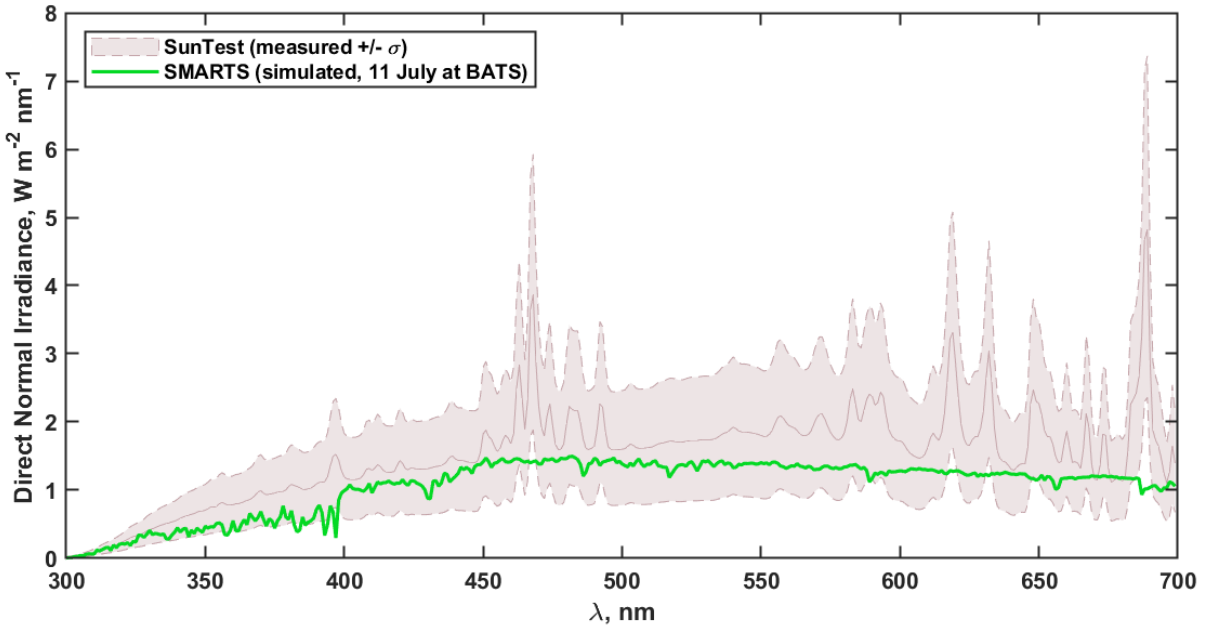

Figure 2-5: Wavelength-dependent radiometry of the Suntest , showing spatial variance (grey area), and a simulated summer irradiance spectrum in the Sargasso Sea.

This data reinforces the idea that for a metabolite to have an environmentally relevant photochemical decay, the estimated reaction rate must be short enough that a less-intense and time-varying irradiance could still yield a half-life in days.

2.6.5 Spectrometry and Dissolved Organic Carbon

Natural aqueous photochemistry is dictated in large part by the chromophoricity (light absorption) and concentration of the organic material dissolved in the water. Consequently, dissolved organic carbon (DOC) and UV-Visible absorbance

spectroscopy go together when teasing out the photoreactive potential of a sample. DOC concentrations in the various matrices are displayed in Table 2-2 along with total nitrogen (TN), which includes all nitrogen species—organic and inorganic.

Table 2-3: DOC and TN measurements from raw and metabolite-spiked matrices (columns 2,3,5, and 6) and calculation of DOC/TN added from metabolite spike (fourth column).

Matrix	Raw DOC (µM)	Spiked DOC (µM)	DOC added (µM)	Raw TN (µM)	Spiked TN (µM)	TN added (µM)
MQ	3.7 ± 2.0	426.8 ± 20.9	423.2 ± 22.9	0.5 ± 0.1	3.5 ± 0.4	3.0 ± 0.6
ASW	12.7 ± 0.7	417.9 ± 28.9	405.3 ± 29.6	1.3 ± 0.2	4.5 ± 0.4	3.2 ± 0.6
VSW	100.1 ± 0.4	524.3 ± 21.2	424.3 ± 21.6	7.6 ± 0.2	10.8 ± 0.2	3.2 ± 0.3

Raw ASW had higher DOC than the MQ in which it was made, though ~60% less than a previous test owing to the precombustion of NaCl, which composed most of the mass of the added salts. We advise any future experiments using such scant concentrations of organic analytes to take similar precautions. Raw VSW can contain >300 µM DOC depending on the time of collection, but the water we collected for this experiment was much lower (100.1 µM). Metabolite spikes, on average, added 417.6 µM DOC to the matrix.

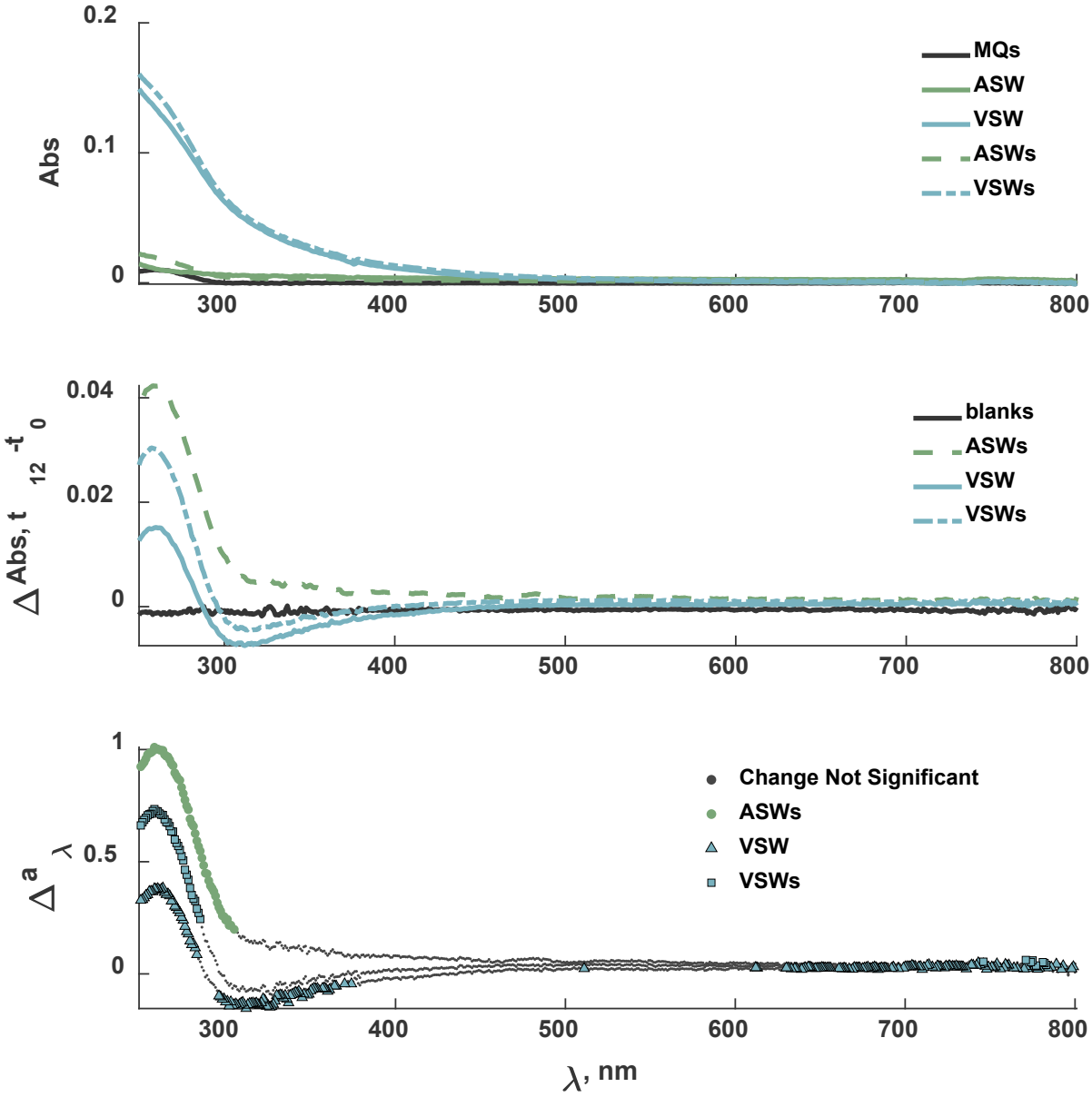

Figure 2-6: Top: Absorbance data, MQ blank subtracted. Small "s" denotes a matrix with metabolite spike. Middle: Difference in absorbance between final and initial time point. Bottom: Difference in Napierian absorbance coefficients between initial and final time points. Values shown are based on the average of three spectral measurements, and the "not significant" differences are based on a significance level of 0.01 on Student's t-test.

The irradiated (12 h) ASW sample did not contain enough water to be accurately measured on the spectrophotometer. When we subtracted the MQ blank from the initial (0 h) spectra, every matrix had Napierian absorbance coefficients < 4.4 m^{-1} at all wavelengths.

In the interest of estimating roughly how terrigenous organic matter may have influenced the VSW results, we approximated the total dissolved lignin phenols (derived from land plants) using the equations of Fichot and Benner (2012) and the spectral slope coefficient $S_{275-295}$ for VSW.[101] The spectral slope coefficient of this water was beyond the range of the regression—high enough where we assumed terrigenous DOM in our samples was negligible. We sampled at high tide (1 December 2023, 6:20 am local time) and thus may have minimized terrestrial influence on our results.

2.6.6 Light Absorption

Irradiance within the solar simulator varied depending on a sample's position relative to the lamp. Based on the calculated absorption coefficients of the two different sample types, the actual photon absorption rates varied by less than ±5% in the 280-650 nm wavelength range. Above 650 nm, variance appears to increase greatly; however, this region is also where the absorbance measurements themselves were nearing the lower limit of the spectrophotometer and small differences there would be inflated in downstream calculations. We assume that these negligibly-absorbed parts of the spectrum are irrelevant to the observed reactions.

2.6.7 Photon Absorption by Samples

Due to a lack of actinometry, we calculated photon absorption by the samples through integrating the product of downwelling irradiance (Figure 2-3) and the absorbance of the different matrix waters (ASW, VSW, sASW, sVSW).

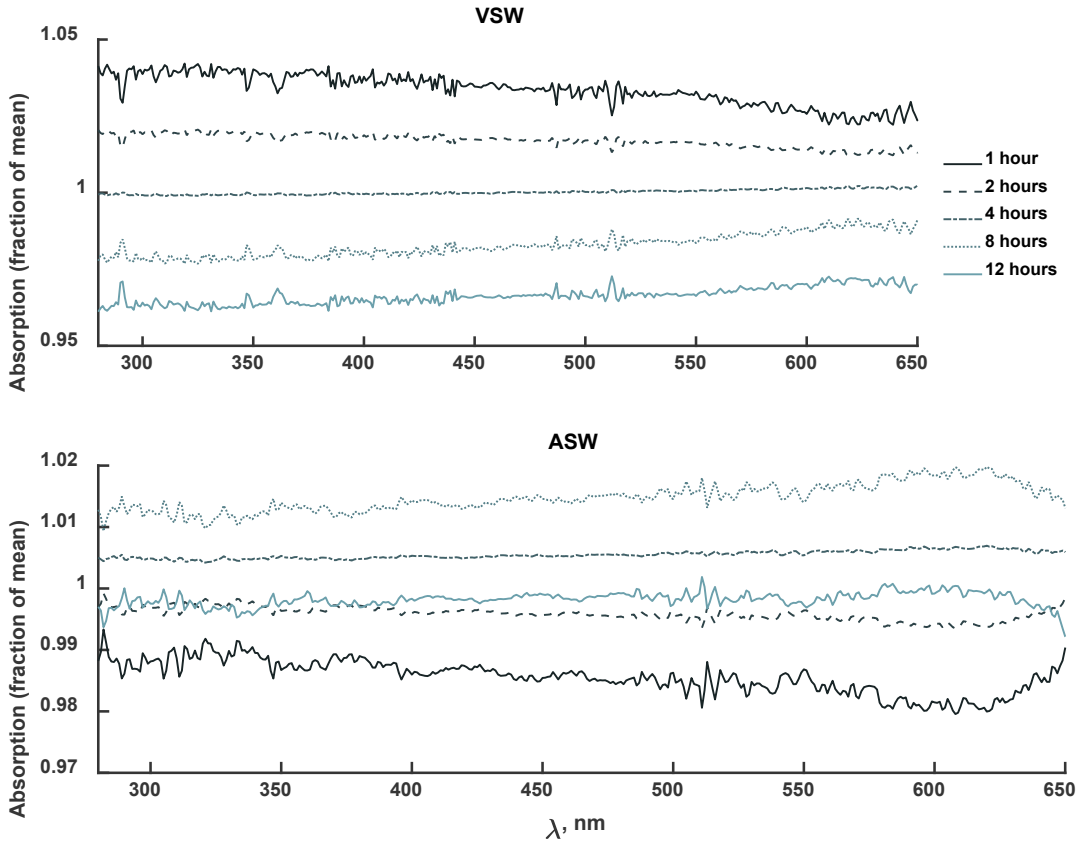

Figure 2-7: Relative photon absorption of each time-point sample by wavelength. Wavelengths >650 nm have been excluded to show the relative consistency of the higher-energy wavelengths. Absorbed irradiance was calculated by integrating the products of absorption coefficients and measured incident radiation over the prone quartz cylinders containing the samples.

The absorption values in Figure 2-7 vary, but while they are noted by sample time, the reason for variance was position in the SunTest relative to the lamp, thus representing variable irradiance rather than absorptivity.

As for the individual compounds for which we measured extinction coefficients, their specific absorption rates are compared below.

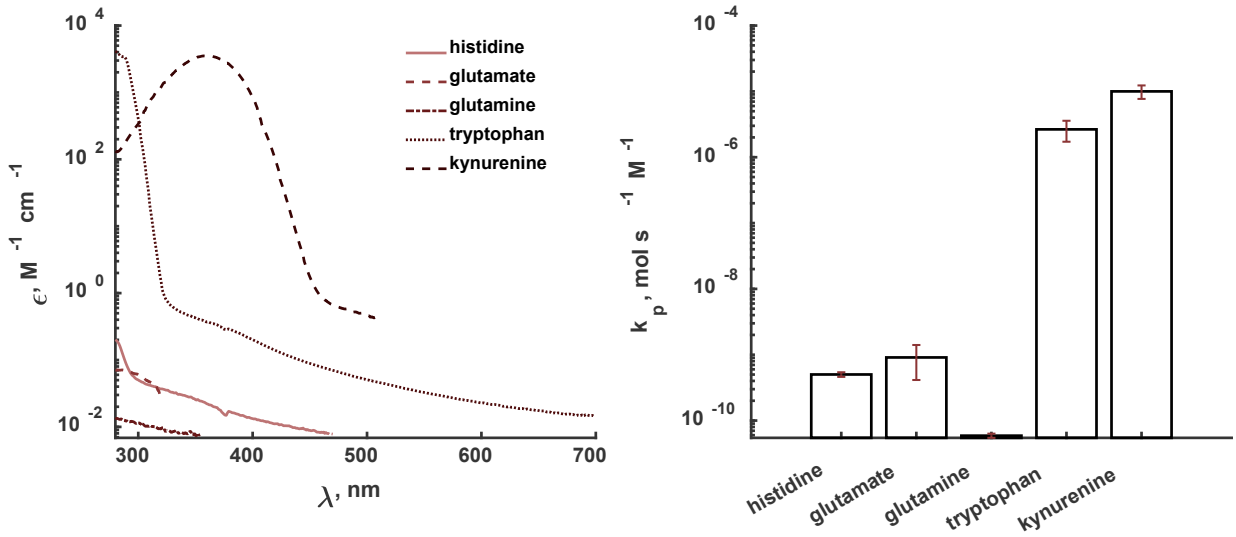

Figure 2-8: Molar extinction (280-699) nm for five compounds (left). Compound-specific photon absorption (right) for the same five compounds at t = 0 h.

The extinction coefficients in Figure 2-8 were those used to calculate apparent quantum yields.

Chapter 3: The metabolite excretion rates of four migratory zooplankton

Co-authors: Amy E. Maas[d,e], Krista Longnecker[f], Melisa C. Kido Soule[f], Elizabeth B. Kujawinski[f]

Abstract

Zooplankton, both migratory and non-migratory, are critical intermediaries in the ocean's food webs—and in its chemical flows. By consuming particulate organic matter in surface waters, they package nutrients from lower trophic levels as biomass and sinking fecal matter. Zooplankton may additionally play a critical supply role in microbial food webs, as they directly release organic compounds through their production of dissolved organic carbon and nitrogen. The identities and quantities of these waste products are poorly characterized, however, preventing an adequate analysis of their role in microbial ecology. We measured 42 excreted metabolites—17 of which had never been quantified as zooplankton excreta—from four taxonomic orders of zooplankton, including a calanoid copepod, an amphipod, a euphausiid, and a pteropod. We found that this modest set of targeted analytes compose up to 18% of the total excreted nitrogen. Glycine and taurine together comprise up to 3.5 and 2.1 % of excreted dissolved organic carbon and total dissolved nitrogen, respectively. Our findings demonstrate that not only do excreta from multiple zooplankton taxa consistently contain specific organic nutrients, but that the rates of excretion can be measured and applied to extant data about zooplankton abundance to estimate source terms for individual ecologically important chemicals.

3.1 Introduction

The trophic web of ocean ecology is undergirded by the reactions and exchanges of individual organic metabolites, and zooplankton are an understudied player in these exchanges as a source of these metabolites. In both oceanic and limnic systems, zooplankton span multiple trophic levels and fill a variety of ecological niches. As metazoan heterotrophs, they serve as important grazers, consolidators of biomass, and synthesizers of complex organic molecules. The production of solid waste by zooplankton is an important nutrient exchange process in pelagic ecosystems, and an

[d]Bermuda Institute of Ocean Sciences, St. George's, Bermuda
[e]School of Ocean Futures, Arizona State University, Tempe, AZ, USA
[f]Woods Hole Oceanographic Institution, Woods Hole, MA, USA

ongoing and active area of research—fecal pellets are both a known source of nutrients for microorganisms and a source of sinking carbon which can quickly make its way out of the epipelagic zone [70,151,152].

Analysis of zooplankton particulate waste is useful for the purpose of calculating export of organic matter to depth and analysis of predator-prey dynamics [153,154], but the influence of this waste upon food webs is broader than what escapes from their fecal pellets. There is ample evidence that the respiratory and excretory contributions of zooplankton to elemental cycles are significant: they consume oxygen (dioxygen gas) and produce nitrogen (ammonia, urea, dissolved organic nitrogen) and carbon (carbon dioxide, dissolved organic carbon) [30,73,75,155]. These metabolic products are labile and change the composition and behavior of the microbial community [75,94,156]. Amino acids, lipids, nucleic acids, and other metabolites are comprised of major elements (C, N, P, S) occurring simultaneously—not in isolated bulk pools, but as a linear combination of individual stoichiometry. Beyond the basic ratios of elements present in zooplankton excreta, the precise identities of the compounds making up a metabolite excretion profile may be important, as each unique functional moiety may be more or less labile to the surrounding microbial community. For example, phosphonate-P may be less labile than phosphate-P, and the sulfur in dimethylsulfoniopropionate (DMSP) can be more labile than in a sulfated polysaccharide [52,157,158]. If the ocean's microbiome feeds in part on the excreta of zooplankton, and the process of breaking down organic matter is specific at the molecular level, it follows that the underlying chemical ecology depends on both the quantity and identity of excreta.

There is preliminary evidence demonstrating the impacts of specific zooplankton metabolites on microbial communities. Taurine, for example, is excreted in large quantities by copepods, providing a valuable source of organic carbon, nitrogen, and sulfur to the microbial food web—calculated to be up to 71% of the organic sulfur required by the North Atlantic's heterotrophic prokaryotes [74]. *Pleuromamma xiphias* copepods also excreted six non-amino acid metabolites (nucleosides and B vitamins/derivatives) in Maas et al (2020)[75]. While the production rates of these compounds were much lower than those measured for taurine, the excreted metabolites were metabolically valuable, such as pantothenic acid (vitamin B_5), folate (vitamin B_9), and thymidine. Amendment of heterotrophic communities with zooplankton excretions, results in exponential growth of microbial communities and a preferential use of nitrogen compounds.[75,159] The taxonomic specificity of microbial responses suggests a specific niche supported by the compositional diversity of this excreta. SAR11, *Roseobacter, Alteromonas*, and the Thaumarchaeota were the dominant consumers of taurine in Clifford et al. (2020), while the presence of zooplankton excreta increased the abundances of *Flavobacteriales, Rhodobacterales* and *Pseudoalteromonadaceae* clades in multiple studies.[75,160,161] These findings suggest a dependence of certain fractions of the planktonic microbial food web on zooplankton behavior and metabolism.

Until recently, a major issue with existing quantitative methods for metabolites in seawater was the high loss incurred in solid-phase extraction, a step that is required to separate small polar metabolites from seawater salts for downstream mass spectrometry analysis. In Maas et al. (2020), one liter of water and 50 copepods per replicate were required to produce sufficient material for the quantification of six novel

metabolites. One year later, Widner et al. (2021) demonstrated a new derivatization regime for seawater with the sensitivity to detect the expected metabolite excretions of a single copepod while using only 25 mL of sample.[17] With this method, quantitative and structural information became sensitive enough for single-organism experiments with zooplankton. With these new methods, it is experimentally tractable to study a larger number of biological replicates over a larger taxonomic diversity, and to conduct a more comprehensive analysis of the relationship between zooplankton size and metabolite production.

Using an updated version of the Widner et al. (2021) method, we have evaluated metabolite excretion rates for four species of migratory zooplankton: *Pleuromamma xiphias*, a copepod; *Clio pyramidata,* a pteropod; *Hansarsia microps*, a euphausiid; and *Scina* spp., a predatory amphipod. We tested three hypotheses in this work: (1) zooplankton excrete a diversity of identifiable labile metabolites beyond that which has been previously measured, (2) organic non-urea metabolites are a large contributor to the total pool of excreted labile nitrogen, and (3) some metabolites are consistently excreted at quantifiable rates by the animals.

3.2 Methods and Materials

3.2.1 Collection of Water and Animals

Three months prior to our experiment, technicians for the Bermuda Atlantic Time-series Study (BATS) collected 10 L of unfiltered seawater from 1000 m depth in a polycarbonate carboy, which aged in the dark until 29 May 2023—the day our experiment began. This process allows the removal of dissolved organic compounds by resident microbes, providing a clean background seawater medium with minimal labile

metabolites for subsequent experimental manipulation. We gravity-filtered this aged seawater (through a 0.2 μm PTFE membrane, Millipore-Sigma) 5 hours before collecting zooplankton and used this filtered, aged seawater (FSW) for all standards, incubations, and animal rinses. We cleaned all incubation bottles, tubing, animal handling tools, and filtering hardware with 10% HCl before final triplicate MilliQ rinses, reducing the probability of microbial contamination of our experimental setup.

We captured zooplankton at night with a small boat at the first 1000 m isobath off the Southeast edge of the Bermuda platform (32^{o} 20.338' N, 64^{o} 33.099' W). Using a 1 m Reeve net outfitted with a 150 μm mesh and a 20 L cod-end, we performed two 20-minute tows, targeting the chlorophyll maximum (~85 m) after sundown, with the first tow beginning at 20:50 local time. We returned to shore for processing immediately after collection.

We picked 15 animals from 5 species (8 *Pleuromamma xiphias,* a copepod; 2 *Hansarsia microps* and 1 *Stylocheiron abbreviatum*, euphausiids; 2 *Clio pyramidata*, a pteropod; and 2 *Scina spp.*, an amphipod) with either a (clean) spoon or wide-bore pipette and rinsed each three times with FSW before depositing individuals into glass bottles (60 mL BOD with ground-glass stopper) for incubation in the dark (21.5 °C, 0-12 h), with 11 additional bottles of FSW for controls (Table 3-1). The *S. abbreviatum* euphausiid and one pteropod died during the incubation, and their results will not be discussed further. After each sampling, we retrieved and weighed each animal on a microbalance, and weighed them again after 24 h of desiccation in an oven (65 °C).

3.2.2 Metabolite Sampling

At 0, 6, and 12 hours we sampled abiotic controls. At 6 h and 12 h we sampled *P. xiphias* in triplicate. All other species (ranging in replication from 1-3) were sampled at 12 h. We collected 25 mL for metabolites using a 200-µm Nitex mesh prefilter, peristaltic pump, and 0.2-µm PTFE membrane filter in sequence. This setup avoided sucking up animals or fecal pellets. We used a fresh set of filters and acid-washed the tubing (10% HCl) between each set of replicates and collected the filtrate in combusted (450 °C) amber-glass EPA vials (40 mL).

3.2.3 Derivatization of Metabolites

We immediately derivatized metabolite samples using a modified version of the benzoyl chloride (BzCl) method by Widner et al [17]. Briefly, we basified each sample or standard with NaOH (250 µL, 8 M), then added BzCl (5 mL, 5% v/v in acetone), mixed by inversion for 5 min, and quenched with concentrated H_3PO_4 (125 µL), added internal standards, and shipped the samples/standards back to the laboratory at the Woods Hole Oceanographic Institution (WHOI) at 4 °C. We concentrated the samples with solid-phase extraction at WHOI in accordance with the original method.[17]

Rather than using one standard curve as in the original method, we generated two isotopically-labeled curves to extend our range of quantification. We targeted 111 metabolites with a 17-point standard curve ranging from 5-7000 pg mL^{-1}. We spiked each sample and standard with 250 µL of two stable isotope-labeled internal standard (SIL-IS) solutions: $^{13}C_6$-BzCl-derivatized (20 ng mL^{-1}) and D_5-BzCl-derivatized (100 ng mL^{-1}). Both SIL-IS mixtures contained isotopologues of the complete set of metabolite targets.

3.2.4 Dissolved Organic Carbon and Dissolved Nitrogen

We filtered water (40 mL) for dissolved organic carbon (DOC) and total dissolved nitrogen (TDN) analysis into a combusted 40 mL EPA vial using the same procedure as for metabolites. We took three control (FSW) samples at the start of the experiment and another set of three at 12 h. One replicate of *P. xiphias* was dedicated for DOC/TDN, but we took four more samples by pooling surplus water from live 12 h incubations within each separate species (*P. xiphias*, *H. microps*, *Scina* spp., and *C. pyrimidata*).

We acidified DOC/TDN sample (pH < 2) with HCl (12 M) after collection and shipped them back to WHOI at 4 °C, where we quantified DOC and TDN in tandem using a Shimadzu TOC-L equipped with a TNM-L module. We quantified both elements (C, N) using standard curves of potassium hydrogen phthalate (C) and potassium nitrate (N). Each calibration curve had at least four points spanning the sample ranges and we injected each sample 3-5 times to minimize the signal coefficient of variation [100].

3.2.5 Cell Counts

To quantify microbial influences on our results, we fixed 40 mL aliquots of azoic FSW before and after 12 h incubation and one aliquot of 12 h *P. xiphias* incubation water (no 0.2 µm secondary filtration) with formalin (4 mL 37% v/v, 0.2 µm filtered)[162].

We stained 15 mL of each fixed sample with 0.5 mL DAPI (4′,6-diamidino-2-phenylindole, 5 µg mL^{-1}) on a 0.2 µm polycarbonate filter stained with Irgalan Black (0.2 g in 100 mL 2% acetic acid) in darkness. Immediately after staining, we counted cells on the filters using an ultraviolet epifluorescence microscope (AX70; Olympus, Shinjuku, Japan). We counted 12-26 fields (1000x magnification) for each sample, ensuring the mean value had <0.2 coefficient of variation.

3.2.6 Metabolite Quantification

The Vanquish UPLC and Orbitrap Fusion Lumos used to quantify metabolites, as well as their parameters and solvent gradients, were the same as previously published work [17], and are provided in the 3.6 Appendix A: Supplementary Methods. We injected each sample in both positive and negative ion modes in a randomized order with a pooled QC injection every 11 samples. We gave the Orbitrap an inclusion list of user-defined parent ion masses and known retention times to determine what ions the Orbitrap should collect for diagnostic fragmentation.

3.2.7 LCMS Peak Integration and Calibration

We integrated three chromatographic peaks for each metabolite (analyte, $^{13}C_6$-SIL-IS, D_5-SIL-IS) in Skyline [103] based on retention times and exact masses (error <5 ppm). The deuterated targets typically had an RT shift of -6 s relative to the other two isotopologues.

We used a new data pipeline, SkyMat (github.com/WHOIGit/SkyMat) to calculate concentrations (pM) from integrated peak areas. The scripts included in the package import peak areas from Skyline, convert them to light/heavy ratios, and calibrate the sample concentrations based on a linear regression of the standards. Because there were up to two ion modes and two isotope ratios per metabolite, we selected the best ion mode/isotope combination for each sample based on the lowest regression uncertainty. We converted concentrations from pg mL^{-1} to pM based on molar masses and used the stoichiometry of each analyte to calculate elemental N and C contributions.

3.2.8 Excretion Rates

We evaluated excretion rates (pmol mg^{-1} h^{-1}) by subtracting the time-matched control metabolite concentrations (pM) from each animal sample, multiplying by incubation volume (0.06 L) to get an inventory in pmol, then divided these by incubation duration (h) and each animal's dry biomass (mg).

3.2.9 Difference Testing

We calculated the inter-sample distance matrix for each 12 h animal and control sample based on metabolite concentrations using the Bray-Curtis dissimilarity (function `f_braycurtis` in the Fathom toolbox [163]). We used this distance matrix to construct a phylogenetic tree with 10^5 bootstraps (function `phytree` in MATLAB) and performed ANOSIM with dissimilarity matrices constructed both from the concentration (pM, with controls included) and the derived rates (pmol mg^{-1} h^{-1}, controls subtracted) by using the `f_anosim` function (also from the Fathom toolbox).

3.2.10 Data and Code Availability

The original datafiles used in this experiment are available in MetaboLights (https://www.ebi.ac.uk/metabolights/editor/study/MTBLS9061/) and the codes used for figure generation and data processing are available at GitHub (https://github.com/germo006/zoopee). Processed metabolite concentrations for every sample are in the Supplemental Information, along with InChI keys for each metabolite.

3.3 Results and Discussion

3.3.1 Measurements and Elemental Contributions

Our results have expanded the number of known metabolites in zooplankton excreta from 28 to 45. We quantified the excretion of all formerly known molecules in this group

except for urea, folate, and beta-alanine, which were not analyzed in this study. Individual metabolite concentrations spanned six orders of magnitude, from <30 pM to 10 μM. Measurements in the high-nanomolar to micromolar range for an individual metabolite are unusual for ambient marine organic matter [45], and underscore that zooplankton excreta is both diverse and highly concentrated with respect to some labile metabolites.

We measured dissolved organic carbon (DOC) and total dissolved nitrogen (TDN) for each animal species and control. TDN includes inorganic species such as ammonium and nitrate. The incubation water initially contained 57.41 ± 0.04 μM DOC and 9.62 ± 0.05 μM TDN (n = 3), which increased in the controls to 80.51 μM DOC and 11.24 μM TDN at the end of 12 h (n = 1). This increase in ambient DOC and TDN was measurable; however, the excreta of the incubated animals eclipsed this change, with all except the copepod pushing DOC to >100 μM (ΔDOC of 5.22 - 30.28 μM relative to t_{12} controls) and TDN to 18.49 - 36.27 μM (ΔTDN of 7.09 - 25.03 μM relative to t_{12} controls).

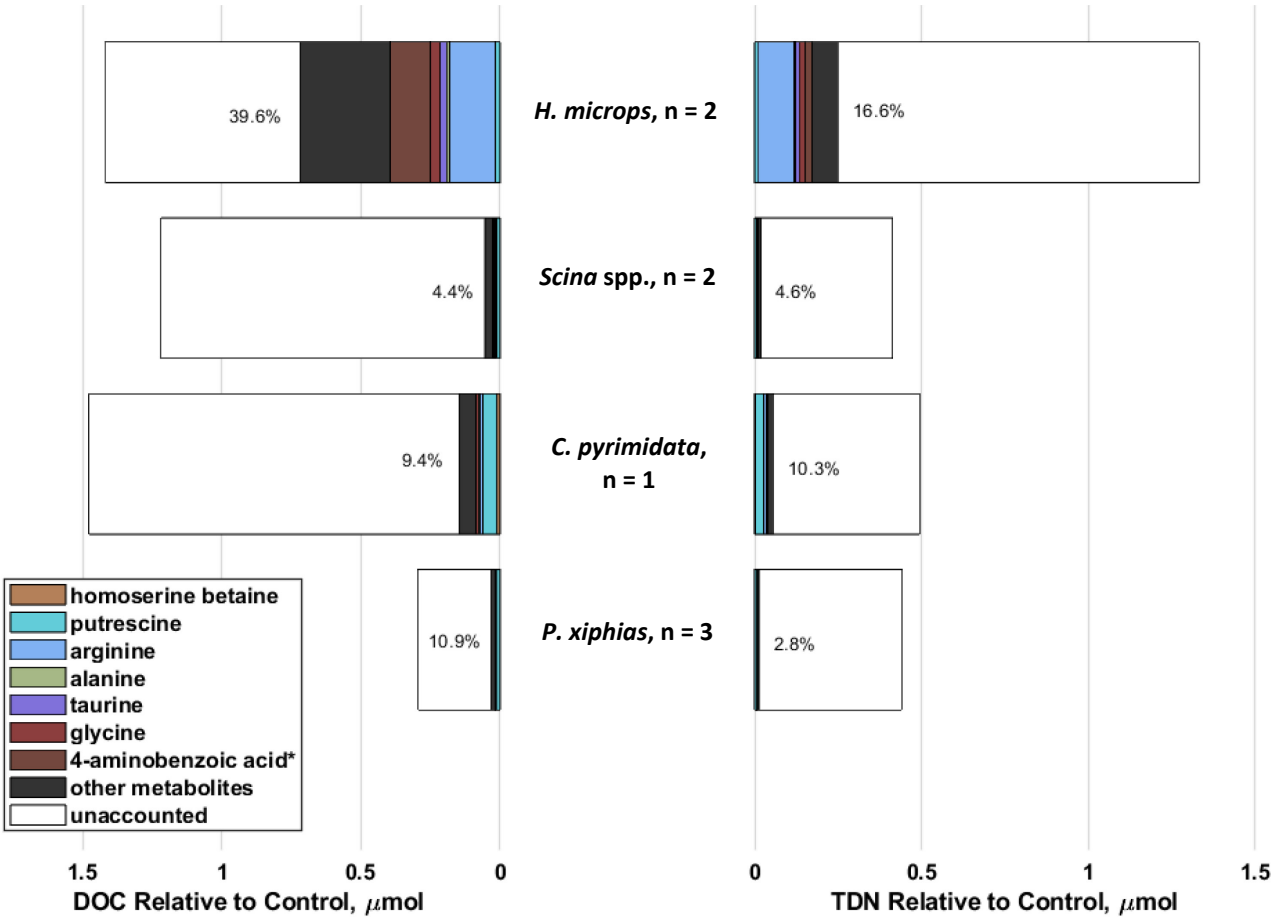

Figure 3-1: Metabolite excretion as a fraction of DOC/TDN excretion. Numerical values are shown as inventories; concentration (μM) multiplied by incubation volume (0.06 L). Bars represent DOC or TDN change relative to control and filled portions of the bar represent the carbon or nitrogen content of excreted metabolites. The colored bar segments are specific metabolites with large excretion totals, while the black remainder is the sum of all other metabolites. *4-aminobenzoic acid in *H. microps* was above the standard curve; data extrapolated. Metabolite measurements are means of *n* live, 12-h incubations.

As bulk elemental excretions, the targeted metabolites accounted for 4.4-39.6% of dissolved organic carbon and 2.8-16.6% of dissolved nitrogen (Figure 3-1). The five highest overall contributors to excretion by median across the animal species were arginine, putrescine, glycine, taurine, and lysine. These molecules were not observed in our previous work because all have very low (or non-existent) extraction efficiencies on the PPL resin, but are detectable after benzoylation [16,17].

3.3.2 Excretion Rates and Biological Variability

While excretion rates of carbon and nitrogen have been successfully linked to body size, this does not seem to be the case for specific metabolites. Fitting power-law relationships to each metabolite with more than five valid measurements only resulted in four relationships with $R^2>0.5$: glutamine (n=5, $R^2=0.927$), 3'-adenosine monophosphate (n=6, $R^2=0.589$), 5'-adenosine monophosphate (n=6, $R^2=0.586$), and *N,N'*-diacetylchitobiose (n=7, $R^2=0.576$). Out of caution, the full table of these regressions is not included, as allometric scaling generally requires much larger sample sizes to merit making such comparisons across orders of magnitude.[164]

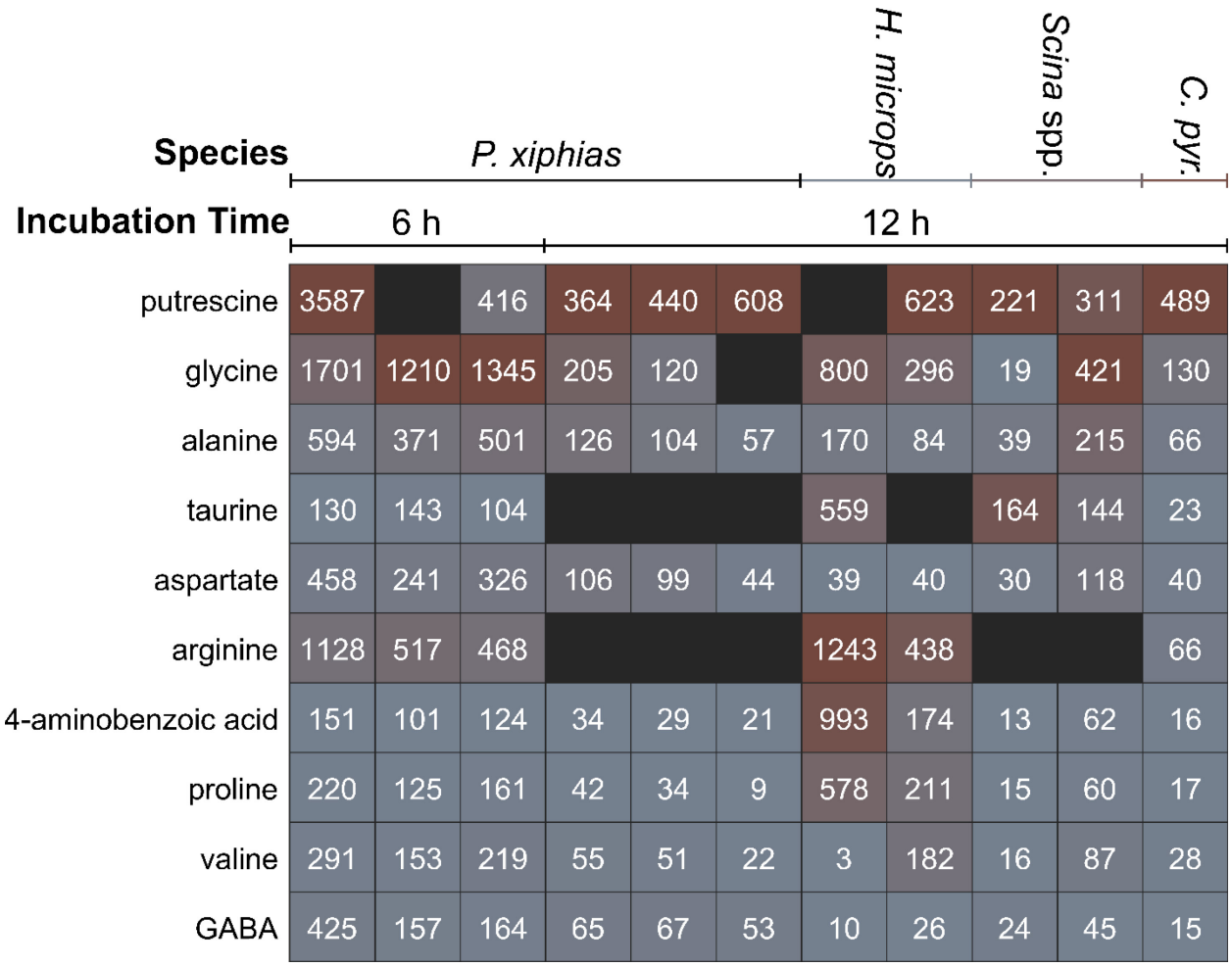

Figure 3-2: Excretion rates (pmol mg^{-1} h^{-1}) of all live zooplankton samples (individual replicates as columns), rounded to the nearest whole number and colored by magnitude within the sample. The metabolites shown are the ten highest-excreted, based on median. GABA = *gamma*-aminobutyric acid.

In terms of such specific biochemistry, this lack of obvious scaling may be unsurprising. Biomass-dependent excretion rates might, however, be assumed based on the literature on total DOC production in zooplankton, and this data is not sufficient to uphold or upend that paradigm.[72,165] An allometric relationship cannot be ruled out, but with ≤ 6 samples per species, differences in excretion (pmol hr^{-1}) vary more by species than they do by size. Nonetheless, Figure 3-2 and subsequent others are presented as dry-biomass-normalized out of convention.

The top ten metabolite excretion rates relative to dry biomass (pmol hr^{-1} mg^{-1}) per sample tend to be similar among the species (Figure 3-2), although the scope of these data does not permit the use of targeted metabolites as a "fingerprint" of each organism. Using ANOSIM on the Bray-Curtis semi-metric pairwise differences, the only two groups with a significant difference were the animals and the control samples ($R = 0.796$, $p = 0.001$).

Intraspecies similarity in excretion rates in conjunction with high variability for individual compounds has some precedent. In Clifford et al. (2017), taurine excretion (nmol hr^{-1} mg_{DW}^{-1}) had a relative standard deviation of 17-25% depending on the species of calanoid copepod (n = 15). For other amino acids, variability was as high as 93% (leucine, *Centropagus* spp., n = 3) and as low as 1.8% (histidine, *Calanus* spp. n = 3). This suggests that non-biomass variables (feeding history, reproductive status) may also modulate the production of some metabolites. A simple case can be made with the data from Clifford et al. (2020) where the composition of amino acids within the community excretions of zooplankton changes by season: glycine is dominant during the whole year, but second place changes from aspartic acid (spring) to alanine (summer) to serine (fall) and to an ambiguous tie between several others in the winter.

Some prominent metabolites are most likely derived from prey or the gut microbiome rather than the organism itself. The euphausiid, *Hansarsia microps*, produced remarkable amounts of 4-aminobenzoic acid; this compound is generally manufactured by plants and prokaryotes, and its use in the synthesis of folate is not known in animals, to the point where its receptors are the target of some antibacterial sulfonamides [166,167]. Of the crustacean genomes that are annotated in the Kyoto

Encyclopedia of Genes and Genomes (KEGG), none have enzymes that can utilize this compound [168,169]. *Hansarsia microps* and *Clio pyramidata* also excreted 2,3-dihydroxypropane-1-sulfonate, which almost certainly comes from their diet and passes through the digestive process unscathed. This sulfonate is a known product of phytoplankton metabolism [170], and if it is processed within the animals, it is likely due to their gut microbiomes [171–173].

The exact impact of digestive processing—or the lack thereof—is beyond the scope of this paper. Rather, we focus on the impact of zooplankton excretion on the dissolved metabolite pool in its aqueous vicinity. Each zooplankton species takes in, processes, and releases organic matter in ways that differ depending on the species and their respective microbiomes—among other variables.[153,171] Each animal is a point source of metabolites that moves throughout the water column; in this case, all species studied perform diel vertical migration. We can therefore ask: Is this a process that measurably impacts the flux of dissolved metabolites into different ocean strata?

Extrapolating these measured excretion rates will assume that organisms trapped in a bottle behave similarly to native behavior *in situ* and that the results were not simply due to stress response, but this assumption is largely taken for granted due to the constraints of experimental work with zooplankton (Amy Maas, personal communication). The effects of bottle incubations may depend on the number and diversity of zooplankton in the incubation: based on previous reports of amino acid excretion, rates for each specific compound seem to decrease when moving from a mixed consortium[74] to single-species[75], but in comparing numbers with Maas et al. (2020), going from ~50 *P. xiphias* copepods to one per sample increased observed

amino acid excretion rates by a median of 3.4-fold (in both cases normalized to biomass). What follows is a sort of thought experiment, and will be explored more fully in the context of field data in Chapter 4; regardless, the scaling involved in taking laboratory measurements to field modeling will take more work to constrain the variance among zooplankton.

3.3.3 Implications for the Microbial Ecosystem

In Figure 3-2, we present the top 8 (by median) metabolite excretion rates of each animal, as well as their matching measurements from the other species. Most critically, the four horizontal lines matching the colors of the various data represent "measurability"—that is, the excretion rate necessary for a zooplankter of average dry weight to change one liter of water by 10 picomoles of a metabolite in six hours. With the benzoylation method, this is roughly what would be required to measure a confident difference in field samples, although this will differ by metabolite. All but two metabolites in Figure 3-3 (sarcosine, ciliatine) are unilaterally above the measurability line for every animal species. Every putrescine rate estimate is two orders of magnitude above its respective threshold, indicating zooplankton excretion may be a major source of this linear diamine in the water column, supplying substantially more organic nitrogen than even taurine.

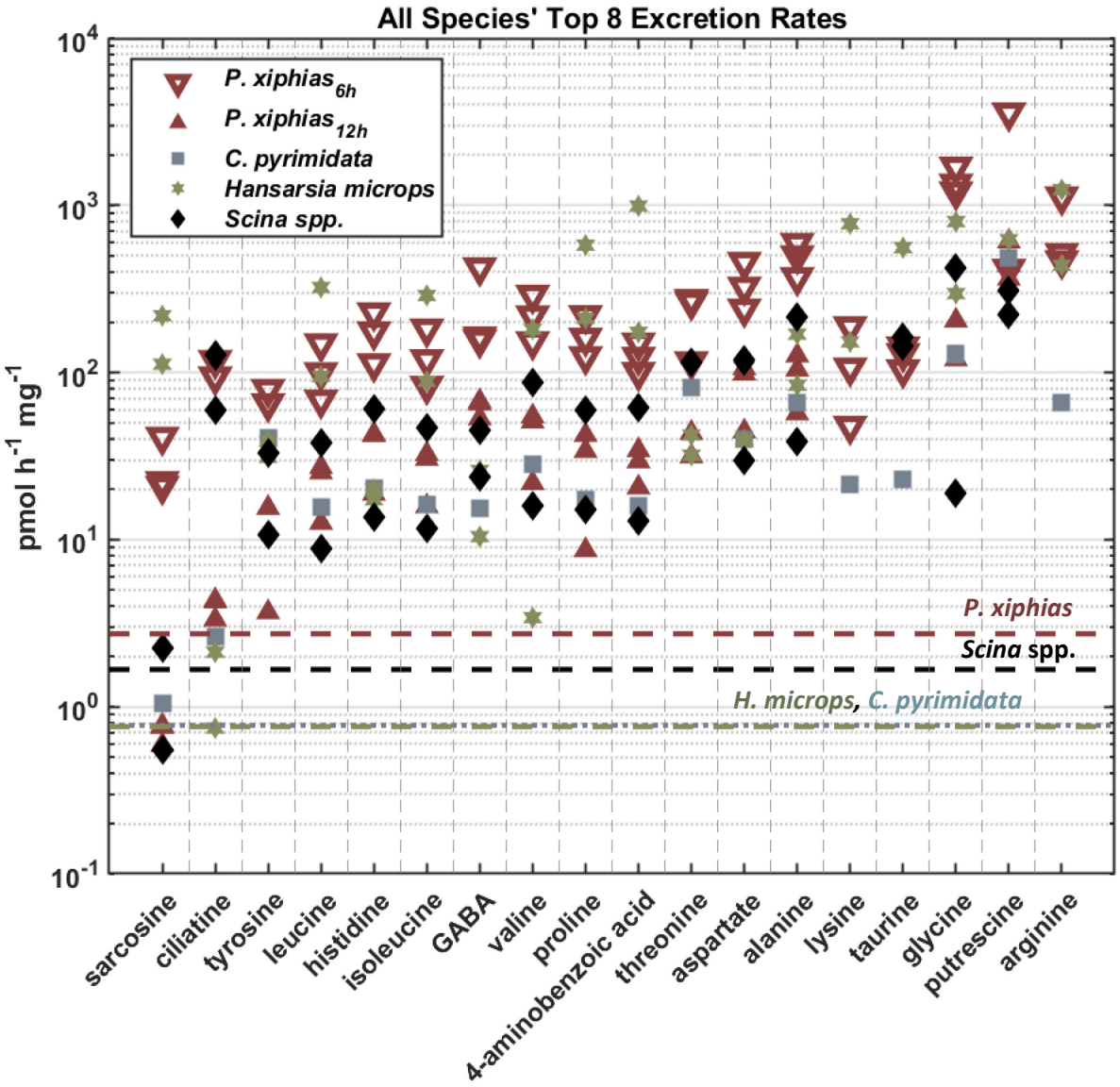

Figure 3-3: Most highly-excreted metabolites relative to field-relevance, sorted by increasing median excretion rate. Colored horizontal lines are the minimum rate for an animal of each species' average mass to increase the metabolite inventory in 1 L of water by 10 pM. Metabolites displayed are the union of each species' top eight excreta by median. Lines for *C. pyrimidata* and *H. microps* are the same.

The rates plotted for *P. xiphias* decrease over time: every six-hour metabolite excretion rate is higher than the 12-hour rates. Figure 3-2 displays similar information: the composition of excreted metabolites changed when the copepods were starved for 12 hours. Excretion rates of organic nitrogen are known to level off or decrease after

even four hours [71,174], so we assume our measurements are a lower bound compared to field conditions where animals continually feed.

Using the data and a modified version of the code from [165], we multiplied the excretion rates for *P. xiphias* at 6 hours (more metabolically active) by the approximate dry mass data from two multi-net, multi-depth plankton tows from cruise AE1712 (October 2017). We assumed a 12-hour residence time, as did Steinberg et al. (2002) when calculating organic N excretion. We used only data for live animals at the taxonomic level of Copepoda. While a conservative estimate, copepods composed >70% of the identified zooplankton in the 2021 dataset.

The results show that copepods alone may be an unparalleled source of amino acids, and a salient indicator of how fast the microbial mill can grind. Both the chlorophyll maximum and maximum heterotrophic production commonly occur at BATS between 50 and 200 m [80]. In this range, we estimated a 12-h copepod contribution of 17.8 nM (day) or 36.2 nM (night) contribution to glycine alone. Both of these numbers are larger than the ambient dissolved glycine concentrations measured in all samples from [175] at BATS, but their sampling was done during the day and at 5-20 m. We recalculated copepod glycine excretion as an hourly rate from the 0-50 m daytime net tow in [165] (0.563 nM h^{-1}) and divided this into their mean concentration (4.98 ± 3.54 nM): this results in a residence time of 8.84 ± 6.29 h for glycine. Strikingly, Suttle et al. (1991) estimated a glycine residence time of 10.4 ± 4.3 h from uptake by the *in-situ* bacterial community. Not only are these estimates astonishingly close; together they imply that there is a tight coupling between highly-excreted molecules from zooplankton and the ambient microbes.

3.4 Conclusions

Our intention was to expand the scope of ocean metabolomics beyond the actions of unicellular organisms and to provide novel insights into what is knowable about zooplankton physiology, at the molecular level. The manifold species of zooplankton in the upper ocean impact the microbial web that sits trophically below it in more specific ways than just elemental contributions. In comparing those contributions to our measurements, we can name and quantify up to 40% of the molecules within those pools.

Both the biology and the chemistry of the work described here leave much to be further explored. There are many metabolites that cannot be captured with benzoylation. Some can be measured with the more well-tested approach of acidic solid-phase extraction alone, and some that may require another method, such as aniline derivatization of carboxylic acids.[75] To truly test species differences, starvation responses, and allometric scaling, experiments with greater sample sizes and different species are required.

Acknowledgments

This research was made possible by help from Dr. Leo Blanco-Bercial and Yuuki Niimi (zooplankton collection and ID), Rachel Parsons and Marcus Simons-Rewan (instruction in cell counts), Dr. Craig Carlson (advice on getting clean water), Gretchen Swarr (maintenance of metabolite standards), and the small boat operators and technicians of the Bermuda Institute of Ocean Sciences. This work was funded by Simons Foundation International (Award 409923), The George F. Jewett Ocean

Ventures Fund, the MIT-BIOS Fund, and WHOI Academic Programs Endowed Funds.

The colors in this paper's figures were drawn from the album *Conversation Piece* (2011) by A Lot Like Birds.

3.6 Appendix A: Supplementary Methods

3.6.1 Benzoyl Chloride Derivatization and Workup

We dried acetone from the samples under nitrogen at 30 °C until they lost the mass of acetone added (3.786 g).

We extracted metabolites with 1 g BondElut PPL cartridges and evaporated the MeOH eluent in a Vacufuge (Eppendorf). We partially redissolved the analytes in 500 µL 5% (v/v) acetonitrile in MQ, then mixed with a vortexer. The liquid contained benzoic acid precipitate, so we centrifuged it at 20,000 x g for 15 minutes, moved the supernatant to a combusted 2 mL glass vial, and repeated this rinse/centrifuge a second time, combining the supernatants. We evaporated the ~1 mL of solvent again on the Vacufuge and did a final 100 µL 5% (v/v) acetonitrile rinse/centrifuge, this time transferring the supernatant to chromatography vials and adding 5 µL acetonitrile to prevent additional precipitation.

3.6.2 UHPLC-Orbitrap MS Conditions

Using an autosampler set to 4 °C, we injected samples (5 µL per ion mode) onto a reversed phase Waters Acquity HSS T3 column (2.1 × 100 mm, 1.8 µm) equipped with a Vanguard pre-column (Waters) held at 40 °C. We used mobile phases (A) 0.1% (v/v) formic acid in water and (B) 0.1% (v/v) formic acid in acetonitrile. The gradient, at 0.5 mL min-1, was: 0-0.5 min (1% B), 2 min (10% B), 2-5 min (10% B), 7 min (25% B), 7-9 min (25% B), 12.5 min (50% B), 13 min (95% B), 13-14.5 min (95% B) and re-equilibration with 1% B (total run time = 16 min). Other instrument parameters were: ESI voltages = 3600 V (positive) and 2600 V (negative); source gases = 55 (sheath), 20 (auxillary), and 1 (sweep); capillary temperature = 350 °C; vaporizer temperature = 400

°C. We collected MS data from 170-1000 m/z at resolution 60,000 fwhm (at m/z 200), automatic gain control (AGC) at 4e5, and max injection time 50 msec.

Upon detection of a target compound's mass, we isolated the parent ion in the quadrupole at a width of 1 m/z, and collected MS/MS data at resolution 7,500 fwhm, AGC at 5e4, and max injection time 22 msec using higher energy collisional dissociation (HCD) with 35% collision energy and intensity threshold at 2e4.

3.7 Appendix B: Incubation Metadata

I have included the complete table of metabolite measurements with a copy of the embedded metadata in the Supplemental Information file (Germolus_germolus_PhD_CEE_2024_tables_supplemental.xlsx); however, [] includes the information about incubation start times, stop times, animal species, and their dry weights. The “Sample Name” column corresponds to the name of the processed metabolite sample ID in the Supplementary Information sheet Chapter3_Measurements.

Table 3-4: Incubation metadata for zooplankton excretion experiment. Additional metadata, including exact start-stop times, can be found in the Supplemental Information file. CTRL = control; t_x = time point, with subscript being the nominal duration; Px = *P. xiphias*; Euph = Euphausiid; Cp = *C, pyramidata*; Amph = Amphipod. Numbers in the sample name denote unique IDs for both the incubation bottles and the derivatization process.

Sample_Name	***Species***	***Duration (h)***	***dry mass (mg)***	***Notes***
Zoop2_20_t0_ctrl_4	CTRL	0.8		
Zoop2_18_t0_ctrl_6	CTRL	0.8		
Zoop2_19_t0_ctrl_16	CTRL	0.8		
Zoop2_22_t6_ctrl_26	CTRL	6.1		
Zoop2_21_t6_ctrl_53	CTRL	6.1		
Zoop2_23_t6_ctrl_22	CTRL	6.1		
Zoop2_25_t6_Px_12	*Pleuromamma xiphias*	6.1	0.652	alive
Zoop2_24_t6_Px_52	*Pleuromamma xiphias*	6.2	0.647	alive
Zoop2_26_t6_Px_11	*Pleuromamma xiphias*	6.2	0.515	alive
Zoop2_28_t12_ctrl_5	CTRL	12.0		
Zoop2_29_t12_ctrl_25	CTRL	12.0		
Zoop2_27_t12_ctrl_2	CTRL	12.0		
Zoop2_32_t12_Px_18	*Pleuromamma xiphias*	12.1	0.567	alive
Zoop2_33_t12_Euph_24	*Hansarsia microps*	12.1	1.14	alive
Zoop2_34_t12_Euph_68	*Hansarsia microps*	12.1	3.244	alive
Zoop2_37_t12_Cpy_9	*Clio pyrimidata*	12.1	2.219	DEAD
Zoop2_30_t12_Px_57	*Pleuromamma xiphias*	12.1	0.726	alive
Zoop2_35_t12_Euph_15	*Stylocheiron abbreviatum*	12.1	9.878	DEAD
Zoop2_31_t12_Px_10	*Pleuromamma xiphias*	12.1	0.555	alive
Zoop2_36_t12_Cpy_3	*Clio pyrimidata*	12.2	2.151	alive
Zoop2_39_t12_Amph_21	*Scina* spp.	12.2	1.228	alive
Zoop2_38_t12_Amph_17	*Scina* spp.	12.2	0.765	alive

3.8 Appendix C: Metabolite Measurements

Table 3-5: All metabolite concentrations for Chapter 3. This sheet contains "raw preprocessed data": In other words, the concentrations have been calculated, but I have not removed metabolites that I consider suspect, nor have I done anything to account for the controls. Red text indicates an animal that died by the incubation end, blue cells contain values below the LOD, and orange cells are extrapolated (above standard curve).

				Sample Name and Concentration (pM)																					
Trivial Name	LOD #bz (pM)		Max Std. (pM)	Zoop2_37_t12_Cpy_9	Zoop2_29_t12_ctrl_25	Zoop2_22_t6_ctrl_26	Zoop2_25_t6_Px_12	Zoop2_20_t0_ctrl_4	Zoop2_18_t0_ctrl_6	Zoop2_34_t12_Euph_68	Zoop2_35_t12_Euph_15	Zoop2_30_t12_Px_57	Zoop2_39_t12_Amph_21	Zoop2_28_t12_ctrl_5	Zoop2_27_t12_ctrl_2	Zoop2_33_t12_Euph_24	Zoop2_23_t6_ctrl_22	Zoop2_32_t12_Px_18	Zoop2_26_t6_Px_11	Zoop2_31_t12_Px_10	Zoop2_24_t6_Px_52	Zoop2_36_t12_Cpy_3	Zoop2_38_t12_Amph_17	Zoop2_21_t6_ctrl_53	Zoop2_19_t0_ctrl_16
2'deoxycytidine	1	54.5	30807.1	0	0	0	3531	0	0	0	0	0	0	0	0	0	0	0	0	0	0	0	0	1037	0
2'deoxyguanosine	1	46.3	26193.7	7	0	0	0	0	0	20	11	0	0	0	0	0	0	0	0	0	0	0	0	0	0
2'deoxyuridine	1	54.3	30674.8	118	132	122	230	293	200	311	9684	218	121	78	141	134	145	246	120	248	233	78	272	78	334
adenosine 3′-monophosphate	1	35.7	20160.1	732	24	0	1133	0	37	300	355	224	2575	202	0	110	0	343	91	103	155	451	1196	0	0
4-aminobenzoic acid	1	90.3	51042.7	7836	775	1124	7085	742	1078	647999	2930000	4321	2523	1085	804	39292	877	2654	2361	1599	5258	6247	8965	844	1085
adenosine 5′-monophosphate	1	31.7	17894.6	663	14	0	847	0	36	259	277	207	2262	195	0	82	0	272	91	77	137	422	1323	0	18
inosine 5′-monophosphate	1	31.6	17849.4	490	151	127	132	138	120	3865	62270	141	133	121	132	390	150	124	125	127	120	268	165	121	139
uridine 5′-monophosphate	1	33.6	19014.0	363	36	36	218	36	36	766	858	111	123	90	36	1027	36	36	45	39	72	200	107	36	36
5'deoxyadenosine	1	49.3	27861.8	0	0	0	0	0	0	0	0	0	0	0	0	0	0	0	296	0	0	791	0	0	0
2,3-dihydroxypropane-1-sulfonate	1	79.3	44825.8	8245	0	0	339	0	0	5776	3876	243	390	0	0	1439	0	423	327	385	0	3763	333	0	0
gamma-aminobutyric acid	1	120.1	67882.1	1099	0	0	21118	404	0	853	25225	3600	0	1217	0	0	0	1718	1109	0	3676	800	1048	0	0
4-methyl-5 -hydroxyethylthiazole	1	86.5	48879.3	248	248	248	248	248	248	248	252	248	248	248	248	248	248	248	248	248	313	248	248	248	248
4-amino-5-hydroxymethyl-2-methylpyrimidine	1	89.0	50301.8	0	0	0	6502	14043	7656	0	5534	15112	0	0	7358	0	11627	10651	0	23515	0	5134	8338	0	19897
N-acetyl-D-glucosamine	1	56.0	31645.6	3369	532	2042	532	0	1118	10398	36244	420	0	0	580	5437	993	3688	1897	1039	1773	4605	4631	0	0
N-acetyl-muramic acid	1	42.2	23868.8	128	86	58	77	0	58	291	187	61	0	47	141	118	128	99	0	125	90	316	178	100	213
(1,2-dicarboxyethyl) glutathione	1	29.2	16532.8	0	0	0	0	0	0	0	0	0	0	0	0	0	0	0	0	0	3	3	0	0	2

Sample Name and Concentration (pM)

Trivial Name	LOD #bz	LOD (pM)	Max Std. (pM)	Zoop2_37_t12_Cpy_9	Zoop2_29_t12_ctrl_25	Zoop2_22_t6_ctrl_26	Zoop2_25_t6_Px_12	Zoop2_20_t0_ctrl_4	Zoop2_18_t0_ctrl_6	Zoop2_34_t12_Euph_68	Zoop2_35_t12_Euph_15	Zoop2_30_t12_Px_57	Zoop2_39_t12_Amph_21	Zoop2_28_t12_ctrl_5	Zoop2_27_t12_ctrl_2	Zoop2_33_t12_Euph_24	Zoop2_23_t6_ctrl_22	Zoop2_32_t12_Px_18	Zoop2_26_t6_Px_11	Zoop2_31_t12_Px_10	Zoop2_24_t6_Px_52	Zoop2_36_t12_Cpy_3	Zoop2_38_t12_Amph_17	Zoop2_21_t6_ctrl_53	Zoop2_19_t0_ctrl_16
alanine	1	139.0	78572.2	27349	716	1108	28745	947	1792	107003	1529531	14700	5823	1528	857	15452	920	8061	8786	2575	22458	24859	29615	1607	2823
arginine	1	71.1	40183.7	120073	0	823	65555	0	3109	838532		26421	18623	5436	0	127329	723	18143	17710	13155	21437	55655	19495	2109	751
asparagine	1	93.7	52982.1	11228	0	0	7476	0	180	19949	37261	3313	1928	0	0	6513	0	2141	2677	311	4808	9598	5467	0	0
aspartate	1	93.0	52592.0	11776	295	1041	22778	363	1405	21954	43147	12113	3961	1266	282	5697	829	7815	4979	1545	13876	14080	15009	1198	1421
chitobiose	2	29.2	16493.9	580	0	354	0	0	491	14436	3207	0	383	283	0	8104	245	0	0	233	378	959	296	0	0
chitotriose	1	19.7	11159.1	55	31	31	63	31	31	805	189	31	31	31	31	475	31	31	31	31	40	81	31	31	31
ciliatine	1	99.0	55973.1	3707	0	0	0	0	0	0	1778	0	14394	0	0	0	0	0	0	0	0	660	19562	0	0
citrulline	1	70.7	39956.6	988	0	165	3479	0	260	654	5537	1790	359	143	0	425	131	1087	783	164	1471	1463	1839	278	72
cysteate	1	73.2	41383.4	1649	0	0	0	0	0	8694	64749	0	0	0	0	3024	0	0	0	0	0	1962	0	0	0
cysteine	1	102.2	57774.8	7506	905	905	1280	907	910	11705	32849	1061	1131	930	914	2895	905	1117	1020	1018	1023	5162	1090	905	905
cytidine	1	50.9	28780.5	1730	167	145	333	153	158	825	5724	198	221	241	111	526	197	0	240	222	183	653	168	200	218
cytosine	1	111.5	63006.3	38327	12659	0	23036	0	4294	0	8698	17190	18675	0	0	8244	3057	0	7686	3376	17683	2735	51494	8708	34231
desthiobiotin	1	57.8	32670.6	0	0	0	0	0	0		0	0	0	816	0	0	0		0	0	0	0	0	0	0
ectoine	1	87.1	49240.3	7231	0	0	8391	0	0	11011	78840	0	0	0	0	0	0	0	0	0	0	3333	0	0	0
folate	1	28.1	15858.6	94	96	103	93	97	93			94	93	93	96	173		93	93	93	93	94	131	97	94
glucosamine-6-phosphate	1	47.8	27021.8	604	335	335	335	335	335	335	335	335	335	335	335	335	335	335	335	335	335	5555	335	335	335
glucose 6-phosphate	1	40.7	23018.7	265	109	109	247	109	109	379	1903	140	109	109	109	200	109	138	109	109	110	113	109	109	109
glutamic acid	1	84.2	47577.0	24439	0	0	8013	0	359	23040	40528	5291	1836	0	0	5914	0	3522	2168	599	4048	13557	3537	0	0
glutamine	1	84.7	47899.3	40012	0	0	5997	0	0	33214	246972	3164	1189	0	0	11546	0	2588	5258	913	6499	21160	2549	0	0
glutathione	2	40.3	22779.0	2278	0	0	305	0	0	822	2213	415	0	0	0	173	0	165	317	107	177	1742	0	0	0
glycine	1	165.0	93246.3	137837	604	3398	82880	1116	3528	533993	11113832	41472	16222	3185	0	79555	1785	25193	33584	7124	58851	68006	77044	3686	7172
glyphosate	1	73.2	41403.0	169	169	169	169	169	169	169	169	169	169	169	169	169	169	169	169	169	169	169	169	169	169

				Sample Name and Concentration (pM)																					
Trivial Name	LOD #bz (pM)		Max Std. (pM)	Zoop2_37_t12_Cpy_9	Zoop2_29_t12_ctrl_25	Zoop2_22_t6_ctrl_26	Zoop2_25_t6_Px_12	Zoop2_20_t0_ctrl_4	Zoop2_18_t0_ctrl_6	Zoop2_34_t12_Euph_68	Zoop2_35_t12_Euph_15	Zoop2_30_t12_Px_57	Zoop2_39_t12_Amph_21	Zoop2_28_t12_ctrl_5	Zoop2_27_t12_ctrl_2	Zoop2_33_t12_Euph_24	Zoop2_23_t6_ctrl_22	Zoop2_32_t12_Px_18	Zoop2_26_t6_Px_11	Zoop2_31_t12_Px_10	Zoop2_24_t6_Px_52	Zoop2_36_t12_Cpy_3	Zoop2_38_t12_Amph_17	Zoop2_21_t6_ctrl_53	Zoop2_19_t0_ctrl_16
guanosine	1	43.7	24717.5	505	0	0	127	0	0	1252	18220	91	322	106	0	656	0	0	0	0	0	230	192	0	125
histidine	1	79.8	45117.6	8376	0	909	11283	0	916	9938	33771	4906	2066	600	0	3243	580	3455	2045	746	7728	7496	8154	532	348
homoserine	1	104.0	58764.3	94	0	0	118	0	57	120	535	7755	0	108	0	0	0	0	142	0	81	76	0	57	105
homoserine betaine	1	76.9	43478.3	266832	0	0	1577	0	0	30991	34251	0	10308	0	0	6184	0	0	0	0	0	117123	4309	0	0
inosine	1	46.2	26097.0	1763	0	0	634	392	880	14657	320650	399	1871	443	0	2654	510	382	0	0	0	709	484	0	1837
isethionate	1	83.6	47262.2	113942	0	0	4348	0	0	35433	21992	1346	0	0	0	14491	0	949	2070	696	3957	28213	0	0	0
isoleucine	1	94.4	53365.9	6058	0	550	9113	0	636	187499	182736	3418	1540	515	0	18979	181	2127	1321	427	4881	5753	5943	458	327
kynurenine	1	59.5	33619.9	1949	0	0	1237	0	0	4582	18143	702	0	0	0	697	0	233	108	0	690	942	510	0	0
leucine	1	94.4	53365.9	5873	252	712	7730	245	708	210024	139389	3038	1248	544	174	20817	298	1936	1421	470	4435	5880	5015	502	493
lysine	1	84.7	47882.9	51891	0	499	13004	0	668	520444	134865	5930	3294	472	0	48291	189	3888	2947	953	7513	22532	8335	481	290
malic acid	1	92.4	52203.7	5657	432	498	6065	1896	1017	6121	40321	9135	2748	1727	727	3321	872	3728	1216	1316	893	2782	3416	1355	3145
methionine	1	83.0	46913.7	3411	0	0	1019	0	0	10021	70454	1095	179	0	0	1294	0	0	210	0	254	2073	995	0	0
muramic acid	1	49.3	27862.9	0	0	78	0	0	114	59	0	0	0	95	0	63	0	354	0	45	108	63	190	53	0
ornithine	1	73.3	41439.7	1093	0	115	3613	0	247	576	6598	1949	254	73	0	448	77	1158	655	86	1639	1695	1765	248	0
pantothenic acid	1	52.0	29378.4	1749	0	0	195	0	0	1820	2114	204	117	0	0	429	0	223	76	194	139	985	64	0	13
phenylalanine	1	75.0	42375.4	5814	0	439	5794	0	305	11286	76594	2395	990	335	0	5487	161	1296	954	281	3664	3859	3737	262	146
proline	1	107.6	60800.8	10015	0	312	10634	0	286	377629	9675003	6203	3778	831	230	48414	282	3881	2583	975	6676	7557	9345	293	219
putrescine	1	76.9	43459.4	882	55	1066	461	0	30	2915	1227	1309	88	0	0	565	0	91	119	69	372	547	186	796	0
pyridoxine	1	60.2	34040.1	0	15609	0	0	0	0	0	0	0	0	19459	3739	0	0	0	79117	0	0	0	0	0	0
sarcosine	1	139.0	78572.2	1423	0	0	2156	0	0	142832	770540	0	472	0	0	25652	0	0	592	0	799	367	0	0	0
serine	1	117.8	66609.6	31554	1564	4827	72670	1505	6744	43530	204667	42249	16945	6723	1282	16318	3218	27520	19725	6924	50924	52465	61027	4919	4694

				Sample Name and Concentration (pM)																					
Trivial Name	LOD #bz (pM)		Max Std. (pM)	Zoop2_37_t12_Cpy_9	Zoop2_29_t12_ctrl_25	Zoop2_22_t6_ctrl_26	Zoop2_25_t6_Px_12	Zoop2_20_t0_ctrl_4	Zoop2_18_t0_ctrl_6	Zoop2_34_t12_Euph_68	Zoop2_35_t12_Euph_15	Zoop2_30_t12_Px_57	Zoop2_39_t12_Amph_21	Zoop2_28_t12_ctrl_5	Zoop2_27_t12_ctrl_2	Zoop2_33_t12_Euph_24	Zoop2_23_t6_ctrl_22	Zoop2_32_t12_Px_18	Zoop2_26_t6_Px_11	Zoop2_31_t12_Px_10	Zoop2_24_t6_Px_52	Zoop2_36_t12_Cpy_3	Zoop2_38_t12_Amph_17	Zoop2_21_t6_ctrl_53	Zoop2_19_t0_ctrl_16
glycerol 3-phosphate	1	33.4	18897.5	17178	179	0	6200	149	167	62503	236228	1269	14450	175	0	25406	0	2556	549	448	777	10889	6035	169	177
spermidine	1	85.3	48192.8	3482	0	0	989	0	0	1312	2391	0	0	0	0	0	0	0	0	0	0	1594	0	0	0
syringic acid	1	62.5	35323.2	1303	144	144	144	144	144	144	1030	144	144	144	144	144	144	144	144	144	144	1541	144	144	144
taurine	1	99.0	55932.9	129850	0	0	3413	0	0	414693	10632225	3222	90243	0	0	47225	0	2878	2325	1744	1666	59404	71823	0	0
thiamine monophosphate	1	29.7	16793.8	8	0	0	7	0	0	0	13	7	0	0	0	0	0	3	0	0	0	10	0	0	0
threonine	1	104.0	58764.3	37981	234	897	18289	0	945	31313	124188	10049	2976	667	279	11023	1255	7275	6137	2105	17607	39299	21687	1149	1181
thymidine	1	51.1	28898.2	405	0	0	86	0	0	1508	44063	0	0	0	0	936	0	71	0	0	0	0	92	0	0
tryptamine	1	77.3	43689.9	8	5	6	5	6	6	7	9	6	6	6	5	6	6	5	7	5	6	8	6	5	5
tryptophan	1	60.6	34275.1	2784	0	0	1072	0	0	7489	23855	285	88	0	0	960	0	102	0	0	877	1556	901	0	0
tyrosine	1	68.3	38633.5	10157	0	0	7102	0	0	21729	99178	3680	4065	0	0	10291	0	1829	1631	0	6150	19054	6570	0	0
uridine	1	50.7	28665.0	1039	196	207	605	208	189	4590	45240	349	600	304	203	2294	199	289	317	244	314	494	475	179	217
valine	1	105.7	59752.5	12712	167	944	14307	0	829	666	14180	6438	2423	561	0	40118	326	4239	3027	882	9460	10688	11955	647	682
xanthosine	1	38.7	21857.2	282	16	16	16	22	16	24	269	16	16	16	16	16	16	16	16	16	16	292	16	16	16

Chapter 4: Interpreting dissolved metabolites in the Sargasso Sea through mixing, photochemistry, and zooplankton excretion

Co-authors[g]: Krista Longnecker, Melissa C. Kido Soule, Elizabeth B. Kujawinski

Abstract

Metabolites are the unique molecular species that together make up much of the labile dissolved organic matter in the ocean. These molecules are the signals and resources on which the microbial loop depends, and they are also chemical species with diverse arrays of sources and sinks. We quantified several metabolites over the course of a two-day sampling period in the <0.2 μm phase at Hydrostation S in the North Altantic Ocean. Using aqueous derivatization and LC-MS, we quantified 60 different dissolved metabolites at six-hour intervals. Here we describe the general patterns and pair the measurements with novel estimates of photochemical, excretory, and physical sources and sinks to separate the underlying microbial ecosystem from the other variables impinging upon its influence on the dissolved organic compounds of the ocean. We found that mixing plays a large role in shaping dissolved metabolite profiles, that copepods alone may supply the entire daily inventory of many metabolites through excretion, and that photochemistry plays a gradual role in shaping the available labile compounds.

4.1 Introduction

Dissolved (DOM) and particulate (POM) organic matter in the ocean has often been a quantity observed through elemental totals (ex. organic carbon) or ratios (ex. C:N:P).[51,176,177] Such quantities are invaluable for understanding the mechanics of the ocean as a physical system,[178] an ecosystem,[15] and a climate-controlling mechanism.[179] Even so, there is more complexity within the broad umbrella of DOM, of which metabolites comprise an ecologically critical subset. The metabolite subset of organic matter is defined either strictly by its biogenic origins and/or functionally through its size and lability; either way, it is the group of individual molecular species on which cells subsist and the language in which they speak to each other.[13,14] Language,[180] or

[g]Woods Hole Oceanographic Institution, Woods Hole, MA, USA

sometimes currency,[181] are both analogic frameworks applied in the metabolite literature. These modalities evoke a complexity of signaling,[8] cooperation,[94] and competition that can only be resolved by examining the words—metabolites—of the language.

It is increasingly common to apply the techniques of metabolomics to extracellular, or dissolved, organic matter in environmental samples, resulting in tens to thousands of simultaneous chemical measurements.[6,182,183] Questions for these tools began modestly: what is *in* DOM?[184,185] This naturally led to trying to identify the dominant functional groups within DOM,[186] to the conclusion that the most highly-labile components of DOM are those with concentrations approaching the limit of what a cell can use, with short (often <1 d) lifetimes and appreciable concentration gradients at every spatial scale from microns to kilometers.[6,187,188] The measurements used for this purpose of teasing apart dissolved organic chemicals—variations on nuclear magnetic resonance and chromatography/mass spectrometry—when applied to organismal tissue are commonly colloquialized as a "snapshot"[189–191] of the biological metabolism. The extracellular, or dissolved, phase is often treated as a reservoir among the microbes that interact with dissolved organic matter as a fleeting commerce, with labile metabolites such as amino acids and nucleotides turning over on timescales of hours to weeks.[10,187,192]

The chemical interactions between organisms occur with such rapidity and on such small spatial scales that discussions of dissolved metabolites generally omit non-biological flux mechanisms, as they are assumed to be negligible compared to microbial exchange. When specific molecules are analyzed, this is often not the case. For

example, dimethylsulfoniopropionate (DMSP) and its subsequent degradation products undergo photochemical reactions *in situ*, and many extremely labile compounds are known to be produced from the photochemical breakdown of organic matter.[58,92,193] The amino acids histidine, tryptophan, kynurenine, and methionine, as well as the B-vitamins riboflavin and cobalamin are all photolabile to various extents.[60,105,109,194,195] Thiamine, a known auxophore, spontaneously hydrolyzes in slightly basic conditions.[83,85,196] Amino acids (among other metabolites) are both susceptible to complexation by metals and known to be excreted by zooplankton.[65,75,197] Even more strikingly, some of these interactions enhance each other: copper complexes can be photoreduced,[65] and some metabolites can accelerate the breakdown of others.[93,198,199] It is already a daunting task to model the ecology of the ocean's microbiome at a chemical level, but doing so must consider which production and consumption terms occur on similar time scales to metabolism and account for the unique chemical behaviors of each metabolite.

Expanding metabolite analysis to allow both microbiological and physical interpretations parallelizes the rates, fluxes, and structures we can directly evaluate, and provides insight that cannot be gained through conventional approaches that look at bulk dissolved organic matter or divide it into broad classes.[200,201] Applying this perspective to the extracellular environment of the ocean allows the fullness of chemical ecology to come into focus in a way that modeling monadic microbes in terms of their internality—their genomes, transcriptomes, endometabolomes, etc.—does not, while caring for the molecule-specific interdependencies upon which microbial ecosystems rely.[94,95,202] In this paper, we report a novel set of benzoyl chloride-derivatized metabolite measurements from the Sargasso Sea in November 2021 and ask what

factors might participate in their fluxes using a few illustrative examples. We evaluated, based on experiments described elsewhere, the influence of zooplankton excreta and photochemical decay on metabolite concentrations. We also fold in new estimates of vertical eddy mixing to evaluate an apparent pulse (and disappearance) of several compounds at distinct points in space and time.

4.2 Methods and Materials

4.2.1 Site Description

Hydrostation S (32° 10′ N, 64° 30′ W) has been profiled biweekly for temperature, dissolved oxygen, and salinity since 1954, and its nearby (60 km, 31° 40′ N, 64° 10′ W) sibling, the Bermuda Atlantic Time-series Study site (BATS) has a shorter history (monthly, 1988-present) but broader scope of chemical and biological measurements such as bacterial production, chlorophyll, and nutrients.[80,203] The two are sometimes treated as one superset of observations, as hydrography between the sites is "statistically indistinguishable".[203,204] In November 2021 we occupied Hydrostation S aboard the R/V *Atlantic Explorer* as part of BIOS-SCOPE cruise AE2123, sampling nutrients, dissolved organic carbon, microbial diversity, and metabolites in CTD casts every six hours for two days. This work focuses on the dissolved metabolites, which we sampled on eight casts—three "day" and five "night" casts as defined by sunrise/sunset. Four casts were more accurately "dusk" or "dawn" and, as marginal cases, will not be used to assess day/night differences.

4.2.2 Collection of Water and Derivatization

During each cast, we sampled 4-8 depths in triplicate 25 mL aliquots, which we filtered through a 0.2 μm PTFE membrane (Omnipore) into an amber glass 40 mL EPA vial.

Immediately following collection, we derivatized samples using the procedure of Widner et al. (2021). Briefly: we basified each sample to pH 12 with 750 µL 8 M NaOH, added 5 mL 5% (v/v) benzoyl chloride in acetone, agitated for five minutes, and quenched the reaction with 375 µL H_3PO_4. To each sample we then added 250 µL of a $^{13}C_6$-benzoyl chloride derivatized mix of 111 standards (the stable isotope labeled internal standard, or SIL-IS). Quantification based on the analyte-isotopologue ratio is sensitive to variation when the analyte (numerator) is far more concentrated than the SIL-IS (denominator), with measurement variance inversely proportional to the SIL-IS signal. Hence, we chose the specific volume of SIL-IS (equivalent to a 164 pg/mL spike) to produce analyte-isotopologue signal ratios ≤ 1. All samples were frozen at -20 ^{o}C until workup back at the Woods Hole Oceanographic Institution (Woods Hole, MA, USA).

4.2.3 Auxiliary Measurements

We paired other data collected on cruise AE2123 casts with the metabolite data, including direct (photosynthetically active radiation (PAR), temperature, salinity, chlorophyll fluorescence) and derived (density, buoyancy frequency (N^2)) measurements from the SBE9 sonde (Seabird Electronics, Inc.) on the Niskin rosette. We also used bacterial cell counts collected in tandem by Shuting Liu (Kean University) and examined by Rachel Parsons (ASU Bermuda Institute of Ocean Sciences) with epifluorescence microscopy.

Using the wind speed data collected from the R/V Atlantic Explorer's main mast anemometer, along with the profile measurements, we calculated an estimate of vertical eddy diffusivity K_z following the formula of Haskell et al. (2016) after replacing all negative N^2 values with small non-zero values (10^{-5}).[77]

Amy Maas (ASU BIOS) provided zooplankton counts and biomass estimates from two multi-level net tows taken in October 2017. We filtered the data from two tows (day and night) down to live copepods (~70% of collected organisms) and estimated the biomass in eight depth bins using a published algorithm recoded in MATLAB R2023a.[165]

4.2.4 Standards and Processing of Metabolite Samples

Our standard curves had 9 points and 111 metabolites, ranging from 5 pg mL^{-1} to 1 ng mL^{-1} (per metabolite) and employing the same derivatization method and SIL-IS mix as the samples. We made four standard curves: a duplicate set at the beginning of the cruise (~1 day before sample collection) and at the end of the cruise (~2 days after sample collection). The SIL-IS yielded isotopologues for every analytical target. We performed solvent removal (dry-down), solid-phase extraction, and concentration in accordance with Widner et al. (2021).

We used a Vanquish UHPLC system (Thermo Fisher Scientific) to perform chromatographic separation on each sample, coupled to heated electrospray ionization (H-ESI) and an Orbitrap Fusion Lumos for mass spectrometric analysis. The Lumos used a full-scan MS mode with data-dependent tandem MS specified by a list of user-defined parent ions with a retention time (RT) window (full MS/ddMS^2 with inclusion list). All MS scans occurred in the Orbitrap analyzer, with MS peak areas used for quantification and MS/MS scans used for confirmation. Sample order was randomized, except for standard curves and a pooled sample every ten samples. Additional information on the column, mobile phases, and MS parameters is in section 4.5.2.

We integrated the chromatographic peaks in Skyline[103] for each target and its corresponding SIL-IS while monitoring both diagnostic mass fragments and retention times against known values.

We used an in-house data pipeline, SkyMat (github.com/WHOIGit/SkyMat), to pull in the integrated peak areas for the analytes and their ^{13}C isotopologues in both positive and negative ionization modes. Using the ratios of light-to-heavy peak areas (light-to-heavy ratio or LHR), this generated up to two standard curves for each ion mode (post-cruise and pre-cruise duplicates folded into one curve each). Rather than keeping one ionization mode for each metabolite, we used a new algorithm to sort measurements based on the regions of each curve that had lower error. First, we converted the data to a molar basis and evaluated the 95% prediction intervals of each regressed standard curve.

$$PI(x) = \text{tinv}(0.975, n-2) \cdot S_{yy} \cdot \left(\frac{(1-R^2)(n-1)}{(n-2)S_{xx}}\right)^{\frac{1}{2}} \cdot \left(\frac{(n+1)S_{xx}}{n} + (x-\bar{x})^2\right)^{1/2}$$

Equation 4-1: 95% prediction interval on a standard curve where y (LHR of an analyte) is regressed on x (the concentration of a standard).

In Equation 4-1, the 95% prediction region on y is $y \pm PI(x)$. The function *tinv* is the inverse CDF of the t-distribution with $n-2$ degrees of freedom; S_{xx} and S_{yy} are the sum of squared deviations from the mean of x (concentration) and y (LHR). R^2 is the coefficient of determination for the regression, and n is the number of points in the regression. "Mean of x" is notated as $\bar{x}$. PI is a smooth paraboloid function and symmetric about y, which in this case is the LHR of metabolites in a standard—what we needed was the uncertainty in concentration (x). We inverted $PI(x)$ around the calibration curve by treating the symmetric y-intervals as components of congruent right

triangles sharing a vertex at $y(x)$ and bearing two horizontal prediction intervals $\Delta x = \pm PI(x)/m$ corresponding to concentrations at $x \pm \Delta x$. Because each x produces two values ($x \pm \Delta x$) that do not match the original value of x but are offset by Δx, we calculated both values for every x in the curve and interlaced the two smooth functions to yield one paraboloid spanning the entire range of the calibration curve. We found the intersection x_{crit} (if it existed) of the curves in both positive (Δx^{pos}) and negative (Δx^{neg}) ion modes, which marked the location where the confidence of one curve overtook the other. For example, if $\Delta x^{pos} < \Delta x^{neg}\ \forall\ x < 100\ pM$, we kept the positive mode values below that concentration and used negative mode above 100 pM. If the two curves had no intersection, we simply used data from whichever mode performed better unilaterally.

After all calibration and sorting steps, we eliminated each metabolite measurement below its respective limit-of-detection (LOD; $3.3 \cdot s_b/m$, where s_b is the standard deviation of the calibration y-intercept and m is the calibration slope).[205]

We evaluated zooplankton (copepod) excretion rates based on metabolite excreted, minus time-matched azoic control, normalized to biomass and incubation time (pmol mg^{-1} h^{-1}). The original datafiles used in this experiment are available in MetaboLights (www.ebi.ac.uk/metabolights/MTBLS9057) and the codes used for figure generation and data processing are available at GitHub (https://github.com/germo006/Chemstation-S).

4.2.5 Rate Approximations and Notation

We evaluated three non-microbiological factors (copepod excretion, direct photolysis, and mixing) that may have affected our observed concentrations through three separate forms of rate/flux modeling. For the sections that follow, we presented mathematical

representations of these processes with concentration, rate, extinction coefficient, and quantum yields represented using symbols (C, or subscript i) generalizable to any metabolite.

4.2.6 Metabolite Mixing

We used the K_z profiles to evaluate how vertical mixing would or would not affect detection of a large input provided by a source such as a dense population of migratory zooplankton during a period of residence at a single depth. Because of the local importance of metabolite inputs and the relatively large spatial distances between samples (>10 m), we simulated a pulse input at two depths z_0: 25 m (in the mixed layer) and 115 m (below the mixed layer). We set the pulse magnitude C_0 to the mean concentrations in one abnormally concentrated sample set (Cast 6 Niskin 13; C6N13) from 115 m. We estimated a background concentration C_b equivalent to the mean of all measurements less than twice the median for the whole dataset, excluding non-detects. We set two vertical scale parameters of the pulse based on our sampling strategy: z_b, the minimum distance between C6N13 and its nearest sampled neighbor (15 m); and z_g, a gradient width parameter set to 5 m and defined as the distance from the pulse center where $C(z_0 \pm z_g) = C_{peak}/2$, or the distributional parameter half width at half maximum. We fit splines over the five points determined by these boundaries using a method less sensitive to overshoots than normal cubic fits in 0.1 m intervals,[206] and padded the boundary conditions out to $z_0 \pm 2z_b$ with C_b to allow diffusion to extend beyond the peak itself.

We used two casts' K_z profiles, Cast 6 (upon which C_0 was based) and Cast 7, its temporal successor (+ 6.5 hours). Each K_z profile was dictated by the CTD's depth

measurements, so we aligned these profiles with the simulation depths and with each other through bilinear interpolation across space (to match depth) and then time (to create a gridded $K_z(z,t)$).

Using the vectors of concentration and depth, and the matrix of vertical diffusivity, we solved the standard diffusion equation forward in time for six hours using the `ode45` function in MATLAB.

$$\frac{dC}{dt}(z) = -\frac{d}{dz}\left(K_z\left(\frac{dC}{dz}\right)\right)$$

Equation 4-2: Vertical mixing by eddy diffusion.

We calculated all derivatives based on a two-point central difference formula, or in the cases of endpoints, a three-point formula of equivalent accuracy.[207]

4.2.7 Comparing Excretion to Standing Stocks

We applied our copepod biomass density estimates to the metabolite excretion rates calculated for *Pleuromamma xiphias* in Chapter 3 via the formula of Steinberg et al. (2002) to calculate excreted metabolite quantity as a concentration change (ΔC, pM) at a depth assuming a zooplankton residence time t_r of 1 h (as opposed to Steinberg et al.'s 12 h, due to the evidence that metabolic rates may be subject to change on >6 hour scales):[71]

$$\Delta C = \frac{m_{dry}}{V_{tow}} \cdot r_{mtab} \cdot t_r$$

Equation 4-3: Zooplankton metabolite excretion in the water column.

The variable m_{dry} here was the sum of copepod dry mass estimates in a given net tow, V_{tow} was the volume of water filtered by that tow (L), and r_{mtab} was the dry-mass normalized metabolite excretion rate (pmol mg_{DW}^{-1} h^{-1}).

To estimate a residence time based solely on this production, we used an hourly rate of change ($\Delta C/12$, pM h^{-1}) and divided the ambient concentrations by this value for each metabolite sample. To align day/night differences between the metabolite and zooplankton data, we performed this calculation only on casts that were distinctly "day" (Casts 4 and 8, around noon) and "night" (Casts 2 and 6, around midnight). We restricted the residence time calculation to the depths where we had densely sampled metabolites (<200 m).

4.2.8 Photochemical Decay

We calculated a rate of photolysis for two metabolites whose apparent quantum yields of photolysis were calculated in Chapter 2. As there was no spectrally-resolved irradiance measured during the cruise, we modeled the downwelling irradiance for the two midday casts (both normal and diffuse horizontal from 280-800 nm) using SMARTS, and adjusted these surface values for diffraction and scattering upon entering the water using the routine of Zepp and Cline to give a combined surface photon fluence for each wavelength, $Z_{\lambda,SMARTS}$ (μmol photons s^{-1} m^{-2} nm^{-1}).[119,148] We scaled these simulated surface-level values based on measurements of photosynthetically active (400-700 nm) radiation taken by the PAR sensor on the CTD. This involved fitting an exponential curve to PAR as a function of depth and taking PAR_0 as the intercept, as the CTD did not record measurements shallower than about 3 m. We adjusted the SMARTS values to Z_λ (μmol photons s^{-1} m^{-2}) as follows:

$$Z_\lambda = Z_{\lambda,SMARTS} \cdot \left(\frac{PAR_0}{\sum_{\lambda=400}^{700} Z_{\lambda,SMARTS}}\right)$$

Equation 4-4: Simulated Z values, corrected for measured PAR.

This adjustment was <10% but fitting a curve to PAR revealed that the fraction of absorbed radiation in the mixed layer near solar noon was near-complete, leading to a simplification of absorbance calculations. Combined with the results from mixing rates (see Results and Section 4.6), we decided to calculate photodegradation as an integrated process across the mixed layer, using the mean analyte concentration C_{ML} within that layer (<75 m). This approach was similar to others, but due to the deep mixed layer and the empirical evidence from PAR data, we assumed all light is absorbed within the mixed layer.[119,201]

$$\frac{dC}{dt} \cong u\Phi \mathrm{C} \int_{\lambda=280\ nm}^{800} \frac{Z_\lambda \varepsilon_\lambda}{z_{mix}\alpha_{D,\lambda}} d\lambda$$

Equation 4-5: Photochemical decay in the mixed layer.

In Equation 4-5, Φ is the apparent quantum yield of direct photolysis (moles of metabolite photolyzed per mole photons absorbed) and ε_λ is the molar extinction coefficient of the metabolite ($M^{-1}\ cm^{-1}\ nm^{-1}$), both obtained from Chapter 2. The mixed layer depth z_{mix} is 75 m, and $\alpha_{D,\lambda}$ is the diffuse attenuation coefficient of the water column ($m^{-1}\ nm^{-1}$) as reported by Shifrin.[208] The constant u is a conversion factor of 3.6 x 10^{-4} to put the final rate into units of pM h^{-1}.

4.3 Results and Discussion

4.3.1 Water Column Conditions

In November 2021, the Sargasso Sea's annual mixed layer deepening had begun. In Figure 4-1 the mixed layer depth of ~75 m was just above the chlorophyll maximum and lined up with the start of the thermocline. Average water temperature dropped from 24.4 ± 0.1 °C in the mixed layer to 18.9 °C at 250 m, and salinity began to change from an average of 36.6 ppt to 36.7 ppt at 100 m, then relaxed back to 26.6 ppt

by 250 m. These parameters are within the ranges reported for the nearby Bermuda Atlantic Time-series Study site (BATS), although estimates for November tend to vary as the mixing depth moves towards the bottom of the photic zone.[80]

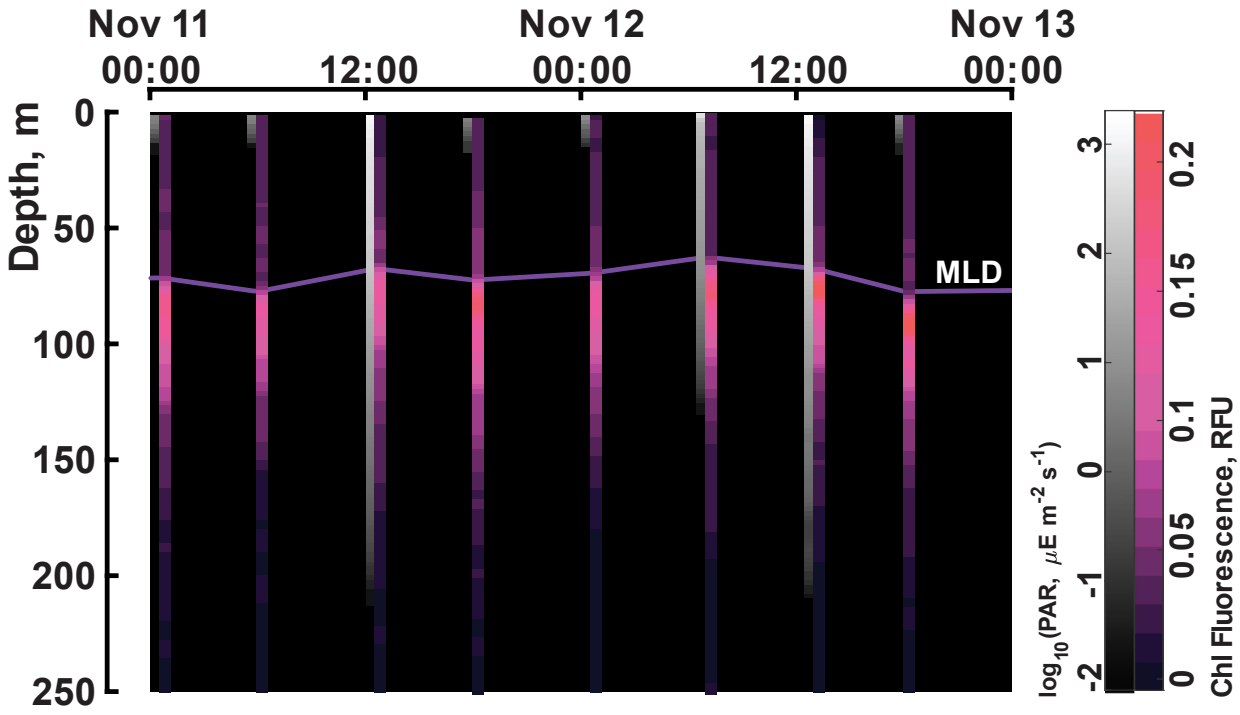

Figure 4-1: Chlorophyll fluorescence and photosynthetically active radiation (PAR; color-scaled bars), aligned with cast timing (local time). Mixed layer depth is represented across casts (solid purple line).

Chlorophyll fluorescence was highest at 77.4-93.3 m depending on the cast, and peaked generally between noon and 18:00, although in general the 6-hour spacing between casts was too long to adequately capture diel patterns. Photosynthetically active radiation (PAR) in Figure 4-1 demonstrates this issue: the PAR profiles do not show penetration of sunlight (as opposed to moonlight or onboard ship lights) except for the two midday casts (4 and 8) and cast 7, which was just after sunrise. PAR and chlorophyll together cannot be said to show synchrony in this dataset, nor were they correlated: PAR, both at the surface (PAR_0) and at the fluorescence maximum were uncorrelated with fluorescence magnitude itself (one-way ANOVA, $p = 0.51$). These

distinctions provide a lens of nuance to the following metabolite analyses, as we generally looked at day/night distinctions, time-independent correlations, profile structures, and inferred fluxes—which do not involve interpolating metabolite data across casts.

4.3.2 Metabolites

We quantified 60 unique metabolites at 54 unique points in time-depth space, totaling 3240 triplicate sets. In all there were 1380 non-detects (where no replicate had a measurement >LOD), 616 singleton measurements eliminated from further consideration, and 1244 metabolite-sample pairs satisfying all QC criteria. For eight metabolites (taurine, homoserine betaine, glutamic acid, ciliatine, aspartic acid, 4-aminobenzoic acid, and *gamma*-aminobutyric acid), our measurements are semiquantitative, as the stock mix used for their calibration leaked in transit to Bermuda and forced us to add an approximate and smaller amount (~1/2) to the final stock mix of all compounds. These semi-quantified compounds, when analyzed, have been notated with * in text and tables and with a “corrected” subscript in figures and we reported their measured concentrations as half the calibrated value.

Of the detected metabolites, six (2’-deoxyuridine, homoserine betaine, 5’-deoxyadenosine, adenosine-5’-monophosphate, 2’-deoxycitidine, adenosine-3’-monophosphate) had not previously been quantified in seawater samples, and for at least two others (putrescine, spermidine), the proof-of-concept in Widner and colleagues’ benzoyl chloride method paper is the only instance of seawater detection.[17,45] The true importance of the benzoyl chloride (BC) method lies both in its capture of a broad range of amines and alcohols and its sensitivity. Amino acids alone

are a widely-studied group of nitrogen-rich labile metabolites, but the O-phthaldialdehyde (OPA) derivatization-HPLC method used to commonly detect them has limits of detection (~0.5 nM) two orders of magnitude higher than the BC method (0.0002-0.001 nM).[209,210] For places such as the fall and winter Sargasso Sea, the benzoyl chloride method can give quantitative measurements where previous methods could not—and can do so with only 25 mL (75 mL of water per triplicate set). While less water is sometimes required for amino acid measurements using the OPA method (15 mL for a triplicate set),[197] using an extra 60 mL to measure more than twice as many metabolites greatly expands the questions that can be examined. These additional metabolites in our case included nucleic acid monomers, B-vitamins, catabolic intermediates, polyamines, and putative osmolytes, but any other targets with a BC-derivatizable group can be added to the method (provided commercially-available or synthesizable standards).

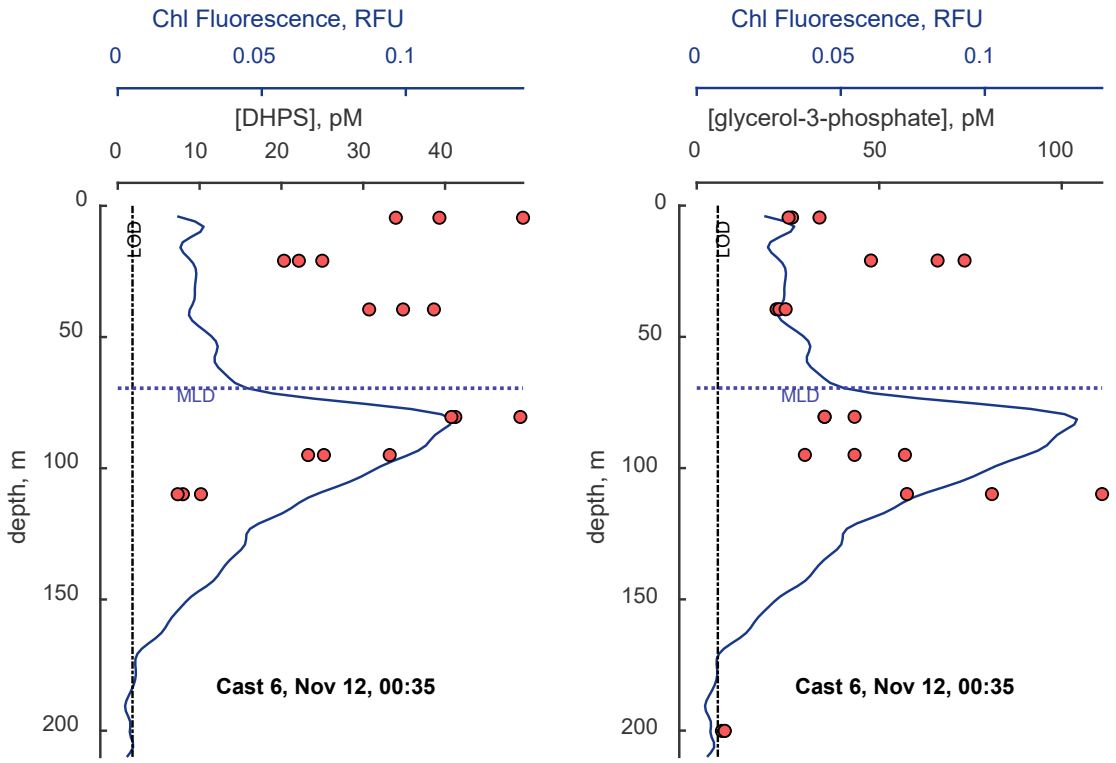

Figure 4-2: Depth profiles of two metabolites : 2,3-dihydroxypropane-1-sulfonate (DHPS, left), and glycerol-3-phosphate (right), shown as individual replicates (circles), alongside its limit of detection (LOD), the mixed layer depth (MLD), and the chlorophyll fluorescence profile.

In general, metabolites with data dense enough for profiles followed one or more spatial patterns: surface maxima (sarcosine, glycerol-3-phosphate), peaking near the chlorophyll maximum (homoserine, ciliatine*, cysteate), and/or occasionally present below 200 m (2'deoxyuridine, glutathione). As an example, Figure 4-2 showcases 2,3-dihydroxypropane-1-sulfonate (DHPS), a metabolite mainly produced by diatoms and a breakdown product of sulfolipids.[170,173] In every cast, DHPS concentrations were highest at the chlorophyll fluorescence maximum, but in the mixed layer either were uniform (overall mean concentration 38.1 ± 13.3 pM) or had a secondary maximum at the surface, although Cast 6 (Figure 4-2) was the only cast where this surface maximum (40.9 ± 7.9 pM at 4.54 m) was significantly different (t-test, $p < 0.05$) from its neighbor (22.5 ± 2.6 pM at 20.9 m). Glycerol-3-phosphate (G3P), DHPS' phosphate analog, has

an opposing pattern of dual peaks in the mixed layer and below the chlorophyll maximum, which may indicate differential lipid reconstruction schemes in the microbial residents of these two areas—DHPS may be a degradation product of phytoplankton sulfolipids, and G3P is a component of phospholipids, although the two also have myriad other roles in cellular catabolism and regulation as labile C_3 scaffolds.[173,211–213] Transient mixed-layer peaks such as those in Figure 4-2 may have multiple time-varying explanations, which will be expounded upon later.

The most common pattern was that metabolites peaked around the chlorophyll max, but this pattern has multiple possible explanations. Twenty metabolites correlated (Spearman rank correlation, $p < 0.05$) positively with fluorescence; none had a significant negative correlation. Taurine* was among the metabolites correlated to fluorescence, although Figure 4-3 illustrates caveats to this relationship—while it would be natural to assume that a region of concentrated primary production might have a high concentration of dissolved metabolites, the highest measured concentrations did not align with the chlorophyll max. Twelve metabolites had their highest concentrations ($> 3 \cdot$ cruise median) at 115 m depth during one night (00:35 local time) cast. This anomaly prompted both the analysis of mixing rates and zooplankton excretion, which will be discussed later.

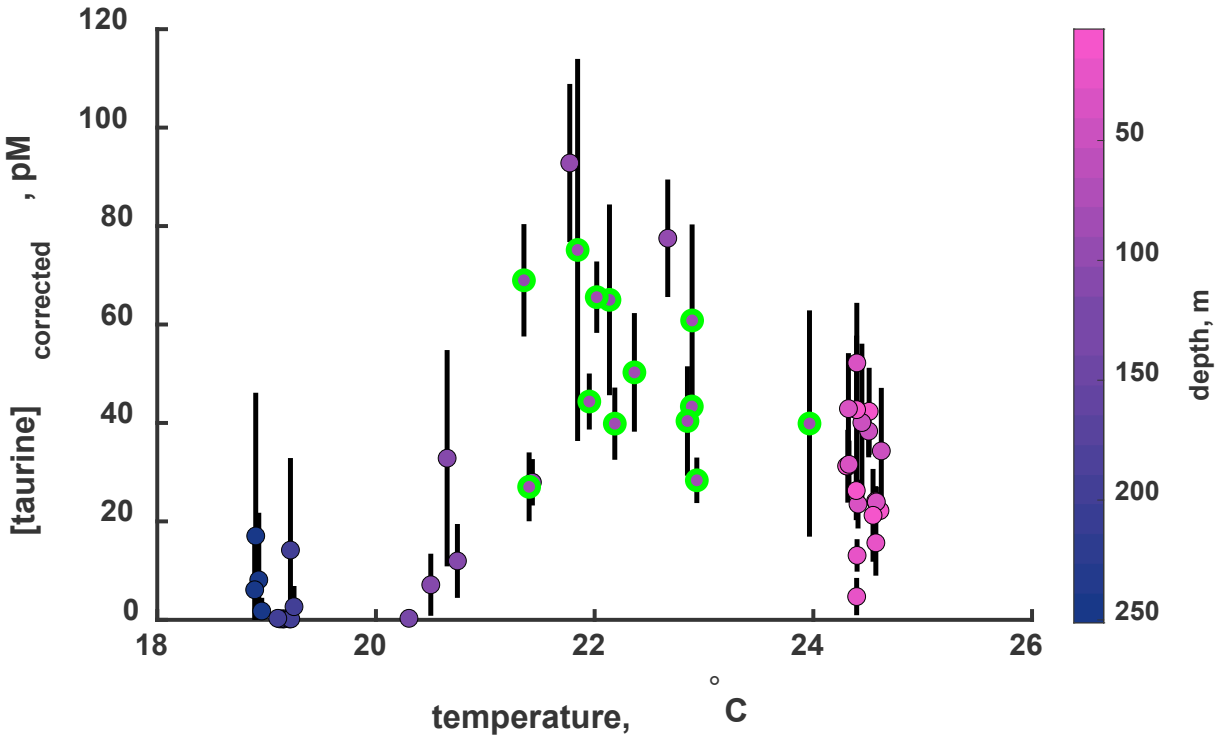

Figure 4-3: Taurine* vs. temperature and depth. Error bars are ±σ of triplicates, and color represents depth. Green outlines denote the sample is near the chlorophyll maximum (78-93 m). Data are plotted as a function of temperature to show the prominent break where chlorophyll max samples generally occur below the thermocline (below 23 °C).

Of all possible correlations, three metabolites correlated with depth and temperature but not chlorophyll: isethionate, malic acid, and *N*-acetylmuramic acid. The significance of these correlations vanishes ($p = 0.28$-1.0) when re-evaluated using only data within the mixed layer. This lack of within-layer correlation between hydrographic variables points to the limited usefulness of such relationships, as the apparent correlations discussed previously were driven by three distinct groups of samples structured by depth: mixed layer (high), chlorophyll max, and deep samples (low, >200 m). These three non-chlorophyll-correlated metabolites (isethionate, malic acid, *N*-acetylmuramic acid) are, however, are a group with interesting differences that give

more insight into water-column processes when examined outside the context of simple hydrography.

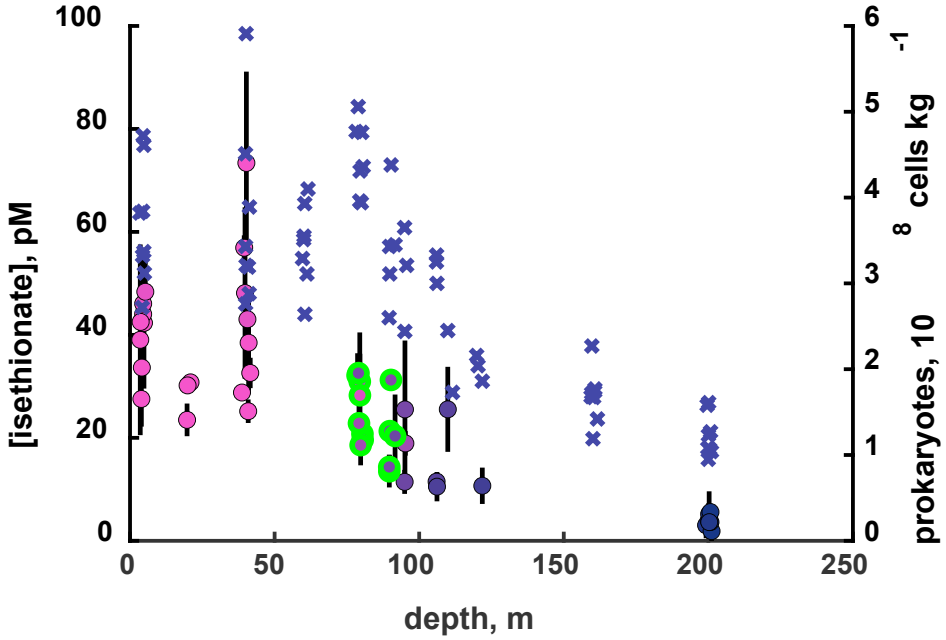

Figure 4-4: Isethionate vs. depth with temperature noted by marker color and chlorophyll max samples bordered in green. The additional y-axis (right) corresponds to epifluorescence microscopy-based cell counts (blue "x" markers).

Isethionate is a C_2-sulfonate that has received attention as a part of the same network of sulfonate exchange to which DHPS also belongs.[170] The fact that isethionate exhibits a different pattern than DHPS is actually mirrored in TARA Oceans metagenomes: orthologs for *iseK*, an isethionate transporter, are present in generally <1% of bacterial genomes above the mesopelagic zone, while the DHPS transporter gene *hpsN* is relatively uniform across vertical zones and generally more common (~5% of bacterial genomes).[214] Assuming the cited metagenomes' trends applied to these specific two days—and/or that these sulfonates share the observed patterns globally—the colocation of genes for their use could reflect uptake rates. The sulfonate picture is complicated by taurine, another widely-metabolized sulfonate (Figure 4-3). It (taurine)

did not share the same accord with the TARA metagenomes, as its transporter gene *tauA* is common (often >5%) in the mixed layer and chlorophyll max, but highest (~10% of genomes) in the mesopelagic.[214] Correlations, or lack thereof, of genes and metabolites is circumstantial evidence at best for production and consumption, but the uniqueness of taurine in this instance will be especially relevant later (see *Zooplankton Contributions*).

N-acetylmuramic acid, a peptidoglycan monomer in bacterial cell walls, follows a similar pattern to isethionate and prokaryotic cells (Figure 4-4); that is, it is relatively uniform in the mixed layer with lower concentrations in deeper zones. Bacteria are likely the source of this compound, but the exact mechanics of how this amide sugar ended up in the dissolved phase are beyond our scope, and for this compound the measurements were extremely dilute (<40 pM) and had an average coefficient of variation (CV) of 1.1 (replicate standard deviation divided by mean). Malic acid, a dicarboxylate shared by all known metabolisms, is a hybrid profile of mixed-layer uniformity, general variability (mean replicate CV = 0.72), and one of the metabolites that spiked at 115 m depth in a single sample (along with taurine and 10 others).

Metabolite concentrations were lower than in one previous dataset employing the same method, at the same location, by an order of magnitude or more.[6] Malic acid, for example, reached 1500-2000 pM in the mixed layer in July 2019 at nearby BATS, while for our dataset this number was 81.0 ± 40.2 pM. Taking these numbers and comparing the depths of the mixed layer (average 14.4 m for the data in [111]), the total mixed-layer inventory of malic acid was, on average, 25.2 ± 3.6 μmol m^{-2} in July 2019 and 6.1 ± 3.0 μmol m^{-2} in November 2021, implying that during the mixing period, malic acid becomes

dilute, but the total inventory remains less variable. This contrasts with, for example, pantothenic acid and riboflavin, two B-vitamins that were higher during winter mixing and lower during summer stratification.[111] Malic acid is not an essential vitamin, although it is a valuable intermediate in the citric acid cycle and may be a way for diatoms to shunt excess light energy into a benign form,[215] a process that would be more important in the summer than in the fall or winter.

Part of the reasoning for relying on areal inventories here is that deposited marine aerosols contain malic acid, among other metabolites.[216]As a first estimate for depositional compensation, Kawamura et al.'s value of 0.19 ng m^{-3} (1.4 pmol m^{-2}) malic acid in Arctic aerosols can be used with the range of sulfur aerosol deposition velocities reported by Sievering et al. (1989) for the North Atlantic to calculate a malic acid deposition range from 240 to 2400 nmol h^{-1} m^{-2}.[217] This is capable of completely replenishing mixed layer concentrations in 9.5 ± 8.1 d for the summer 2019 or 2.3 ± 2.2 d in November 2021. Such a fast rate of deposition is striking, but it is a loose estimate that does not account for wet deposition or surface microlayer processes,[218] all of which are critical to near-surface concentrations. These surface processes may be the cause of the surface maxima that we observed for some compounds, especially those of low molecular weight (such as DHPS, Figure 4-2), where there must be a source that operates faster than mixing can erase its signature. This is both plausible and likely varies in time with respect to both deposition and mixing (see 4.3.4 and 4.5).

4.3.3 Dominant Metabolites and The Use of Summary Values

General statistics (mean, median, standard deviation, interquartile range, number of observations, and limits of detection) for all metabolites with >5 measurements within

the mixed layer are in Table 4-1, while the full set of metabolite names, InChI keys, LODs, and individual measurements can be found in the Supplemental Information. Because Table 4-1 provides distributional statistics over a broad spatiotemporal range of the cruise, even singleton measurements were counted. We ordered the data by median because some metabolites had low sample numbers but high variability, like tyrosine, where one sample at 41.0 m was above the range of the standard curve, at (roughly) 10 nM.

In general, the subsequent calculations in this work will not rely on imputation methods for values <LOD, although these do exist.[219,220] Measurements consistently hovering near the LOD (see Supplemental Information and Chapter 5), some of them singletons within a triplicate set, are often interpreted as equivalent to zero, i.e., that the molecule is absent. However, sparse measurements are better interpreted as an upper bound, due to analytical variability around the LOD. Confidence in metabolite concentrations will increase as more samples are taken, and the LOD is continually improved by analytical methods. Until complete replicate sets can be reliably obtained for a metabolite, singleton measurements may be used with caution, and their distributional parameters in the water column are not to be relied upon except in cases where most samples are within the range of detection.

Table 4-6: Summary of metabolite measurements in the mixed layer, ordered by descending median and only where n > 5. All values except for n are pM. LOD is the limit of detection calculated from two standard curve replicates. *Denotes compounds whose absolute magnitudes were inflated due to standard spill (see Methods). Abbreviations: HMP = 4-amino-5-hydroxymethyl-2-methylpyrimidine; DHPS = 2,3-dihydroxyproane-1-sulfonate; amMP = 4-amino-5-aminomethyl-2-methylpyrimidine

Name	**Mean**	**Std. Deviation**	**n**	**LOD**	**Median**	**Interquartile Range**
HMP	291.1	159.6	7	20.4	255.7	124.7
malic acid	81.0	40.2	57	19.9	72.3	65.8
glycine	62.2	40.3	25	1.8	63.6	58.8

Name	Mean	Std. Deviation	n	LOD	Median	Interquartile Range
tyrosine	443.0	1866.8	29	3.5	63.2	113.4
*homoserine betaine**	33.1	16.4	57	3.2	28.5	15.5
*taurine**	30.2	13.1	56	1.0	27.4	17.3
5'-deoxyadenosine	64.7	34.2	16	27.0	54.0	29.9
*glutamic acid**	24.7	16.3	46	0.2	19.8	14.7
DHPS	38.1	13.3	57	1.8	36.7	22.4
alanine	76.8	73.6	16	2.3	36.3	74.2
isethionate	39.7	14.0	57	1.5	35.5	18.3
2'-deoxyuridine	33.8	15.7	54	8.2	34.8	27.1
ectoine	45.0	30.2	8	12.1	34.2	31.3
serine	79.2	115.1	27	1.2	32.9	27.1
2'-deoxycitidine	35.0	12.3	8	24.6	32.7	16.1
thymidine	30.6	8.4	27	20.2	30.4	6.1
cytidine	37.7	20.6	13	8.7	30.3	26.0
glycerol-3-phosphate	29.4	11.2	57	5.8	27.4	12.2
*aspartate**	14.6	10.6	22	4.6	12.6	10.8
chitobiose	29.9	9.2	10	62.5	24.8	17.0
putrescine	48.1	97.9	33	2.5	20.9	19.1
xanthosine	23.7	5.4	10	55.6	20.8	6.9
threonine	34.6	41.7	33	2.7	19.6	15.8
citrulline	40.7	51.2	14	2.3	18.8	46.8
N-acetyl-muramic acid	20.9	10.1	30	9.2	17.4	14.8
glutamine	24.1	36.3	55	0.2	17.1	10.2
cysteine	17.3	7.5	57	4.6	16.9	7.8
amMP	18.1	6.0	11	1.3	16.2	9.3
glutathione	19.1	10.6	14	7.6	15.2	15.8
arginine	41.8	56.3	10	3.8	12.0	50.2
glucose 6-phosphate	11.3	0.8	9	7.8	11.5	1.2
5'-adenosine monophosphate	16.2	23.6	23	9.8	11.3	8.2
histidine	26.2	43.8	27	1.9	11.0	15.3
uridine	11.5	2.2	23	3.6	10.6	1.8
phenylalanine	15.4	18.2	31	4.2	8.9	5.9
5'-inosine monophosphate	7.8	1.3	11	7.0	7.5	1.8
cysteate	7.4	2.0	23	6.1	7.3	2.3
sarcosine	8.3	4.5	53	1.2	7.3	4.3
5'-uridine monophosphate	6.7	0.7	7	7.8	6.9	1.4
tryptophan	6.5	1.7	50	1.3	6.3	2.0
asparagine	9.3	8.8	28	1.7	5.9	6.9
muramic acid	7.5	5.3	22	5.1	5.9	5.1
homoserine	5.5	0.7	53	1.2	5.4	1.2
kynurenine	4.0	1.5	35	1.9	3.5	1.0

Name	Mean	Std. Deviation	n	LOD	Median	Interquartile Range
pantothenic acid	2.9	0.7	28	1.8	2.9	1.1
*ciliatine**	1.8	1.4	12	0.2	1.4	0.1
2'deoxyguanosine	2.8	1.8	35	0.7	2.4	0.2
adenosine	2.7	1.8	37	0.8	2.4	0.2

4.3.4 Water-Column Mixing

We simulated the mixing of metabolites on a short (~6 h) time-scale, because during Cast 6 (00:35), a single set of replicates at 115 m contained concentrations of proteinogenic amino acids, as well as 4-aminobenzoic acid, citrulline, kynurenine, malic acid, and putrescine at several times the median value across all samples. These samples passed quality control, and more importantly, were not unanimous anomalies across metabolites—about half of the measured compounds were *not* different from other measurements. While the reason for the pulse was unknown, its presence led to questions about whether the event that produced it would lead to visible anomalies if it was localized to other depths.

We found that mixing, even with a well-parametrized diffusivity field, made little difference at the original depth (115 m) of the pulse. The K_z field provided by R. Curry (ASU BIOS), when applied through Equation 4-2 to any variable within the water column, indicates that the distinction between mixed layer and below should be physically dominant even on timescales of 6 h, explaining both patterns of homogeneity within the mixed layer and the localized persistence of labile compounds below. The "pulse" we observed at 115 m—below the mixed layer—during Cast 6 could not have been attenuated more than 5% by mixing in the time between casts. This attenuation varied by metabolite, because the gradient established by the pulse input could be

steeper or shallower depending on the pulse's magnitude. Generally, this means that at least below the mixed layer, pulses such as this may be encountered in the future, and they are likely to be locally-relevant phenomena—the sort of heterogeneities to which chemotactic bacteria and archaea flock.[78]

Within the mixed layer, small heterogeneities caused K_z estimates to be much larger and more erratic. Their values were generally lognormal (Supplemental Figure 4-1) and affected more strongly by density gradients than wind speed, which varied from 0-15 m s^{-1} and resulted in K_z values from 2.05 x 10^{-6} to 3.9 x 10^{-4} m^2 s^{-1}. The least inter-profile K_z variance was between casts 6 and 7, hence their use in the mixing model by way of interpolation.

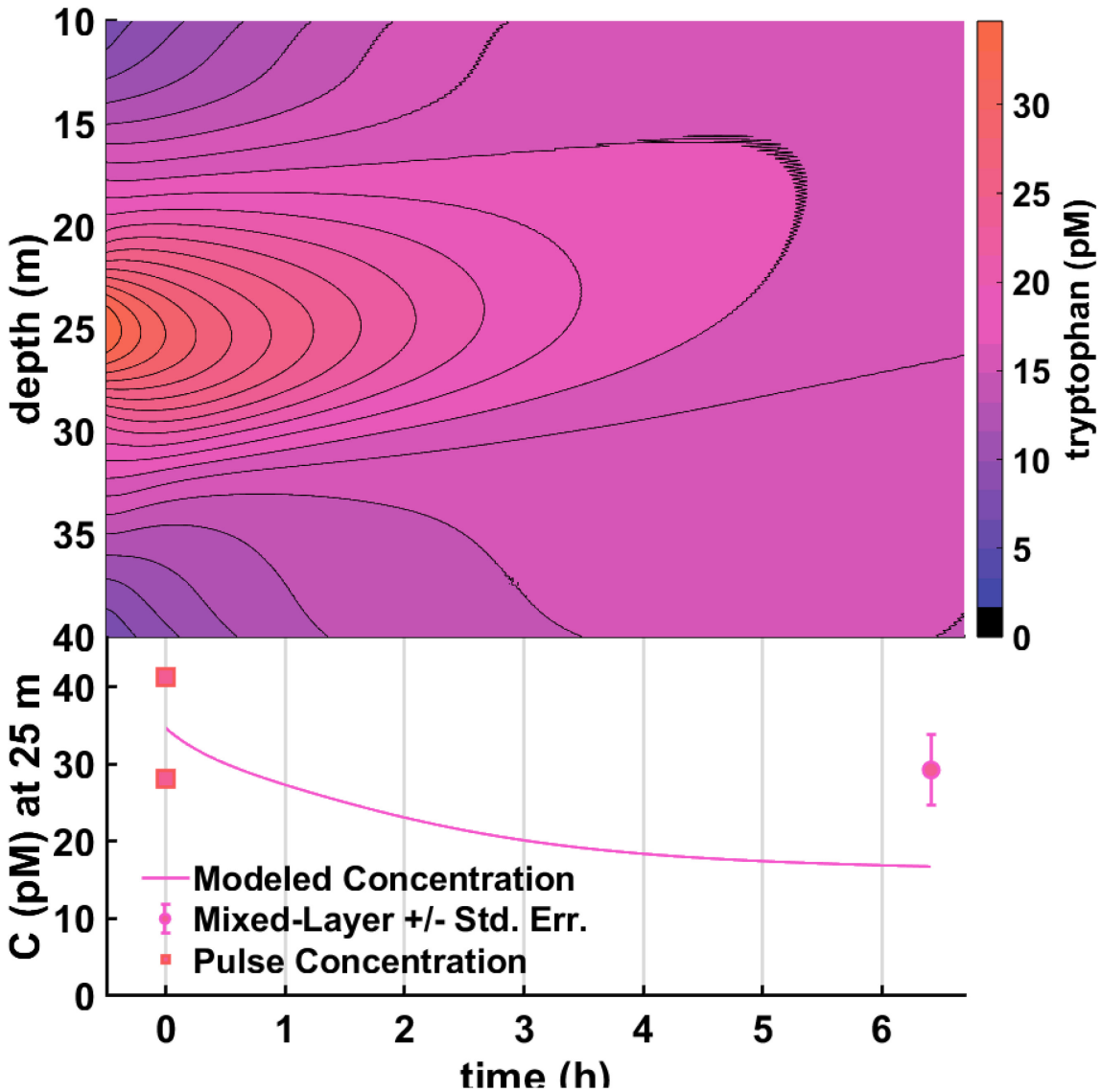

Figure 4-5: Mixing of a tryptophan pulse within the mixed layer. Top: contour plot of simulated tryptophan field. Bottom: Comparison of simulation results to 115 m pulse and average mixed layer concentration (see section 4.2.6).

When the same routine was used with eddy diffusivities around 25 m, many metabolites mixed close to background levels—close enough to be statistically indistinguishable within the error of the field measurements. It is simply unlikely that such a pulse would be observed in the mixed layer. Any similar inputs would be likely be mixed to the point of statistical indistinction from the background within 6 h, and

definitely within 12 h. This idea impacts the interpretation of metabolites broadly; differences that are observed within this layer are likely not due to slower standing processes, but sub-daily processes that change concentrations in under 12 hours. Processes operating on slower scales can be modeled as acting uniformly across the mixed layer when compared to observations.

The reason for reporting this interpretation is that mixing, and incorporating it into models, is not new for DOC;[4] however, it is more important for analyzing metabolite fluxes than seems to be commonly considered. High concentrations of a chemical moiety in the mixed layer can be sustained by spatially-restricted but unseen inputs several times the ambient concentrations because mixing distributes them quickly over tens of meters. Meanwhile, inputs even a few meters below the pycnocline may lead to profiles that would be considered erroneous if this difference is not considered. The labile organics encountered by microbes are then not only dictated by the uniqueness of their sources, but the vigor of the indifferent process of mixing.

As mentioned in the Methods, negative buoyancy frequency values did not factor into K_z calculations; however, mixing due to density inversion is not the only problem. A central limitation for the approach taken here is that of one-dimensionality. We had neither lateral advection nor lateral mixing parameters, and only one sampling location.

4.3.5 Zooplankton Contributions

In Chapter 3, the copepod *Pleuromamma xiphias*, a dominant migrator near Bermuda, excreted 31 metabolites at a rate capable of changing one liter of water by 10 pM in 6 h, a change that our methods would generally be able to detect. Through association alone, zooplankton excretion is a likely candidate for concentrated inputs: of the 22

metabolites that were detected as the “pulse,” 19 were among the compounds excreted at a high rate for *P. xiphias.*

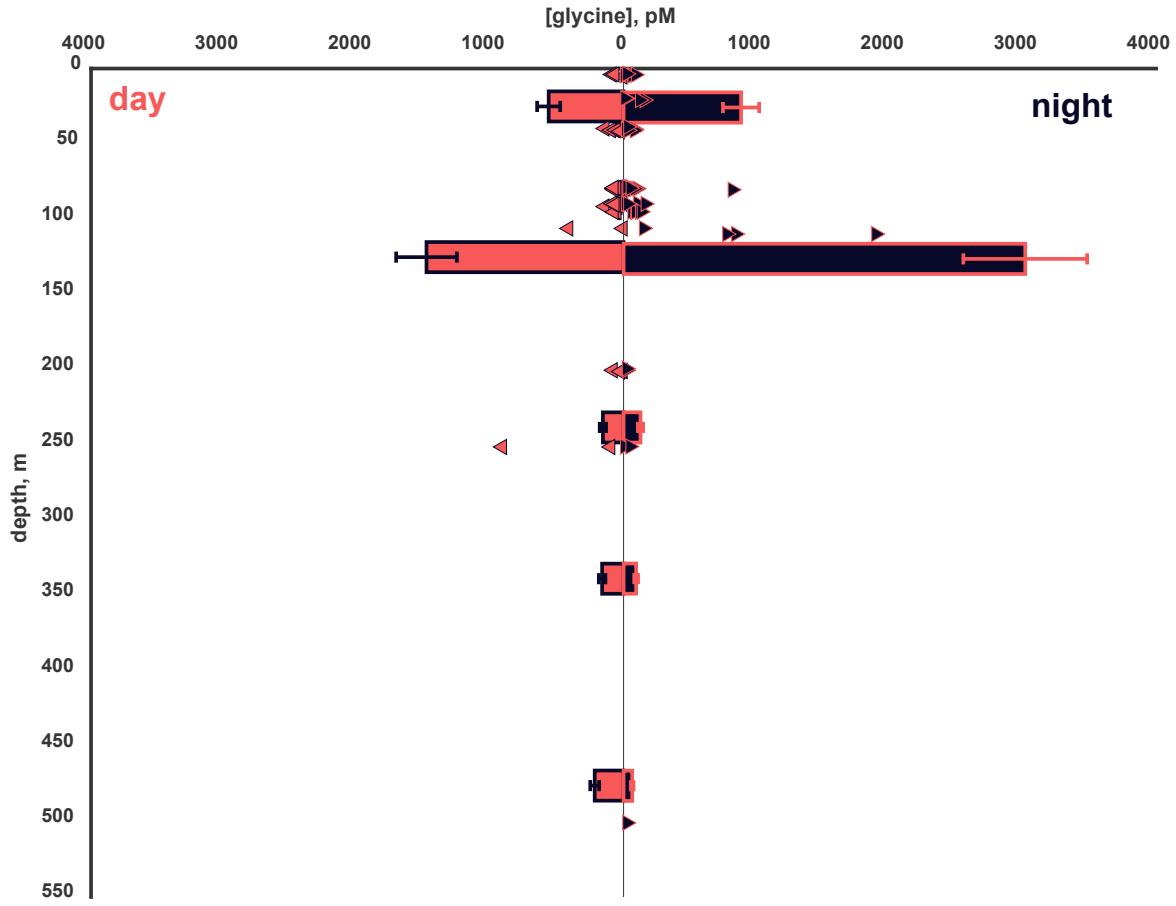

Figure 4-6: Ambient glycine concentrations versus estimated copepod excretion during a 1-hour residence time. Scattered triangles are the ambient AE2123 glycine concentrations; bars are the copepod excretion estimates, with error bars representing variance in excretion rate measurements (n = 3).

To provide a more substantial line of evidence we paired our measurements with the zooplankton biomass abundance data (using Equation 4-3) to estimate potential water-column excretion. A residence time of 1 hour (as opposed to 12) obviated the need to treat migration as a sort of teleportation and brings the contributions (bars in Figure 4-6) closer to measured field values (triangles in Figure 4-6) The excretion maximum both at day and at night would occur between 100 and 200 m—a range covering the depth of the pulse and corresponding to maximal respiration and feeding

(Figure 4-6).[165] The second-highest excretion depth range includes the mixed layer, implying that zooplankton supply not just ammonium and/or taurine,[74,197] but also a suite of biologically labile compounds to the mixed layer and, importantly, to depths of up to 1000 m.

The magnitude of the potential zooplankton contributions is quite large. Figure 4-6 assumes a 1-hour residence time, showing that copepods could supply the entire inventory of their prominent excreta to the mixed layer and below—not through sloppy feeding and not due to the excretions of phytoplankton, but by recycling microbial biomass through digestion. This would not only explain the 115 m pulse, but the high concentrations of some compounds near the chlorophyll maximum that lies below the mixed layer.

Table 4-7: Turnover times based on copepod excretion rates. "Day" is after sunrise; "Night" is after sunset. Error calculated based on standard deviation of copepod excretion measurements (n=3, Chapter 3) and standard deviation of all measurements in the specified space-time range (n = 2-36). *denotes were corrected by a factor of 0.5 (see Methods)

	Turnover Time (h)			
	0-75 m		**75-200 m**	
metabolite	Day	Night	Day	Night
arginine	0.05±0.03	0.19±0.22	0.05±0.06	0.12±0.33
alanine	0.16±0.03	0.28±0.25	0.13±0.20	0.34±0.52
asparagine	0.15±0.06	0.18±0.18	0.12±0.13	0.23±0.50
glycine	0.12±0.07	0.07±0.05	0.05±0.05	0.08±0.15
threonine	0.17±0.09	0.27±0.31	0.12±0.19	0.37±0.75
phenylalanine	0.26±0.11	0.41±0.47	0.14±0.12	0.40±0.91
histidine	0.19±0.13	0.30±0.49	0.14±0.36	0.54±1.17
kynurenine	0.63±0.30	0.43±0.26	0.33±0.22	0.32±0.49
citrulline	0.84±0.39	2.04±2.32	3.30±2.59	3.23±6.89
tryptophan	1.04±0.50	0.64±0.35	0.44±0.25	0.42±0.60
putrescine	0.13±0.50	0.23±0.99	0.12±0.46	0.21±1.08
sarcosine	1.08±0.71	0.47±0.30	0.29±0.16	0.14±0.08
glutamine	1.56±0.86	1.66±2.72	0.90±0.64	0.50±0.71
homoserine	6.58±2.22	4.29±1.44	3.48±1.77	1.29±0.49
ectoine	1.69±3.11	2.53±4.85	1.56±2.91	1.11±2.25
tyrosine	3.90±5.11	15.13±55.84	0.69±0.54	0.53±0.54
glycerol-3-phosphate	3.32±6.92	2.63±5.51	2.35±4.91	0.96±2.03
adenosine-5'-monophosphate	4.34±7.74	1.54±0.98	0.72±0.40	0.43±0.34

	Turnover Time (h)			
	0-75 m		**75-200 m**	
thymidine	66.50±35.85	41.42±24.51	27.65±18.26	14.59±10.24
guanosine	n.d.	22.88±35.45	13.71±21.24	14.93±23.13
methionine	n.d.	8.29±12.45	n.d.	8.31±13.79
adenosine-3'-monophosphate	n.d.	0.58±0.38	0.28±0.21	0.18±0.09
leucine	n.d.	0.41±0.40	0.23±0.24	0.60±0.87
isoleucine	n.d.	0.55±0.46	0.20±0.18	0.93±1.50
proline	n.d.	0.38±0.41	0.20±0.05	0.70±0.67
valine	n.d.	0.36±0.22	0.17±0.25	0.53±0.64
*ciliatine**	0.07±0.01	0.07±0.06	0.05±0.02	0.02±0.01
*gamma-aminobutyric acid**	0.07±0.05	0.10±0.08	0.20±0.15	0.03±0.03
*aspartate**	0.17±0.08	0.16±0.13	0.11±0.13	0.19±0.36
*taurine**	1.28±0.41	0.62±0.34	0.70±0.33	0.32±0.19
*glutamic acid**	2.35±2.36	1.48±1.31	1.11±1.68	0.76±1.24
*4-aminobenzoic acid**	n.d.	0.54±0.57	0.54±0.09	1.00±0.87

One analysis that the combination of excretion and field data allows is calculating a turnover time, and the results of this calculation for excreted compounds is in Table 4-2. We performed this analysis as $C_{ambient}/R_{production}$, the ratio of ambient concentration to excretion rate. The ranges are large, accounting for error in both measurements of zooplankton excretion and of field metabolite concentrations, but indicate that the microbial production of these compounds is slow, or consumption is high, or a combination of both. We used only copepods in our calculations as they made up 70% of the identified organisms in the data provided for 2017, but other organisms excrete different profiles of metabolites, sometimes at much higher rates than *P. xiphias* (Chapter 3).

Values in Table 4-7 vary widely in every possible dimension: by time of day, by metabolite, by depth, and internally (error). The latter will be addressed as more measurements are conducted and the factors involved in zooplankton excretions investigated more thoroughly.[221] As for the time of day, zooplankton abundance varies up to 50% due to diel migration—without even factoring in variation in microbial

metabolism.[7,165] The latter, in addition to differences in depth and by metabolite, are not independent factors: different consumers and producers with different metabolic regimes live at different depths, resulting in unique ambient stocks of metabolites.[222,223] The reported turnover times represent a malleable estimate that considers only zooplankton production and no other production terms—it would be much more surprising if they had been uniform.

With zooplankton, the one spatial dimension of the metabolite data deserves some scrutiny. Zooplankton are not a uniform cloud of biochemical activity, but millimeter-scale motile units, and in the dataset provided by Maas, zooplankton abundance in general ranged from 5-800 m^{-3}, or as a median, one animal per 61 L. Depending on the depth range and assuming some avoidant behavior, one zooplankter might be caught in a 12 L Niskin about one in five times. It may be that an animal caught during filtering (rather than being diluted in the entire Niskin volume) produced the “pulse” during cast 6, which would partially explain why something like it had not been seen in any of the hundreds of dissolved metabolite samples on record. There was, however, no note of any animal caught on the PTFE membrane. Zooplankton are generally captured via net tows, giving a lateral average of abundance and biomass, but difficult to use as explanations for single points in vertical space.

4.3.6 Metabolite Photodegradation

For two casts near solar noon, and for two metabolites (tryptophan and kynurenine) we have simulated irradiance, concentrations throughout the mixed layer, and apparent quantum yields. Applying Equation 4-5 to the mean concentrations from the mixed layer in Casts 4 and 8 resulted in low reaction rates (0.98-1.24x10^{-3} pM h^{-1} for

tryptophan; 3.03-5.31x10^{-3} pM h^{-1} for kynurenine) and corresponding turnover times ($\ln(2)\ /k_p$) in the range of months—if irradiance was constantly as intense as a solar noon in November. These estimations for two metabolites do not represent a large proportion of their total fluxes, but rather are likely to be a slow leak in the system of metabolite exchange, where biological products become other DOM components that may or may not be labile.

Here, we accounted only for direct photolysis, and due to the simulated irradiance excluded some of the most highly absorbent wavelengths of light for the two compounds, those below 280 nm. While these higher-energy wavelengths are unlikely to filter down more than a few centimeters in the water column,[224] their impact on the surface layer may be visible through the extent to which products are mixed downwards.

The presence of secondary photochemical reactions is unlikely to have a more dramatic impact. While the reaction of tryptophan with singlet oxygen can be fast, even the nearly diffusion-limited ~3.2x10^{7} M s^{-1}, open-water steady-state concentrations of $^1O_2$ are 10^{-15}-10^{-12} M.[32,225] When acting on <10^{-11} M levels of tryptophan, the reaction rates are negligible, and there is evidence to support the idea that in natural waters, triplet dissolved organic matter ^{3}CDOM is the primary culprit in tryptophan degradation, with direct photodegradation in second place.[109,110] In the oligotrophic ocean, ^{3}CDOM is unlikely to overcome the low standing concentrations, both of itself and of reactive metabolites,[32] even if the bimolecular rate is in the diffusion-limited 10^9 M s^{-1} range.

We have presented these photolysis estimates as a null result with respect to overall metabolite fluxes, but they are only a start. There are other metabolites that the

benzoyl chloride method does not capture, such as riboflavin, which are remarkably susceptible to photodegradation but lack the kind of parameters that would allow us to directly model their fate in the open ocean.[60,108] Moreover, there is a great deal of unexplained diversity in DOM, and if even two of 64 (3%) of metabolites can be slowly transformed into photoproducts, the next step is to find out what those products are and whether they are labile—a goal which has had some notable progress already and depends on the character of the DOM.[57,226,227]

Assuming that direct photolysis over 24 h is ~40% of solar noon values extrapolated to 24 h,[48] the mixed layer would still accumulate 0.06-0.10 μmol m^{-2} kynurenine degradation products over the course of November (which has lower irradiance compared to summer months), and these products must be consumed by some process to achieve the approximate seasonal steady-state of DOM within an oligotrophic ocean ecosystem.[80] Genomic and experimental data for import and use of dissolved tryptophan and kynurenine degradation products (such as *N*-formylkynurenine and kynurenic acid) is nonexistent. Anthranilate, one of the eventual photodegradation products of both metabolites, is also not discussed except in the context of cellular internality, but can be used as ready fodder for the prokaryotic kynurenine pathway.[228–230]

4.3.7 Open Questions and the Microbial Remainder Rate

While microbial life is capable of making large adjustments to its metabolism in response to environmental changes and producing different dissolved metabolites under different conditions,[8,10,231] the actions of the sun, of mixing, and (to some extent) of zooplankton are inexorable, even if gradual.

While the compounds tryptophan and kynurenine are two isolated cases related to photochemistry, they are also among compounds excreted by zooplankton (Chapter 3), and the potential impact of that dataset on interpretation of the microbial loop needs constraining. The three processes we examined here are not the totality of the puzzle; we cited others such as hydrolysis and complexation whose impacts on DOM-microbe interactions are functionally unconstrained.[65,85] Thousands more species of DOM exist to be examined for such factors, and for the major species require quantitative analysis.[232] This is a rich field which tools for parallelization such as the LC-MS based method can help greatly in exploring. Incorporating simple models such as the mixing model we used can help in interpreting the field data we do have; for example, noting that mixing evens out profiles within the mixed layer on time-scales of 6-12 hours—without even considering lateral mixing or advection.

We can hypothesize that the life cycle of a single molecule of kynurenine may be that it is produced by a phytoplankter,[222] who is eaten by a copepod. The molecule is excreted in the surface, broken into a different product by sunlight, and perhaps consumed as a new molecule (ex. anthranilic acid) by a heterotrophic bacterium and reincorporated in a richly complex variation of the microbial loop.[233] Much more has been written about the production of dissolved metabolites than has been determined about their import and use, which lead to the assumption that the same organisms which live through interacting with labile DOM are also its main controls. We hypothesize, for the broad diversity of metabolites and derivative products, that there is much more at play. These factors act on different time-scales and at different

magnitudes, but exert a large collective degree of influence over the chemical environment to which microorganisms must adapt.

4.4 Conclusions

The possible fates of labile DOM species depend upon both their biological function and their chemical identities. The processes governing the biomolecules studied as metabolites do not apply evenly to them, nor do they adhere to steady-state assumptions. We applied three somewhat well-studied frameworks to a field dataset and found that a subset of compounds is rapidly produced as the products of zooplankton metabolism. These excretions are subject to physical mixing, which explains differences in apparent metabolite distribution between and within hydrographic layers and—due to the gradient-dependent nature of mixing—acts more strongly on those compounds whose inputs are highly localized. Photochemistry affects the system in ways that are subtle but depend entirely on a metabolite's structure and need to be investigated further for compounds with a higher degree of chomophoricity. More importantly, we see that the active alteration of dissolved metabolites is a slow leak in the neat picture of the metabolite exchange cycle and could be either the first step on a process that decreases lability, or a reason for certain metabolic preferences for one substrate over another, or a combination of both. There is an enormous well of research remaining here, but primarily this work should serve as a demonstration of quantitative LC-MS analysis for putting labile DOM in a broader physical context. It is a first step in building dissolved organic matter from the bottom up by examining how each chemical brick is laid.

Acknowledgments

This work was funded by the Simons Foundation International through the BIOS-SCOPE collaboration. Hydrographic data was provided by the technical staff of the R/V Atlantic Explorer; Shuting Liu and Rachel Parsons collected prokaryote abundance data. The metabolite stocks in the Kujawinski lab were (and are) maintained by Gretchen Swarr, and the mass spec worked only by the deft hands of Melissa Kido Soule. Ruth Curry graciously pointed me to new algorithms for vertical eddy diffusivity and provided implementation in MATLAB. The colors used in the figures were drawn from the cover of *Wave Machine* (2023) by Makari.

4.5 Appendix A: Supplemental Methods:

4.5.1 Sample Drydown and Workup

We dried acetone from the samples under nitrogen at 30 °C until they lost the mass of acetone added (3.786 g).

We extracted metabolites with 1 g BondElut PPL cartridges and evaporated the MeOH eluent in a Vacufuge (Eppendorf). We partially redissolved the analytes in 500 µL 5% (v/v) acetonitrile in MQ, then mixed with a vortexer. The liquid contained benzoic acid precipitate, so we centrifuged it at 20,000 x g for 15 minutes and moved the supernatant to a combusted 2 mL glass vial. We evaporated the of solvent again on the Vacufuge and did a final 100 µL 5% (v/v) acetonitrile rinse/centrifuge, this time transferring the supernatant to chromatography vials and adding 5 µL acetonitrile to prevent additional precipitation.

4.5.2 UHPLC-Orbitrap MS Conditions

Using an autosampler set to 4 °C, we injected samples (5 µL per ion mode) onto a reversed phase Waters Acquity HSS T3 column (2.1 × 100 mm, 1.8 µm) equipped with a Vanguard pre-column (Waters) held at 40 °C. We used mobile phases (A) 0.1% (v/v) formic acid in water and (B) 0.1% (v/v) formic acid in acetonitrile. The gradient, at 0.5 mL min-1, was: 0-0.5 min (1% B), 2 min (10% B), 2-5 min (10% B), 7 min (25% B), 7-9 min (25% B), 12.5 min (50% B), 13 min (95% B), 13-14.5 min (95% B) and re-equilibration with 1% B (total run time = 16 min). Other instrument parameters were: ESI voltages = 3600 V (positive) and 2600 V (negative); source gases = 55 (sheath), 20 (auxillary), and 1 (sweep); capillary temperature = 350 °C; vaporizer temperature = 400

°C. We collected MS data from 170-1000 m/z at resolution 60,000 fwhm (at m/z 200), automatic gain control (AGC) at 4e5, and max injection time 50 msec.

Upon detection of a target compound's mass, we isolated the parent ion in the quadrupole at a width of 1 m/z, and collected MS/MS data at resolution 7,500 fwhm, AGC at 5e4, and max injection time 22 msec using higher energy collisional dissociation (HCD) with 35% collision energy and intensity threshold at 2e4.

4.6 Appendix B: Supplemental Results

4.6.1 All Metabolites

Below I have included the complete set of measurements. As with the other chapters, they are also provided in spreadsheet format in the Supplemental Information file. I have provided the essential metadata here as well: local date and time, depth of the sample, and the cast and Niskin numbers—samples with the same cast and Niskin IDs are replicates.

Table 4-8: All metabolite measurements for Chapter 4. The measurements are raw values, filtered by LOD but not by blanks or pooled samples. All metabolites are in units of pmol L^{-1}, and NaN values represent a values <LOD. Because this table is split across the next 52 pages, the row names repeat with every new group of samples, while the headers repeat every page. C0N0 is a MilliQ blank. Abbreviations: HMP (4-amino-5-hydroxymethyl-2-methylpyrimidine); amMP (4-amino-5-aminomethyl-2-methylpyrimidine); HET (4-methyl-5-hydroxyethylthiazole).

name	AE2123_BC36_C0N0	AE2123_BC19_C2N2	AE2123_BC20_C2N2	AE2123_BC21_C2N2	AE2123_BC22_C2N6	AE2123_BC23_C2N6	AE2123_BC24_C2N6	AE2123_BC25_C2N9	AE2123_BC26_C2N9	AE2123_BC27_C2N9	AE2123_BC28_C2N11	AE2123_BC29_C2N11	AE2123_BC30_C2N11
cast	0	2	2	2	2	2	2	2	2	2	2	2	2
niskin	0	2	2	2	6	6	6	9	9	9	11	11	11
depth (m)	0	4.084	4.084	4.084	41.012	41.012	41.012	78.691	78.691	78.691	95.074	95.074	95.074
date (YYYYmmdd)	0	20211111	20211111	20211111	20211111	20211111	20211111	20211111	20211111	20211111	20211111	20211111	20211111
time (hhMM)	0	435	435	435	435	435	435	435	435	435	435	435	435
2'deoxycitidine	NaN	38.3	NaN	NaN	NaN	NaN	NaN	NaN	NaN	NaN	NaN	NaN	31.0
2'deoxyguanosine	2.3	2.3	2.5	2.3	2.3	13.2	2.4	NaN	2.5	NaN	2.7	2.5	NaN
2'deoxyuridine	NaN	37.0	11.0	12.9	38.9	16.1	35.3	43.1	8.4	12.4	9.1	30.2	15.9

name	AE2123_BC36_C0N0	AE2123_BC19_C2N2	AE2123_BC20_C2N2	AE2123_BC21_C2N2	AE2123_BC22_C2N6	AE2123_BC23_C2N6	AE2123_BC24_C2N6	AE2123_BC25_C2N9	AE2123_BC26_C2N9	AE2123_BC27_C2N9	AE2123_BC28_C2N11	AE2123_BC29_C2N11	AE2123_BC30_C2N11
cast	0	2	2	2	2	2	2	2	2	2	2	2	2
niskin	0	2	2	2	6	6	6	9	9	9	11	11	11
depth (m)	0	4.084	4.084	4.084	41.012	41.012	41.012	78.691	78.691	78.691	95.074	95.074	95.074
date (YYYYmmdd)	0	20211111	20211111	20211111	20211111	20211111	20211111	20211111	20211111	20211111	20211111	20211111	20211111
time (hhMM)	0	435	435	435	435	435	435	435	435	435	435	435	435
adenosine 3'-monophosphate	NaN	NaN	NaN	NaN	NaN	NaN	NaN	NaN	NaN	NaN	NaN	NaN	NaN
4-aminobenzoic acid	NaN	NaN	18.6	NaN	111.4	NaN	NaN	NaN	NaN	NaN	NaN	NaN	NaN
uridine 5'-monophosphate	NaN	NaN	NaN	NaN	NaN	NaN	NaN	NaN	NaN	NaN	NaN	NaN	10.2
adenosine 5'-monophosphate	NaN	11.8	11.5	NaN	15.5	30.6	NaN	NaN	20.1	NaN	NaN	NaN	33.3
inosine 5'-monophosphate	NaN	NaN	NaN	NaN	NaN	NaN	NaN	NaN	NaN	10.8	NaN	NaN	7.7
5'deoxyadenosine	36.9	NaN	NaN	NaN	NaN	NaN	NaN	48.8	NaN	NaN	NaN	NaN	NaN
2,3-dihydroxypropane-1-sulfonate	NaN	36.6	38.6	45.4	42.1	36.8	57.2	37.3	34.9	40.6	29.1	33.6	78.2
gamma-aminobutyric acid	NaN	NaN	NaN	NaN	NaN	NaN	NaN	NaN	NaN	NaN	NaN	NaN	NaN
HET	NaN	NaN	NaN	NaN	NaN	NaN	NaN	NaN	NaN	NaN	NaN	NaN	NaN
HMP	126.3	NaN	NaN	623.2	94.4	278.8	NaN	241.6	NaN	NaN	197.1	325.0	107.7
N-acetyl-muramic acid	NaN	12.5	NaN	35.8	NaN	35.5	39.6	23.7	49.3	31.4	NaN	11.6	NaN
adenine	NaN	NaN	NaN	NaN	NaN	NaN	NaN	NaN	NaN	NaN	NaN	NaN	NaN
adenosine	2.3	2.4	2.7	2.3	2.3	13.2	2.4	2.3	2.3	2.4	2.7	2.4	2.4
alanine	30.3	24.1	150.1	33.6	184.7	NaN	35.2	30.2	19.8	50.1	32.7	51.6	148.2
amMP	11.3	NaN	8.1	7.9	NaN	4.7	NaN	14.3	6.2	11.3	17.4	NaN	8.4
arginine	NaN	NaN	74.0	NaN	187.5	NaN	NaN	NaN	10.6	11.8	9.2	8.0	10.7
asparagine	3.5	3.5	18.0	3.3	11.1	8.0	8.3	8.5	13.7	11.8	6.8	10.2	16.4

name	AE2123_BC36_C0N0	AE2123_BC19_C2N2	AE2123_BC20_C2N2	AE2123_BC21_C2N2	AE2123_BC22_C2N6	AE2123_BC23_C2N6	AE2123_BC24_C2N6	AE2123_BC25_C2N9	AE2123_BC26_C2N9	AE2123_BC27_C2N9	AE2123_BC28_C2N11	AE2123_BC29_C2N11	AE2123_BC30_C2N11
cast	0	2	2	2	2	2	2	2	2	2	2	2	2
niskin	0	2	2	2	6	6	6	9	9	9	11	11	11
depth (m)	0	4.084	4.084	4.084	41.012	41.012	41.012	78.691	78.691	78.691	95.074	95.074	95.074
date (YYYYmmdd)	0	20211111	20211111	20211111	20211111	20211111	20211111	20211111	20211111	20211111	20211111	20211111	20211111
time (hhMM)	0	435	435	435	435	435	435	435	435	435	435	435	435
aspartate	NaN	10.8	66.7	NaN	73.2	35.9	27.7	NaN	28.5	21.7	25.9	42.9	19.8
chitobiose	NaN	NaN	NaN	NaN	NaN	NaN	NaN	NaN	NaN	NaN	NaN	NaN	NaN
chitotriose	NaN	NaN	NaN	NaN	NaN	NaN	NaN	NaN	NaN	NaN	NaN	NaN	NaN
ciliatine	NaN	NaN	NaN	NaN	NaN	2.8	2.8	2.8	2.6	3.9	4.1	4.8	16.3
citrulline	NaN	6.9	99.0	6.8	188.0	NaN	7.9	NaN	NaN	NaN	NaN	NaN	4.7
cysteate	NaN	NaN	7.3	NaN	NaN	9.9	13.1	NaN	9.9	NaN	7.6	8.2	16.2
cysteine	NaN	19.8	40.0	14.7	10.0	19.6	17.8	14.9	32.2	11.2	22.3	30.2	27.0
cystine	NaN	NaN	NaN	NaN	NaN	NaN	NaN	NaN	NaN	NaN	NaN	NaN	NaN
cytidine	NaN	NaN	NaN	NaN	NaN	24.6	25.9	NaN	NaN	38.3	NaN	19.8	76.6
ectoine	NaN	NaN	NaN	NaN	NaN	23.8	NaN	NaN	NaN	NaN	29.3	45.1	NaN
glucosamine-6-phosphate	NaN	NaN	NaN	NaN	NaN	NaN	NaN	NaN	NaN	NaN	NaN	NaN	NaN
glucose 6-phosphate	NaN	NaN	NaN	NaN	NaN	NaN	NaN	NaN	11.3	NaN	NaN	NaN	NaN
glutamic acid	NaN	9.7	47.1	NaN	98.7	97.3	57.3	25.5	81.0	38.5	35.8	54.5	89.3
glutamine	2.9	9.1	24.7	12.7	22.7	27.1	24.1	18.0	30.5	20.1	17.6	22.1	33.7
glutathione	NaN	NaN	NaN	NaN	NaN	NaN	26.2	NaN	NaN	NaN	NaN	NaN	NaN
glycine	NaN	NaN	91.5	NaN	83.1	35.7	NaN	NaN	48.1	27.1	91.9	122.8	135.1
guanosine	NaN	NaN	NaN	NaN	NaN	NaN	NaN	NaN	NaN	NaN	NaN	NaN	NaN
histidine	NaN	NaN	68.3	11.1	30.1	NaN	9.2	5.6	5.0	6.1	NaN	NaN	18.6
homoserine	4.4	4.2	6.2	6.1	6.5	5.5	4.3	7.1	6.5	4.6	5.6	5.3	10.4

name	AE2123_BC36_C0N0	AE2123_BC19_C2N2	AE2123_BC20_C2N2	AE2123_BC21_C2N2	AE2123_BC22_C2N6	AE2123_BC23_C2N6	AE2123_BC24_C2N6	AE2123_BC25_C2N9	AE2123_BC26_C2N9	AE2123_BC27_C2N9	AE2123_BC28_C2N11	AE2123_BC29_C2N11	AE2123_BC30_C2N11
cast	0	2	2	2	2	2	2	2	2	2	2	2	2
niskin	0	2	2	2	6	6	6	9	9	9	11	11	11
depth (m)	0	4.084	4.084	4.084	41.012	41.012	41.012	78.691	78.691	78.691	95.074	95.074	95.074
date (YYYYmmdd)	0	20211111	20211111	20211111	20211111	20211111	20211111	20211111	20211111	20211111	20211111	20211111	20211111
time (hhMM)	0	435	435	435	435	435	435	435	435	435	435	435	435
homoserine betaine	NaN	48.4	51.9	37.0	68.0	66.1	98.3	70.4	75.7	73.0	44.1	52.6	104.2
isethionate	NaN	33.3	34.0	33.6	39.9	28.0	47.6	34.3	27.2	34.9	15.7	20.0	40.8
isoleucine	NaN	NaN	22.5	NaN	88.7	NaN	NaN	NaN	NaN	NaN	25.5	28.6	56.8
kynurenine	NaN	3.6	7.1	3.1	4.5	5.1	3.2	4.0	4.0	4.8	4.2	6.3	5.5
leucine	NaN	NaN	15.9	NaN	66.1	NaN	NaN	NaN	NaN	NaN	18.4	19.3	35.7
malic acid	NaN	52.1	150.2	28.6	184.9	81.2	131.6	49.0	79.5	29.4	43.8	57.7	122.6
methionine	NaN	NaN	NaN	NaN	NaN	NaN	NaN	NaN	NaN	NaN	NaN	NaN	NaN
muramic acid	NaN	NaN	NaN	NaN	NaN	NaN	NaN	5.5	NaN	NaN	NaN	NaN	11.1
pantothenic acid	NaN	NaN	NaN	2.8	NaN	4.1	2.7	NaN	2.0	NaN	NaN	NaN	2.0
phenylalanine	6.4	5.1	41.0	6.4	98.0	NaN	4.9	7.2	5.2	9.3	8.6	11.8	25.5
proline	NaN	NaN	NaN	NaN	70.1	NaN	NaN	NaN	NaN	NaN	NaN	NaN	NaN
putrescine	NaN	NaN	190.3	21.2	544.1	NaN	NaN	38.8	30.5	55.2	NaN	24.7	67.9
sarcosine	NaN	7.0	6.3	6.0	6.8	4.3	6.6	7.5	4.6	7.8	5.4	6.1	12.5
serine	NaN	30.4	252.2	35.0	360.6	NaN	17.6	19.8	11.1	51.2	NaN	9.6	35.8
glycerol 3-phosphate	NaN	35.9	31.4	27.0	24.3	24.0	28.4	40.4	29.2	32.4	36.3	38.8	65.4
spermidine	NaN	NaN	NaN	433.8	NaN	NaN	NaN	NaN	NaN	NaN	NaN	NaN	NaN
taurine	NaN	42.3	42.5	48.4	54.9	98.2	52.8	92.4	84.5	83.2	150.9	214.2	191.8
thiamine monophosphate	8.3	NaN	NaN	NaN	NaN	NaN	NaN	8.0	NaN	19.8	15.9	NaN	NaN
threonine	10.7	18.5	109.3	21.4	184.3	4.9	22.4	15.7	11.4	27.4	5.0	6.4	30.6

name	AE2123_BC36_C0N0	AE2123_BC19_C2N2	AE2123_BC20_C2N2	AE2123_BC21_C2N2	AE2123_BC22_C2N6	AE2123_BC23_C2N6	AE2123_BC24_C2N6	AE2123_BC25_C2N9	AE2123_BC26_C2N9	AE2123_BC27_C2N9	AE2123_BC28_C2N11	AE2123_BC29_C2N11	AE2123_BC30_C2N11
cast	0	2	2	2	2	2	2	2	2	2	2	2	2
niskin	0	2	2	2	6	6	6	9	9	9	11	11	11
depth (m)	0	4.084	4.084	4.084	41.012	41.012	41.012	78.691	78.691	78.691	95.074	95.074	95.074
date (YYYYmmdd)	0	20211111	20211111	20211111	20211111	20211111	20211111	20211111	20211111	20211111	20211111	20211111	20211111
time (hhMM)	0	435	435	435	435	435	435	435	435	435	435	435	435
thymidine	NaN	NaN	NaN	26.2	40.9	28.7	34.1	NaN	31.6	28.4	30.1	26.9	97.8
tryptamine	NaN	NaN	NaN	NaN	NaN	NaN	NaN	NaN	NaN	NaN	NaN	NaN	NaN
tryptophan	4.0	4.2	5.5	5.0	6.4	NaN	NaN	4.3	6.3	7.0	10.6	9.8	19.2
tyrosine	NaN	19.7	398.6	81.7	10132.6	109.0	NaN	226.5	143.0	57.8	21.3	38.6	105.4
uridine	9.6	9.7	10.8	8.7	14.3	9.6	11.0	10.1	8.8	9.8	8.3	9.2	6.6
valine	NaN	NaN	25.5	NaN	91.0	NaN	NaN	NaN	NaN	NaN	20.8	27.1	51.0
xanthosine	NaN	NaN	NaN	NaN	NaN	NaN	NaN	NaN	NaN	NaN	NaN	NaN	NaN

name	AE2123_BC31_C2N16	AE2123_BC32_C2N16	AE2123_BC33_C2N16	AE2123_BC34_C2N21	AE2123_BC35_C2N21	AE2123_BC37_C2N21	AE2123_BC38_C2N22	AE2123_BC39_C2N22	AE2123_BC40_C2N22	AE2123_BC41_C3N2	AE2123_BC42_C3N2	AE2123_BC43_C3N2	AE2123_BC44_C3N4
cast	2	2	2	2	2	2	2	2	2	3	3	3	3
niskin	16	16	16	21	21	21	22	22	22	2	2	2	4
depth (m)	199.216	199.216	199.216	500.793	500.793	500.793	1000.522	1000.522	1000.522	3.539	3.539	3.539	19.723
date (YYYYmmdd)	20211111	20211111	20211111	20211111	20211111	20211111	20211111	20211111	20211111	20211111	20211111	20211111	20211111
time (hhMM)	435	435	435	435	435	435	435	435	435	1000	1000	1000	1000
2'deoxycitidine	NaN	NaN	55.4	NaN	NaN	NaN	NaN	NaN	NaN	NaN	NaN	NaN	NaN
2'deoxyguanosine	NaN	2.3	NaN	NaN	NaN	NaN	2.3	2.6	2.4	2.3	2.5	2.5	2.7
2'deoxyuridine	31.5	13.2	29.9	14.3	26.1	NaN	NaN	NaN	NaN	13.9	36.0	35.6	8.9
adenosine 3'-monophosphate	NaN	NaN	NaN	NaN	NaN	NaN	NaN	NaN	NaN	NaN	NaN	NaN	8.2
4-aminobenzoic acid	NaN	NaN	NaN	NaN	NaN	NaN	NaN	NaN	NaN	NaN	NaN	NaN	NaN
uridine 5'-monophosphate	NaN	NaN	NaN	NaN	NaN	NaN	NaN	NaN	NaN	NaN	NaN	NaN	NaN
adenosine 5'-monophosphate	NaN	NaN	NaN	NaN	NaN	NaN	NaN	NaN	NaN	NaN	NaN	NaN	13.0
inosine 5'-monophosphate	NaN	NaN	NaN	NaN	NaN	NaN	NaN	NaN	NaN	NaN	NaN	7.2	7.7
5'deoxyadenosine	83.9	NaN	NaN	NaN	NaN	NaN	NaN	NaN	NaN	NaN	85.5	40.2	NaN
2,3-dihydroxypropane-1-sulfonate	NaN	NaN	NaN	NaN	NaN	NaN	NaN	NaN	NaN	24.4	37.3	37.5	25.0
gamma-aminobutyric acid	7.4	NaN	NaN	NaN	NaN	NaN	6.7	NaN	68.5	NaN	NaN	NaN	11.5
HET	NaN	NaN	NaN	NaN	NaN	NaN	NaN	NaN	NaN	NaN	NaN	NaN	NaN
HMP	NaN	NaN	NaN	NaN	NaN	450.4	NaN	314.6	NaN	240.3	NaN	NaN	57.8
N-acetyl-muramic acid	NaN	NaN	NaN	NaN	NaN	NaN	NaN	NaN	NaN	NaN	9.4	15.6	13.8
adenine	NaN	NaN	NaN	NaN	NaN	NaN	NaN	NaN	NaN	NaN	NaN	NaN	NaN
adenosine	NaN	2.3	NaN	NaN	NaN	NaN	2.3	2.6	2.4	NaN	2.4	2.6	2.7
alanine	NaN	26.2	35.5	127.7	NaN	NaN	6.5	20.9	20.0	NaN	16.7	4.1	37.0

name	AE2123_BC31_C2N16	AE2123_BC32_C2N16	AE2123_BC33_C2N16	AE2123_BC34_C2N21	AE2123_BC35_C2N21	AE2123_BC37_C2N21	AE2123_BC38_C2N22	AE2123_BC39_C2N22	AE2123_BC40_C2N22	AE2123_BC41_C3N2	AE2123_BC42_C3N2	AE2123_BC43_C3N2	AE2123_BC44_C3N4
cast	2	2	2	2	2	2	2	2	2	3	3	3	3
niskin	16	16	16	21	21	21	22	22	22	2	2	2	4
depth (m)	199.216	199.216	199.216	500.793	500.793	500.793	1000.522	1000.522	1000.522	3.539	3.539	3.539	19.723
date (YYYYmmdd)	20211111	20211111	20211111	20211111	20211111	20211111	20211111	20211111	20211111	20211111	20211111	20211111	20211111
time (hhMM)	435	435	435	435	435	435	435	435	435	1000	1000	1000	1000
amMP	NaN	7.5	11.9	11.4	NaN	NaN	7.3	16.0	5.4	NaN	NaN	NaN	NaN
arginine	NaN	NaN	NaN	9.3	NaN	NaN	NaN	NaN	NaN	NaN	NaN	NaN	9.7
asparagine	17.2	NaN	4.6	14.2	NaN	NaN	NaN	NaN	NaN	3.6	2.7	5.7	2.4
aspartate	13.2	NaN	14.4	15.5	NaN	NaN	NaN	NaN	9.4	NaN	NaN	NaN	NaN
chitobiose	NaN	NaN	NaN	NaN	NaN	NaN	NaN	NaN	NaN	NaN	NaN	NaN	NaN
chitotriose	NaN	NaN	NaN	NaN	NaN	NaN	NaN	NaN	NaN	NaN	NaN	NaN	NaN
ciliatine	2.4	NaN	NaN	NaN	NaN	NaN	NaN	NaN	NaN	NaN	NaN	NaN	NaN
citrulline	NaN	10.0	34.0	81.7	NaN	NaN	NaN	NaN	NaN	NaN	NaN	NaN	NaN
cysteate	NaN	NaN	NaN	NaN	NaN	NaN	NaN	NaN	NaN	NaN	NaN	NaN	NaN
cysteine	NaN	NaN	9.4	NaN	NaN	NaN	NaN	NaN	NaN	18.3	17.0	13.3	25.5
cystine	NaN	NaN	NaN	NaN	NaN	NaN	NaN	NaN	NaN	NaN	NaN	NaN	NaN
cytidine	NaN	12.7	NaN	28.0	NaN	NaN	NaN	11.2	31.0	NaN	NaN	NaN	NaN
ectoine	NaN	NaN	NaN	NaN	NaN	NaN	NaN	NaN	NaN	NaN	54.7	NaN	NaN
glucosamine-6-phosphate	NaN	NaN	NaN	NaN	NaN	NaN	NaN	NaN	NaN	NaN	NaN	NaN	NaN
glucose 6-phosphate	NaN	NaN	NaN	NaN	NaN	NaN	NaN	NaN	NaN	NaN	NaN	10.2	NaN
glutamic acid	NaN	NaN	NaN	NaN	NaN	NaN	NaN	NaN	NaN	30.4	NaN	51.3	28.0
glutamine	NaN	NaN	5.6	14.3	2.3	NaN	NaN	NaN	NaN	13.4	15.1	20.7	65.7
glutathione	NaN	NaN	NaN	NaN	NaN	NaN	NaN	NaN	NaN	NaN	NaN	NaN	NaN

name	AE2123_BC31_C2N16	AE2123_BC32_C2N16	AE2123_BC33_C2N16	AE2123_BC34_C2N21	AE2123_BC35_C2N21	AE2123_BC37_C2N21	AE2123_BC38_C2N22	AE2123_BC39_C2N22	AE2123_BC40_C2N22	AE2123_BC41_C3N2	AE2123_BC42_C3N2	AE2123_BC43_C3N2	AE2123_BC44_C3N4
cast	2	2	2	2	2	2	2	2	2	3	3	3	3
niskin	16	16	16	21	21	21	22	22	22	2	2	2	4
depth (m)	199.216	199.216	199.216	500.793	500.793	500.793	1000.522	1000.522	1000.522	3.539	3.539	3.539	19.723
date (YYYYmmdd)	20211111	20211111	20211111	20211111	20211111	20211111	20211111	20211111	20211111	20211111	20211111	20211111	20211111
time (hhMM)	435	435	435	435	435	435	435	435	435	1000	1000	1000	1000
glycine	23.1	NaN	NaN	26.9	NaN	NaN	NaN	NaN	NaN	26.0	NaN	NaN	12.1
guanosine	NaN	NaN	NaN	NaN	NaN	NaN	NaN	NaN	NaN	NaN	NaN	NaN	NaN
histidine	NaN	5.9	16.1	59.2	NaN	NaN	NaN	NaN	NaN	NaN	NaN	5.6	17.4
homoserine	4.6	4.4	4.2	4.5	4.2	4.4	4.1	5.3	5.2	5.3	4.8	6.6	6.0
homoserine betaine	NaN	NaN	NaN	NaN	NaN	NaN	NaN	NaN	NaN	35.8	50.3	34.3	21.4
isethionate	NaN	4.4	4.5	7.7	NaN	NaN	NaN	NaN	NaN	21.7	36.9	58.5	25.8
isoleucine	NaN	NaN	NaN	NaN	NaN	NaN	NaN	NaN	NaN	NaN	NaN	NaN	NaN
kynurenine	NaN	NaN	3.0	4.2	NaN	NaN	NaN	NaN	NaN	2.9	2.9	2.9	4.5
leucine	NaN	NaN	NaN	6.7	NaN	NaN	NaN	NaN	NaN	NaN	NaN	NaN	NaN
malic acid	NaN	NaN	30.0	NaN	NaN	NaN	NaN	NaN	240.9	106.5	31.6	104.7	85.5
methionine	NaN	NaN	NaN	NaN	NaN	NaN	NaN	NaN	NaN	NaN	NaN	NaN	NaN
muramic acid	8.0	11.9	NaN	NaN	NaN	NaN	NaN	6.6	NaN	7.0	6.4	NaN	NaN
pantothenic acid	NaN	NaN	NaN	NaN	NaN	NaN	NaN	NaN	NaN	2.7	2.7	NaN	3.9
phenylalanine	NaN	NaN	8.4	11.4	NaN	NaN	NaN	NaN	NaN	NaN	NaN	NaN	8.9
proline	NaN	NaN	NaN	NaN	NaN	NaN	NaN	NaN	NaN	NaN	NaN	NaN	NaN
putrescine	NaN	NaN	12.5	61.9	NaN	NaN	NaN	NaN	NaN	NaN	20.9	11.3	22.1
sarcosine	NaN	NaN	3.9	NaN	NaN	NaN	4.0	NaN	NaN	NaN	7.2	7.8	5.1
serine	NaN	39.4	60.7	191.8	NaN	NaN	NaN	NaN	16.1	NaN	NaN	NaN	16.4

name	AE2123_BC31_C2N16	AE2123_BC32_C2N16	AE2123_BC33_C2N16	AE2123_BC34_C2N21	AE2123_BC35_C2N21	AE2123_BC37_C2N21	AE2123_BC38_C2N22	AE2123_BC39_C2N22	AE2123_BC40_C2N22	AE2123_BC41_C3N2	AE2123_BC42_C3N2	AE2123_BC43_C3N2	AE2123_BC44_C3N4
cast	2	2	2	2	2	2	2	2	2	3	3	3	3
niskin	16	16	16	21	21	21	22	22	22	2	2	2	4
depth (m)	199.216	199.216	199.216	500.793	500.793	500.793	1000.522	1000.522	1000.522	3.539	3.539	3.539	19.723
date (YYYYmmdd)	20211111	20211111	20211111	20211111	20211111	20211111	20211111	20211111	20211111	20211111	20211111	20211111	20211111
time (hhMM)	435	435	435	435	435	435	435	435	435	1000	1000	1000	1000
glycerol 3-phosphate	12.2	20.1	8.1	12.5	NaN	NaN	NaN	NaN	NaN	19.8	24.2	16.4	45.8
spermidine	NaN	NaN	NaN	NaN	NaN	NaN	NaN	NaN	NaN	NaN	NaN	NaN	NaN
taurine	NaN	NaN	NaN	NaN	NaN	NaN	NaN	NaN	NaN	47.3	54.7	42.8	16.9
thiamine monophosphate	10.1	7.1	NaN	NaN	NaN	NaN	NaN	NaN	NaN	6.7	NaN	NaN	NaN
threonine	NaN	15.0	20.1	60.7	NaN	NaN	NaN	NaN	NaN	NaN	9.5	20.1	18.2
thymidine	NaN	NaN	NaN	NaN	NaN	NaN	NaN	NaN	NaN	NaN	26.3	24.5	30.9
tryptamine	NaN	NaN	NaN	NaN	NaN	NaN	NaN	NaN	NaN	NaN	NaN	NaN	NaN
tryptophan	NaN	NaN	4.8	NaN	NaN	NaN	NaN	NaN	NaN	4.0	6.3	5.1	4.7
tyrosine	17.4	NaN	27.3	131.8	NaN	1362.4	59.0	73.1	NaN	NaN	24.3	NaN	NaN
uridine	NaN	NaN	7.4	5.6	5.2	4.4	NaN	7.7	NaN	5.5	10.6	6.9	19.5
valine	NaN	NaN	NaN	12.4	NaN	NaN	NaN	NaN	NaN	NaN	NaN	NaN	NaN
xanthosine	NaN	NaN	NaN	NaN	NaN	NaN	NaN	NaN	NaN	NaN	NaN	NaN	NaN

name	AE2123_BC45_C3N4	AE2123_BC46_C3N4	AE2123_BC47_C3N6	AE2123_BC48_C3N6	AE2123_BC49_C3N6	AE2123_BC50_C3N9	AE2123_BC51_C3N9	AE2123_BC52_C3N9	AE2123_BC53_C3N11	AE2123_BC54_C3N11	AE2123_BC55_C3N11	AE2123_BC56_C3N13	AE2123_BC57_C3N13
cast	3	3	3	3	3	3	3	3	3	3	3	3	3
niskin	4	4	6	6	6	9	9	9	11	11	11	13	13
depth (m)	19.723	19.723	38.714	38.714	38.714	79.455	79.455	79.455	89.839	89.839	89.839	106.019	106.019
date (YYYYmmdd)	20211111	20211111	20211111	20211111	20211111	20211111	20211111	20211111	20211111	20211111	20211111	20211111	20211111
time (hhMM)	1000	1000	1000	1000	1000	1000	1000	1000	1000	1000	1000	1000	1000
2'deoxycitidine	NaN	NaN	NaN	NaN	NaN	NaN	NaN	NaN	NaN	NaN	NaN	NaN	NaN
2'deoxyguanosine	2.3	2.3	NaN	2.5	2.4	2.3	2.3	2.3	NaN	NaN	2.6	NaN	2.5
2'deoxyuridine	63.3	20.6	37.6	43.6	40.8	89.0	16.7	11.9	12.6	40.0	24.9	19.4	25.5
adenosine 3'-monophosphate	NaN	NaN	NaN	NaN	NaN	NaN	NaN	NaN	NaN	NaN	NaN	NaN	NaN
4-aminobenzoic acid	NaN	NaN	NaN	NaN	NaN	NaN	NaN	NaN	NaN	NaN	NaN	NaN	NaN
uridine 5'-monophosphate	NaN	NaN	NaN	NaN	NaN	NaN	NaN	NaN	NaN	NaN	NaN	NaN	NaN
adenosine 5'-monophosphate	NaN	NaN	11.6	NaN	NaN	NaN	NaN	NaN	NaN	NaN	32.6	NaN	NaN
inosine 5'-monophosphate	9.1	NaN	NaN	NaN	8.6	NaN	NaN	NaN	NaN	NaN	10.0	NaN	NaN
5'deoxyadenosine	75.5	NaN	49.0	NaN	NaN	NaN	NaN	NaN	NaN	NaN	NaN	NaN	37.4
2,3-dihydroxypropane-1-sulfonate	17.5	24.2	31.8	27.8	37.3	46.1	26.4	30.3	40.2	48.4	50.1	18.2	25.3
gamma-aminobutyric acid	NaN	NaN	NaN	NaN	NaN	NaN	NaN	NaN	NaN	NaN	4.5	NaN	NaN
HET	NaN	NaN	NaN	NaN	NaN	NaN	NaN	NaN	NaN	NaN	NaN	NaN	NaN
HMP	NaN	NaN	NaN	NaN	111.4	NaN	NaN	NaN	NaN	NaN	NaN	NaN	NaN
N-acetyl-muramic acid	NaN	NaN	20.5	22.8	26.3	21.0	NaN	NaN	NaN	NaN	65.7	NaN	NaN
adenine	NaN	NaN	NaN	NaN	NaN	227.6	NaN	NaN	NaN	NaN	NaN	NaN	NaN
adenosine	2.5	2.3	NaN	2.4	2.3	2.5	NaN	2.3	2.4	2.3	2.5	NaN	2.6
alanine	NaN	NaN	16.0	NaN	22.2	34.0	NaN	35.0	24.2	20.3	11.1	21.9	4.8

name	AE2123_BC45_C3N4	AE2123_BC46_C3N4	AE2123_BC47_C3N6	AE2123_BC48_C3N6	AE2123_BC49_C3N6	AE2123_BC50_C3N9	AE2123_BC51_C3N9	AE2123_BC52_C3N9	AE2123_BC53_C3N11	AE2123_BC54_C3N11	AE2123_BC55_C3N11	AE2123_BC56_C3N13	AE2123_BC57_C3N13
cast	3	3	3	3	3	3	3	3	3	3	3	3	3
niskin	4	4	6	6	6	9	9	9	11	11	11	13	13
depth (m)	19.723	19.723	38.714	38.714	38.714	79.455	79.455	79.455	89.839	89.839	89.839	106.019	106.019
date (YYYYmmdd)	20211111	20211111	20211111	20211111	20211111	20211111	20211111	20211111	20211111	20211111	20211111	20211111	20211111
time (hhMM)	1000	1000	1000	1000	1000	1000	1000	1000	1000	1000	1000	1000	1000
amMP	NaN	5.5	12.6	16.7	NaN	8.2	NaN	5.3	NaN	10.4	NaN	NaN	NaN
arginine	NaN	NaN	NaN	NaN	NaN	NaN	NaN	NaN	NaN	NaN	37.4	NaN	NaN
asparagine	NaN	NaN	4.5	3.2	6.1	8.6	4.6	8.5	7.7	9.1	15.9	9.6	NaN
aspartate	NaN	NaN	NaN	9.8	NaN	NaN	10.3	NaN	NaN	NaN	48.1	23.0	NaN
chitobiose	NaN	NaN	NaN	NaN	NaN	NaN	NaN	NaN	NaN	NaN	NaN	NaN	NaN
chitotriose	NaN	NaN	NaN	NaN	NaN	NaN	NaN	NaN	NaN	NaN	NaN	NaN	NaN
ciliatine	NaN	NaN	NaN	NaN	NaN	NaN	NaN	NaN	3.6	4.0	9.4	2.6	4.9
citrulline	NaN	NaN	NaN	NaN	NaN	NaN	NaN	8.3	NaN	NaN	NaN	NaN	NaN
cysteate	NaN	NaN	NaN	NaN	NaN	NaN	6.9	NaN	NaN	NaN	15.2	NaN	NaN
cysteine	15.9	9.9	14.5	14.1	23.7	18.5	19.1	15.9	29.0	17.5	44.9	24.5	12.2
cystine	NaN	NaN	NaN	NaN	NaN	NaN	NaN	NaN	NaN	NaN	NaN	NaN	NaN
cytidine	31.7	NaN	NaN	NaN	NaN	NaN	40.7	NaN	28.5	NaN	NaN	20.9	NaN
ectoine	NaN	NaN	NaN	NaN	41.1	31.1	NaN	NaN	NaN	NaN	NaN	NaN	NaN
glucosamine-6-phosphate	NaN	NaN	NaN	NaN	NaN	NaN	NaN	NaN	NaN	NaN	NaN	NaN	NaN
glucose 6-phosphate	NaN	NaN	NaN	NaN	NaN	10.0	NaN	NaN	NaN	11.3	NaN	NaN	NaN
glutamic acid	NaN	NaN	NaN	21.5	NaN	NaN	23.1	NaN	10.2	28.1	107.2	19.5	NaN
glutamine	13.3	9.9	13.0	13.3	11.4	21.6	10.9	15.9	19.8	21.4	32.8	10.7	5.0
glutathione	NaN	NaN	NaN	NaN	NaN	NaN	NaN	NaN	NaN	NaN	NaN	NaN	NaN

name	AE2123_BC45_C3N4	AE2123_BC46_C3N4	AE2123_BC47_C3N6	AE2123_BC48_C3N6	AE2123_BC49_C3N6	AE2123_BC50_C3N9	AE2123_BC51_C3N9	AE2123_BC52_C3N9	AE2123_BC53_C3N11	AE2123_BC54_C3N11	AE2123_BC55_C3N11	AE2123_BC56_C3N13	AE2123_BC57_C3N13
cast	3	3	3	3	3	3	3	3	3	3	3	3	3
niskin	4	4	6	6	6	9	9	9	11	11	11	13	13
depth (m)	19.723	19.723	38.714	38.714	38.714	79.455	79.455	79.455	89.839	89.839	89.839	106.019	106.019
date (YYYYmmdd)	20211111	20211111	20211111	20211111	20211111	20211111	20211111	20211111	20211111	20211111	20211111	20211111	20211111
time (hhMM)	1000	1000	1000	1000	1000	1000	1000	1000	1000	1000	1000	1000	1000
glycine	NaN	NaN	NaN	33.5	NaN	NaN	52.2	NaN	33.0	NaN	164.4	151.7	NaN
guanosine	NaN	NaN	NaN	NaN	NaN	NaN	NaN	NaN	NaN	NaN	NaN	NaN	NaN
histidine	NaN	NaN	5.2	NaN	11.0	10.9	NaN	13.1	6.1	4.4	6.2	25.4	NaN
homoserine	4.6	5.6	5.2	5.4	5.0	5.1	4.7	5.8	4.6	6.0	7.0	4.7	4.0
homoserine betaine	23.2	38.6	46.8	41.5	36.4	56.2	35.3	48.1	63.8	53.2	112.3	16.7	10.6
isethionate	19.9	24.8	29.9	27.9	28.6	41.9	24.4	26.5	21.1	19.7	23.1	9.8	11.9
isoleucine	NaN	NaN	NaN	NaN	NaN	NaN	NaN	NaN	NaN	NaN	NaN	NaN	NaN
kynurenine	3.0	NaN	4.1	3.6	3.8	6.2	2.9	4.0	2.9	3.4	4.6	3.1	NaN
leucine	NaN	NaN	NaN	NaN	NaN	NaN	NaN	NaN	NaN	NaN	NaN	2.2	NaN
malic acid	33.1	41.1	NaN	58.5	28.7	32.9	46.6	NaN	NaN	NaN	100.2	NaN	NaN
methionine	NaN	NaN	NaN	NaN	NaN	NaN	NaN	NaN	NaN	NaN	NaN	NaN	NaN
muramic acid	NaN	NaN	NaN	NaN	NaN	8.6	NaN	NaN	NaN	NaN	NaN	11.7	NaN
pantothenic acid	2.5	NaN	NaN	3.9	2.4	3.3	3.3	2.4	NaN	2.1	3.9	NaN	NaN
phenylalanine	NaN	NaN	5.2	NaN	5.8	8.2	NaN	6.8	5.4	5.6	6.7	5.4	NaN
proline	NaN	NaN	NaN	NaN	NaN	NaN	NaN	NaN	NaN	NaN	NaN	NaN	NaN
putrescine	NaN	NaN	NaN	NaN	NaN	12.0	NaN	13.7	27.0	13.9	39.3	NaN	NaN
sarcosine	5.9	5.0	4.7	4.3	6.0	6.9	4.3	6.2	8.4	6.8	6.3	3.8	NaN
serine	NaN	NaN	25.3	NaN	20.7	9.6	NaN	18.2	8.5	NaN	11.8	39.3	NaN

name	AE2123_BC45_C3N4	AE2123_BC46_C3N4	AE2123_BC47_C3N6	AE2123_BC48_C3N6	AE2123_BC49_C3N6	AE2123_BC50_C3N9	AE2123_BC51_C3N9	AE2123_BC52_C3N9	AE2123_BC53_C3N11	AE2123_BC54_C3N11	AE2123_BC55_C3N11	AE2123_BC56_C3N13	AE2123_BC57_C3N13
cast	3	3	3	3	3	3	3	3	3	3	3	3	3
niskin	4	4	6	6	6	9	9	9	11	11	11	13	13
depth (m)	19.723	19.723	38.714	38.714	38.714	79.455	79.455	79.455	89.839	89.839	89.839	106.019	106.019
date (YYYYmmdd)	20211111	20211111	20211111	20211111	20211111	20211111	20211111	20211111	20211111	20211111	20211111	20211111	20211111
time (hhMM)	1000	1000	1000	1000	1000	1000	1000	1000	1000	1000	1000	1000	1000
glycerol 3-phosphate	35.8	29.2	30.4	24.4	27.1	33.2	23.9	25.6	44.8	40.2	64.1	31.5	39.1
spermidine	NaN	NaN	NaN	NaN	NaN	NaN	NaN	NaN	NaN	NaN	NaN	NaN	NaN
taurine	33.8	43.2	47.7	54.2	41.9	55.2	48.3	66.6	132.2	83.3	235.4	40.8	12.1
thiamine monophosphate	NaN	NaN	NaN	NaN	NaN	NaN	NaN	NaN	NaN	14.1	NaN	NaN	NaN
threonine	NaN	NaN	11.6	NaN	13.5	19.2	NaN	17.0	5.4	7.0	10.9	15.8	NaN
thymidine	56.0	NaN	NaN	NaN	45.3	52.9	29.2	40.2	27.1	51.8	35.0	NaN	NaN
tryptamine	NaN	NaN	NaN	NaN	NaN	NaN	NaN	NaN	NaN	NaN	NaN	NaN	NaN
tryptophan	NaN	5.8	NaN	NaN	NaN	NaN	NaN	NaN	NaN	5.1	NaN	4.8	NaN
tyrosine	NaN	NaN	23.8	14.3	22.5	NaN	26.6	24.4	116.6	26.6	177.3	NaN	NaN
uridine	8.8	8.1	11.7	6.6	8.1	10.1	6.6	8.2	7.6	8.1	6.6	NaN	NaN
valine	NaN	NaN	NaN	NaN	NaN	NaN	NaN	NaN	NaN	NaN	NaN	NaN	NaN
xanthosine	NaN	NaN	NaN	NaN	NaN	NaN	NaN	NaN	NaN	NaN	NaN	NaN	NaN

name	AE2123_BC58_C3N13	AE2123_BC59_C3N16	AE2123_BC60_C3N16	AE2123_BC61_C3N16	AE2123_BC62_C3N18	AE2123_BC63_C3N18	AE2123_BC64_C3N18	AE2123_BC65_C4N2	AE2123_BC66_C4N2	AE2123_BC67_C4N2	AE2123_BC71_C4N6	AE2123_BC72_C4N6	AE2123_BC73_C4N6
cast	3	3	3	3	3	3	3	4	4	4	4	4	4
niskin	13	16	16	16	18	18	18	2	2	2	6	6	6
depth (m)	106.019	200.63	200.63	200.63	250.283	250.283	250.283	3.923	3.923	3.923	40.867	40.867	40.867
date (YYYYmmdd)	20211111	20211111	20211111	20211111	20211111	20211111	20211111	20211111	20211111	20211111	20211111	20211111	20211111
time (hhMM)	1000	1000	1000	1000	1000	1000	1000	1635	1635	1635	1635	1635	1635
2'deoxycitidine	NaN	NaN	NaN	NaN	29.8	NaN	29.4	NaN	NaN	NaN	NaN	NaN	NaN
2'deoxyguanosine	2.4	2.3	NaN	NaN	3.2	2.3	2.5	2.4	2.6	NaN	2.3	2.6	2.4
2'deoxyuridine	35.0	NaN	NaN	NaN	24.0	26.0	27.9	NaN	45.7	48.3	13.7	14.2	51.7
adenosine 3'-monophosphate	NaN	NaN	NaN	NaN	NaN	NaN	NaN	NaN	NaN	NaN	NaN	NaN	NaN
4-aminobenzoic acid	NaN	NaN	NaN	NaN	NaN	NaN	NaN	NaN	NaN	NaN	NaN	NaN	NaN
uridine 5'-monophosphate	NaN	NaN	NaN	NaN	NaN	NaN	NaN	NaN	NaN	NaN	NaN	NaN	NaN
adenosine 5'-monophosphate	NaN	NaN	NaN	NaN	11.6	NaN	NaN	NaN	NaN	NaN	NaN	NaN	NaN
inosine 5'-monophosphate	NaN	NaN	NaN	NaN	NaN	NaN	NaN	NaN	NaN	NaN	NaN	NaN	NaN
5'deoxyadenosine	NaN	NaN	NaN	43.7	NaN	52.0	36.5	NaN	NaN	NaN	NaN	79.0	NaN
2,3-dihydroxypropane-1-sulfonate	18.8	NaN	NaN	NaN	22.9	NaN	NaN	26.0	24.6	34.7	23.7	25.1	25.2
gamma-aminobutyric acid	NaN	NaN	NaN	NaN	NaN	NaN	NaN	4.8	NaN	NaN	NaN	NaN	NaN
HET	NaN	NaN	NaN	NaN	NaN	NaN	NaN	NaN	NaN	NaN	NaN	NaN	NaN
HMP	NaN	NaN	NaN	NaN	NaN	NaN	414.5	NaN	80.0	174.2	NaN	78.2	118.6
N-acetyl-muramic acid	19.3	NaN	NaN	NaN	16.7	NaN	NaN	15.2	NaN	22.7	41.9	28.7	14.6
adenine	NaN	NaN	NaN	NaN	NaN	NaN	NaN	NaN	NaN	NaN	NaN	NaN	NaN
adenosine	2.3	2.3	NaN	2.3	3.2	2.3	2.5	2.4	2.5	2.3	2.3	2.3	2.4
alanine	4.1	5.1	54.2	NaN	NaN	NaN	NaN	15.7	10.4	33.4	16.5	18.3	7.4

name	AE2123_BC58_C3N13	AE2123_BC59_C3N16	AE2123_BC60_C3N16	AE2123_BC61_C3N16	AE2123_BC62_C3N18	AE2123_BC63_C3N18	AE2123_BC64_C3N18	AE2123_BC65_C4N2	AE2123_BC66_C4N2	AE2123_BC67_C4N2	AE2123_BC71_C4N6	AE2123_BC72_C4N6	AE2123_BC73_C4N6
cast	3	3	3	3	3	3	3	4	4	4	4	4	4
niskin	13	16	16	16	18	18	18	2	2	2	6	6	6
depth (m)	106.019	200.63	200.63	200.63	250.283	250.283	250.283	3.923	3.923	3.923	40.867	40.867	40.867
date (YYYYmmdd)	20211111	20211111	20211111	20211111	20211111	20211111	20211111	20211111	20211111	20211111	20211111	20211111	20211111
time (hhMM)	1000	1000	1000	1000	1000	1000	1000	1635	1635	1635	1635	1635	1635
amMP	24.3	NaN	NaN	NaN	NaN	NaN	29.2	NaN	NaN	3.6	NaN	NaN	NaN
arginine	NaN	NaN	NaN	NaN	NaN	NaN	NaN	10.1	NaN	NaN	11.0	NaN	NaN
asparagine	NaN	NaN	2.4	NaN	3.4	NaN	NaN	7.7	3.3	1.9	5.8	6.1	3.2
aspartate	NaN	NaN	NaN	NaN	NaN	NaN	NaN	37.0	25.7	NaN	30.8	34.0	15.5
chitobiose	NaN	NaN	NaN	NaN	NaN	NaN	NaN	NaN	NaN	NaN	NaN	NaN	NaN
chitotriose	NaN	NaN	NaN	NaN	NaN	NaN	NaN	NaN	NaN	NaN	NaN	NaN	NaN
ciliatine	2.6	NaN	NaN	NaN	NaN	NaN	NaN	NaN	NaN	2.4	NaN	NaN	NaN
citrulline	NaN	NaN	NaN	NaN	NaN	NaN	NaN	NaN	14.0	NaN	20.0	17.6	11.9
cysteate	NaN	NaN	NaN	NaN	NaN	NaN	NaN	NaN	7.5	NaN	7.9	8.0	NaN
cysteine	12.3	NaN	6.2	NaN	NaN	NaN	NaN	15.5	29.2	11.3	25.0	24.5	18.3
cystine	NaN	NaN	NaN	NaN	NaN	NaN	NaN	NaN	NaN	NaN	NaN	NaN	NaN
cytidine	NaN	NaN	NaN	22.4	41.8	NaN	NaN	NaN	50.4	50.3	11.0	NaN	NaN
ectoine	NaN	NaN	NaN	NaN	NaN	NaN	NaN	NaN	NaN	NaN	NaN	NaN	NaN
glucosamine-6-phosphate	NaN	NaN	NaN	NaN	NaN	NaN	NaN	NaN	NaN	NaN	NaN	NaN	NaN
glucose 6-phosphate	10.6	NaN	NaN	NaN	20.5	NaN	NaN	NaN	NaN	NaN	NaN	NaN	NaN
glutamic acid	NaN	NaN	NaN	NaN	18.7	NaN	NaN	65.9	45.7	18.1	29.5	32.7	27.7
glutamine	5.9	NaN	4.2	NaN	24.6	3.0	NaN	9.4	7.1	10.2	9.9	9.0	10.1
glutathione	NaN	NaN	NaN	NaN	NaN	NaN	NaN	NaN	NaN	NaN	NaN	NaN	NaN
glycine	NaN	NaN	NaN	NaN	NaN	NaN	NaN	88.4	67.7	NaN	61.0	94.8	59.3

name	AE2123_BC58_C3N13	AE2123_BC59_C3N16	AE2123_BC60_C3N16	AE2123_BC61_C3N16	AE2123_BC62_C3N18	AE2123_BC63_C3N18	AE2123_BC64_C3N18	AE2123_BC65_C4N2	AE2123_BC66_C4N2	AE2123_BC67_C4N2	AE2123_BC71_C4N6	AE2123_BC72_C4N6	AE2123_BC73_C4N6
cast	3	3	3	3	3	3	3	4	4	4	4	4	4
niskin	13	16	16	16	18	18	18	2	2	2	6	6	6
depth (m)	106.019	200.63	200.63	200.63	250.283	250.283	250.283	3.923	3.923	3.923	40.867	40.867	40.867
date (YYYYmmdd)	20211111	20211111	20211111	20211111	20211111	20211111	20211111	20211111	20211111	20211111	20211111	20211111	20211111
time (hhMM)	1000	1000	1000	1000	1000	1000	1000	1635	1635	1635	1635	1635	1635
guanosine	NaN	NaN	NaN	NaN	NaN	NaN	NaN	NaN	NaN	NaN	NaN	NaN	NaN
histidine	NaN	9.1	11.8	3.5	NaN	NaN	NaN	14.8	13.8	5.0	20.2	18.2	9.4
homoserine	4.1	5.1	4.5	4.2	4.3	4.7	6.1	4.8	4.9	5.8	5.4	4.4	5.3
homoserine betaine	9.1	NaN	NaN	NaN	34.8	NaN	NaN	57.1	46.1	41.6	30.3	38.1	45.0
isethionate	12.8	5.5	NaN	4.7	8.2	4.8	NaN	24.4	24.5	33.8	22.5	26.4	26.5
isoleucine	NaN	NaN	NaN	NaN	NaN	NaN	NaN	NaN	NaN	NaN	NaN	NaN	NaN
kynurenine	NaN	NaN	2.9	NaN	NaN	NaN	NaN	3.5	3.7	NaN	NaN	5.6	NaN
leucine	NaN	NaN	NaN	NaN	NaN	NaN	NaN	NaN	NaN	NaN	NaN	NaN	NaN
malic acid	NaN	25.1	NaN	NaN	NaN	NaN	NaN	70.9	41.4	44.1	45.4	45.8	76.5
methionine	NaN	NaN	NaN	NaN	NaN	NaN	NaN	NaN	NaN	NaN	NaN	NaN	NaN
muramic acid	NaN	NaN	NaN	NaN	NaN	NaN	NaN	6.2	NaN	11.0	NaN	NaN	NaN
pantothenic acid	NaN	NaN	NaN	NaN	NaN	NaN	NaN	3.6	NaN	NaN	3.3	2.2	2.9
phenylalanine	NaN	NaN	11.4	NaN	NaN	NaN	NaN	8.0	8.3	6.7	6.4	6.0	5.6
proline	NaN	NaN	NaN	NaN	NaN	NaN	NaN	NaN	NaN	NaN	NaN	NaN	NaN
putrescine	6.6	NaN	NaN	NaN	8.2	NaN	NaN	10.3	NaN	13.6	NaN	13.1	NaN
sarcosine	3.9	NaN	NaN	NaN	5.2	NaN	NaN	8.0	3.8	13.5	4.0	NaN	NaN
serine	NaN	NaN	79.0	11.3	NaN	NaN	NaN	77.6	27.5	23.3	37.2	39.8	19.6
glycerol 3-phosphate	41.1	6.2	14.7	9.2	17.1	27.1	14.1	23.0	20.4	21.1	21.6	26.9	22.1
spermidine	NaN	NaN	NaN	NaN	NaN	NaN	NaN	NaN	NaN	NaN	NaN	NaN	NaN

name	AE2123_BC58_C3N13	AE2123_BC59_C3N16	AE2123_BC60_C3N16	AE2123_BC61_C3N16	AE2123_BC62_C3N18	AE2123_BC63_C3N18	AE2123_BC64_C3N18	AE2123_BC65_C4N2	AE2123_BC66_C4N2	AE2123_BC67_C4N2	AE2123_BC71_C4N6	AE2123_BC72_C4N6	AE2123_BC73_C4N6
cast	3	3	3	3	3	3	3	4	4	4	4	4	4
niskin	13	16	16	16	18	18	18	2	2	2	6	6	6
depth (m)	106.019	200.63	200.63	200.63	250.283	250.283	250.283	3.923	3.923	3.923	40.867	40.867	40.867
date (YYYYmmdd)	20211111	20211111	20211111	20211111	20211111	20211111	20211111	20211111	20211111	20211111	20211111	20211111	20211111
time (hhMM)	1000	1000	1000	1000	1000	1000	1000	1635	1635	1635	1635	1635	1635
taurine	18.9	NaN	NaN	NaN	101.3	NaN	NaN	60.8	43.4	23.1	85.2	64.7	80.1
thiamine monophosphate	NaN	NaN	NaN	NaN	NaN	NaN	NaN	NaN	NaN	NaN	NaN	NaN	NaN
threonine	NaN	5.6	26.5	NaN	NaN	NaN	NaN	19.6	11.9	23.5	15.9	17.5	10.6
thymidine	26.2	NaN	NaN	NaN	NaN	25.1	NaN	NaN	NaN	NaN	27.7	26.4	31.3
tryptamine	NaN	NaN	NaN	NaN	NaN	NaN	NaN	NaN	NaN	NaN	NaN	NaN	NaN
tryptophan	NaN	NaN	NaN	4.2	5.3	NaN	NaN	5.4	8.2	5.4	6.9	5.6	4.8
tyrosine	15.0	NaN	19.7	NaN	NaN	NaN	NaN	467.4	166.0	38.7	67.9	63.2	38.6
uridine	6.6	NaN	7.7	5.3	7.3	5.7	5.6	8.2	8.0	8.2	9.5	6.2	6.0
valine	NaN	NaN	NaN	NaN	NaN	NaN	NaN	NaN	NaN	NaN	NaN	NaN	NaN
xanthosine	NaN	NaN	NaN	NaN	NaN	NaN	NaN	NaN	NaN	NaN	NaN	NaN	NaN

name	AE2123_BC74_C4N9	AE2123_BC75_C4N9	AE2123_BC76_C4N9	AE2123_BC77_C4N11	AE2123_BC78_C4N11	AE2123_BC79_C4N11	AE2123_BC80_C4N13	AE2123_BC81_C4N13	AE2123_BC82_C4N13	AE2123_BC83_C4N16	AE2123_BC84_C4N16	AE2123_BC85_C4N16	AE2123_BC86_C4N18
cast	4	4	4	4	4	4	4	4	4	4	4	4	4
niskin	9	9	9	11	11	11	13	13	13	16	16	16	18
depth (m)	80.374	80.374	80.374	89.668	89.668	89.668	106.147	106.147	106.147	201.113	201.113	201.113	251.214
date (YYYYmmdd)	20211111	20211111	20211111	20211111	20211111	20211111	20211111	20211111	20211111	20211111	20211111	20211111	20211111
time (hhMM)	1635	1635	1635	1635	1635	1635	1635	1635	1635	1635	1635	1635	1635
2'deoxycitidine	NaN	55.0	NaN	NaN	NaN	NaN	NaN	NaN	31.8	NaN	NaN	NaN	NaN
2'deoxyguanosine	2.4	NaN	NaN	NaN	2.4	2.6	NaN	2.3	2.3	2.4	2.4	2.3	2.4
2'deoxyuridine	20.7	28.8	30.1	43.4	37.0	17.6	24.5	32.6	18.4	26.4	17.5	16.9	11.9
adenosine 3'-monophosphate	NaN	NaN	NaN	NaN	NaN	NaN	7.6	NaN	NaN	NaN	NaN	NaN	NaN
4-aminobenzoic acid	NaN	NaN	NaN	NaN	NaN	NaN	72.9	NaN	NaN	NaN	NaN	NaN	220.4
uridine 5'-monophosphate	NaN	NaN	NaN	NaN	NaN	NaN	NaN	NaN	NaN	NaN	NaN	NaN	NaN
adenosine 5'-monophosphate	NaN	NaN	NaN	NaN	NaN	NaN	NaN	NaN	NaN	NaN	NaN	NaN	NaN
inosine 5'-monophosphate	9.3	NaN	NaN	12.5	13.8	NaN	NaN	NaN	NaN	NaN	11.1	9.6	NaN
5'deoxyadenosine	NaN	NaN	40.6	NaN	NaN	29.2	NaN	NaN	NaN	NaN	NaN	NaN	NaN
2,3-dihydroxypropane-1-sulfonate	37.7	41.3	33.9	28.0	26.8	23.8	11.1	8.0	21.7	NaN	NaN	NaN	NaN
gamma-aminobutyric acid	NaN	NaN	NaN	NaN	NaN	NaN	36.7	NaN	NaN	NaN	NaN	NaN	8.2
HET	NaN	NaN	NaN	NaN	NaN	NaN	NaN	NaN	NaN	NaN	NaN	NaN	NaN
HMP	NaN	NaN	NaN	181.5	NaN	NaN	NaN	NaN	NaN	NaN	NaN	79.7	NaN
N-acetyl-muramic acid	NaN	NaN	NaN	NaN	NaN	12.0	NaN	NaN	NaN	NaN	NaN	NaN	NaN
adenine	NaN	NaN	NaN	NaN	NaN	NaN	NaN	NaN	NaN	NaN	NaN	NaN	NaN
adenosine	2.5	2.3	2.3	NaN	2.3	2.9	2.3	2.4	2.5	2.3	2.4	2.3	2.4
alanine	38.9	32.7	38.6	28.2	NaN	22.6	437.7	7.1	40.1	NaN	17.7	19.2	1152.3

name	AE2123_BC74_C4N9	AE2123_BC75_C4N9	AE2123_BC76_C4N9	AE2123_BC77_C4N11	AE2123_BC78_C4N11	AE2123_BC79_C4N11	AE2123_BC80_C4N13	AE2123_BC81_C4N13	AE2123_BC82_C4N13	AE2123_BC83_C4N16	AE2123_BC84_C4N16	AE2123_BC85_C4N16	AE2123_BC86_C4N18
cast	4	4	4	4	4	4	4	4	4	4	4	4	4
niskin	9	9	9	11	11	11	13	13	13	16	16	16	18
depth (m)	80.374	80.374	80.374	89.668	89.668	89.668	106.147	106.147	106.147	201.113	201.113	201.113	251.214
date (YYYYmmdd)	20211111	20211111	20211111	20211111	20211111	20211111	20211111	20211111	20211111	20211111	20211111	20211111	20211111
time (hhMM)	1635	1635	1635	1635	1635	1635	1635	1635	1635	1635	1635	1635	1635
amMP	NaN	3.5	NaN	10.1	9.0	NaN	7.6	NaN	24.2	NaN	15.7	7.1	NaN
arginine	NaN	7.7	NaN	NaN	NaN	NaN	115.7	NaN	36.2	NaN	NaN	NaN	383.6
asparagine	5.1	9.2	7.2	2.1	4.1	6.3	58.4	NaN	NaN	NaN	NaN	NaN	216.7
aspartate	NaN	NaN	NaN	NaN	NaN	NaN	125.6	NaN	NaN	NaN	NaN	NaN	349.3
chitobiose	NaN	NaN	NaN	NaN	NaN	NaN	NaN	NaN	NaN	NaN	NaN	NaN	NaN
chitotriose	NaN	NaN	NaN	NaN	NaN	NaN	NaN	NaN	NaN	NaN	NaN	NaN	NaN
ciliatine	3.1	5.0	5.6	3.4	4.6	4.3	2.6	NaN	2.9	NaN	NaN	NaN	NaN
citrulline	NaN	NaN	NaN	NaN	NaN	76.0	224.6	NaN	NaN	NaN	NaN	NaN	718.5
cysteate	NaN	NaN	NaN	NaN	NaN	8.9	NaN	NaN	NaN	NaN	NaN	NaN	NaN
cysteine	17.9	26.0	15.9	10.8	31.7	15.7	42.3	6.4	12.4	6.3	NaN	NaN	47.3
cystine	NaN	NaN	NaN	NaN	NaN	NaN	NaN	NaN	NaN	NaN	NaN	NaN	NaN
cytidine	NaN	22.1	100.3	NaN	NaN	80.3	20.1	NaN	NaN	23.5	37.2	NaN	64.9
ectoine	NaN	NaN	NaN	NaN	41.0	NaN	29.1	NaN	NaN	NaN	NaN	26.3	23.1
glucosamine-6-phosphate	NaN	NaN	NaN	NaN	NaN	NaN	NaN	NaN	NaN	NaN	NaN	NaN	NaN
glucose 6-phosphate	NaN	NaN	NaN	11.3	14.0	NaN	NaN	NaN	NaN	NaN	NaN	NaN	11.8
glutamic acid	19.8	37.9	31.4	12.9	54.1	36.7	74.1	NaN	NaN	NaN	NaN	NaN	256.9
glutamine	19.1	17.1	19.0	10.9	17.2	10.5	58.6	NaN	6.8	NaN	NaN	NaN	105.2
glutathione	NaN	NaN	NaN	NaN	NaN	NaN	NaN	NaN	NaN	NaN	NaN	NaN	NaN

name	AE2123_BC74_C4N9	AE2123_BC75_C4N9	AE2123_BC76_C4N9	AE2123_BC77_C4N11	AE2123_BC78_C4N11	AE2123_BC79_C4N11	AE2123_BC80_C4N13	AE2123_BC81_C4N13	AE2123_BC82_C4N13	AE2123_BC83_C4N16	AE2123_BC84_C4N16	AE2123_BC85_C4N16	AE2123_BC86_C4N18
cast	4	4	4	4	4	4	4	4	4	4	4	4	4
niskin	9	9	9	11	11	11	13	13	13	16	16	16	18
depth (m)	80.374	80.374	80.374	89.668	89.668	89.668	106.147	106.147	106.147	201.113	201.113	201.113	251.214
date (YYYYmmdd)	20211111	20211111	20211111	20211111	20211111	20211111	20211111	20211111	20211111	20211111	20211111	20211111	20211111
time (hhMM)	1635	1635	1635	1635	1635	1635	1635	1635	1635	1635	1635	1635	1635
glycine	73.1	42.5	NaN	10.3	85.4	38.3	414.6	NaN	6.3	26.2	NaN	NaN	912.0
guanosine	NaN	NaN	NaN	NaN	NaN	NaN	NaN	NaN	NaN	NaN	NaN	NaN	NaN
histidine	13.4	14.6	6.9	NaN	3.1	18.0	328.4	9.5	10.8	NaN	10.0	9.3	1079.1
homoserine	5.7	7.1	7.8	8.0	6.5	6.9	5.5	5.1	6.7	5.0	4.1	4.8	6.3
homoserine betaine	46.7	54.9	54.2	18.7	25.1	20.3	NaN	NaN	NaN	NaN	NaN	NaN	NaN
isethionate	22.4	20.4	19.5	13.8	10.2	16.5	12.4	7.2	11.9	NaN	NaN	5.1	13.7
isoleucine	NaN	NaN	NaN	NaN	NaN	NaN	50.7	NaN	NaN	NaN	NaN	NaN	208.5
kynurenine	NaN	3.7	3.4	5.9	NaN	3.7	12.0	NaN	NaN	NaN	NaN	NaN	32.3
leucine	NaN	NaN	NaN	NaN	NaN	NaN	54.2	NaN	NaN	NaN	NaN	NaN	170.9
malic acid	NaN	NaN	NaN	50.3	NaN	NaN	59.5	NaN	20.4	NaN	NaN	NaN	122.4
methionine	NaN	NaN	NaN	NaN	NaN	NaN	NaN	NaN	NaN	NaN	NaN	NaN	18.8
muramic acid	7.4	NaN	9.6	NaN	NaN	NaN	NaN	NaN	NaN	5.6	NaN	NaN	8.4
pantothenic acid	NaN	NaN	NaN	NaN	NaN	NaN	NaN	NaN	NaN	NaN	NaN	NaN	NaN
phenylalanine	7.8	6.7	5.3	6.8	NaN	13.4	54.8	4.8	8.7	NaN	NaN	4.8	155.0
proline	NaN	NaN	NaN	NaN	NaN	NaN	35.2	NaN	NaN	3.9	NaN	NaN	144.1
putrescine	44.3	28.0	16.8	21.3	NaN	NaN	236.6	NaN	97.4	NaN	NaN	NaN	695.8
sarcosine	6.4	6.6	5.1	4.4	NaN	NaN	4.8	NaN	4.1	NaN	NaN	4.8	6.7
serine	38.7	85.9	15.2	19.5	11.9	53.7	695.6	39.2	75.9	10.9	39.2	30.5	2061.7

name	AE2123_BC74_C4N9	AE2123_BC75_C4N9	AE2123_BC76_C4N9	AE2123_BC77_C4N11	AE2123_BC78_C4N11	AE2123_BC79_C4N11	AE2123_BC80_C4N13	AE2123_BC81_C4N13	AE2123_BC82_C4N13	AE2123_BC83_C4N16	AE2123_BC84_C4N16	AE2123_BC85_C4N16	AE2123_BC86_C4N18
cast	4	4	4	4	4	4	4	4	4	4	4	4	4
niskin	9	9	9	11	11	11	13	13	13	16	16	16	18
depth (m)	80.374	80.374	80.374	89.668	89.668	89.668	106.147	106.147	106.147	201.113	201.113	201.113	251.214
date (YYYYmmdd)	20211111	20211111	20211111	20211111	20211111	20211111	20211111	20211111	20211111	20211111	20211111	20211111	20211111
time (hhMM)	1635	1635	1635	1635	1635	1635	1635	1635	1635	1635	1635	1635	1635
glycerol 3-phosphate	34.3	42.1	24.3	40.1	29.6	30.2	98.2	42.3	52.7	12.5	17.8	13.3	45.5
spermidine	NaN	NaN	NaN	NaN	NaN	NaN	NaN	NaN	NaN	NaN	NaN	NaN	NaN
taurine	78.4	95.0	65.7	44.5	70.1	47.5	18.2	NaN	24.4	NaN	NaN	NaN	47.7
thiamine monophosphate	NaN	NaN	NaN	NaN	13.7	NaN	NaN	NaN	NaN	11.1	NaN	NaN	8.3
threonine	17.4	20.0	11.1	21.6	6.1	42.7	245.8	9.3	21.7	NaN	7.5	8.3	616.6
thymidine	NaN	73.9	NaN	NaN	NaN	26.8	NaN	NaN	NaN	NaN	NaN	25.8	NaN
tryptamine	NaN	NaN	NaN	NaN	NaN	NaN	NaN	NaN	NaN	NaN	NaN	NaN	28.2
tryptophan	5.7	6.6	5.9	5.3	5.3	4.8	14.5	4.3	NaN	4.1	NaN	NaN	54.2
tyrosine	50.5	39.9	70.7	126.3	55.3	55.0	35.5	NaN	83.0	NaN	54.1	NaN	72.6
uridine	9.1	9.9	7.2	12.2	5.5	9.7	17.1	NaN	5.6	5.8	NaN	5.3	13.2
valine	NaN	NaN	NaN	NaN	NaN	NaN	110.1	NaN	NaN	NaN	NaN	NaN	330.5
xanthosine	NaN	NaN	NaN	NaN	NaN	NaN	NaN	NaN	NaN	NaN	NaN	NaN	NaN

name	AE2123_BC87_C4N18	AE2123_BC88_C4N18	AE2123_BC89_C5N2	AE2123_BC90_C5N2	AE2123_BC91_C5N2	AE2123_BC92_C5N6	AE2123_BC93_C5N6	AE2123_BC94_C5N6	AE2123_BC95_C5N9	AE2123_BC96_C5N9	AE2123_BC97_C5N9	AE2123_BC100_C5N11	AE2123_BC98_C5N11
cast	4	4	5	5	5	5	5	5	5	5	5	5	5
niskin	18	18	2	2	2	6	6	6	9	9	9	11	11
depth (m)	251.214	251.214	4.817	4.817	4.817	41.574	41.574	41.574	79.178	79.178	79.178	90.229	90.229
date (YYYYmmdd)	20211111	20211111	20211111	20211111	20211111	20211111	20211111	20211111	20211111	20211111	20211111	20211111	20211111
time (hhMM)	1635	1635	2202	2202	2202	2202	2202	2202	2202	2202	2202	2202	2202
2'deoxycitidine	NaN	NaN	NaN	44.1	29.1	NaN	NaN	NaN	26.9	NaN	53.8	NaN	NaN
2'deoxyguanosine	2.7	NaN	2.4	2.4	NaN	NaN	NaN	2.7	NaN	NaN	2.3	2.3	2.4
2'deoxyuridine	21.0	22.1	22.8	50.8	29.2	19.3	60.4	35.7	18.3	67.9	45.4	16.7	48.5
adenosine 3'-monophosphate	NaN	NaN	NaN	NaN	NaN	NaN	NaN	NaN	NaN	NaN	NaN	NaN	NaN
4-aminobenzoic acid	5.3	NaN	NaN	NaN	NaN	NaN	NaN	NaN	NaN	NaN	NaN	NaN	NaN
uridine 5'-monophosphate	NaN	NaN	NaN	NaN	NaN	NaN	NaN	NaN	NaN	NaN	NaN	NaN	NaN
adenosine 5'-monophosphate	NaN	NaN	NaN	NaN	NaN	NaN	NaN	NaN	NaN	NaN	NaN	NaN	11.0
inosine 5'-monophosphate	NaN	NaN	NaN	NaN	NaN	NaN	NaN	NaN	NaN	NaN	7.7	8.6	NaN
5'deoxyadenosine	NaN	NaN	NaN	NaN	58.9	63.3	40.6	NaN	NaN	31.5	NaN	NaN	NaN
2,3-dihydroxypropane-1-sulfonate	NaN	NaN	26.5	45.9	52.1	35.9	27.9	30.2	25.2	25.7	32.7	71.7	57.4
gamma-aminobutyric acid	NaN	NaN	NaN	NaN	NaN	NaN	NaN	NaN	NaN	NaN	NaN	NaN	NaN
HET	NaN	NaN	NaN	NaN	NaN	NaN	NaN	NaN	NaN	NaN	NaN	NaN	NaN
HMP	NaN	257.9	NaN	NaN	NaN	NaN	NaN	NaN	204.6	160.6	NaN	NaN	NaN
N-acetyl-muramic acid	NaN	NaN	NaN	NaN	21.1	NaN	12.9	40.5	NaN	10.8	NaN	NaN	NaN
adenine	NaN	NaN	NaN	NaN	NaN	NaN	NaN	NaN	NaN	NaN	NaN	NaN	NaN
adenosine	2.6	NaN	NaN	2.4	NaN	NaN	NaN	2.5	NaN	NaN	2.3	2.3	2.5
alanine	123.2	18.2	NaN	31.5	35.8	8.5	NaN	NaN	19.4	NaN	18.7	25.9	34.5

name	AE2123_BC87_C4N18	AE2123_BC88_C4N18	AE2123_BC89_C5N2	AE2123_BC90_C5N2	AE2123_BC91_C5N2	AE2123_BC92_C5N6	AE2123_BC93_C5N6	AE2123_BC94_C5N6	AE2123_BC95_C5N9	AE2123_BC96_C5N9	AE2123_BC97_C5N9	AE2123_BC100_C5N11	AE2123_BC98_C5N11
cast	4	4	5	5	5	5	5	5	5	5	5	5	5
niskin	18	18	2	2	2	6	6	6	9	9	9	11	11
depth (m)	251.214	251.214	4.817	4.817	4.817	41.574	41.574	41.574	79.178	79.178	79.178	90.229	90.229
date (YYYYmmdd)	20211111	20211111	20211111	20211111	20211111	20211111	20211111	20211111	20211111	20211111	20211111	20211111	20211111
time (hhMM)	1635	1635	2202	2202	2202	2202	2202	2202	2202	2202	2202	2202	2202
amMP	15.0	NaN	NaN	NaN	7.7	19.7	6.1	6.4	8.8	5.9	10.4	10.7	NaN
arginine	NaN	NaN	NaN	NaN	NaN	NaN	NaN	NaN	NaN	NaN	NaN	NaN	NaN
asparagine	18.9	NaN	NaN	4.2	2.1	NaN	NaN	3.0	2.0	3.7	NaN	6.5	7.8
aspartate	28.4	NaN	NaN	NaN	NaN	NaN	NaN	14.5	NaN	NaN	NaN	NaN	NaN
chitobiose	NaN	NaN	NaN	NaN	NaN	NaN	NaN	NaN	NaN	NaN	NaN	NaN	NaN
chitotriose	NaN	NaN	NaN	NaN	NaN	NaN	NaN	NaN	NaN	NaN	NaN	NaN	NaN
ciliatine	NaN	NaN	3.0	NaN	NaN	NaN	NaN	NaN	2.5	NaN	NaN	6.2	5.3
citrulline	396.3	NaN	NaN	NaN	NaN	NaN	NaN	NaN	NaN	NaN	NaN	NaN	NaN
cysteate	NaN	NaN	NaN	NaN	NaN	NaN	NaN	7.9	NaN	NaN	NaN	8.4	8.7
cysteine	8.5	47.5	13.2	10.8	17.8	6.6	17.9	24.6	23.6	30.5	22.2	11.2	20.4
cystine	NaN	NaN	NaN	NaN	NaN	NaN	NaN	NaN	NaN	NaN	NaN	NaN	NaN
cytidine	18.9	NaN	24.6	NaN	30.3	NaN	NaN	NaN	NaN	NaN	NaN	NaN	93.4
ectoine	NaN	NaN	NaN	NaN	NaN	NaN	19.1	NaN	NaN	NaN	NaN	NaN	NaN
glucosamine-6-phosphate	NaN	NaN	NaN	NaN	NaN	NaN	NaN	NaN	NaN	NaN	NaN	NaN	NaN
glucose 6-phosphate	NaN	NaN	10.8	NaN	11.5	NaN	NaN	12.4	11.4	NaN	11.0	12.5	13.1
glutamic acid	19.4	NaN	41.6	37.7	36.3	36.7	35.0	80.6	17.9	22.4	14.1	26.4	30.9
glutamine	5.4	NaN	14.9	19.4	17.1	24.3	15.8	29.8	9.1	12.4	15.0	16.1	33.8
glutathione	NaN	NaN	17.1	NaN	11.7	25.9	21.3	44.5	27.5	23.7	NaN	NaN	NaN
glycine	98.7	NaN	NaN	NaN	NaN	NaN	NaN	27.2	54.4	73.9	NaN	40.0	55.4

name	AE2123_BC87_C4N18	AE2123_BC88_C4N18	AE2123_BC89_C5N2	AE2123_BC90_C5N2	AE2123_BC91_C5N2	AE2123_BC92_C5N6	AE2123_BC93_C5N6	AE2123_BC94_C5N6	AE2123_BC95_C5N9	AE2123_BC96_C5N9	AE2123_BC97_C5N9	AE2123_BC100_C5N11	AE2123_BC98_C5N11
cast	4	4	5	5	5	5	5	5	5	5	5	5	5
niskin	18	18	2	2	2	6	6	6	9	9	9	11	11
depth (m)	251.214	251.214	4.817	4.817	4.817	41.574	41.574	41.574	79.178	79.178	79.178	90.229	90.229
date (YYYYmmdd)	20211111	20211111	20211111	20211111	20211111	20211111	20211111	20211111	20211111	20211111	20211111	20211111	20211111
time (hhMM)	1635	1635	2202	2202	2202	2202	2202	2202	2202	2202	2202	2202	2202
guanosine	NaN	NaN	NaN	NaN	NaN	NaN	NaN	NaN	NaN	NaN	NaN	NaN	NaN
histidine	145.9	14.3	NaN	4.8	NaN	NaN	NaN	NaN	5.7	NaN	NaN	3.3	10.9
homoserine	5.6	5.8	5.7	4.9	4.7	4.6	5.3	5.1	6.5	5.1	4.9	7.3	5.8
homoserine betaine	NaN	18.1	73.5	75.8	112.4	48.9	47.0	64.3	32.4	47.7	49.3	50.7	42.8
isethionate	7.7	7.0	27.6	50.6	48.7	35.5	32.8	29.6	24.2	17.9	26.3	33.5	30.7
isoleucine	18.0	NaN	NaN	NaN	NaN	NaN	NaN	NaN	NaN	NaN	NaN	NaN	NaN
kynurenine	4.2	NaN	NaN	3.1	4.1	NaN	NaN	NaN	NaN	NaN	3.1	NaN	3.4
leucine	20.7	NaN	NaN	NaN	NaN	NaN	NaN	NaN	NaN	NaN	NaN	NaN	NaN
malic acid	62.0	NaN	140.6	70.4	69.8	128.3	111.4	91.2	95.6	80.5	25.1	NaN	25.2
methionine	NaN	NaN	NaN	NaN	NaN	NaN	NaN	NaN	NaN	NaN	NaN	NaN	NaN
muramic acid	NaN	10.2	NaN	5.5	NaN	NaN	NaN	NaN	NaN	NaN	NaN	NaN	NaN
pantothenic acid	NaN	NaN	2.6	NaN	NaN	NaN	2.1	3.1	NaN	2.9	NaN	NaN	NaN
phenylalanine	22.4	5.1	NaN	6.5	6.5	NaN	NaN	4.6	NaN	NaN	4.7	4.8	5.5
proline	4.3	NaN	NaN	NaN	NaN	NaN	NaN	NaN	NaN	NaN	NaN	NaN	NaN
putrescine	42.1	NaN	NaN	23.8	18.5	NaN	NaN	NaN	30.4	NaN	20.3	29.2	35.7
sarcosine	NaN	NaN	5.3	15.4	21.8	7.6	24.7	7.3	6.7	4.3	6.6	8.6	8.0
serine	181.9	12.6	NaN	8.7	NaN	NaN	NaN	NaN	NaN	NaN	NaN	NaN	NaN
glycerol 3-phosphate	14.5	12.1	8.7	24.3	22.0	15.0	15.4	11.8	14.3	25.8	32.6	36.2	38.9
spermidine	NaN	NaN	NaN	NaN	NaN	NaN	NaN	NaN	NaN	NaN	NaN	NaN	NaN

name	AE2123_BC87_C4N18	AE2123_BC88_C4N18	AE2123_BC89_C5N2	AE2123_BC90_C5N2	AE2123_BC91_C5N2	AE2123_BC92_C5N6	AE2123_BC93_C5N6	AE2123_BC94_C5N6	AE2123_BC95_C5N9	AE2123_BC96_C5N9	AE2123_BC97_C5N9	AE2123_BC100_C5N11	AE2123_BC98_C5N11
cast	4	4	5	5	5	5	5	5	5	5	5	5	5
niskin	18	18	2	2	2	6	6	6	9	9	9	11	11
depth (m)	251.214	251.214	4.817	4.817	4.817	41.574	41.574	41.574	79.178	79.178	79.178	90.229	90.229
date (YYYYmmdd)	20211111	20211111	20211111	20211111	20211111	20211111	20211111	20211111	20211111	20211111	20211111	20211111	20211111
time (hhMM)	1635	1635	2202	2202	2202	2202	2202	2202	2202	2202	2202	2202	2202
taurine	NaN	NaN	66.7	85.4	102.0	44.5	106.4	89.6	74.8	105.4	62.2	125.3	93.9
thiamine monophosphate	NaN	NaN	NaN	NaN	NaN	10.8	NaN	NaN	NaN	NaN	NaN	NaN	NaN
threonine	108.1	6.1	NaN	12.6	NaN	5.1	NaN	NaN	8.5	NaN	5.4	5.4	13.6
thymidine	NaN	NaN	NaN	NaN	NaN	NaN	NaN	NaN	NaN	46.9	26.9	24.2	NaN
tryptamine	NaN	NaN	NaN	NaN	NaN	NaN	NaN	NaN	NaN	NaN	NaN	NaN	NaN
tryptophan	NaN	4.6	6.2	6.9	6.8	5.9	4.8	7.5	5.2	5.5	6.1	9.4	6.9
tyrosine	NaN	NaN	NaN	35.4	NaN	NaN	NaN	NaN	NaN	NaN	NaN	NaN	NaN
uridine	5.4	5.8	9.8	8.5	10.2	9.6	12.0	10.6	14.6	10.1	11.7	6.6	12.6
valine	21.2	NaN	NaN	NaN	NaN	NaN	NaN	NaN	NaN	NaN	NaN	NaN	NaN
xanthosine	NaN	NaN	NaN	NaN	NaN	NaN	NaN	NaN	NaN	NaN	NaN	NaN	NaN

name	AE2123_BC99_C5N11	AE2123_BC101_C5N16	AE2123_BC102_C5N16	AE2123_BC103_C5N16	AE2123_BC104_C6N2	AE2123_BC105_C6N2	AE2123_BC106_C6N2	AE2123_BC107_C6N4	AE2123_BC108_C6N4	AE2123_BC109_C6N4	AE2123_BC110_C6N6	AE2123_BC111_C6N6	AE2123_BC112_C6N6
cast	5	5	5	5	6	6	6	6	6	6	6	6	6
niskin	11	16	16	16	2	2	2	4	4	4	6	6	6
depth (m)	90.229	200.722	200.722	200.722	4.541	4.541	4.541	20.922	20.922	20.922	39.485	39.485	39.485
date (YYYYmmdd)	20211111	20211111	20211111	20211111	20211112	20211112	20211112	20211112	20211112	20211112	20211112	20211112	20211112
time (hhMM)	2202	2202	2202	2202	435	435	435	435	435	435	435	435	435
2'deoxycitidine	NaN	NaN	NaN	NaN	NaN	NaN	NaN	NaN	NaN	NaN	NaN	NaN	NaN
2'deoxyguanosine	NaN	NaN	NaN	NaN	2.4	2.7	2.4	NaN	2.3	2.4	2.4	2.5	2.4
2'deoxyuridine	39.6	15.3	NaN	13.4	26.8	61.0	32.0	22.7	11.5	27.6	8.5	12.0	23.5
adenosine 3'-monophosphate	NaN	NaN	NaN	NaN	NaN	NaN	NaN	4.9	3.8	NaN	NaN	NaN	NaN
4-aminobenzoic acid	NaN	NaN	NaN	NaN	NaN	NaN	NaN	NaN	30.8	14.3	NaN	NaN	NaN
uridine 5'-monophosphate	NaN	NaN	NaN	NaN	NaN	NaN	NaN	NaN	NaN	NaN	NaN	NaN	NaN
adenosine 5'-monophosphate	NaN	NaN	NaN	NaN	12.9	21.7	NaN	NaN	11.3	NaN	NaN	NaN	NaN
inosine 5'-monophosphate	NaN	NaN	NaN	NaN	NaN	NaN	NaN	NaN	NaN	NaN	NaN	NaN	NaN
5'deoxyadenosine	NaN	NaN	NaN	NaN	NaN	180.2	41.0	48.0	NaN	NaN	NaN	NaN	NaN
2,3-dihydroxypropane-1-sulfonate	72.4	NaN	NaN	NaN	49.5	34.0	39.3	22.1	20.3	25.0	38.6	30.7	34.9
gamma-aminobutyric acid	NaN	NaN	NaN	NaN	NaN	6.6	NaN	15.0	NaN	8.1	NaN	NaN	NaN
HET	NaN	NaN	NaN	NaN	NaN	NaN	NaN	NaN	NaN	NaN	NaN	NaN	NaN
HMP	NaN	430.4	359.1	NaN	NaN	NaN	NaN	NaN	NaN	NaN	NaN	NaN	NaN
N-acetyl-muramic acid	NaN	NaN	NaN	NaN	29.6	10.8	12.3	NaN	NaN	19.1	10.7	NaN	NaN
adenine	NaN	NaN	NaN	NaN	NaN	NaN	NaN	NaN	NaN	NaN	NaN	NaN	NaN
adenosine	2.4	NaN	NaN	NaN	2.4	2.4	2.7	2.3	2.3	2.3	2.3	2.7	2.4
alanine	65.2	17.4	4.4	NaN	36.5	NaN	12.8	30.6	254.2	191.4	37.8	36.1	17.7

name	AE2123_BC99_C5N11	AE2123_BC101_C5N16	AE2123_BC102_C5N16	AE2123_BC103_C5N16	AE2123_BC104_C6N2	AE2123_BC105_C6N2	AE2123_BC106_C6N2	AE2123_BC107_C6N4	AE2123_BC108_C6N4	AE2123_BC109_C6N4	AE2123_BC110_C6N6	AE2123_BC111_C6N6	AE2123_BC112_C6N6
cast	5	5	5	5	6	6	6	6	6	6	6	6	6
niskin	11	16	16	16	2	2	2	4	4	4	6	6	6
depth (m)	90.229	200.722	200.722	200.722	4.541	4.541	4.541	20.922	20.922	20.922	39.485	39.485	39.485
date (YYYYmmdd)	20211111	20211111	20211111	20211111	20211112	20211112	20211112	20211112	20211112	20211112	20211112	20211112	20211112
time (hhMM)	2202	2202	2202	2202	435	435	435	435	435	435	435	435	435
amMP	NaN	NaN	11.3	4.1	NaN	10.6	13.5	12.7	16.2	NaN	NaN	4.3	9.4
arginine	13.1	NaN	NaN	NaN	NaN	NaN	NaN	NaN	60.1	33.2	NaN	NaN	NaN
asparagine	10.8	NaN	NaN	NaN	12.7	4.6	4.6	NaN	46.6	22.6	5.7	4.1	3.7
aspartate	NaN	NaN	NaN	NaN	NaN	19.3	NaN	NaN	78.0	56.3	NaN	NaN	NaN
chitobiose	NaN	NaN	NaN	NaN	NaN	NaN	NaN	NaN	NaN	NaN	NaN	NaN	NaN
chitotriose	NaN	NaN	NaN	NaN	NaN	NaN	NaN	NaN	NaN	NaN	NaN	NaN	NaN
ciliatine	5.5	NaN	NaN	NaN	2.7	NaN	NaN	NaN	13.0	NaN	NaN	NaN	3.0
citrulline	NaN	NaN	NaN	NaN	20.5	NaN	NaN	NaN	77.7	56.2	NaN	33.9	NaN
cysteate	NaN	NaN	NaN	NaN	NaN	NaN	NaN	NaN	NaN	NaN	NaN	NaN	NaN
cysteine	24.1	10.1	5.8	9.5	16.9	26.9	17.4	22.7	33.8	23.2	13.2	11.8	16.6
cystine	NaN	NaN	NaN	NaN	NaN	NaN	NaN	NaN	NaN	NaN	NaN	NaN	NaN
cytidine	43.1	NaN	NaN	NaN	NaN	NaN	NaN	NaN	68.3	NaN	NaN	NaN	NaN
ectoine	NaN	NaN	37.8	NaN	NaN	NaN	NaN	NaN	NaN	110.8	NaN	NaN	NaN
glucosamine-6-phosphate	NaN	NaN	NaN	NaN	NaN	NaN	NaN	NaN	NaN	NaN	NaN	NaN	NaN
glucose 6-phosphate	NaN	NaN	NaN	NaN	NaN	NaN	11.2	NaN	NaN	NaN	NaN	NaN	NaN
glutamic acid	28.3	NaN	NaN	NaN	89.1	57.3	55.9	16.5	50.9	35.1	32.1	33.9	21.5
glutamine	25.2	2.4	NaN	NaN	273.2	18.1	11.0	18.4	23.3	22.6	17.1	17.2	15.1
glutathione	NaN	NaN	NaN	NaN	NaN	9.8	13.4	NaN	NaN	NaN	NaN	NaN	7.9

name	AE2123_BC99_C5N11	AE2123_BC101_C5N16	AE2123_BC102_C5N16	AE2123_BC103_C5N16	AE2123_BC104_C6N2	AE2123_BC105_C6N2	AE2123_BC106_C6N2	AE2123_BC107_C6N4	AE2123_BC108_C6N4	AE2123_BC109_C6N4	AE2123_BC110_C6N6	AE2123_BC111_C6N6	AE2123_BC112_C6N6
cast	5	5	5	5	6	6	6	6	6	6	6	6	6
niskin	11	16	16	16	2	2	2	4	4	4	6	6	6
depth (m)	90.229	200.722	200.722	200.722	4.541	4.541	4.541	20.922	20.922	20.922	39.485	39.485	39.485
date (YYYYmmdd)	20211111	20211111	20211111	20211111	20211112	20211112	20211112	20211112	20211112	20211112	20211112	20211112	20211112
time (hhMM)	2202	2202	2202	2202	435	435	435	435	435	435	435	435	435
glycine	67.0	NaN	NaN	5.7	65.6	65.3	9.5	NaN	157.4	122.4	NaN	NaN	NaN
guanosine	NaN	NaN	NaN	NaN	NaN	NaN	NaN	NaN	NaN	NaN	NaN	NaN	NaN
histidine	19.1	10.2	NaN	NaN	5.3	NaN	NaN	4.7	212.3	107.0	7.0	4.0	3.6
homoserine	5.8	6.4	5.3	4.8	4.9	4.9	7.0	5.0	5.8	6.1	6.1	4.9	6.1
homoserine betaine	62.4	NaN	NaN	NaN	136.9	59.2	70.5	52.7	34.0	32.6	78.0	77.1	77.6
isethionate	29.6	5.7	5.1	NaN	56.5	32.7	42.9	29.7	31.0	31.6	59.4	56.9	54.5
isoleucine	NaN	NaN	NaN	NaN	NaN	NaN	NaN	NaN	43.6	16.6	NaN	NaN	NaN
kynurenine	4.0	NaN	NaN	NaN	3.5	3.7	NaN	3.4	8.8	9.0	3.0	NaN	NaN
leucine	NaN	NaN	NaN	NaN	NaN	NaN	NaN	NaN	35.2	15.7	NaN	NaN	NaN
malic acid	45.0	NaN	NaN	NaN	88.7	54.0	147.0	29.9	41.2	130.4	53.7	77.2	47.6
methionine	NaN	NaN	NaN	NaN	NaN	NaN	NaN	NaN	19.5	NaN	NaN	NaN	NaN
muramic acid	NaN	NaN	8.4	5.6	NaN	NaN	8.4	NaN	NaN	18.0	12.9	NaN	NaN
pantothenic acid	NaN	NaN	NaN	NaN	NaN	3.6	2.4	NaN	2.0	3.6	NaN	NaN	NaN
phenylalanine	7.1	8.1	NaN	NaN	17.8	7.1	9.3	10.1	45.2	35.7	9.7	16.7	6.7
proline	NaN	NaN	NaN	NaN	NaN	NaN	NaN	NaN	10.4	NaN	NaN	NaN	NaN
putrescine	45.1	7.1	NaN	NaN	29.7	NaN	10.7	42.8	164.4	87.2	12.1	46.3	21.2
sarcosine	7.9	NaN	NaN	4.7	21.6	3.6	10.7	4.7	3.6	5.6	4.0	8.6	7.4
serine	38.5	13.0	NaN	NaN	27.2	NaN	13.5	41.9	387.4	364.0	44.9	49.2	NaN

name	AE2123_BC99_C5N11	AE2123_BC101_C5N16	AE2123_BC102_C5N16	AE2123_BC103_C5N16	AE2123_BC104_C6N2	AE2123_BC105_C6N2	AE2123_BC106_C6N2	AE2123_BC107_C6N4	AE2123_BC108_C6N4	AE2123_BC109_C6N4	AE2123_BC110_C6N6	AE2123_BC111_C6N6	AE2123_BC112_C6N6
cast	5	5	5	5	6	6	6	6	6	6	6	6	6
niskin	11	16	16	16	2	2	2	4	4	4	6	6	6
depth (m)	90.229	200.722	200.722	200.722	4.541	4.541	4.541	20.922	20.922	20.922	39.485	39.485	39.485
date (YYYYmmdd)	20211111	20211111	20211111	20211111	20211112	20211112	20211112	20211112	20211112	20211112	20211112	20211112	20211112
time (hhMM)	2202	2202	2202	2202	435	435	435	435	435	435	435	435	435
glycerol 3-phosphate	55.0	8.9	13.9	NaN	33.6	26.1	25.2	73.4	66.0	47.7	21.9	22.6	24.4
spermidine	NaN	NaN	NaN	NaN	NaN	NaN	NaN	NaN	NaN	NaN	NaN	NaN	NaN
taurine	170.9	70.9	NaN	13.3	105.0	100.4	50.8	22.1	22.7	33.8	52.6	35.6	52.9
thiamine monophosphate	NaN	NaN	NaN	NaN	NaN	NaN	NaN	NaN	NaN	NaN	NaN	NaN	NaN
threonine	25.1	14.8	NaN	NaN	31.3	3.7	28.3	17.0	145.5	119.6	20.4	40.2	12.4
thymidine	NaN	NaN	NaN	NaN	26.4	32.5	NaN	31.9	NaN	32.0	NaN	27.9	NaN
tryptamine	NaN	NaN	NaN	NaN	NaN	NaN	NaN	NaN	26.5	NaN	NaN	NaN	NaN
tryptophan	8.0	5.4	4.1	4.4	7.7	7.1	7.2	4.9	14.4	7.5	7.8	6.5	5.9
tyrosine	NaN	32.3	NaN	NaN	137.3	72.8	69.2	NaN	228.8	228.8	38.3	33.9	14.7
uridine	6.8	NaN	NaN	5.9	12.4	12.2	7.5	7.3	10.1	15.0	10.3	11.1	9.2
valine	NaN	NaN	NaN	NaN	NaN	NaN	NaN	NaN	56.8	36.2	NaN	NaN	NaN
xanthosine	NaN	NaN	NaN	NaN	NaN	NaN	NaN	NaN	NaN	NaN	NaN	NaN	NaN

name	AE2123_BC113_C6N9	AE2123_BC114_C6N9	AE2123_BC115_C6N9	AE2123_BC116_C6N11	AE2123_BC117_C6N11	AE2123_BC118_C6N11	AE2123_BC119_C6N13	AE2123_BC120_C6N13	AE2123_BC121_C6N13	AE2123_BC122_C6N16	AE2123_BC123_C6N16	AE2123_BC124_C6N16	AE2123_BC125_C6N18
cast	6	6	6	6	6	6	6	6	6	6	6	6	6
niskin	9	9	9	11	11	11	13	13	13	16	16	16	18
depth (m)	80.46	80.46	80.46	94.966	94.966	94.966	109.889	109.889	109.889	200.111	200.111	200	250.946
date (YYYYmmdd)	20211112	20211112	20211112	20211112	20211112	20211112	20211112	20211112	20211112	20211112	20211112	####	20211112
time (hhMM)	435	435	435	435	435	435	435	435	435	435	435	435	435
2'deoxycitidine	49.9	NaN	NaN	NaN	55.7	NaN	NaN	NaN	NaN	NaN	NaN	NaN	31.1
2'deoxyguanosine	3.0	2.6	2.3	2.3	NaN	NaN	2.3	NaN	NaN	NaN	2.3	2.3	NaN
2'deoxyuridine	13.8	38.1	27.7	28.4	21.9	34.0	24.3	14.4	23.4	13.8	11.4	16.0	12.9
adenosine 3'-monophosphate	NaN	NaN	NaN	NaN	NaN	NaN	5.5	NaN	NaN	NaN	NaN	NaN	NaN
4-aminobenzoic acid	NaN	629.5	NaN	NaN	NaN	6.4	379.5	196.0	172.1	NaN	NaN	NaN	NaN
uridine 5'-monophosphate	NaN	NaN	NaN	NaN	NaN	NaN	NaN	NaN	NaN	NaN	NaN	NaN	NaN
adenosine 5'-monophosphate	NaN	NaN	NaN	12.4	NaN	NaN	19.3	NaN	NaN	NaN	NaN	NaN	17.5
inosine 5'-monophosphate	NaN	NaN	NaN	NaN	NaN	NaN	NaN	NaN	NaN	NaN	NaN	NaN	NaN
5'deoxyadenosine	49.1	NaN	28.4	NaN	34.8	NaN	NaN	47.8	NaN	NaN	NaN	32.1	47.7
2,3-dihydroxypropane-1-sulfonate	49.2	41.3	40.8	23.3	33.2	25.2	8.0	7.3	10.2	NaN	NaN	NaN	35.1
gamma-aminobutyric acid	NaN	22.4	NaN	NaN	NaN	NaN	22.4	4.5	6.9	NaN	NaN	NaN	7.7
HET	NaN	NaN	NaN	NaN	NaN	NaN	NaN	NaN	NaN	NaN	NaN	NaN	NaN
HMP	53.8	NaN	NaN	NaN	NaN	NaN	NaN	NaN	NaN	151.4	NaN	49.7	NaN
N-acetyl-muramic acid	NaN	NaN	NaN	10.7	11.9	13.4	NaN	NaN	13.1	14.4	NaN	NaN	NaN
adenine	NaN	NaN	NaN	NaN	NaN	NaN	NaN	NaN	NaN	NaN	NaN	NaN	NaN
adenosine	3.4	3.2	2.3	NaN	NaN	2.3	2.4	2.3	NaN	NaN	2.3	2.3	NaN
alanine	48.6	1607.7	21.9	NaN	30.6	138.6	1605.0	854.7	651.9	NaN	13.9	10.0	83.9

name	AE2123_BC113_C6N9	AE2123_BC114_C6N9	AE2123_BC115_C6N9	AE2123_BC116_C6N11	AE2123_BC117_C6N11	AE2123_BC118_C6N11	AE2123_BC119_C6N13	AE2123_BC120_C6N13	AE2123_BC121_C6N13	AE2123_BC122_C6N16	AE2123_BC123_C6N16	AE2123_BC124_C6N16	AE2123_BC125_C6N18
cast	6	6	6	6	6	6	6	6	6	6	6	6	6
niskin	9	9	9	11	11	11	13	13	13	16	16	16	18
depth (m)	80.46	80.46	80.46	94.966	94.966	94.966	109.889	109.889	109.889	200.111	200.111	200	250.946
date (YYYYmmdd)	20211112	20211112	20211112	20211112	20211112	20211112	20211112	20211112	20211112	20211112	20211112	#######	20211112
time (hhMM)	435	435	435	435	435	435	435	435	435	435	435	435	435
amMP	NaN	NaN	NaN	19.7	25.8	NaN	7.4	NaN	3.7	6.0	8.4	NaN	22.0
arginine	13.3	1462.7	NaN	9.5	NaN	16.5	297.3	112.3	126.5	NaN	NaN	NaN	8.4
asparagine	7.1	386.6	5.5	NaN	4.3	17.5	339.5	148.2	147.6	NaN	NaN	NaN	11.1
aspartate	NaN	720.6	NaN	NaN	NaN	25.4	870.7	449.0	406.1	NaN	NaN	NaN	10.2
chitobiose	NaN	NaN	NaN	NaN	NaN	NaN	NaN	NaN	NaN	NaN	NaN	NaN	NaN
chitotriose	NaN	NaN	NaN	NaN	NaN	NaN	NaN	NaN	NaN	NaN	NaN	NaN	NaN
ciliatine	5.9	4.9	4.7	3.4	4.6	3.9	12.7	5.3	5.3	NaN	2.6	NaN	3.9
citrulline	NaN	2043.5	20.7	NaN	NaN	52.7	476.5	163.8	182.6	NaN	NaN	10.0	7.5
cysteate	NaN	17.5	8.1	NaN	NaN	NaN	13.7	7.6	NaN	NaN	NaN	NaN	NaN
cysteine	25.9	96.1	17.1	39.3	20.8	21.7	153.6	72.6	52.4	6.6	NaN	NaN	9.1
cystine	NaN	NaN	NaN	NaN	NaN	NaN	NaN	NaN	NaN	NaN	NaN	NaN	NaN
cytidine	43.2	NaN	NaN	NaN	NaN	34.5	NaN	NaN	NaN	38.6	NaN	NaN	NaN
ectoine	NaN	NaN	NaN	70.2	NaN	134.0	93.5	NaN	257.4	NaN	NaN	NaN	NaN
glucosamine-6-phosphate	NaN	NaN	NaN	NaN	NaN	NaN	NaN	NaN	NaN	NaN	NaN	13.3	NaN
glucose 6-phosphate	10.9	11.6	NaN	NaN	NaN	NaN	NaN	NaN	NaN	NaN	NaN	NaN	NaN
glutamic acid	29.1	562.2	47.2	22.6	NaN	15.9	377.7	147.6	167.1	NaN	NaN	NaN	59.7
glutamine	39.3	237.5	17.4	8.6	12.4	20.0	102.0	41.8	42.8	NaN	NaN	NaN	33.5
glutathione	NaN	10.4	7.8	NaN	NaN	NaN	NaN	NaN	NaN	NaN	NaN	NaN	NaN

name	AE2123_BC113_C6N9	AE2123_BC114_C6N9	AE2123_BC115_C6N9	AE2123_BC116_C6N11	AE2123_BC117_C6N11	AE2123_BC118_C6N11	AE2123_BC119_C6N13	AE2123_BC120_C6N13	AE2123_BC121_C6N13	AE2123_BC122_C6N16	AE2123_BC123_C6N16	AE2123_BC124_C6N16	AE2123_BC125_C6N18
cast	6	6	6	6	6	6	6	6	6	6	6	6	6
niskin	9	9	9	11	11	11	13	13	13	16	16	16	18
depth (m)	80.46	80.46	80.46	94.966	94.966	94.966	109.889	109.889	109.889	200.111	200.111	200	250.946
date (YYYYmmdd)	20211112	20211112	20211112	20211112	20211112	20211112	20211112	20211112	20211112	20211112	20211112	####	20211112
time (hhMM)	435	435	435	435	435	435	435	435	435	435	435	435	435
glycine	62.5	818.3	28.8	65.0	NaN	86.3	1896.4	844.7	777.6	NaN	NaN	NaN	9.9
guanosine	NaN	18.9	NaN	NaN	NaN	NaN	NaN	NaN	NaN	NaN	NaN	NaN	NaN
histidine	13.4	928.7	5.0	NaN	14.3	82.9	1745.4	825.9	723.6	NaN	3.6	NaN	43.7
homoserine	5.0	5.2	7.3	5.4	6.1	5.6	5.2	5.5	4.9	4.8	4.9	5.8	5.3
homoserine betaine	50.9	54.5	52.9	13.9	20.3	19.3	23.5	9.0	12.2	NaN	10.1	NaN	68.5
isethionate	17.5	21.4	19.9	8.9	11.8	13.6	34.7	23.2	18.7	5.9	5.9	NaN	27.7
isoleucine	NaN	1182.9	NaN	NaN	NaN	3.7	354.7	162.6	177.7	NaN	NaN	NaN	NaN
kynurenine	5.0	37.7	2.9	NaN	NaN	6.5	64.3	31.1	31.2	NaN	NaN	NaN	6.1
leucine	NaN	580.9	NaN	NaN	NaN	9.7	267.3	140.5	129.7	NaN	NaN	NaN	4.1
malic acid	NaN	1083.5	33.6	NaN	NaN	NaN	189.9	21.7	77.2	NaN	NaN	42.4	NaN
methionine	NaN	134.7	NaN	NaN	NaN	NaN	60.2	40.8	31.3	NaN	NaN	NaN	NaN
muramic acid	NaN	NaN	NaN	NaN	NaN	15.3	NaN	9.5	NaN	NaN	6.6	NaN	NaN
pantothenic acid	NaN	2.5	NaN	NaN	NaN	NaN	NaN	NaN	NaN	NaN	NaN	NaN	NaN
phenylalanine	10.7	704.7	10.0	4.9	10.2	19.3	320.3	158.6	145.0	5.7	7.1	8.3	15.8
proline	NaN	593.6	NaN	NaN	NaN	NaN	222.8	96.6	98.1	NaN	NaN	NaN	NaN
putrescine	23.4	3299.2	37.9	NaN	22.8	65.5	395.5	185.8	213.5	NaN	NaN	NaN	35.4
sarcosine	9.1	7.3	4.0	3.6	3.9	6.1	9.6	8.3	10.7	NaN	NaN	NaN	6.9
serine	73.9	2078.8	31.1	NaN	45.0	214.4	2807.0	1644.7	1277.6	NaN	9.8	13.5	76.7

name	AE2123_BC113_C6N9	AE2123_BC114_C6N9	AE2123_BC115_C6N9	AE2123_BC116_C6N11	AE2123_BC117_C6N11	AE2123_BC118_C6N11	AE2123_BC119_C6N13	AE2123_BC120_C6N13	AE2123_BC121_C6N13	AE2123_BC122_C6N16	AE2123_BC123_C6N16	AE2123_BC124_C6N16	AE2123_BC125_C6N18
cast	6	6	6	6	6	6	6	6	6	6	6	6	6
niskin	9	9	9	11	11	11	13	13	13	16	16	16	18
depth (m)	80.46	80.46	80.46	94.966	94.966	94.966	109.889	109.889	109.889	200.111	200.111	200	250.946
date (YYYYmmdd)	20211112	20211112	20211112	20211112	20211112	20211112	20211112	20211112	20211112	20211112	20211112	####	20211112
time (hhMM)	435	435	435	435	435	435	435	435	435	435	435	435	435
glycerol 3-phosphate	35.0	43.2	35.0	29.6	43.2	57.0	111.1	57.6	80.9	7.6	6.9	7.7	62.5
spermidine	NaN	NaN	NaN	NaN	NaN	NaN	189.4	NaN	NaN	NaN	NaN	NaN	NaN
taurine	107.3	120.6	73.8	66.8	50.7	50.2	115.5	32.6	48.9	NaN	NaN	NaN	35.6
thiamine monophosphate	NaN	NaN	NaN	NaN	NaN	NaN	NaN	NaN	NaN	NaN	NaN	NaN	NaN
threonine	21.3	1640.9	26.9	NaN	21.7	72.3	993.3	512.1	458.0	NaN	9.0	8.1	35.3
thymidine	NaN	30.5	36.2	NaN	NaN	NaN	NaN	29.3	NaN	NaN	NaN	NaN	NaN
tryptamine	NaN	31.3	NaN	NaN	NaN	NaN	84.0	25.7	NaN	NaN	NaN	NaN	NaN
tryptophan	6.4	70.8	6.8	5.4	6.1	7.8	75.6	41.3	28.1	4.4	NaN	NaN	7.0
tyrosine	123.9	265.3	50.1	NaN	89.6	71.4	93.8	64.0	37.3	39.6	NaN	617.6	46.7
uridine	5.1	102.0	10.7	6.4	5.4	9.6	20.8	13.8	14.9	5.8	6.1	5.5	8.9
valine	NaN	840.6	NaN	NaN	NaN	17.3	582.7	273.8	261.8	NaN	NaN	NaN	NaN
xanthosine	NaN	NaN	NaN	NaN	NaN	NaN	NaN	NaN	NaN	NaN	NaN	NaN	NaN

name	AE2123_BC126_C6N18	AE2123_BC127_C6N18	AE2123_BC128_C7N2	AE2123_BC129_C7N2	AE2123_BC130_C7N2	AE2123_BC131_C7N4	AE2123_BC132_C7N4	AE2123_BC133_C7N4	AE2123_BC134_C7N6	AE2123_BC135_C7N6	AE2123_BC136_C7N6	AE2123_BC137_C7N9	AE2123_BC138_C7N9
cast	6	6	7	7	7	7	7	7	7	7	7	7	7
niskin	18	18	2	2	2	4	4	4	6	6	6	9	9
depth (m)	250.946	250.946	3.676	3.676	3.676	19.903	19.903	19.903	40.236	40.236	40.236	79.751	79.751
date (YYYYmmdd)	20211112	20211112	20211112	20211112	20211112	20211112	20211112	20211112	20211112	20211112	20211112	20211112	20211112
time (hhMM)	435	435	1100	1100	1100	1100	1100	1100	1100	1100	1100	1100	1100
2'deoxycitidine	NaN	NaN	NaN	NaN	NaN	25.7	NaN	NaN	36.4	NaN	59.1	NaN	NaN
2'deoxyguanosine	NaN	2.3	2.3	2.3	2.3	2.6	2.3	2.7	NaN	2.9	NaN	2.3	2.3
2'deoxyuridine	9.3	21.1	47.7	29.9	34.2	55.7	49.5	53.4	41.8	48.4	63.2	66.4	53.9
adenosine 3'-monophosphate	NaN	NaN	NaN	NaN	NaN	3.2	NaN	NaN	NaN	NaN	NaN	NaN	NaN
4-aminobenzoic acid	NaN	NaN	NaN	NaN	NaN	NaN	NaN	NaN	NaN	NaN	NaN	NaN	NaN
uridine 5'-monophosphate	NaN	NaN	NaN	NaN	NaN	NaN	NaN	NaN	NaN	NaN	NaN	NaN	NaN
adenosine 5'-monophosphate	NaN	NaN	NaN	NaN	NaN	NaN	NaN	NaN	NaN	16.7	NaN	NaN	NaN
inosine 5'-monophosphate	NaN	NaN	NaN	NaN	NaN	NaN	NaN	8.9	10.6	NaN	NaN	NaN	NaN
5'deoxyadenosine	NaN	NaN	NaN	65.7	NaN	NaN	NaN	NaN	NaN	NaN	72.1	NaN	NaN
2,3-dihydroxypropane-1-sulfonate	NaN	NaN	34.6	48.5	53.0	15.7	26.8	23.4	62.1	59.1	73.4	63.4	62.9
gamma-aminobutyric acid	NaN	NaN	NaN	NaN	NaN	NaN	NaN	NaN	NaN	NaN	NaN	NaN	NaN
HET	NaN	NaN	NaN	NaN	NaN	NaN	NaN	NaN	NaN	NaN	NaN	NaN	NaN
HMP	NaN	123.0	NaN	NaN	NaN	NaN	NaN	NaN	NaN	NaN	NaN	NaN	112.5
N-acetyl-muramic acid	NaN	NaN	NaN	11.8	NaN	NaN	NaN	10.8	NaN	27.0	NaN	NaN	NaN
adenine	NaN	NaN	NaN	NaN	NaN	NaN	NaN	NaN	NaN	NaN	NaN	NaN	NaN
adenosine	NaN	2.3	2.3	2.4	2.3	2.7	2.4	2.4	2.3	2.7	NaN	2.3	NaN
alanine	5.8	56.1	10.4	10.8	12.8	NaN	NaN	66.2	12.8	NaN	16.0	NaN	NaN

name	AE2123_BC126_C6N18	AE2123_BC127_C6N18	AE2123_BC128_C7N2	AE2123_BC129_C7N2	AE2123_BC130_C7N2	AE2123_BC131_C7N4	AE2123_BC132_C7N4	AE2123_BC133_C7N4	AE2123_BC134_C7N6	AE2123_BC135_C7N6	AE2123_BC136_C7N6	AE2123_BC137_C7N9	AE2123_BC138_C7N9
cast	6	6	7	7	7	7	7	7	7	7	7	7	7
niskin	18	18	2	2	2	4	4	4	6	6	6	9	9
depth (m)	250.946	250.946	3.676	3.676	3.676	19.903	19.903	19.903	40.236	40.236	40.236	79.751	79.751
date (YYYYmmdd)	20211112	20211112	20211112	20211112	20211112	20211112	20211112	20211112	20211112	20211112	20211112	20211112	20211112
time (hhMM)	435	435	1100	1100	1100	1100	1100	1100	1100	1100	1100	1100	1100
amMP	10.0	NaN	15.4	5.2	NaN	5.5	NaN	7.9	NaN	NaN	12.5	NaN	NaN
arginine	24.3	NaN	NaN	NaN	NaN	NaN	NaN	NaN	NaN	12.9	NaN	7.5	7.9
asparagine	4.1	3.0	2.3	NaN	NaN	NaN	NaN	4.7	14.4	16.9	11.5	12.5	9.4
aspartate	33.6	NaN	NaN	NaN	NaN	NaN	NaN	NaN	NaN	17.4	NaN	23.4	14.7
chitobiose	NaN	NaN	NaN	NaN	NaN	NaN	NaN	NaN	NaN	NaN	NaN	NaN	NaN
chitotriose	NaN	NaN	NaN	NaN	NaN	NaN	NaN	NaN	NaN	NaN	NaN	NaN	NaN
ciliatine	NaN	NaN	NaN	NaN	NaN	NaN	NaN	NaN	3.0	3.3	2.7	5.0	5.5
citrulline	NaN	NaN	NaN	NaN	NaN	NaN	NaN	NaN	NaN	NaN	NaN	NaN	NaN
cysteate	10.6	NaN	NaN	NaN	NaN	NaN	NaN	NaN	NaN	NaN	NaN	13.2	11.4
cysteine	28.3	NaN	13.9	7.9	17.7	13.5	8.9	9.2	7.5	30.7	17.4	46.4	32.9
cystine	NaN	NaN	NaN	NaN	NaN	NaN	NaN	NaN	NaN	NaN	NaN	NaN	NaN
cytidine	NaN	NaN	48.3	NaN	NaN	NaN	NaN	NaN	NaN	NaN	NaN	NaN	NaN
ectoine	NaN	NaN	NaN	NaN	NaN	NaN	NaN	57.5	NaN	27.2	NaN	54.0	39.3
glucosamine-6-phosphate	NaN	NaN	NaN	NaN	NaN	NaN	NaN	NaN	NaN	NaN	NaN	NaN	NaN
glucose 6-phosphate	NaN	NaN	NaN	NaN	NaN	NaN	NaN	NaN	11.8	NaN	11.9	NaN	NaN
glutamic acid	NaN	NaN	13.3	NaN	NaN	NaN	NaN	NaN	76.7	97.1	60.0	47.5	56.2
glutamine	5.2	NaN	12.9	13.6	12.7	NaN	2.7	5.0	43.8	49.4	54.6	23.9	20.4
glutathione	NaN	NaN	10.4	12.7	NaN	NaN	NaN	NaN	27.3	NaN	30.2	30.2	20.0

name	AE2123_BC126_C6N18	AE2123_BC127_C6N18	AE2123_BC128_C7N2	AE2123_BC129_C7N2	AE2123_BC130_C7N2	AE2123_BC131_C7N4	AE2123_BC132_C7N4	AE2123_BC133_C7N4	AE2123_BC134_C7N6	AE2123_BC135_C7N6	AE2123_BC136_C7N6	AE2123_BC137_C7N9	AE2123_BC138_C7N9
cast	6	6	7	7	7	7	7	7	7	7	7	7	7
niskin	18	18	2	2	2	4	4	4	6	6	6	9	9
depth (m)	250.946	250.946	3.676	3.676	3.676	19.903	19.903	19.903	40.236	40.236	40.236	79.751	79.751
date (YYYYmmdd)	20211112	20211112	20211112	20211112	20211112	20211112	20211112	20211112	20211112	20211112	20211112	20211112	20211112
time (hhMM)	435	435	1100	1100	1100	1100	1100	1100	1100	1100	1100	1100	1100
glycine	50.1	NaN	NaN	NaN	NaN	NaN	NaN	21.6	16.8	84.8	NaN	103.5	82.6
guanosine	NaN	NaN	NaN	NaN	NaN	NaN	NaN	NaN	NaN	NaN	NaN	NaN	NaN
histidine	6.1	33.5	NaN	NaN	NaN	NaN	NaN	51.8	NaN	NaN	NaN	NaN	NaN
homoserine	4.5	6.4	5.9	6.4	4.5	4.3	4.5	5.2	5.7	5.3	6.3	5.8	5.8
homoserine betaine	NaN	NaN	53.1	55.8	56.6	23.6	37.0	32.5	134.4	125.0	167.0	54.1	66.1
isethionate	5.5	5.3	44.5	39.8	43.3	28.8	29.8	31.9	85.2	53.0	82.0	15.9	16.8
isoleucine	NaN	NaN	NaN	NaN	NaN	NaN	NaN	NaN	NaN	NaN	NaN	NaN	NaN
kynurenine	4.3	NaN	NaN	3.4	3.2	NaN	2.8	5.3	3.1	2.8	NaN	NaN	NaN
leucine	NaN	NaN	NaN	NaN	NaN	NaN	NaN	2.2	NaN	NaN	NaN	NaN	NaN
malic acid	32.0	NaN	127.3	112.7	42.5	35.5	82.4	62.7	155.1	94.2	60.1	46.5	50.9
methionine	NaN	NaN	NaN	NaN	NaN	NaN	NaN	NaN	NaN	NaN	NaN	NaN	NaN
muramic acid	NaN	6.2	NaN	NaN	NaN	NaN	7.5	22.8	NaN	NaN	NaN	NaN	NaN
pantothenic acid	NaN	NaN	NaN	NaN	NaN	NaN	NaN	3.2	NaN	3.0	NaN	2.0	1.9
phenylalanine	11.7	11.3	6.1	5.7	6.1	5.2	4.4	13.0	8.0	6.0	6.9	7.1	NaN
proline	NaN	NaN	NaN	NaN	NaN	NaN	NaN	NaN	NaN	NaN	NaN	NaN	NaN
putrescine	23.2	NaN	5.6	6.7	13.1	NaN	NaN	15.8	15.9	9.1	25.8	NaN	8.2
sarcosine	NaN	NaN	9.3	8.3	10.5	NaN	4.8	4.9	7.7	6.4	10.7	6.1	4.7
serine	63.2	130.3	NaN	NaN	NaN	NaN	NaN	112.3	NaN	NaN	NaN	NaN	NaN

name	AE2123_BC126_C6N18	AE2123_BC127_C6N18	AE2123_BC128_C7N2	AE2123_BC129_C7N2	AE2123_BC130_C7N2	AE2123_BC131_C7N4	AE2123_BC132_C7N4	AE2123_BC133_C7N4	AE2123_BC134_C7N6	AE2123_BC135_C7N6	AE2123_BC136_C7N6	AE2123_BC137_C7N9	AE2123_BC138_C7N9
cast	6	6	7	7	7	7	7	7	7	7	7	7	7
niskin	18	18	2	2	2	4	4	4	6	6	6	9	9
depth (m)	250.946	250.946	3.676	3.676	3.676	19.903	19.903	19.903	40.236	40.236	40.236	79.751	79.751
date (YYYYmmdd)	20211112	20211112	20211112	20211112	20211112	20211112	20211112	20211112	20211112	20211112	20211112	20211112	20211112
time (hhMM)	435	435	1100	1100	1100	1100	1100	1100	1100	1100	1100	1100	1100
glycerol 3-phosphate	18.4	21.0	30.7	27.4	42.9	35.0	34.7	27.3	36.3	37.1	22.5	49.8	47.1
spermidine	NaN	NaN	NaN	NaN	NaN	NaN	NaN	NaN	NaN	NaN	NaN	NaN	NaN
taurine	NaN	NaN	39.0	56.7	62.0	NaN	15.2	12.3	82.1	130.4	100.7	128.4	156.9
thiamine monophosphate	NaN	NaN	NaN	NaN	NaN	NaN	NaN	NaN	NaN	NaN	NaN	NaN	NaN
threonine	11.3	25.1	5.3	5.1	6.2	5.3	NaN	38.9	11.6	NaN	9.1	NaN	NaN
thymidine	NaN	NaN	NaN	NaN	29.3	NaN	NaN	NaN	NaN	31.8	NaN	NaN	NaN
tryptamine	NaN	NaN	NaN	NaN	NaN	NaN	NaN	NaN	NaN	NaN	NaN	NaN	NaN
tryptophan	5.8	NaN	6.4	5.3	5.6	3.9	4.4	7.8	7.8	4.9	7.7	7.3	5.1
tyrosine	421.0	57.5	NaN	NaN	NaN	NaN	23.6	NaN	NaN	NaN	NaN	NaN	NaN
uridine	5.9	5.3	6.8	5.5	7.9	7.2	7.8	7.2	10.4	6.7	10.3	7.9	9.1
valine	NaN	NaN	NaN	NaN	NaN	NaN	NaN	NaN	NaN	NaN	NaN	NaN	NaN
xanthosine	NaN	NaN	NaN	NaN	NaN	NaN	NaN	NaN	NaN	NaN	NaN	NaN	NaN

name	AE2123_BC139_C7N9	AE2123_BC140_C7N11	AE2123_BC141_C7N11	AE2123_BC142_C7N11	AE2123_BC143_C7N13	AE2123_BC144_C7N13	AE2123_BC145_C7N13	AE2123_BC146_C7N16	AE2123_BC147_C7N16	AE2123_BC148_C7N16	AE2123_BC149_C7N18	AE2123_BC150_C7N18	AE2123_BC151_C7N18
cast	7	7	7	7	7	7	7	7	7	7	7	7	7
niskin	9	11	11	11	13	13	13	16	16	16	18	18	18
depth (m)	79.751	89.651	89.651	89.651	121.829	121.829	121.829	200.275	200.275	200.275	250.944	250.944	250.944
date (YYYYmmdd)	20211112	20211112	20211112	20211112	20211112	20211112	20211112	20211112	20211112	20211112	20211112	20211112	20211112
time (hhMM)	1100	1100	1100	1100	1100	1100	1100	1100	1100	1100	1100	1100	1100
2'deoxycitidine	NaN	NaN	NaN	NaN	NaN	NaN	NaN	NaN	NaN	NaN	NaN	NaN	NaN
2'deoxyguanosine	2.3	2.5	NaN	2.3	NaN	2.3	2.8	NaN	2.3	NaN	2.3	2.3	2.4
2'deoxyuridine	NaN	11.7	NaN	NaN	32.2	11.3	34.5	14.2	10.7	13.4	NaN	13.8	NaN
adenosine 3'-monophosphate	NaN	NaN	NaN	NaN	NaN	NaN	NaN	NaN	NaN	NaN	NaN	NaN	NaN
4-aminobenzoic acid	NaN	NaN	NaN	NaN	NaN	NaN	NaN	NaN	NaN	NaN	NaN	NaN	NaN
uridine 5'-monophosphate	NaN	NaN	NaN	NaN	NaN	NaN	NaN	NaN	NaN	NaN	NaN	NaN	NaN
adenosine 5'-monophosphate	NaN	NaN	NaN	NaN	NaN	NaN	NaN	NaN	NaN	NaN	NaN	NaN	NaN
inosine 5'-monophosphate	NaN	NaN	NaN	NaN	NaN	NaN	NaN	NaN	NaN	NaN	NaN	NaN	NaN
5'deoxyadenosine	NaN	69.7	NaN	NaN	NaN	59.3	33.4	NaN	NaN	NaN	NaN	NaN	43.4
2,3-dihydroxypropane-1-sulfonate	73.7	50.8	50.2	28.0	NaN	NaN	5.3	NaN	NaN	NaN	NaN	NaN	6.1
gamma-aminobutyric acid	NaN	NaN	NaN	NaN	NaN	NaN	NaN	NaN	NaN	NaN	NaN	NaN	NaN
HET	NaN	NaN	NaN	NaN	NaN	NaN	NaN	NaN	NaN	NaN	NaN	NaN	NaN
HMP	NaN	NaN	165.9	NaN	NaN	64.4	103.0	196.1	NaN	NaN	NaN	NaN	NaN
N-acetyl-muramic acid	NaN	NaN	NaN	10.4	NaN	NaN	NaN	NaN	NaN	NaN	NaN	NaN	20.7
adenine	NaN	NaN	NaN	NaN	NaN	NaN	NaN	NaN	NaN	NaN	NaN	NaN	NaN
adenosine	2.4	2.7	NaN	2.3	NaN	2.3	2.8	NaN	2.3	NaN	2.3	2.3	2.5
alanine	15.9	22.1	19.2	NaN	NaN	NaN	NaN	NaN	NaN	NaN	NaN	NaN	13.0

name	AE2123_BC139_C7N9	AE2123_BC140_C7N11	AE2123_BC141_C7N11	AE2123_BC142_C7N11	AE2123_BC143_C7N13	AE2123_BC144_C7N13	AE2123_BC145_C7N13	AE2123_BC146_C7N16	AE2123_BC147_C7N16	AE2123_BC148_C7N16	AE2123_BC149_C7N18	AE2123_BC150_C7N18	AE2123_BC151_C7N18
cast	7	7	7	7	7	7	7	7	7	7	7	7	7
niskin	9	11	11	11	13	13	13	16	16	16	18	18	18
depth (m)	79.751	89.651	89.651	89.651	121.829	121.829	121.829	200.275	200.275	200.275	250.944	250.944	250.944
date (YYYYmmdd)	20211112	20211112	20211112	20211112	20211112	20211112	20211112	20211112	20211112	20211112	20211112	20211112	20211112
time (hhMM)	1100	1100	1100	1100	1100	1100	1100	1100	1100	1100	1100	1100	1100
amMP	NaN	NaN	13.9	4.3	10.7	15.3	7.1	NaN	NaN	16.1	NaN	10.9	13.9
arginine	NaN	NaN	NaN	NaN	NaN	NaN	NaN	NaN	NaN	NaN	NaN	NaN	NaN
asparagine	9.7	NaN	3.0	5.9	NaN	NaN	NaN	NaN	NaN	NaN	NaN	NaN	NaN
aspartate	NaN	NaN	NaN	NaN	NaN	NaN	NaN	NaN	NaN	NaN	NaN	NaN	NaN
chitobiose	NaN	NaN	NaN	NaN	NaN	NaN	NaN	NaN	NaN	NaN	NaN	NaN	NaN
chitotriose	NaN	NaN	NaN	NaN	NaN	NaN	NaN	NaN	NaN	NaN	NaN	NaN	NaN
ciliatine	7.7	5.1	6.0	4.3	2.6	NaN	NaN	NaN	NaN	NaN	NaN	NaN	2.4
citrulline	NaN	NaN	NaN	NaN	NaN	NaN	NaN	NaN	NaN	NaN	NaN	NaN	NaN
cysteate	9.4	NaN	NaN	7.3	NaN	NaN	NaN	NaN	NaN	NaN	NaN	NaN	NaN
cysteine	14.5	16.4	10.2	21.5	NaN	10.3	NaN	7.4	NaN	NaN	NaN	NaN	NaN
cystine	NaN	NaN	NaN	NaN	NaN	NaN	NaN	NaN	NaN	NaN	NaN	NaN	NaN
cytidine	NaN	27.6	NaN	27.7	NaN	NaN	29.5	20.9	NaN	NaN	48.6	NaN	NaN
ectoine	NaN	NaN	32.9	NaN	NaN	NaN	NaN	NaN	NaN	NaN	NaN	27.1	81.0
glucosamine-6-phosphate	NaN	NaN	NaN	NaN	NaN	NaN	NaN	NaN	NaN	NaN	NaN	NaN	NaN
glucose 6-phosphate	NaN	15.8	NaN	13.7	NaN	NaN	NaN	NaN	10.0	NaN	NaN	NaN	NaN
glutamic acid	41.4	NaN	16.0	28.0	NaN	NaN	NaN	NaN	NaN	NaN	NaN	NaN	NaN
glutamine	21.2	16.1	16.3	14.4	NaN	NaN	NaN	NaN	NaN	NaN	NaN	NaN	3.3
glutathione	19.9	NaN	NaN	15.2	NaN	NaN	NaN	NaN	NaN	NaN	NaN	NaN	NaN

name	AE2123_BC139_C7N9	AE2123_BC140_C7N11	AE2123_BC141_C7N11	AE2123_BC142_C7N11	AE2123_BC143_C7N13	AE2123_BC144_C7N13	AE2123_BC145_C7N13	AE2123_BC146_C7N16	AE2123_BC147_C7N16	AE2123_BC148_C7N16	AE2123_BC149_C7N18	AE2123_BC150_C7N18	AE2123_BC151_C7N18
cast	7	7	7	7	7	7	7	7	7	7	7	7	7
niskin	9	11	11	11	13	13	13	16	16	16	18	18	18
depth (m)	79.751	89.651	89.651	89.651	121.829	121.829	121.829	200.275	200.275	200.275	250.944	250.944	250.944
date (YYYYmmdd)	20211112	20211112	20211112	20211112	20211112	20211112	20211112	20211112	20211112	20211112	20211112	20211112	20211112
time (hhMM)	1100	1100	1100	1100	1100	1100	1100	1100	1100	1100	1100	1100	1100
glycine	NaN	22.4	16.2	109.1	NaN	NaN	NaN	25.5	NaN	NaN	NaN	NaN	NaN
guanosine	NaN	NaN	NaN	NaN	NaN	NaN	NaN	NaN	NaN	NaN	NaN	NaN	NaN
histidine	4.9	NaN	NaN	NaN	NaN	NaN	NaN	NaN	NaN	NaN	NaN	NaN	NaN
homoserine	7.4	5.4	7.0	5.0	5.1	4.2	4.8	4.4	4.8	5.1	4.6	4.4	NaN
homoserine betaine	63.3	31.6	31.4	28.9	7.4	NaN	27.3	NaN	NaN	NaN	NaN	NaN	16.6
isethionate	23.1	16.5	14.8	11.7	14.6	7.8	9.6	NaN	8.2	7.3	6.5	4.5	8.5
isoleucine	NaN	NaN	NaN	NaN	NaN	NaN	NaN	NaN	NaN	NaN	NaN	NaN	NaN
kynurenine	4.4	3.6	NaN	NaN	NaN	NaN	4.1	3.8	NaN	NaN	NaN	NaN	NaN
leucine	NaN	NaN	NaN	NaN	NaN	NaN	NaN	NaN	NaN	NaN	NaN	NaN	NaN
malic acid	36.0	27.1	NaN	38.6	NaN	NaN	NaN	23.4	NaN	NaN	NaN	NaN	NaN
methionine	NaN	NaN	NaN	NaN	NaN	NaN	NaN	NaN	NaN	NaN	NaN	NaN	NaN
muramic acid	NaN	NaN	NaN	NaN	NaN	7.6	NaN	NaN	NaN	NaN	NaN	NaN	27.4
pantothenic acid	NaN	NaN	NaN	NaN	NaN	NaN	NaN	NaN	NaN	NaN	NaN	NaN	NaN
phenylalanine	7.1	6.7	5.6	5.7	NaN	NaN	4.9	NaN	5.3	4.3	NaN	NaN	6.3
proline	NaN	NaN	NaN	NaN	NaN	NaN	NaN	NaN	NaN	NaN	NaN	NaN	NaN
putrescine	44.2	46.6	53.3	NaN	NaN	NaN	NaN	NaN	NaN	NaN	NaN	NaN	NaN
sarcosine	10.1	11.3	14.2	6.6	NaN	4.3	3.8	NaN	NaN	NaN	NaN	4.4	4.3
serine	NaN	NaN	NaN	NaN	NaN	NaN	NaN	NaN	NaN	NaN	NaN	NaN	NaN

name	AE2123_BC139_C7N9	AE2123_BC140_C7N11	AE2123_BC141_C7N11	AE2123_BC142_C7N11	AE2123_BC143_C7N13	AE2123_BC144_C7N13	AE2123_BC145_C7N13	AE2123_BC146_C7N16	AE2123_BC147_C7N16	AE2123_BC148_C7N16	AE2123_BC149_C7N18	AE2123_BC150_C7N18	AE2123_BC151_C7N18
cast	7	7	7	7	7	7	7	7	7	7	7	7	7
niskin	9	11	11	11	13	13	13	16	16	16	18	18	18
depth (m)	79.751	89.651	89.651	89.651	121.829	121.829	121.829	200.275	200.275	200.275	250.944	250.944	250.944
date (YYYYmmdd)	20211112	20211112	20211112	20211112	20211112	20211112	20211112	20211112	20211112	20211112	20211112	20211112	20211112
time (hhMM)	1100	1100	1100	1100	1100	1100	1100	1100	1100	1100	1100	1100	1100
glycerol 3-phosphate	42.2	48.8	25.2	32.8	24.9	38.0	15.2	11.1	16.8	15.5	25.2	20.6	18.8
spermidine	NaN	NaN	NaN	NaN	NaN	NaN	NaN	NaN	NaN	NaN	NaN	NaN	NaN
taurine	79.7	87.9	100.5	77.8	NaN	NaN	NaN	NaN	NaN	NaN	NaN	NaN	9.8
thiamine monophosphate	NaN	NaN	NaN	NaN	NaN	NaN	NaN	NaN	NaN	NaN	NaN	NaN	14.5
threonine	8.5	NaN	NaN	NaN	NaN	NaN	NaN	NaN	NaN	NaN	NaN	NaN	NaN
thymidine	NaN	25.3	NaN	NaN	NaN	NaN	NaN	37.8	NaN	NaN	NaN	NaN	NaN
tryptamine	NaN	NaN	NaN	NaN	NaN	NaN	NaN	25.9	NaN	NaN	NaN	NaN	NaN
tryptophan	6.3	5.2	5.4	6.0	3.9	NaN	4.7	3.8	3.6	4.7	4.1	NaN	4.5
tyrosine	67.1	14.3	NaN	31.2	NaN	NaN	NaN	NaN	NaN	NaN	NaN	NaN	NaN
uridine	7.9	6.6	NaN	NaN	NaN	NaN	5.6	7.8	5.2	5.4	NaN	NaN	NaN
valine	NaN	NaN	NaN	NaN	NaN	NaN	NaN	NaN	NaN	NaN	NaN	NaN	NaN
xanthosine	NaN	NaN	NaN	NaN	NaN	NaN	NaN	NaN	NaN	NaN	NaN	NaN	NaN

name	AE2123_BC152_C8N2	AE2123_BC153_C8N2	AE2123_BC154_C8N2	AE2123_BC155_C8N6	AE2123_BC156_C8N6	AE2123_BC157_C8N6	AE2123_BC158_C8N9	AE2123_BC159_C8N9	AE2123_BC160_C8N9	AE2123_BC161_C8N11	AE2123_BC162_C8N11	AE2123_BC163_C8N11	AE2123_BC164_C8N16
cast	8	8	8	8	8	8	8	8	8	8	8	8	8
niskin	2	2	2	6	6	6	9	9	9	11	11	11	16
depth (m)	4.546	4.546	4.546	40.595	40.595	40.595	79.003	79.003	79.003	91.657	91.657	91.657	200.734
date (YYYYmmdd)	20211112	20211112	20211112	20211112	20211112	20211112	20211112	20211112	20211112	20211112	20211112	20211112	20211112
time (hhMM)	1700	1700	1700	1700	1700	1700	1700	1700	1700	1700	1700	1700	1700
2'deoxycitidine	NaN	NaN	NaN	NaN	NaN	NaN	NaN	NaN	NaN	NaN	148.6	NaN	NaN
2'deoxyguanosine	NaN	NaN	NaN	2.5	2.4	NaN	2.4	2.3	NaN	2.8	2.3	2.6	2.4
2'deoxyuridine	48.3	24.2	29.7	29.8	15.3	41.6	39.8	NaN	9.4	45.0	15.8	65.5	21.1
adenosine 3'-monophosphate	NaN	NaN	NaN	NaN	NaN	NaN	3.2	2.6	NaN	3.1	NaN	NaN	NaN
4-aminobenzoic acid	NaN	NaN	NaN	NaN	NaN	NaN	NaN	NaN	NaN	NaN	NaN	NaN	NaN
uridine 5'-monophosphate	NaN	NaN	NaN	NaN	NaN	NaN	NaN	NaN	NaN	NaN	10.6	NaN	NaN
adenosine 5'-monophosphate	NaN	NaN	NaN	NaN	NaN	NaN	NaN	10.7	NaN	14.4	NaN	14.2	NaN
inosine 5'-monophosphate	NaN	NaN	NaN	NaN	7.5	NaN	NaN	NaN	NaN	NaN	NaN	NaN	NaN
5'deoxyadenosine	NaN	NaN	45.7	NaN	49.0	NaN	NaN	NaN	NaN	NaN	NaN	NaN	59.1
2,3-dihydroxypropane-1-sulfonate	49.9	52.4	53.0	39.8	56.5	42.8	137.5	142.4	107.3	111.7	45.4	53.7	NaN
gamma-aminobutyric acid	NaN	NaN	NaN	NaN	NaN	NaN	NaN	NaN	NaN	NaN	NaN	NaN	NaN
HET	NaN	NaN	NaN	NaN	NaN	NaN	NaN	NaN	NaN	NaN	NaN	NaN	NaN
HMP	NaN	NaN	327.6	NaN	NaN	NaN	NaN	NaN	752.7	148.0	132.8	69.0	156.1
N-acetyl-muramic acid	NaN	NaN	NaN	13.6	12.9	NaN	NaN	11.3	NaN	NaN	NaN	NaN	NaN
adenine	NaN	NaN	NaN	NaN	NaN	NaN	NaN	NaN	NaN	NaN	NaN	NaN	NaN
adenosine	NaN	NaN	NaN	2.3	2.7	NaN	2.4	2.4	NaN	3.0	2.3	2.3	2.4
alanine	16.0	18.5	20.9	NaN	28.4	NaN	30.7	26.5	14.8	48.1	24.7	25.7	6.3

name	AE2123_BC152_C8N2	AE2123_BC153_C8N2	AE2123_BC154_C8N2	AE2123_BC155_C8N6	AE2123_BC156_C8N6	AE2123_BC157_C8N6	AE2123_BC158_C8N9	AE2123_BC159_C8N9	AE2123_BC160_C8N9	AE2123_BC161_C8N11	AE2123_BC162_C8N11	AE2123_BC163_C8N11	AE2123_BC164_C8N16
cast	8	8	8	8	8	8	8	8	8	8	8	8	8
niskin	2	2	2	6	6	6	9	9	9	11	11	11	16
depth (m)	4.546	4.546	4.546	40.595	40.595	40.595	79.003	79.003	79.003	91.657	91.657	91.657	200.734
date (YYYYmmdd)	20211112	20211112	20211112	20211112	20211112	20211112	20211112	20211112	20211112	20211112	20211112	20211112	20211112
time (hhMM)	1700	1700	1700	1700	1700	1700	1700	1700	1700	1700	1700	1700	1700
amMP	NaN	NaN	NaN	3.4	8.2	NaN	NaN	NaN	8.7	3.8	26.1	5.2	13.2
arginine	NaN	NaN	NaN	NaN	NaN	NaN	19.2	19.0	12.5	29.2	31.6	55.3	NaN
asparagine	NaN	NaN	NaN	2.7	2.2	3.2	9.7	13.7	9.1	22.9	11.1	16.1	NaN
aspartate	NaN	NaN	NaN	26.3	NaN	14.3	NaN	NaN	NaN	NaN	NaN	42.9	NaN
chitobiose	NaN	NaN	NaN	NaN	NaN	NaN	NaN	NaN	NaN	NaN	NaN	NaN	NaN
chitotriose	NaN	NaN	NaN	NaN	NaN	NaN	NaN	NaN	NaN	NaN	NaN	NaN	NaN
ciliatine	NaN	NaN	NaN	NaN	NaN	2.4	6.3	5.0	5.1	12.8	4.8	9.9	NaN
citrulline	NaN	NaN	NaN	NaN	NaN	NaN	NaN	NaN	NaN	NaN	NaN	NaN	NaN
cysteate	NaN	NaN	NaN	8.8	NaN	10.4	6.5	6.6	NaN	NaN	NaN	15.9	NaN
cysteine	19.3	14.7	6.0	19.8	24.3	14.2	22.9	33.6	27.5	19.3	27.8	59.3	7.0
cystine	NaN	NaN	NaN	NaN	NaN	NaN	NaN	NaN	NaN	NaN	NaN	NaN	NaN
cytidine	NaN	23.4	NaN	NaN	NaN	NaN	77.2	NaN	NaN	NaN	NaN	20.6	50.4
ectoine	NaN	NaN	NaN	25.9	NaN	NaN	NaN	69.9	79.7	NaN	NaN	69.6	NaN
glucosamine-6-phosphate	NaN	NaN	NaN	NaN	NaN	NaN	NaN	NaN	NaN	NaN	NaN	NaN	NaN
glucose 6-phosphate	NaN	NaN	NaN	NaN	11.6	NaN	12.3	NaN	NaN	22.1	18.4	15.3	NaN
glutamic acid	29.1	33.1	47.1	62.4	37.7	70.5	49.5	44.9	53.8	196.9	60.3	135.8	NaN
glutamine	19.9	21.1	22.8	17.9	18.3	18.2	32.4	28.9	26.8	60.9	34.7	42.0	NaN
glutathione	NaN	NaN	NaN	NaN	NaN	NaN	8.2	NaN	10.1	15.3	NaN	14.6	NaN

name	AE2123_BC152_C8N2	AE2123_BC153_C8N2	AE2123_BC154_C8N2	AE2123_BC155_C8N6	AE2123_BC156_C8N6	AE2123_BC157_C8N6	AE2123_BC158_C8N9	AE2123_BC159_C8N9	AE2123_BC160_C8N9	AE2123_BC161_C8N11	AE2123_BC162_C8N11	AE2123_BC163_C8N11	AE2123_BC164_C8N16
cast	8	8	8	8	8	8	8	8	8	8	8	8	8
niskin	2	2	2	6	6	6	9	9	9	11	11	11	16
depth (m)	4.546	4.546	4.546	40.595	40.595	40.595	79.003	79.003	79.003	91.657	91.657	91.657	200.734
date (YYYYmmdd)	20211112	20211112	20211112	20211112	20211112	20211112	20211112	20211112	20211112	20211112	20211112	20211112	20211112
time (hhMM)	1700	1700	1700	1700	1700	1700	1700	1700	1700	1700	1700	1700	1700
glycine	NaN	NaN	NaN	63.6	NaN	67.0	32.7	32.3	17.1	47.0	45.9	142.9	NaN
guanosine	NaN	NaN	NaN	NaN	NaN	NaN	8.5	NaN	NaN	NaN	NaN	NaN	NaN
histidine	NaN	NaN	NaN	NaN	NaN	NaN	3.6	4.9	NaN	36.9	29.2	15.5	201.1
homoserine	6.1	6.5	6.2	5.7	4.6	4.6	11.1	10.6	10.0	19.9	7.9	9.1	5.6
homoserine betaine	82.8	77.8	114.9	91.2	100.8	89.8	84.4	69.1	88.3	120.0	64.3	59.4	NaN
isethionate	46.9	46.9	44.4	39.4	50.3	39.4	33.3	34.7	29.6	29.6	16.0	15.4	7.0
isoleucine	NaN	NaN	NaN	NaN	NaN	NaN	NaN	NaN	NaN	12.1	NaN	14.5	NaN
kynurenine	NaN	NaN	NaN	NaN	NaN	3.5	3.9	3.5	4.2	10.0	NaN	5.2	NaN
leucine	NaN	NaN	NaN	NaN	NaN	NaN	NaN	NaN	NaN	10.9	NaN	9.2	NaN
malic acid	111.7	108.9	67.2	126.0	70.8	98.1	31.8	27.1	26.1	34.2	NaN	34.8	NaN
methionine	NaN	NaN	NaN	NaN	NaN	NaN	NaN	NaN	NaN	NaN	NaN	NaN	NaN
muramic acid	NaN	NaN	13.6	NaN	NaN	NaN	NaN	NaN	NaN	NaN	NaN	NaN	NaN
pantothenic acid	NaN	NaN	3.5	3.7	NaN	3.5	NaN	2.5	NaN	NaN	NaN	NaN	NaN
phenylalanine	7.3	8.2	8.0	6.2	7.8	6.9	8.1	8.3	8.7	17.6	14.3	19.3	7.0
proline	NaN	NaN	NaN	NaN	NaN	NaN	NaN	NaN	NaN	NaN	NaN	NaN	NaN
putrescine	18.5	NaN	NaN	NaN	18.3	22.0	47.2	33.3	23.6	78.3	34.6	67.2	NaN
sarcosine	8.4	12.2	11.3	6.9	10.2	6.0	9.7	9.2	11.8	13.8	8.7	6.3	NaN
serine	NaN	NaN	NaN	NaN	NaN	NaN	NaN	NaN	NaN	23.0	22.4	39.6	NaN

name	AE2123_BC152_C8N2	AE2123_BC153_C8N2	AE2123_BC154_C8N2	AE2123_BC155_C8N6	AE2123_BC156_C8N6	AE2123_BC157_C8N6	AE2123_BC158_C8N9	AE2123_BC159_C8N9	AE2123_BC160_C8N9	AE2123_BC161_C8N11	AE2123_BC162_C8N11	AE2123_BC163_C8N11	AE2123_BC164_C8N16
cast	8	8	8	8	8	8	8	8	8	8	8	8	8
niskin	2	2	2	6	6	6	9	9	9	11	11	11	16
depth (m)	4.546	4.546	4.546	40.595	40.595	40.595	79.003	79.003	79.003	91.657	91.657	91.657	200.734
date (YYYYmmdd)	20211112	20211112	20211112	20211112	20211112	20211112	20211112	20211112	20211112	20211112	20211112	20211112	20211112
time (hhMM)	1700	1700	1700	1700	1700	1700	1700	1700	1700	1700	1700	1700	1700
glycerol 3-phosphate	35.7	36.9	37.8	28.4	33.9	33.7	69.4	68.9	69.0	51.9	45.8	66.2	16.1
spermidine	NaN	NaN	NaN	NaN	NaN	NaN	NaN	NaN	NaN	NaN	NaN	NaN	NaN
taurine	46.1	66.0	75.1	93.0	60.6	103.9	140.5	138.4	114.4	131.1	119.3	163.4	NaN
thiamine monophosphate	NaN	NaN	NaN	NaN	NaN	NaN	NaN	NaN	NaN	NaN	NaN	NaN	NaN
threonine	7.7	10.8	12.8	NaN	14.7	NaN	6.9	9.7	8.4	37.7	18.7	34.3	NaN
thymidine	24.3	30.8	NaN	30.4	43.7	34.4	NaN	31.1	NaN	29.0	NaN	NaN	NaN
tryptamine	NaN	NaN	NaN	28.3	NaN	NaN	NaN	NaN	NaN	NaN	NaN	NaN	NaN
tryptophan	5.7	6.2	6.1	7.5	6.1	8.1	8.1	7.3	6.5	11.9	9.6	10.6	4.1
tyrosine	NaN	NaN	NaN	NaN	NaN	NaN	NaN	NaN	NaN	NaN	28.4	13.5	NaN
uridine	10.6	8.7	8.8	9.6	9.1	8.4	6.1	7.3	5.9	12.8	8.3	9.6	NaN
valine	NaN	NaN	NaN	NaN	NaN	NaN	NaN	NaN	NaN	7.0	NaN	6.6	NaN
xanthosine	NaN	NaN	NaN	NaN	NaN	NaN	NaN	NaN	NaN	NaN	NaN	NaN	NaN

name	AE2123_BC165_C8N16	AE2123_BC166_C8N16	AE2123_BC167_C9N2	AE2123_BC168_C9N2	AE2123_BC169_C9N2	AE2123_BC170_C9N6	AE2123_BC171_C9N6	AE2123_BC172_C9N6	AE2123_BC173_C9N9	AE2123_BC174_C9N9	AE2123_BC175_C9N9	AE2123_BC176_C9N11	AE2123_BC177_C9N11
cast	8	8	9	9	9	9	9	9	9	9	9	9	9
niskin	16	16	2	2	2	6	6	6	9	9	9	11	11
depth (m)	200.734	200.734	5.284	5.284	5.284	39.767	39.767	39.767	79.498	79.498	79.498	95.223	95.223
date (YYYYmmdd)	20211112	20211112	20211112	20211112	20211112	20211112	20211112	20211112	20211112	20211112	20211112	20211112	20211112
time (hhMM)	1700	1700	2203	2203	2203	2203	2203	2203	2203	2203	2203	2203	2203
2'deoxycitidine	NaN	NaN	NaN	NaN	NaN	NaN	NaN	NaN	NaN	NaN	NaN	NaN	NaN
2'deoxyguanosine	NaN	2.3	NaN	2.3	2.4	NaN	2.3	NaN	2.3	2.4	2.4	NaN	NaN
2'deoxyuridine	8.3	19.4	20.4	42.5	55.7	NaN	NaN	25.0	34.0	44.3	55.2	NaN	NaN
adenosine 3'-monophosphate	NaN	NaN	NaN	NaN	NaN	NaN	NaN	NaN	NaN	NaN	NaN	NaN	NaN
4-aminobenzoic acid	NaN	NaN	NaN	NaN	NaN	NaN	NaN	NaN	NaN	NaN	NaN	NaN	NaN
uridine 5'-monophosphate	NaN	NaN	NaN	NaN	NaN	NaN	NaN	NaN	NaN	12.5	NaN	NaN	NaN
adenosine 5'-monophosphate	NaN	NaN	NaN	NaN	NaN	120.9	18.7	NaN	NaN	20.2	NaN	11.5	NaN
inosine 5'-monophosphate	NaN	NaN	NaN	NaN	NaN	NaN	NaN	NaN	NaN	NaN	NaN	NaN	NaN
5'deoxyadenosine	NaN	NaN	NaN	35.5	NaN	42.1	NaN	NaN	NaN	NaN	NaN	NaN	NaN
2,3-dihydroxypropane-1-sulfonate	NaN	NaN	36.7	56.8	47.5	29.5	52.5	66.3	67.2	175.4	79.0	40.7	51.7
gamma-aminobutyric acid	NaN	NaN	NaN	NaN	NaN	NaN	NaN	NaN	NaN	NaN	NaN	NaN	NaN
HET	NaN	NaN	NaN	NaN	NaN	NaN	NaN	NaN	NaN	NaN	NaN	NaN	NaN
HMP	276.9	NaN	NaN	255.7	88.9	46.2	NaN	137.8	89.5	62.7	50.5	NaN	NaN
N-acetyl-muramic acid	NaN	NaN	27.3	NaN	NaN	NaN	NaN	12.3	NaN	NaN	NaN	10.1	NaN
adenine	NaN	NaN	NaN	NaN	NaN	NaN	NaN	NaN	NaN	NaN	NaN	NaN	NaN
adenosine	NaN	2.3	NaN	2.4	2.5	NaN	2.3	NaN	2.4	2.3	2.4	NaN	NaN
alanine	NaN	110.3	29.6	34.4	27.0	NaN	28.5	30.2	17.7	13.6	50.1	40.6	37.3

name	AE2123_BC165_C8N16	AE2123_BC166_C8N16	AE2123_BC167_C9N2	AE2123_BC168_C9N2	AE2123_BC169_C9N2	AE2123_BC170_C9N6	AE2123_BC171_C9N6	AE2123_BC172_C9N6	AE2123_BC173_C9N9	AE2123_BC174_C9N9	AE2123_BC175_C9N9	AE2123_BC176_C9N11	AE2123_BC177_C9N11
cast	8	8	9	9	9	9	9	9	9	9	9	9	9
niskin	16	16	2	2	2	6	6	6	9	9	9	11	11
depth (m)	200.734	200.734	5.284	5.284	5.284	39.767	39.767	39.767	79.498	79.498	79.498	95.223	95.223
date (YYYYmmdd)	20211112	20211112	20211112	20211112	20211112	20211112	20211112	20211112	20211112	20211112	20211112	20211112	20211112
time (hhMM)	1700	1700	2203	2203	2203	2203	2203	2203	2203	2203	2203	2203	2203
amMP	6.9	4.3	26.7	NaN	NaN	9.0	29.8	23.1	4.6	5.7	NaN	NaN	12.9
arginine	NaN	92.8	NaN	9.9	NaN	NaN	9.8	NaN	NaN	21.9	5.2	6.4	37.1
asparagine	NaN	NaN	3.7	2.5	NaN	NaN	8.1	4.4	3.2	28.2	7.1	5.8	5.6
aspartate	NaN	70.6	NaN	NaN	NaN	10.8	24.7	NaN	NaN	72.2	NaN	10.8	NaN
chitobiose	NaN	NaN	NaN	NaN	NaN	NaN	NaN	NaN	NaN	NaN	NaN	NaN	NaN
chitotriose	NaN	NaN	NaN	NaN	NaN	NaN	NaN	NaN	NaN	NaN	NaN	NaN	NaN
ciliatine	NaN	NaN	NaN	NaN	NaN	2.7	NaN	NaN	2.7	4.5	4.2	5.8	4.5
citrulline	NaN	100.5	NaN	NaN	NaN	NaN	9.4	NaN	NaN	NaN	NaN	NaN	NaN
cysteate	NaN	NaN	NaN	8.1	NaN	7.4	10.2	NaN	NaN	13.6	NaN	11.0	NaN
cysteine	NaN	NaN	9.2	14.8	6.7	35.4	6.9	20.0	22.0	55.3	22.2	22.2	25.9
cystine	NaN	NaN	NaN	NaN	NaN	NaN	NaN	NaN	NaN	NaN	NaN	NaN	NaN
cytidine	32.9	NaN	19.5	81.3	NaN	NaN	NaN	NaN	NaN	50.1	42.7	NaN	NaN
ectoine	NaN	20.1	NaN	NaN	NaN	NaN	NaN	NaN	NaN	38.1	NaN	NaN	NaN
glucosamine-6-phosphate	NaN	NaN	NaN	NaN	NaN	NaN	NaN	NaN	NaN	NaN	NaN	NaN	NaN
glucose 6-phosphate	NaN	NaN	10.3	NaN	NaN	NaN	NaN	NaN	11.2	24.2	NaN	NaN	NaN
glutamic acid	NaN	33.2	58.6	30.4	19.6	59.8	204.7	55.8	36.4	415.6	58.3	35.1	32.8
glutamine	NaN	NaN	12.1	10.2	12.7	12.5	46.7	30.3	14.2	84.5	28.4	26.3	22.2
glutathione	NaN	NaN	9.2	NaN	NaN	NaN	NaN	NaN	NaN	38.3	NaN	NaN	8.4

name	AE2123_BC165_C8N16	AE2123_BC166_C8N16	AE2123_BC167_C9N2	AE2123_BC168_C9N2	AE2123_BC169_C9N2	AE2123_BC170_C9N6	AE2123_BC171_C9N6	AE2123_BC172_C9N6	AE2123_BC173_C9N9	AE2123_BC174_C9N9	AE2123_BC175_C9N9	AE2123_BC176_C9N11	AE2123_BC177_C9N11
cast	8	8	9	9	9	9	9	9	9	9	9	9	9
niskin	16	16	2	2	2	6	6	6	9	9	9	11	11
depth (m)	200.734	200.734	5.284	5.284	5.284	39.767	39.767	39.767	79.498	79.498	79.498	95.223	95.223
date (YYYYmmdd)	20211112	20211112	20211112	20211112	20211112	20211112	20211112	20211112	20211112	20211112	20211112	20211112	20211112
time (hhMM)	1700	1700	2203	2203	2203	2203	2203	2203	2203	2203	2203	2203	2203
glycine	NaN	12.7	7.7	NaN	NaN	142.7	50.9	NaN	10.5	77.7	60.3	62.8	52.0
guanosine	NaN	NaN	NaN	NaN	NaN	NaN	NaN	NaN	NaN	NaN	NaN	NaN	NaN
histidine	NaN	NaN	20.7	NaN	8.0	NaN	32.6	5.0	NaN	NaN	4.8	12.3	11.8
homoserine	4.3	4.5	6.3	4.7	5.7	5.4	7.1	6.4	5.5	10.5	5.9	7.7	7.5
homoserine betaine	NaN	NaN	62.5	71.0	74.6	73.5	133.8	118.0	49.8	206.8	81.8	42.2	51.6
isethionate	4.5	5.2	56.1	43.6	45.4	31.7	65.0	47.7	23.4	37.6	23.9	18.6	21.4
isoleucine	NaN	2.7	NaN	NaN	NaN	NaN	NaN	NaN	NaN	NaN	NaN	NaN	NaN
kynurenine	NaN	NaN	NaN	3.7	3.6	NaN	NaN	3.1	NaN	4.0	8.8	4.4	NaN
leucine	NaN	7.8	NaN	NaN	NaN	NaN	NaN	NaN	NaN	NaN	NaN	NaN	NaN
malic acid	NaN	33.4	125.0	94.5	46.0	72.3	150.4	33.8	NaN	31.8	NaN	NaN	36.3
methionine	NaN	NaN	NaN	NaN	NaN	NaN	NaN	NaN	NaN	NaN	NaN	NaN	NaN
muramic acid	NaN	NaN	NaN	NaN	9.1	NaN	NaN	NaN	5.9	9.5	5.8	NaN	NaN
pantothenic acid	NaN	NaN	NaN	NaN	NaN	2.6	NaN	NaN	NaN	2.7	NaN	NaN	NaN
phenylalanine	6.0	20.0	10.1	10.7	13.0	6.9	15.7	12.0	8.4	10.0	12.0	12.4	10.4
proline	NaN	NaN	NaN	NaN	NaN	NaN	NaN	NaN	NaN	NaN	NaN	NaN	NaN
putrescine	NaN	197.0	49.4	39.8	18.4	NaN	NaN	25.8	NaN	28.7	41.3	39.9	135.8
sarcosine	NaN	NaN	13.1	8.4	10.4	8.9	8.0	7.5	5.0	4.1	9.0	5.9	7.8
serine	NaN	155.6	10.5	32.9	NaN	NaN	40.0	21.9	NaN	NaN	39.5	37.8	35.0

name	AE2123_BC165_C8N16	AE2123_BC166_C8N16	AE2123_BC167_C9N2	AE2123_BC168_C9N2	AE2123_BC169_C9N2	AE2123_BC170_C9N6	AE2123_BC171_C9N6	AE2123_BC172_C9N6	AE2123_BC173_C9N9	AE2123_BC174_C9N9	AE2123_BC175_C9N9	AE2123_BC176_C9N11	AE2123_BC177_C9N11
cast	8	8	9	9	9	9	9	9	9	9	9	9	9
niskin	16	16	2	2	2	6	6	6	9	9	9	11	11
depth (m)	200.734	200.734	5.284	5.284	5.284	39.767	39.767	39.767	79.498	79.498	79.498	95.223	95.223
date (YYYYmmdd)	20211112	20211112	20211112	20211112	20211112	20211112	20211112	20211112	20211112	20211112	20211112	20211112	20211112
time (hhMM)	1700	1700	2203	2203	2203	2203	2203	2203	2203	2203	2203	2203	2203
glycerol 3-phosphate	9.4	15.6	15.2	31.3	30.3	37.2	32.6	34.3	35.5	43.1	54.4	56.6	73.6
spermidine	NaN	NaN	NaN	NaN	NaN	NaN	NaN	NaN	NaN	NaN	NaN	NaN	NaN
taurine	NaN	NaN	65.1	60.4	62.1	68.1	52.1	69.3	41.8	130.9	66.7	127.7	166.0
thiamine monophosphate	NaN	NaN	NaN	NaN	NaN	NaN	NaN	NaN	NaN	NaN	NaN	NaN	NaN
threonine	3.6	71.2	28.4	15.7	11.9	4.5	40.2	22.0	12.1	4.6	19.5	28.7	15.3
thymidine	NaN	NaN	NaN	NaN	NaN	NaN	NaN	NaN	NaN	30.6	26.5	32.0	NaN
tryptamine	NaN	NaN	NaN	NaN	23.5	NaN	NaN	NaN	NaN	NaN	NaN	NaN	NaN
tryptophan	NaN	3.8	8.5	6.9	7.0	5.5	9.7	7.4	6.1	6.1	12.9	6.3	6.8
tyrosine	NaN	28.4	NaN	NaN	77.8	17.8	138.4	62.4	NaN	29.2	44.7	NaN	22.3
uridine	NaN	7.4	11.5	9.9	8.2	NaN	9.5	9.1	8.9	9.6	8.0	8.7	9.9
valine	NaN	15.2	NaN	NaN	NaN	NaN	NaN	NaN	NaN	NaN	NaN	NaN	NaN
xanthosine	NaN	NaN	NaN	NaN	NaN	NaN	NaN	NaN	NaN	NaN	NaN	NaN	NaN

name	AE2123_BC178_C9N11	AE2123_BC179_C9N16	AE2123_BC180_C9N16	AE2123_BC181_C9N16	AE2123_BC182_C9N22	AE2123_BC183_C9N22	AE2123_BC184_C9N22
cast	9	9	9	9	9	9	9
niskin	11	16	16	16	22	22	22
depth (m)	95.223	200.306	200.306	200.306	1999.66	1999.66	1999.66
date (YYYYmmdd)	20211112	20211112	20211112	20211112	20211112	20211112	20211112
time (hhMM)	2203	2203	2203	2203	2203	2203	2203
2'deoxycitidine	NaN	NaN	NaN	NaN	NaN	NaN	NaN
2'deoxyguanosine	NaN	2.4	2.3	NaN	2.3	NaN	NaN
2'deoxyuridine	13.6	23.4	11.3	12.5	NaN	NaN	NaN
adenosine 3'-monophosphate	NaN	NaN	NaN	NaN	NaN	13.3	NaN
4-aminobenzoic acid	NaN	NaN	NaN	NaN	NaN	56.8	NaN
uridine 5'-monophosphate	NaN	NaN	NaN	NaN	NaN	9.9	NaN
adenosine 5'-monophosphate	NaN	NaN	NaN	NaN	NaN	33.1	NaN
inosine 5'-monophosphate	NaN	NaN	NaN	NaN	NaN	61.9	NaN
5'deoxyadenosine	61.6	NaN	NaN	NaN	31.8	NaN	NaN
2,3-dihydroxypropane-1-sulfonate	42.6	NaN	NaN	NaN	NaN	NaN	NaN
gamma-aminobutyric acid	NaN	NaN	NaN	NaN	NaN	37.7	NaN
HET	NaN	NaN	NaN	NaN	NaN	NaN	NaN
HMP	NaN	NaN	NaN	NaN	NaN	NaN	72.1
N-acetyl-muramic acid	NaN	NaN	NaN	NaN	NaN	NaN	NaN
adenine	NaN	NaN	NaN	NaN	NaN	NaN	NaN
adenosine	NaN	2.5	2.3	NaN	2.3	2.3	NaN
alanine	31.1	19.5	31.1	9.0	17.8	303.3	20.7
amMP	NaN	13.7	NaN	6.8	19.8	8.4	11.2
arginine	20.9	NaN	NaN	NaN	NaN	73.5	NaN

name	AE2123_BC178_C9N11	AE2123_BC179_C9N16	AE2123_BC180_C9N16	AE2123_BC181_C9N16	AE2123_BC182_C9N22	AE2123_BC183_C9N22	AE2123_BC184_C9N22
cast	9	9	9	9	9	9	9
niskin	11	16	16	16	22	22	22
depth (m)	95.223	200.306	200.306	200.306	1999.66	1999.66	1999.66
date (YYYYmmdd)	20211112	20211112	20211112	20211112	20211112	20211112	20211112
asparagine	5.1	NaN	NaN	2.6	NaN	45.1	NaN
aspartate	NaN	NaN	NaN	34.6	NaN	59.8	NaN
chitobiose	NaN	NaN	NaN	NaN	NaN	NaN	NaN
chitotriose	NaN	NaN	NaN	NaN	NaN	NaN	NaN
ciliatine	3.2	NaN	NaN	NaN	NaN	NaN	NaN
citrulline	NaN	NaN	19.9	NaN	NaN	185.9	NaN
cysteate	NaN	NaN	NaN	NaN	NaN	NaN	NaN
cysteine	34.4	6.4	8.6	5.8	NaN	20.1	NaN
cystine	NaN	NaN	NaN	NaN	NaN	NaN	NaN
cytidine	NaN	NaN	NaN	NaN	NaN	13.2	37.6
ectoine	NaN	NaN	NaN	NaN	NaN	92.9	NaN
glucosamine-6-phosphate	NaN	NaN	NaN	NaN	NaN	NaN	NaN
glucose 6-phosphate	NaN	NaN	NaN	NaN	NaN	NaN	NaN
glutamic acid	15.4	NaN	NaN	NaN	NaN	90.0	NaN
glutamine	20.0	2.1	1.9	3.4	4.4	63.4	NaN
glutathione	NaN	NaN	NaN	NaN	NaN	NaN	NaN
glycine	73.4	NaN	NaN	80.9	NaN	168.6	NaN
guanosine	NaN	NaN	NaN	NaN	NaN	14.3	NaN
histidine	9.6	12.0	36.1	15.0	12.2	195.5	15.9
homoserine	4.8	4.7	5.4	4.8	4.7	4.6	4.8

name	AE2123_BC178_C9N11	AE2123_BC179_C9N16	AE2123_BC180_C9N16	AE2123_BC181_C9N16	AE2123_BC182_C9N22	AE2123_BC183_C9N22	AE2123_BC184_C9N22
cast	9	9	9	9	9	9	9
niskin	11	16	16	16	22	22	22
depth (m)	95.223	200.306	200.306	200.306	1999.66	1999.66	1999.66
date (YYYYmmdd)	20211112	20211112	20211112	20211112	20211112	20211112	20211112
homoserine betaine	53.2	NaN	NaN	NaN	NaN	NaN	NaN
isethionate	16.7	5.5	5.3	NaN	NaN	6.3	NaN
isoleucine	NaN	NaN	NaN	NaN	NaN	39.0	NaN
kynurenine	NaN	NaN	NaN	NaN	NaN	5.9	NaN
leucine	NaN	NaN	NaN	NaN	NaN	32.3	NaN
malic acid	NaN	NaN	NaN	NaN	22.4	24.7	NaN
methionine	NaN	NaN	NaN	NaN	NaN	NaN	NaN
muramic acid	7.1	5.9	NaN	NaN	NaN	11.9	NaN
pantothenic acid	NaN	NaN	NaN	NaN	NaN	3.4	NaN
phenylalanine	9.8	8.1	10.0	7.6	8.9	46.2	8.4
proline	NaN	NaN	NaN	NaN	NaN	20.7	NaN
putrescine	48.3	NaN	25.7	NaN	NaN	193.9	NaN
sarcosine	7.1	NaN	NaN	NaN	NaN	NaN	4.3
serine	9.9	15.1	40.4	33.7	11.3	440.6	16.4
glycerol 3-phosphate	64.2	12.8	8.0	28.4	11.2	53.4	NaN
spermidine	NaN	NaN	NaN	NaN	NaN	NaN	NaN
taurine	171.4	NaN	NaN	15.0	NaN	59.8	NaN
thiamine monophosphate	NaN	NaN	NaN	9.7	NaN	NaN	NaN
threonine	12.7	8.5	23.0	6.9	10.9	161.5	4.7
thymidine	26.8	NaN	NaN	NaN	NaN	NaN	NaN

name	AE2123_BC178_C9N11	AE2123_BC179_C9N16	AE2123_BC180_C9N16	AE2123_BC181_C9N16	AE2123_BC182_C9N22	AE2123_BC183_C9N22	AE2123_BC184_C9N22
cast	9	9	9	9	9	9	9
niskin	11	16	16	16	22	22	22
depth (m)	95.223	200.306	200.306	200.306	1999.66	1999.66	1999.66
date (YYYYmmdd)	20211112	20211112	20211112	20211112	20211112	20211112	20211112
tryptamine	NaN	NaN	NaN	NaN	NaN	NaN	NaN
tryptophan	6.4	4.9	4.8	5.3	4.7	14.4	NaN
tyrosine	35.8	NaN	NaN	NaN	57.0	51.1	32.5
uridine	7.7	4.7	NaN	10.1	NaN	18.2	NaN
valine	NaN	NaN	NaN	NaN	NaN	59.3	NaN
xanthosine	NaN	NaN	NaN	NaN	NaN	NaN	NaN

4.6.2 Variance in Mixing and Timescales

Supplemental Figure 4-1 is a histogram plot of the logarithm of estimated K_z values in the mixed layer, fitted with a normal distribution. I have included it to show that the values even within this top layer varied greatly over this depth and over the cruise.

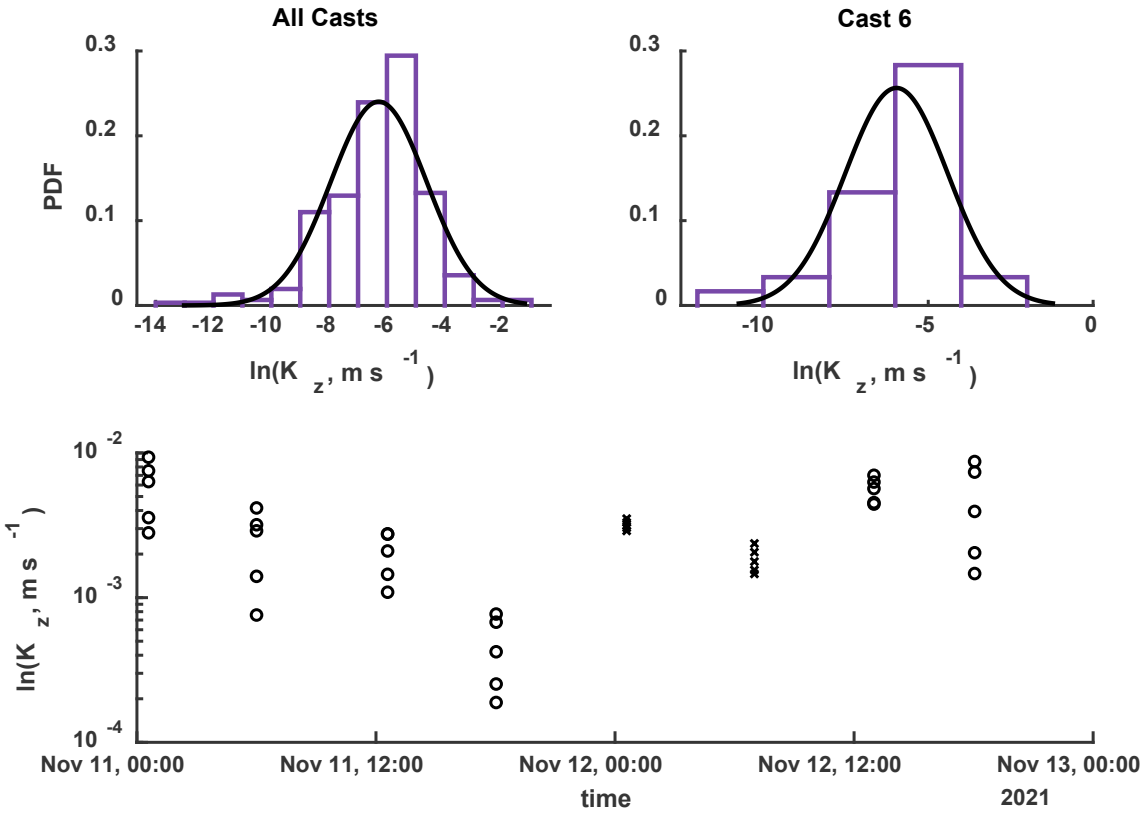

Supplemental Figure 4-1: Distributions of estimated ln(K_z) values. Clockwise from top left: all estimates within the mixed layer (bars) fitted with a normal distribution (black line); estimates within the mixed layer for cast 6; and all estimates between 20 and 30 m depth plotted against the cast time (local).

Spatial variability was high—the K_z values for Cast 6 are on the right in Supplemental Figure 4-1 and show the same type of distribution. Additionally, the bottom panel shows K_z values from 20-30 m depth from each cast to showcase the order-of-magnitude variability in this depth range over the course of the cruise.

One important detail is that the values I used to showcase metabolite mixing (Figure 4-5) were interpolated between Cast 6 and Cast 7 at 25 m. These are marked with “x” and are the two points with the lowest variability, both within and between casts, where interpolation was most justified.

Most importantly, though, is that estimating a characteristic mixing time for this layer has limited practical value. Using distributional parameters for the fitted lognormals of each cast, the mixing time-scale is $t\ \alpha\ z_{ML}^2/\mu_k$ and the uncertainty is $\sigma_t = t \cdot \sigma_k/\mu_k$ (where z_{ML} is the mixed-layer depth, and μ_k and σ_k are the expected value and variance for K_z) ranges from 57 ± 5.4 h in Cast 8 to 3400 ± 3.1 h (about 140 d) in Cast 5. Local mixing times can much higher both due to the spatial scale (5-20 m) and the effects of fluctuations in K_z. For example, a K_z of 5.4 x 10^{-3} m^2 s^{-1} (75^{th} percentile of mixed layer values) operating on a transient metabolite input peak spanning 10 m has a characteristic mixing time of 5.1 h.

4.6.3 Mixing Time Scales, Photochemistry, and Deposition

Given the prevalence of transient rapid mixing and the long half-lives of the photochemistry evaluated in section 4.3.6, the assumption of mixed-layer homogeneity with respect to tryptophan and kynurenine photochemistry seems to stand. In the discursion about aerosol deposition, however, I implied replenishment time-scales from <1 d to about 18 d. If this process is a significant source of small organic compounds such as malate or DHPS, and especially if it is affected by precipitation (wet deposition), then measurable near-surface maxima could be created faster than mixing would erase them. Photochemistry merits a more specific investigation into near-surface processes,

though the intricacies of the surface microlayer—or even a detailed accounting of the near-surface metabolite behaviors—were not the target of this sampling campaign.[218]

Chapter 5: Conclusion

This entire thesis was a step into a set of unknowns, a set of potential sources and sinks of specific chemicals which are daunting in their multiplicity and scale. I considered three processes of many, as introduced in Chapter 1: (mostly) direct photolysis (Chapters 2, 4), zooplankton excretion (Chapters 3, 4), and mixing (Chapter 4). These three factors represent a triune paradigm of chemistry, biology, and physics for dissolved metabolites, but they are by no means complete assessments. It is entirely possible that there is something I completely missed in Chapter 1; after all, the mixing and excretion investigations only ended up as considerations after talking about the field data (Chapter 4) with Ruth Curry (ASU-BIOS) and Amy Maas (ASU-BIOS), and they ended up being far more revelatory in interpreting the field data than did photochemistry.

What started as a purely chemistry-based thesis expanded into something from which I hope the reader can take several different themes. One of them is potentially the oldest theme of chemical oceanography: What is in seawater? I presented brand-new measurements of several compounds in seawater in Chapter 4, and at a locality (November, Hydrostation S) for which no published data using this method exist. Seeing the patterns in this data and in particular the anomaly of the “115 m pulse” of Cast 6, I needed a framework to interpret the data and doubted the sufficiency of correlative relationships and general patterns.

A corollary theme to the first: Why are the constituents of ocean water at the concentrations they are? In Chapters 2 and 3, I examined this question with respect to two processes that both (1) operate differently from each other and (1) depend on the

compound, then applied the results about which I was reasonably confident to the field data of Chapter 4 to evaluate their influence. In no way can this claim the sort of global applicability of, say, Mackenzie and Garrels (1966): metabolites are generally *not* at steady-state, nor are they conservative.[234] They are a set of math problems, which I mean in both the literal and figurative senses. The variables of "what form does the metabolite take" (ionic state, complexation, partitioning) and "what inputs and outputs affect the metabolite" (microbial efflux and uptake, excretion by animals, direct photolytic consumption or production, hydrolysis, reaction with secondary oxidants, mixing) are mostly unknown because each of them is thousands of questions asked simultaneously.[3] While some of these can be examined cursorily through calculations (see depositional processes in Section 4.8; complexation of amino acids in Chapter 1), examining each process using field-relevant concentrations, organic matter compositions, and ionic strengths/acidities yield more applicable results for the marine environment. The benefit of constraining variables that are not subject to microbial metabolism is that once they are known, they might be accounted for, at which point we can apply the microbial network models atop all other forcings, most of which are, basically, chemistry.

That chemistry leads to the potentially contentious theme, simply, "metabolites are chemicals, too." This seems obvious but engaging with it is—to put it mildly—inconvenient. The microbial loop is a much simpler concept if one draws arrows from one cell to the next and ignores the implication that anything other than molecular diffusion happens in the dissolved phase.[27,235] The chemistry of DOM is much simpler if evaluated from the top down by regarding it in terms of *n* classes of labile, semilabile, or

refractory carbon with some C:N:P:S ratio.[4,15,236] These bulk-scale and cell-centric approaches are essential and can give a reasonable approximation of an ecosystem for modeling purposes, but they are fundamentally incapable of comprehending it—not a categorically fatal flaw in such models, as they do capture processes on large scales quite well. However, if we are to ask specific questions about evolution, about unannotated genes, about auxotrophy, and about how DOM changes over time to become less (or more) labile to the ecosystem, it would help to know more about the chemistry beyond what is present. In Chapter 1, these were outlined in detail with some largely theoretical considerations, but the ability to evaluate each at field-relevant salinity, pH, and most importantly, concentration, is now within reach. Given what the last decades of research have gleaned about the structural complexity of labile dissolved organic matter[94,202,213,222,235,237] and the molecular specificity of interactions between microbial species, a molecule-specific DOM paradigm is more than justified.

The capability to do this sort of chemical-by-chemical inventory is still in its infancy; the perceptive reader will note that the method I used to quantify picomolar concentrations of metabolites (with replicate samples, even) was published after I began my graduate research.[17] The utility of the new method goes beyond simply having an idea of knowing, for example, the concentration of dissolved putrescine in the mixed layer. It enables experiments to be run at ambient concentrations or lower volume, which may produce different results than less-sensitive methods. For example, the biomass-normalized excretion rate of individual animo acids for a single zooplankter is lower than an incubation containing many zooplankton of the same species, which is also lower than a consortium of species.[74,197] Acrylate (a byproduct of the osmolyte

DHPS' degradation), may not photolyze below a threshold of 100 nM.[106] The rest of this conclusion chapter is dedicated to setting some parameters for the future, of how metabolites can be treated as chemicals to the benefit of the analysis of ecosystems. These were borne of the decisions that had to be made in the other chapters. The project that I have outlined is hubristic, but there are plenty of decisions to be made about what parts of it are worth tackling—and how.

5.1 The Perils of Conventional Metabolomics: Gradients, Patchiness, and Variance

Chapter 4 contained some discursions about sampling resolution and about gradients with respect to mixing. These came after years of looking at the data in a way its resolution didn't justify; that is, interpolated across time and space as is often done with oceanographic data. The algorithm I used for mixing forces a choice of gradient shape because the sampling intervals of usually >20 m simply did not match the scales on which K_z and other variables operated (K_z was estimated from CTD data at intervals of 1.98 m). Even zooplankton typically migrate in acoustically-visible layers about 10 m thick, so detecting a gradient produced by their residence—and its subsequent disappearance—was a problem spatially and temporally.[238] Trying to interpolate the datasets produced by the casts of AE2123, including those taken by the CTD, using DIVA interpolation produced erroneous interpretations; for example, an appearance that the sun rose around noon (interpolated PAR). Six-hour cast spacing did not capture the diel cycle with the ergodicity required for interpreting periodic patterns, especially for metabolites, where in Chapter 4 we learned that many of their lifetimes might even be shorter than 6 h based on zooplankton production alone.

One thing that the zooplankton project (Chapters 3, 4) also revealed is just how important large and localized inputs might be. At the microscale, this is not new; the "phycosphere" has been a concept with an impressive body of evidence for years.[239,240] For the science of dissolved metabolites, it may be worth considering the existence of an extremely patchy landscape below the mixed layer. The evidence for the "pulse" we observed in Chapter 4 makes a convincing case that it was both real and due to the passage of zooplankton—and nothing like it has ever been observed in a dissolved metabolite sampling campaign. Zooplankton are patchy, potent, and sustain a holobiont including attached and internal microbes that affect their DOM exudations.[171] Based on our observations, microbes are efficient at cleaning up after them. Observing this process within the water column is functionally impossible because it depends not just on sampling the same depth repeatedly, it involves sampling a signal at a unique (x, y, z) coordinate whose metabolite signature is obliterated by the passage of the CTD rosette upon its initial sampling.[241] This is definitively an area of research where lab studies like Chapter 3 and their extrapolation to the water column need to be broadened and repeated and are at the core of this thesis for a reason. *In situ* observations are essential for knowing "what is there," but the "why" requires inferences from chemistry, biology, and physics *ex situ*.

With the introduction of replicate measurements comes variance. While previous dissolved metabolite measurements permitted mostly singleton measurements due to high volume requirements, we must now contend with replicate variation. While the timing of the samples from Chapter 4 (November) was phenologically distinct from most existing metabolite measurements at Bermuda, the metabolites shared by the more

traditional solid-phase extraction (SPE) method (see [16,111,242]) and the benzoyl chloride (BC) method were difficult to directly compare, as the SPE measurements were sparser—eliminating one replicate below the limit of detection (BC) still results in data, whereas eliminating the single sample at a given point in space (SPE) for the same reason eliminates the whole data point. For the places where data could be compared between the two, the SPE number was often higher, and this can be entirely explained by statistics.

Given a population of water samples in a Niskin bottle, if we take the liberty of assuming the actual concentrations vary somewhat, we assume they form a normal distribution $C \sim N(\mu, \sigma)$. Two limits of detection (L_{SPE}, L_{BC}) exist for the two methods, and μ lies close to both, but both $L > \mu$. The probability of making a measurement that is not discarded is $P(C) = 1 - CDF(L)$, where $CDF(L)$ is the cumulative distribution function evaluated at the respective limit. For multiple replicates, the probability of *at least one* valid replicate is $P(C) = 1 - \big(CDF(L)\big)^n$, where n is the number of replicates.

The BC method has two advantages here: generally lower limits of detection and replicates. For a metabolite with $\mu = 15\ pM$ and $\sigma = 10\ pM$, if we assume that $L_{SPE} = L_{BC} = 10\ pM$, both methods produce a valid replicate 69% of the time. With three replicates, that number becomes 97%. If $L_{SPE} > L_{BC}$, not only does this disparity grow, but the SPE method will tend to produce a higher proportion of its valid measurements at what the BC method would consider outliers (especially if $\mu < L_{SPE}$).

Of the metabolites measured in Chapter 4, 30 have published L_{SPE} values. Accounting for PPL extraction efficiency, nine of these L_{SPE} can be compared directly with L_{BC}, and in all but one case (tryptamine), $L_{SPE} > L_{BC}$ by a factor of 2 (guanosine) to

312 (tyrosine). Pantothenic acid had a mean mixed layer concentration of 2.9 ± 0.7 pM in November of 2021; each independent BC replicate had a 94% chance of observing this value with an L_{BC} of 1.78 pM. L_{SPE} is 80 pM, making any observations through the SPE method either observations of highly localized phenomena or extreme outliers. Kynurenine, a more comparable example, was 4.0 ± 1.5 pM, with 92% probability of a BC observation in one sample and a 2% probability of observation in 20 SPE samples.

If one method is substantially more likely to produce measurements at low concentrations and the other is likely to often produce a null or small value (like one-tenth L_{SPE}, as is often performed for statistical analysis of blank-rich data), comparing even means across a dataset must be done with a great deal of care.[220,243] I present this not as an indictment of the data that do exist but as an admonition about interpreting it. We might assume that the axes along which variance would appear are space (location, depth, climate) and time (seasonality, diel cycles), but the method and replication can make even concurrent datasets look like they disagree. Furthermore, many of the practices used for quality control in the metabolite field come from (understandably) a discipline focused on human metabolism, including the treatment of limits of detection and of nondetects.[244,245] Conventional metabolomics guidance may have practices that do not apply if we are interested interpreting a system of aquatic chemistry mechanistically (considering gradients and state variables) rather than only statistically or categorically (presence-absence, pairwise distance, etc.). Dissolved metabolites are still a frontier. Seeking coherency and consistency between datasets with different methods is not yet as simple as a binary distinction (agree/disagree).

5.2 The Kingdoms of Life, the Digestive Shortcut, and the Filling of Metabolic Holes

Other than an approach to zooplankton that was just simplified enough to answer my own questions, I did not write much about biology. There is an astonishingly large body of literature on the metabolisms of some of the most abundant single-celled organisms in the ocean, and this work would not have the implications it does without that previous work. Different species of eukaryotic phytoplankton produce unique suites of labile organic matter, as do the different bacteria and cyanobacteria.[97,222,246] They all have slightly different growth requirements, with enzymes suited to import metabolites often sensitive to a single functional group.[20,95,202] A small number of these organisms possess the diazotrophic capability to feed new fixed nitrogen into the metabolite pool.[247] Even these constraints do not capture the complexity of the microbial loop. Viruses modify the DOM produced by infected microbes;[11] protists probably eat both bacteria and DOM;[154] and it is only recently that anyone started looking into what fungi are doing.[248] At the metabolite level, we certainly do not know yet. These processes are the core of marine metabolomics for good reason, as it is where DOM starts and, in most cases, ends.[3]

Animals, as seen in Chapter 3, might be a remarkably essential shortcut in the microbial loop. In exchange for their own growth, they turn cells and particulate detritus into DOM. This is a known phenomenon for not just zooplankton; fish do the same thing at a higher trophic level, turning multicellular organisms into (1) fish, (2) particulate waste, (4) CO_2, and (3) DOM.[249] The formal logic should be familiar at this point: If DOM (or for that matter DOC or DON) denote quantities comprising metabolites, and some

process is capable of altering that quantity, it is then a potential source or sink of metabolites. As for fish and any other non-plankton animals, there are fewer of them in the water column than microbes or zooplankton, but their relative sparsity and greater mobility (no longer *planktos*, or “drifters”) make them a far more challenging set of entities to constrain chemically.[250–252] For the time being, there is a tremendous amount of opportunity in examining the zooplankton alone. Unlike the metabolic gene webs of microbes, it is far more tractable to survey what the dominant zooplankton of a region produce as a numerical rate, and potentially even narrow their contributions down to variables such as species, body size, temperature, season, and diet.[253]

Knowing what animals contribute to the water column could help in turn to constrain the microbes. While there are reasonable hypotheses for why microbes release some of the DOM they do, such as photosynthetic overflow, viral lysis, or signaling, the dominant paradigm implies that such processes must compensate for *all* labile DOM species within the metabolic web.[8,247,254] If bacteria, archaea, protists, and phytoplankton are the main organisms interacting with DOM for metabolic requirements, knowing a major source term for some metabolites eliminates the need to view microbes as the sole source for that group. We can say with just the evidence presented in Chapter 3 and 4 that this is an unnecessary constraint.

5.3 Physical Chemistry and a Unified Model for Metabolites

Below are two equations that, to the best of my knowledge, denote most of the processes that could likely happen to a metabolite in seawater except microbial release and uptake. For the purpose of simplicity, it is one-dimensional (no lateral diffusion or

advection) and omits surface processes such as wet or dry deposition or the exchange of volatiles. If the air-water interface is of concern, terms for those must be added.

$$\frac{dC_i}{dt} = \frac{d}{dz}\left(K_z\left(\frac{dC_i}{dz}\right)\right) + \sum_{s=1}^{n_s} m_s r_s$$
$$- C_i\left(\Phi_i \int_{\lambda_{min}}^{\lambda_{max}} Z_\lambda \varepsilon_{i,\lambda}\left(1 - 10^{-\alpha_D(\lambda)\cdot z}\right) d\lambda + [OH^-]k_{OH} + k_{H2O}\right.$$
$$\left. + \sum\nolimits_{j=Ox} [Ox]_{j,ss}\, k_j\right)$$

Equation 5-1: One-dimensional water-column process equation. Terms to be independently evaluated are colored for reference in the text.

In Equation 5-1, mixing is notated as it was in Chapter 4 and requires some knowledge of K_z. Animal excretion rates require the biomass (m_s) and excretion rate (r_s) for each species s being evaluated up to n_s species. Direct photolysis is a modification of the equation from Chapter 4, which does not integrate across the mixed layer but rather applies to a point. As alluded to in Chapter 1 and Chapter 4 with respect to the surface layer, applying photochemistry in concert with mixing, deposition (for example, malic acid), and fine-scale characterization here could explain many metabolite behaviors in the first few meters. The next terms contain k values, which are simply pseudo-first or second order rate constants for the corresponding reaction.

Hydrolysis is unlikely to occur via acid catalysis at seawater pH, so I included only terms for neutral and base-catalyzed forms. In addition to thiamine's documented behavior,[85] phosphoesters such 3'-AMP, ATP, and glucose-6-phosphate can be spontaneously dephosphorylated at pH 8, but this process is slow (>months) unless in the presence of a catalyst such as an iron oxide.[255] This could be seen as yet another "slow leak" (4.3.6), but this time to molecules (AMP, ADP, glucose) with known

biological utility.[256–258] Most other metabolites in this thesis are not known to hydrolyze quickly, most being monomers of hydrolysable polysaccharides, proteins, and nucleic acids. There is an inherent logic to this idea: if a metabolite does rapidly hydrolyze, the probability of observing it in the field is low.

Indirect "photochemistry" is a catch-all for reactions with transient oxidants such as singlet oxygen, hydroxyl radical, superoxide, and carbonate radical. Not all these reactions are sustained by photochemistry, as biotic production of superoxide may be the majority of its production in the ocean, even if it is typically thought of as a photochemical intermediate.[259]

For metabolite i, one may view this as a checklist. If we are interested in the net contribution of microbes to the inventory of i in the water column and have a dense sampling of C_i over time and space, we cross off terms that do not apply (for example, a compound does not absorb light above 280 nm—most of the Chapter 2 metabolites—or the observations were below the photic zone, so direct photolysis does not apply). If a term cannot be reasonably ruled out, it can be estimated or evaluated (such as excretion by the dominant zooplankton species). Once a value of the overall rate of change (dC_i/dt) has been estimated, it should be subtracted from the observed rate of change in the field samples. The difference between these two values is that for which the microbial community is responsible, until somebody expands the model to three dimensions or includes the surface layer.

What this result implies is that, for each metabolite, the microbial loop operates slower or faster than we would infer if it were the only process. Chapters 3 and 4 together imply that the loop is operating faster than we realized for the subset of

metabolites excreted by *Pleuromamma xiphias*. Chapter 2 and 4 might lead us to think the sun is not particularly critical to the microbial commerce of these metabolites, even if there are others for which it might matter.

$$C_{i,TOT} = C_i + \sum[i^x] + [i_{coll}] + \sum[iMe^y]$$

Equation 5-2: Abbreviated equilibrium constraints on metabolite *i*.

Recall in Chapter 1 that even the state of the metabolite in question can be altered while still maintaining some identity as speciated components of the total inventory $C_{i,TOT}$: ionic states i^x, colloidal and particulate partitioning i_{coll}, and complexes with metals iMe^y may invoke a tableau approach to the value of C_i and extend to constraining the fraction that gets measured at all (malic acid and glutamate in Chapter 2). Such processes have actually been modeled for iron.[68] Much of this is, for the time being, entirely unknown. For many compounds various equilibrium constants are probably estimable *in silico*, or with stripping voltammetry turned on its conceptual head to measure not a trace metal but the metabolite complexed to it.

Equation 5-1 also contains the assumption that none of the processes that consume a metabolite can produce it. This can be flipped: what does the equation look like for the base-catalyzed hydrolysis product of thiamine (Figure 5-1)?[85] If ATP is more labile to hydrolysis than AMP but AMP is the eventual product of ATP hydrolysis, the sink term of one metabolite becomes a source for another. Perhaps most importantly for dissolved metabolites, recent work has asserted that much of the protein hydrolysis (leads to amino acid production) occurring in the dissolved phase is due to extracellular enzymes, thus blurring the line between cellular action and aqueous chemistry.[260]

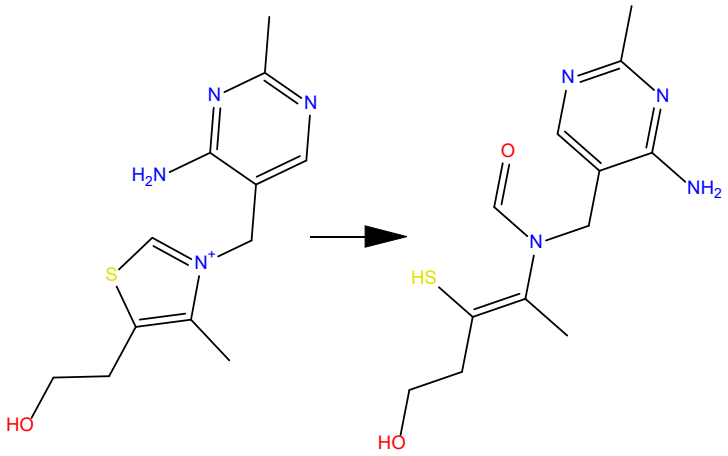

Figure 5-1: Hydrolysis of thiamine, condensed from Scheme 1, Herrmann et al. (1995).

The same sinks-as-sources paradigm applies to photochemistry (riboflavin to lumichrome) or any other system of interconvertible molecules. Equation 5-1 is an entire superset of differential equations containing subfamilies coupled to each other. One major ongoing project that can be helped with quantitative LC-MS is iteration of those families. Untargeted metabolomics was not used for this thesis, but it is the logical next step for cases such as thiamine. Quantify the known metabolite; search for related products in an untargeted dataset (with molecular networking such as GNPS); attempt to quantify the product once a corresponding standard can be found.[8,87] This has its own issues; for example, the BC method and SPE method capture different sets of metabolites, and an untargeted BC method dataset has never been published, as it would require all the binning, integration, and annotating as a normal untargeted dataset, plus an accounting for the benzoyl groups and an assessment of how these groups affect the fragmentation mass spectra, or MS^2.

5.4 Interactive Effects of Equilibrium and the Colloidal Phase

It is worth a few remarks on the interrelationships of equilibria and reactivity, as well. Chapters 1 and 2 paid some attention to the role of acid-base, complexation, and

partitioning, but as explanatory factors they were underexplored. I had not considered these when this project began, as they are not typically the purview of the metabolite literature. The impact of reactive oxygen species (ROS) is hard to truly estimate with the current method. First: we do not know how much of the dissolved metabolite inventory is partitioned in the colloidal fraction (< 0.2 μm; see Section 1.3.3), nor do we know if this process is kinetically competitive with microbial uptake. Second, there is also evidence that the nonpolar $^1O_2$ molecule is preferentially produced within such aggregations of organic matter—where it is more thermodynamically stable and where chromophores to produce it from ground-state O_2 are more abundant.[138]

What looks to us to be "dissolved" may yet be a spectrum of particles, taking in exuded organic matter and transforming it with enzymes and ROS—spatially independent of live cells.[260] While inclusion within organic matter aggregates may protect metabolites somewhat from direct photochemical action, insoluble oxide-forming metals like iron also tend to prefer the colloidal and particulate phases.[261] Given the potential of metabolites to complex iron and be subsequently vulnerable to photolysis *and* the hydrolytic catalysis potential demonstrated for metal oxide minerals,[255,262] aggregation and colloidal partitioning tends to unite almost every relevant abiotic factor in some way. Determining the composition and properties of such nano*particulates* in detail—and their microscale impact on *dissolved*-phase metabolites—is a frontier rich in both impact and irony.

5.5 Final Remarks: The Richness of Dilute Compounds

The ability to not just detect but quantify some of the most labile, transient chemicals in seawater heralds a new era in chemical ecology. It brings to bear the tools

of environmental chemistry and flux balance analysis to bear on a system with a monstrous degree of complexity and begs for a multiplicity of research. It requires both targeted and untargeted approaches. It requires multiple fields of physical, chemical, and biological expertise. It requires developing methods to capture different moieties: SPE; OPA, BC, and aniline derivatization (Halloran et al., in prep), in addition to alternative chromatographic approaches.[17,209,263,264]

The synthesis of this information will produce new insights. We know that photodegradation leaks tryptophan and kynurenine into states that may or may not be labile, depending on things like transporter specificity (Halloran et al., in prep).[265] We know that in the subtropical North Atlantic, zooplankton may meet the entire demand for proteinogenic amino acids, among other metabolites. During the breakdown of stratification, mixing is rapid enough to distribute metabolites though the layer above the pycnocline in a way that changes how measurements there might be interpreted.

If dissolved organic matter is a forest, the trees are individual chemicals. To research metabolites is to risk losing the forest for the trees, but to ignore their characteristics is to define a forest without knowing what trees are. This thesis stands as an account of those trees and the multitudes they contain.

References

(1) Bookchin, M. *The Ecology of Freedom: The Emergence and Dissolution of Hierarchy*; AK Press: Oakland, CA, 2005.

(2) Azam, F.; Fenchel, T.; Field, J.; Gray, J.; Meyer-Reil, L.; Thingstad, F. The Ecological Role of Water-Column Microbes in the Sea. *Mar. Ecol. Prog. Ser.* **1983**, *10*, 257–263. https://doi.org/10.3354/meps010257.

(3) Moran, M. A.; Ferrer-González, F. X.; Fu, H.; Nowinski, B.; Olofsson, M.; Powers, M. A.; Schreier, J. E.; Schroer, W. F.; Smith, C. B.; Uchimiya, M. The Ocean's Labile DOC Supply Chain. *Limnol. Oceanogr.* **2022**, *67* (5), 1007–1021. https://doi.org/10.1002/lno.12053.

(4) Anderson, T. R.; Williams, P. J. le B. A One-Dimensional Model of Dissolved Organic Carbon Cycling in the Water Column Incorporating Combined Biological-Photochemical Decomposition. *Glob. Biogeochem. Cycles* **1999**, *13* (2), 337–349. https://doi.org/10.1029/1999GB900013.

(5) IEA. *CO2 Emissions in 2023*; Paris, 2024. https://www.iea.org/reports/co2-emissions-in-2023 (accessed 2024-04-24).

(6) Longnecker, K.; Soule, M. C. K.; Swarr, G. J.; Parsons, R.; Liu, S.; Johnson, W. M.; Widner, B.; Curry, R.; Carlson, C. A.; Kujawinski, E. B. Seasonal and Daily Patterns in Known Dissolved Metabolites in the Northwestern Sargasso Sea. bioRxiv December 22, 2022, p 2022.12.21.521480. https://doi.org/10.1101/2022.12.21.521480.

(7) Boysen, A. K.; Carlson, L. T.; Durham, B. P.; Groussman, R. D.; Aylward, F. O.; Ribalet, F.; Heal, K. R.; DeLong, E. F.; Armbrust, E. V.; Ingalls, A. E. *Diel Oscillations of Particulate Metabolites Reflect Synchronized Microbial Activity in the North Pacific Subtropical Gyre*; preprint; Ecology, 2020. https://doi.org/10.1101/2020.05.09.086173.

(8) Johnson, W. M.; Kido Soule, M. C.; Kujawinski, E. B. Evidence for Quorum Sensing and Differential Metabolite Production by a Marine Bacterium in Response to DMSP. *ISME J.* **2016**, *10* (9), 2304–2316. https://doi.org/10.1038/ismej.2016.6.

(9) Bjørrisen, P. K. Phytoplankton Exudation of Organic Matter: Why Do Healthy Cells Do It?1. *Limnol. Oceanogr.* **1988**, *33* (1), 151–154. https://doi.org/10.4319/lo.1988.33.1.0151.

(10) Kujawinski, E. B.; Longnecker, K.; Alexander, H.; Dyhrman, S. T.; Fiore, C. L.; Haley, S. T.; Johnson, W. M. Phosphorus Availability Regulates Intracellular Nucleotides in Marine Eukaryotic Phytoplankton. *Limnol. Oceanogr. Lett.* **2017**, *2* (4), 119–129. https://doi.org/10.1002/lol2.10043.

(11) Berdjeb, L.; Pollet, T.; Domaizon, I.; Jacquet, S. Effect of Grazers and Viruses on Bacterial Community Structure and Production in Two Contrasting Trophic Lakes. *BMC Microbiol.* **2011**, *11* (1), 88. https://doi.org/10.1186/1471-2180-11-88.

(12) Patti, G. J.; Yanes, O.; Siuzdak, G. Metabolomics: The Apogee of the Omics Trilogy. *Nat. Rev. Mol. Cell Biol.* **2012**, *13* (4), 263–269. https://doi.org/10.1038/nrm3314.

(13) Kujawinski, E. B. The Impact of Microbial Metabolism on Marine Dissolved Organic Matter. *Annu. Rev. Mar. Sci.* **2011**, *3* (1), 567–599. https://doi.org/10.1146/annurev-marine-120308-081003.
(14) Hansell, D. A. Recalcitrant Dissolved Organic Carbon Fractions. *Annu. Rev. Mar. Sci.* **2013**, *5* (1), 421–445. https://doi.org/10.1146/annurev-marine-120710-100757.
(15) Luo, Y.; Friedrichs, M.; Doney, S.; Church, M.; Ducklow, H. Oceanic Heterotrophic Bacterial Nutrition by Semilabile DOM as Revealed by Data Assimilative Modeling. *Aquat. Microb. Ecol.* **2010**, *60* (3), 273–287. https://doi.org/10.3354/ame01427.
(16) Johnson, W. M.; Kido Soule, M. C.; Kujawinski, E. B. Extraction Efficiency and Quantification of Dissolved Metabolites in Targeted Marine Metabolomics. *Limnol. Oceanogr. Methods* **2017**, *15* (4), 417–428. https://doi.org/10.1002/lom3.10181.
(17) Widner, B.; Kido Soule, M. C.; Ferrer-González, F. X.; Moran, M. A.; Kujawinski, E. B. Quantification of Amine- and Alcohol-Containing Metabolites in Saline Samples Using Pre-Extraction Benzoyl Chloride Derivatization and Ultrahigh Performance Liquid Chromatography Tandem Mass Spectrometry (UHPLC MS/MS). *Anal. Chem.* **2021**, *93* (11), 4809–4817. https://doi.org/10.1021/acs.analchem.0c03769.
(18) Swenson, T. L.; Jenkins, S.; Bowen, B. P.; Northen, T. R. Untargeted Soil Metabolomics Methods for Analysis of Extractable Organic Matter. *Soil Biol. Biochem.* **2015**, *80*, 189–198. https://doi.org/10.1016/j.soilbio.2014.10.007.
(19) Kido Soule, M. C.; Longnecker, K.; Johnson, W. M.; Kujawinski, E. B. Environmental Metabolomics: Analytical Strategies. *Mar. Chem.* **2015**, *177*, 374–387. https://doi.org/10.1016/j.marchem.2015.06.029.
(20) Pochini, L.; Scalise, M.; Galluccio, M.; Indiveri, C. Membrane Transporters for the Special Amino Acid Glutamine: Structure/Function Relationships and Relevance to Human Health. *Front. Chem.* **2014**, *2*. https://doi.org/10.3389/fchem.2014.00061.
(21) Degnan, P. H.; Barry, N. A.; Mok, K. C.; Taga, M. E.; Goodman, A. L. Human Gut Microbes Use Multiple Transporters to Distinguish Vitamin B12 Analogs and Compete in the Gut. *Cell Host Microbe* **2014**, *15* (1), 47–57. https://doi.org/10.1016/j.chom.2013.12.007.
(22) Tang, Y. Z.; Koch, F.; Gobler, C. J. Most Harmful Algal Bloom Species Are Vitamin B $_1$ and B $_{12}$ Auxotrophs. *Proc. Natl. Acad. Sci.* **2010**, *107* (48), 20756–20761. https://doi.org/10.1073/pnas.1009566107.
(23) Mawji, E.; Gledhill, M.; Milton, J. A.; Tarran, G. A.; Ussher, S.; Thompson, A.; Wolff, G. A.; Worsfold, P. J.; Achterberg, E. P. Hydroxamate Siderophores: Occurrence and Importance in the Atlantic Ocean. *Environ. Sci. Technol.* **2008**, *42* (23), 8675–8680. https://doi.org/10.1021/es801884r.
(24) Tang, W.; van der Donk, W. A. Structural Characterization of Four Prochlorosins: A Novel Class of Lantipeptides Produced by Planktonic Marine Cyanobacteria. *Biochemistry* **2012**, *51* (21), 4271–4279. https://doi.org/10.1021/bi300255s.
(25) Behrenfeld, M. J.; Boss, E.; Siegel, D. A.; Shea, D. M. Carbon-Based Ocean Productivity and Phytoplankton Physiology from Space. *Glob. Biogeochem. Cycles* **2005**, *19* (1). https://doi.org/10.1029/2004GB002299.

(26) Mayerhofer, M. M.; Eigemann, F.; Lackner, C.; Hoffmann, J.; Hellweger, F. L. Dynamic Carbon Flux Network of a Diverse Marine Microbial Community. *ISME Commun.* **2021**, *1* (1), 50. https://doi.org/10.1038/s43705-021-00055-7.
(27) Louca, S.; Hawley, A. K.; Katsev, S.; Torres-Beltran, M.; Bhatia, M. P.; Kheirandish, S.; Michiels, C. C.; Capelle, D.; Lavik, G.; Doebeli, M.; Crowe, S. A.; Hallam, S. J. Integrating Biogeochemistry with Multiomic Sequence Information in a Model Oxygen Minimum Zone. *Proc. Natl. Acad. Sci.* **2016**, *113* (40). https://doi.org/10.1073/pnas.1602897113.
(28) Harcombe, W. R.; Riehl, W. J.; Dukovski, I.; Granger, B. R.; Betts, A.; Lang, A. H.; Bonilla, G.; Kar, A.; Leiby, N.; Mehta, P.; Marx, C. J.; Segrè, D. Metabolic Resource Allocation in Individual Microbes Determines Ecosystem Interactions and Spatial Dynamics. *Cell Rep.* **2014**, *7* (4), 1104–1115. https://doi.org/10.1016/j.celrep.2014.03.070.
(29) Alvarez, L.; Aliashkevich, A.; de Pedro, M. A.; Cava, F. Bacterial Secretion of D-Arginine Controls Environmental Microbial Biodiversity. *ISME J.* **2018**, *12* (2), 438–450. https://doi.org/10.1038/ismej.2017.176.
(30) Ikeda, T. Respiration and Ammonia Excretion by Marine Metazooplankton Taxa: Synthesis toward a Global-Bathymetric Model. *Mar. Biol.* **2014**, *161* (12), 2753–2766. https://doi.org/10.1007/s00227-014-2540-5.
(31) Bar-Even, A.; Noor, E.; Savir, Y.; Liebermeister, W.; Davidi, D.; Tawfik, D. S.; Milo, R. The Moderately Efficient Enzyme: Evolutionary and Physicochemical Trends Shaping Enzyme Parameters. *Biochemistry* **2011**, *50* (21), 4402–4410. https://doi.org/10.1021/bi2002289.
(32) Blough, N. V.; Zepp, R. G. Reactive Oxygen Species in Natural Waters. In *Active Oxygen in Chemistry*; Foote, C. S., Valentine, J. S., Greenberg, A., Liebman, J. F., Eds.; Springer Netherlands: Dordrecht, 1995; pp 280–333. https://doi.org/10.1007/978-94-007-0874-7_8.
(33) Voet, D.; Voet, J. G.; Pratt, C. W. *Fundamentals of Biochemistry: Life at the Molecular Level, 5th Edition | Wiley*, 5th ed.; Wiley, 2016.
(34) Williams, R.; Jencks, W. P.; Westheimer, F. H. *pKa Data*; Compiled Data; ACS, Organic Division, 2022; p 33. https://organicchemistrydata.org/hansreich/resources/pka/pka_data/pka-compilation-williams.pdf.
(35) Tanaka, N.; Kolthoff, I. M.; Stricks, W. Iron-Cysteinate Complexes. *J. Am. Chem. Soc.* **1955**, *77* (7), 1996–2004. https://doi.org/10.1021/ja01612a087.
(36) Johnson, D. C.; Dean, D. R.; Smith, A. D.; Johnson, M. K. STRUCTURE, FUNCTION, AND FORMATION OF BIOLOGICAL IRON-SULFUR CLUSTERS. *Annu. Rev. Biochem.* **2005**, *74* (Volume 74, 2005), 247–281. https://doi.org/10.1146/annurev.biochem.74.082803.133518.
(37) Tang, N.; Skibsted, L. H. Calcium Binding to Amino Acids and Small Glycine Peptides in Aqueous Solution: Toward Peptide Design for Better Calcium Bioavailability. *J. Agric. Food Chem.* **2016**, *64* (21), 4376–4389. https://doi.org/10.1021/acs.jafc.6b01534.
(38) Bruland, K. W. Complexation of Zinc by Natural Organic Ligands in the Central North Pacific: Oceanic Zinc Speciation. *Limnol. Oceanogr.* **1989**, *34* (2), 269–285. https://doi.org/10.4319/lo.1989.34.2.0269.

(39) Rue, E. L.; Bruland, K. W. Complexation of Iron(III) by Natural Organic Ligands in the Central North Pacific as Determined by a New Competitive Ligand Equilibration/Adsorptive Cathodic Stripping Voltammetric Method. *Mar. Chem.* **1995**, *50* (1), 117–138. https://doi.org/10.1016/0304-4203(95)00031-L.
(40) Vukosav, P.; Tomišić, V.; Mlakar, M. Iron(III)-Complexes Engaged in the Biochemical Processes in Seawater. II. Voltammetry of Fe(III)-Malate Complexes in Model Aqueous Solution. *Electroanalysis* **2010**, *22* (19), 2179–2186. https://doi.org/10.1002/elan.200900632.
(41) Zabiszak, M.; Frymark, J.; Nowak, M.; Grajewski, J.; Stachowiak, K.; Kaczmarek, M. T.; Jastrząb, R. Influence of D-Electron Divalent Metal Ions in Complex Formation with L-Tartaric and L-Malic Acids. *Molecules* **2021**, *26* (17), 5290. https://doi.org/10.3390/molecules26175290.
(42) Gledhill, M.; Buck, K. N. The Organic Complexation of Iron in the Marine Environment: A Review. *Front. Microbiol.* **2012**, *3*. https://doi.org/10.3389/fmicb.2012.00069.
(43) Park, J.; Durham, B. P.; Key, R. S.; Groussman, R. D.; Bartolek, Z.; Pinedo-Gonzalez, P.; Hawco, N. J.; John, S. G.; Carlson, M. C. G.; Lindell, D.; Juranek, L. W.; Ferrón, S.; Ribalet, F.; Armbrust, E. V.; Ingalls, A. E.; Bundy, R. M. Siderophore Production and Utilization by Marine Bacteria in the North Pacific Ocean. *Limnol. Oceanogr.* **2023**, *68* (7), 1636–1653. https://doi.org/10.1002/lno.12373.
(44) McCormack, P.; Worsfold, P. J.; Gledhill, M. Separation and Detection of Siderophores Produced by Marine Bacterioplankton Using High-Performance Liquid Chromatography with Electrospray Ionization Mass Spectrometry. *Anal. Chem.* **2003**, *75* (11), 2647–2652. https://doi.org/10.1021/ac0340105.
(45) Moran, M. A.; Kujawinski, E. B.; Schroer, W. F.; Amin, S. A.; Bates, N. R.; Bertrand, E. M.; Braakman, R.; Brown, C. T.; Covert, M. W.; Doney, S. C.; Dyhrman, S. T.; Edison, A. S.; Eren, A. M.; Levine, N. M.; Li, L.; Ross, A. C.; Saito, M. A.; Santoro, A. E.; Segrè, D.; Shade, A.; Sullivan, M. B.; Vardi, A. Microbial Metabolites in the Marine Carbon Cycle. *Nat. Microbiol.* **2022**, *7* (4), 508–523. https://doi.org/10.1038/s41564-022-01090-3.
(46) Chin, W.-C.; Orellana, M. V.; Verdugo, P. Spontaneous Assembly of Marine Dissolved Organic Matter into Polymer Gels. *Nature* **1998**, *391* (6667), 568–572. https://doi.org/10.1038/35345.
(47) Orellana, Mó. V.; Verdugo, P. Ultraviolet Radiation Blocks the Organic Carbon Exchange between the Dissolved Phase and the Gel Phase in the Ocean. *Limnol. Oceanogr.* **2003**, *48* (4), 1618–1623. https://doi.org/10.4319/lo.2003.48.4.1618.
(48) Schwarzenbach, Rene P; Gschwend, Philip M.; Imboden, Dieter M. *Environmental Organic Chemistry*, 3rd ed.; Wiley, 2016.
(49) Orellana, M. V.; Leck, C. Chapter 9 - Marine Microgels. In *Biogeochemistry of Marine Dissolved Organic Matter (Second Edition)*; Hansell, D. A., Carlson, C. A., Eds.; Academic Press: Boston, 2015; pp 451–480. https://doi.org/10.1016/B978-0-12-405940-5.00009-1.
(50) Verdugo, P.; Santschi, P. H. Polymer Dynamics of DOC Networks and Gel Formation in Seawater. *Deep Sea Res. Part II Top. Stud. Oceanogr.* **2010**, *57* (16), 1486–1493. https://doi.org/10.1016/j.dsr2.2010.03.002.

(51) Hansell, D.; Carlson, C.; Repeta, D.; Schlitzer, R. Dissolved Organic Matter in the Ocean: A Controversy Stimulates New Insights. *Oceanography* **2009**, *22* (4), 202–211. https://doi.org/10.5670/oceanog.2009.109.
(52) Sichert, A.; Corzett, C. H.; Schechter, M. S.; Unfried, F.; Markert, S.; Becher, D.; Fernandez-Guerra, A.; Liebeke, M.; Schweder, T.; Polz, M. F.; Hehemann, J.-H. Verrucomicrobia Use Hundreds of Enzymes to Digest the Algal Polysaccharide Fucoidan. *Nat. Microbiol.* **2020**, *5* (8), 1026–1039. https://doi.org/10.1038/s41564-020-0720-2.
(53) Aluwihare, L. I.; Repeta, D. J.; Chen, R. F. A Major Biopolymeric Component to Dissolved Organic Carbon in Surface Sea Water. *Nature* **1997**, *387* (6629), 166–169. https://doi.org/10.1038/387166a0.
(54) Orellana, M. V.; Petersen, T. W.; Diercks, A. H.; Donohoe, S.; Verdugo, P.; van den Engh, G. Marine Microgels: Optical and Proteomic Fingerprints. *Mar. Chem.* **2007**, *105* (3), 229–239. https://doi.org/10.1016/j.marchem.2007.02.002.
(55) Mopper, K.; Zhou, X.; Kieber, R. J.; Kieber, D. J.; Sikorski, R. J.; Jones, R. D. Photochemical Degradation of Dissolved Organic Carbon and Its Impact on the Oceanic Carbon Cycle. *Nature* **1991**, *353* (6339), 60–62. https://doi.org/10.1038/353060a0.
(56) Ward, C. P.; L. Sleighter, R.; G. Hatcher, P.; M. Cory, R. Insights into the Complete and Partial Photooxidation of Black Carbon in Surface Waters. *Environ. Sci. Process. Impacts* **2014**, *16* (4), 721–731. https://doi.org/10.1039/C3EM00597F.
(57) Kieber, D. J.; McDaniel, J.; Mopper, K. Photochemical Source of Biological Substrates in Sea Water: Implications for Carbon Cycling. *Nature* **1989**, *341* (6243), 637–639. https://doi.org/10.1038/341637a0.
(58) Zhu, Y.; Kieber, D. J. Concentrations and the Photochemistry of Acetaldehyde, Glyoxal and Methylglyoxal in the Northwest Atlantic Ocean. *Environ. Sci. Technol.* **2019**, *53* (16), 9512–9521. https://doi-org.libproxy.mit.edu/10.1021/acs.est.9b01631.
(59) Tarr, M. A.; Wang, W.; Bianchi, T. S.; Engelhaupt, E. Mechanisms of Ammonia and Amino Acid Photoproduction from Aquatic Humic and Colloidal Matter. *Water Res.* **2001**, *35* (15), 3688–3696. https://doi.org/10.1016/S0043-1354(01)00101-4.
(60) Ahmad, I.; Fasihullah, Q.; Noor, A.; Ansari, I. A.; Ali, Q. N. M. Photolysis of Riboflavin in Aqueous Solution: A Kinetic Study. *Int. J. Pharm.* **2004**, *280* (1–2), 199–208. https://doi.org/10.1016/j.ijpharm.2004.05.020.
(61) Biddanda, B. A.; Cotner, J. B. Enhancement of Dissolved Organic Matter Bioavailability by Sunlight and Its Role in the Carbon Cycle of Lakes Superior and Michigan. *J. Gt. Lakes Res.* **2003**, *29* (2), 228–241. https://doi.org/10.1016/S0380-1330(03)70429-8.
(62) Reitner, B.; Herzig, A.; Herndl, G. Photoreactivity and Bacterioplankton Availability of Aliphatic versus Aromatic Amino Acids and a Protein. *Aquat. Microb. Ecol.* **2002**, *26*, 305–311. https://doi.org/10.3354/ame026305.
(63) Anesio, A.; Denward, C.; Tranvik, L.; Granéli, W. Decreased Bacterial Growth on Vascular Plant Detritus Due to Photochemical Modification. *Aquat. Microb. Ecol.* **1999**, *17*, 159–165. https://doi.org/10.3354/ame017159.

(64) Ward, C. P.; Nalven, S. G.; Crump, B. C.; Kling, G. W.; Cory, R. M. Photochemical Alteration of Organic Carbon Draining Permafrost Soils Shifts Microbial Metabolic Pathways and Stimulates Respiration. *Nat. Commun.* **2017**, *8* (1), 772. https://doi.org/10.1038/s41467-017-00759-2.
(65) Hayase, K.; Zepp, R. G. Photolysis of Copper(II)-Amino Acid Complexes in Water. *Environ. Sci. Technol.* **1991**, *25* (7), 1273–1279. https://doi.org/10.1021/es00019a007.
(66) Qian, Y.; Yin, X.; Lin, H.; Rao, B.; Brooks, S. C.; Liang, L.; Gu, B. Why Dissolved Organic Matter Enhances Photodegradation of Methylmercury. *Environ. Sci. Technol. Lett.* **2014**, *1* (10), 426–431. https://doi.org/10.1021/ez500254z.
(67) Chen, M.; Wang, W.-X.; Guo, L. Phase Partitioning and Solubility of Iron in Natural Seawater Controlled by Dissolved Organic Matter. *Glob. Biogeochem. Cycles* **2004**, *18* (4). https://doi.org/10.1029/2003GB002160.
(68) Weber, L.; Volker, C.; Oschlies, A.; Burchard, H. Iron Profiles and Speciation of the Upper Water Column at the Bermuda Atlantic Time-Series Study Site: A Model Based Sensitivity Study. **2007**.
(69) Kritzberg, E. S.; Ekström, S. M. Increasing Iron Concentrations in Surface Waters – a Factor behind Brownification? *Biogeosciences* **2012**, *9* (4), 1465–1478. https://doi.org/10.5194/bg-9-1465-2012.
(70) Steinberg, D. K.; Landry, M. R. Zooplankton and the Ocean Carbon Cycle. *Annu. Rev. Mar. Sci.* **2017**, *9* (1), 413–444. https://doi.org/10.1146/annurev-marine-010814-015924.
(71) Steinberg, D. K.; Goldthwait, S. A.; Hansell, D. A. Zooplankton Vertical Migration and the Active Transport of Dissolved Organic and Inorganic Nitrogen in the Sargasso Sea. *Deep Sea Res. Part Oceanogr. Res. Pap.* **2002**, *49* (8), 1445–1461. https://doi.org/10.1016/S0967-0637(02)00037-7.
(72) Steinberg, D. K.; Carlson, C. A.; Bates, N. R.; Goldthwait, S. A.; Madin, L. P.; Michaels, A. F. Zooplankton Vertical Migration and the Active Transport of Dissolved Organic and Inorganic Carbon in the Sargasso Sea. *Deep Sea Res. Part Oceanogr. Res. Pap.* **2000**, *47* (1), 137–158. https://doi.org/10.1016/S0967-0637(99)00052-7.
(73) Clifford, E. L.; Hansell, D. A.; Varela, M. M.; Nieto-Cid, M.; Herndl, G. J.; Sintes, E. Crustacean Zooplankton Release Copious Amounts of Dissolved Organic Matter as Taurine in the Ocean: Dissolved Free Taurine in Oceanic Waters. *Limnol. Oceanogr.* **2017**, *62* (6), 2745–2758. https://doi.org/10.1002/lno.10603.
(74) Clifford, E. L.; De Corte, D.; Amano, C.; Paliaga, P.; Ivančić, I.; Ortiz, V.; Najdek, M.; Herndl, G. J.; Sintes, E. Mesozooplankton Taurine Production and Prokaryotic Uptake in the Northern Adriatic Sea. *Limnol. Oceanogr.* **2020**, *65* (11), 2730–2747. https://doi.org/10.1002/lno.11544.
(75) Maas, A. E.; Liu, S.; Bolaños, L. M.; Widner, B.; Parsons, R.; Kujawinski, E. B.; Blanco-Bercial, L.; Carlson, C. A. Migratory Zooplankton Excreta and Its Influence on Prokaryotic Communities. *Front. Mar. Sci.* **2020**, *7*, 573268. https://doi.org/10.3389/fmars.2020.573268.
(76) Fer, I.; Peterson, A. K.; Ullgren, J. E. Microstructure Measurements from an Underwater Glider in the Turbulent Faroe Bank Channel Overflow. *J. Atmospheric*

Ocean. Technol. **2014**, *31* (5), 1128–1150. https://doi.org/10.1175/JTECH-D-13-00221.1.
(77) Haskell. Estimates of Vertical Turbulent Mixing Used to Determine a Vertical Gradient in Net and Gross Oxygen Production in the Oligotrophic South Pacific Gyre. *Geophys. Res. Lett.* **2016**.
(78) Stocker, R.; Seymour, J. R. Ecology and Physics of Bacterial Chemotaxis in the Ocean. *Microbiol. Mol. Biol. Rev.* **2012**, *76* (4), 792–812. https://doi.org/10.1128/MMBR.00029-12.
(79) Blanco-Bercial, L.; Parsons, R.; Bolaños, L. M.; Johnson, R.; Giovannoni, S. J.; Curry, R. The Protist Community Traces Seasonality and Mesoscale Hydrographic Features in the Oligotrophic Sargasso Sea. *Front. Mar. Sci.* **2022**, *9*. https://doi.org/10.3389/fmars.2022.897140.
(80) Steinberg, D. K.; Carlson, C. A.; Bates, N. R.; Johnson, R. J.; Michaels, A. F.; Knap, A. H. Overview of the US JGOFS Bermuda Atlantic Time-Series Study (BATS): A Decade-Scale Look at Ocean Biology and Biogeochemistry. *Deep Sea Res. Part II Top. Stud. Oceanogr.* **2001**, *48* (8–9), 1405–1447. https://doi.org/10.1016/S0967-0645(00)00148-X.
(81) Holmes, M. E.; Sansone, F. J.; Rust, T. M.; Popp, B. N. Methane Production, Consumption, and Air-Sea Exchange in the Open Ocean: An Evaluation Based on Carbon Isotopic Ratios. *Glob. Biogeochem. Cycles* **2000**, *14* (1), 1–10. https://doi.org/10.1029/1999GB001209.
(82) Gutowska, M. A.; Shome, B.; Sudek, S.; McRose, D. L.; Hamilton, M.; Giovannoni, S. J.; Begley, T. P.; Worden, A. Z. Globally Important Haptophyte Algae Use Exogenous Pyrimidine Compounds More Efficiently than Thiamin. *mBio* **2017**, *8* (5), 10.1128/mbio.01459-17. https://doi.org/10.1128/mbio.01459-17.
(83) Croft, M. T.; Warren, M. J.; Smith, A. G. Algae Need Their Vitamins. *Eukaryot. Cell* **2006**, *5* (8), 1175–1183. https://doi.org/10.1128/EC.00097-06.
(84) Suffridge, C. P.; Bolaños, L. M.; Bergauer, K.; Worden, A. Z.; Morré, J.; Behrenfeld, M. J.; Giovannoni, S. J. Exploring Vitamin B1 Cycling and Its Connections to the Microbial Community in the North Atlantic Ocean. *Front. Mar. Sci.* **2020**, *7*, 606342. https://doi.org/10.3389/fmars.2020.606342.
(85) Herrmann, J.; Knoche, W.; Neugebauer, R. Hydrolysis of Thiamine. *J. Chem. Soc. Perkin Trans. 2* **1995**, No. 3, 463. https://doi.org/10.1039/p29950000463.
(86) Paerl, R. W.; Curtis, N. P.; Bittner, M. J.; Cohn, M. R.; Gifford, S. M.; Bannon, C. C.; Rowland, E.; Bertrand, E. M. Use and Detection of a Vitamin B1 Degradation Product Yields New Views of the Marine B1 Cycle and Plankton Metabolite Exchange. *mBio* **2023**, *14* (4), e00061-23. https://doi.org/10.1128/mbio.00061-23.
(87) Aron, A. T.; Gentry, E. C.; McPhail, K. L.; Nothias, L.-F.; Nothias-Esposito, M.; Bouslimani, A.; Petras, D.; Gauglitz, J. M.; Sikora, N.; Vargas, F.; van der Hooft, J. J. J.; Ernst, M.; Kang, K. B.; Aceves, C. M.; Caraballo-Rodríguez, A. M.; Koester, I.; Weldon, K. C.; Bertrand, S.; Roullier, C.; Sun, K.; Tehan, R. M.; Boya P., C. A.; Christian, M. H.; Gutiérrez, M.; Ulloa, A. M.; Tejeda Mora, J. A.; Mojica-Flores, R.; Lakey-Beitia, J.; Vásquez-Chaves, V.; Zhang, Y.; Calderón, A. I.; Tayler, N.; Keyzers, R. A.; Tugizimana, F.; Ndlovu, N.; Aksenov, A. A.; Jarmusch, A. K.; Schmid, R.; Truman, A. W.; Bandeira, N.; Wang, M.; Dorrestein, P. C. Reproducible Molecular Networking of Untargeted Mass Spectrometry Data Using

GNPS. *Nat. Protoc.* **2020**, *15* (6), 1954–1991. https://doi.org/10.1038/s41596-020-0317-5.
(88) Koistinen, V.; Kärkkäinen, O.; Keski-Rahkonen, P.; Tsugawa, H.; Scalbert, A.; Arita, M.; Wishart, D.; Hanhineva, K. Towards a Rosetta Stone for Metabolomics: Recommendations to Overcome Inconsistent Metabolite Nomenclature. *Nat. Metab.* **2023**. https://doi.org/10.1038/s42255-023-00757-3.
(89) Fiore, C. L.; Longnecker, K.; Kido Soule, M. C.; Kujawinski, E. B. Release of Ecologically Relevant Metabolites by the Cyanobacterium *S Ynechococcus Elongatus* CCMP 1631: Metabolomics of *Synechococcus*. *Environ. Microbiol.* **2015**, *17* (10), 3949–3963. https://doi.org/10.1111/1462-2920.12899.
(90) Boysen, A. K.; Durham, B. P.; Kumler, W.; Key, R. S.; Heal, K. R.; Carlson, L. T.; Groussman, R. D.; Armbrust, E. V.; Ingalls, A. E. Glycine Betaine Uptake and Metabolism in Marine Microbial Communities. *Environ. Microbiol.* **2022**, *24* (5), 2380–2403. https://doi.org/10.1111/1462-2920.16020.
(91) Levine, N. M.; Varaljay, V. A.; Toole, D. A.; Dacey, J. W. H.; Doney, S. C.; Moran, M. A. Environmental, Biochemical and Genetic Drivers of DMSP Degradation and DMS Production in the Sargasso Sea: Drivers of DMSP Degradation and DMS Production. *Environ. Microbiol.* **2012**, *14* (5), 1210–1223. https://doi.org/10.1111/j.1462-2920.2012.02700.x.
(92) Moran, M. A.; Zepp, R. G. Role of Photoreactions in the Formation of Biologically Labile Compounds from Dissolved Organic Matter. *Limnol. Oceanogr.* **1997**, *42* (6), 1307–1316. https://doi.org/10.4319/lo.1997.42.6.1307.
(93) Remucal, C. K.; McNeill, K. Photosensitized Amino Acid Degradation in the Presence of Riboflavin and Its Derivatives. *Environ. Sci. Technol.* **2011**, *45* (12), 5230–5237. https://doi.org/10.1021/es200411a.
(94) Johnson, W. M.; Alexander, H.; Bier, R. L.; Miller, D. R.; Muscarella, M. E.; Pitz, K. J.; Smith, H. Auxotrophic Interactions: A Stabilizing Attribute of Aquatic Microbial Communities? *FEMS Microbiol. Ecol.* **2020**, *96* (11), fiaa115. https://doi.org/10.1093/femsec/fiaa115.
(95) Tripp, H. J.; Schwalbach, M. S.; Meyer, M. M.; Kitner, J. B.; Breaker, R. R.; Giovannoni, S. J. Unique Glycine-Activated Riboswitch Linked to Glycine–Serine Auxotrophy in SAR11. *Environ. Microbiol.* **2009**, *11* (1), 230–238. https://doi.org/10.1111/j.1462-2920.2008.01758.x.
(96) Sahu, B.; Ray, M. K. Auxotrophy in Natural Isolate: Minimal Requirements for Growth of the Antarctic Psychrotrophic Bacterium Pseudomonas Syringae Lz4W. *J. Basic Microbiol.* **2008**, *48* (1), 38–47. https://doi.org/10.1002/jobm.200700185.
(97) Durham, B. P.; Boysen, A. K.; Heal, K. R.; Carlson, L. T.; Boccamazzo, R.; Deodato, C. R.; Qin, W.; Cattolico, R. A.; Armbrust, E. V.; Ingalls, A. E. Chemotaxonomic Patterns in Intracellular Metabolites of Marine Microbial Plankton. *Front. Mar. Sci.* **2022**, *9*.
(98) Sunda, W. G.; Price, N. M.; Morel, F. M. M. Trace Metal Ion Buffers and Their Use in Culture Studies (Chapt. 4). In *Algal Culturing Techiques*; Elsevier: Amsterdam; pp 35–63.
(99) Freeman, D. H.; Niles, S. F.; Rodgers, R. P.; French-McCay, D. P.; Longnecker, K.; Reddy, C. M.; Ward, C. P. Hot and Cold: Photochemical Weathering Mediates Oil Properties and Fate Differently Depending on Seawater Temperature. *Environ.*

Sci. Technol. **2023**, *57* (32), 11988–11998. https://doi.org/10.1021/acs.est.3c02962.
(100) Halewood, E.; Opalk, K.; Custals, L.; Carey, M.; Hansell, D. A.; Carlson, C. A. Determination of Dissolved Organic Carbon and Total Dissolved Nitrogen in Seawater Using High Temperature Combustion Analysis. *Front. Mar. Sci.* **2022**, *9*. https://doi.org/10.3389/fmars.2022.1061646.
(101) Fichot, C. G.; Benner, R. The Spectral Slope Coefficient of Chromophoric Dissolved Organic Matter (S275–295) as a Tracer of Terrigenous Dissolved Organic Carbon in River-Influenced Ocean Margins. *Limnol. Oceanogr.* **2012**, *57* (5), 1453–1466. https://doi.org/10.4319/lo.2012.57.5.1453.
(102) Opsahl, S.; Benner, R. Photochemical Reactivity of Dissolved Lignin in River and Ocean Waters. *Limnol. Oceanogr.* **1998**, *43* (6), 1297–1304. https://doi.org/10.4319/lo.1998.43.6.1297.
(103) Adams, K. J.; Pratt, B.; Bose, N.; Dubois, L. G.; St. John-Williams, L.; Perrott, K. M.; Ky, K.; Kapahi, P.; Sharma, V.; MacCoss, M. J.; Moseley, M. A.; Colton, C. A.; MacLean, B. X.; Schilling, B.; Thompson, J. W.; Alzheimer's Disease Metabolomics Consortium. Skyline for Small Molecules: A Unifying Software Package for Quantitative Metabolomics. *J. Proteome Res.* **2020**, *19* (4), 1447–1458. https://doi.org/10.1021/acs.jproteome.9b00640.
(104) Schmid, R.; Heuckeroth, S.; Korf, A.; Smirnov, A.; Myers, O.; Dyrlund, T. S.; Bushuiev, R.; Murray, K. J.; Hoffmann, N.; Lu, M.; Sarvepalli, A.; Zhang, Z.; Fleischauer, M.; Dührkop, K.; Wesner, M.; Hoogstra, S. J.; Rudt, E.; Mokshyna, O.; Brungs, C.; Ponomarov, K.; Mutabdžija, L.; Damiani, T.; Pudney, C. J.; Earll, M.; Helmer, P. O.; Fallon, T. R.; Schulze, T.; Rivas-Ubach, A.; Bilbao, A.; Richter, H.; Nothias, L.-F.; Wang, M.; Orešič, M.; Weng, J.-K.; Böcker, S.; Jeibmann, A.; Hayen, H.; Karst, U.; Dorrestein, P. C.; Petras, D.; Du, X.; Pluskal, T. Integrative Analysis of Multimodal Mass Spectrometry Data in MZmine 3. *Nat. Biotechnol.* **2023**, 1–3. https://doi.org/10.1038/s41587-023-01690-2.
(105) Bannon, C. C.; Mudge, E. M.; Bertrand, E. M. Shedding Light on Cobalamin Photodegradation in the Ocean. *Limnol. Oceanogr. Lett.* **2023**, lol2.10371. https://doi.org/10.1002/lol2.10371.
(106) Xue, L.; Kieber, D. J. Photochemical Production and Photolysis of Acrylate in Seawater. *Environ. Sci. Technol.* **2021**, *55* (10), 7135–7144. https://doi.org/10.1021/acs.est.1c00327.
(107) Sato, M.; Ogata, N.; Wong, K. H.; Obata, H.; Takeda, S. Photodecomposition of Natural Organic Metal-Binding Ligands from Deep Seawater. *Mar. Chem.* **2021**, *230*, 103939. https://doi.org/10.1016/j.marchem.2021.103939.
(108) Vaid, F. H. M.; Gul, W.; Faiyaz, A.; Anwar, Z.; Ejaz, M. A.; Zahid, S.; Ahmad, I. Divalent Anion Catalyzed Photodegradation of Riboflavin: A Kinetic Study. *J. Photochem. Photobiol. Chem.* **2019**, *371*, 59–66. https://doi.org/10.1016/j.jphotochem.2018.10.048.
(109) Boreen, A. L.; Edhlund, B. L.; Cotner, J. B.; McNeill, K. Indirect Photodegradation of Dissolved Free Amino Acids: The Contribution of Singlet Oxygen and the Differential Reactivity of DOM from Various Sources. *Environ. Sci. Technol.* **2008**, *42* (15), 5492–5498. https://doi.org/10.1021/es800185d.

(110) Janssen, E. M.-L.; Erickson, P. R.; McNeill, K. Dual Roles of Dissolved Organic Matter as Sensitizer and Quencher in the Photooxidation of Tryptophan. *Environ. Sci. Technol.* **2014**, *48* (9), 4916–4924. https://doi.org/10.1021/es500535a.
(111) Longnecker, K.; Kido Soule, M. C.; Swarr, G. J.; Parsons, R. J.; Liu, S.; Johnson, W. M.; Widner, B.; Curry, R.; Carlson, C. A.; Kujawinski, E. B. Seasonal and Daily Patterns in Known Dissolved Metabolites in the Northwestern Sargasso Sea. *Limnol. Oceanogr.* **2024**, *69* (3), 449–466. https://doi.org/10.1002/lno.12497.
(112) Saidel, L. J.; Goldfarb, A. R.; Waldman, Sheldon. THE ABSORPTION SPECTRA OF AMINO ACIDS IN THE REGION TWO HUNDRED TO TWO HUNDRED AND THIRTY MILLIMICRONS. *J. Biol. Chem.* **1952**, *197* (1), 285–291. https://doi.org/10.1016/S0021-9258(18)55677-5.
(113) McLean, D. J.; Giese, A. C. ABSORPTION SPECTRA OF PROTEINS AND AMINO ACIDS AFTER ULTRAVIOLET IRRADIATION. *J. Biol. Chem.* **1950**, *187* (2), 537–542. https://doi.org/10.1016/S0021-9258(18)56197-4.
(114) Tsentalovich, Y. P.; Snytnikova, O. A.; Sherin, P. S.; Forbes, M. D. E. Photochemistry of Kynurenine, a Tryptophan Metabolite: Properties of the Triplet State. *J. Phys. Chem. A* **2005**, *109* (16), 3565–3568. https://doi.org/10.1021/jp045142k.
(115) Josimović, Lj.; Janković, I.; Jovanović, S. V. Radiation Induced Decomposition of Tryptophan in the Presence of Oxygen. *Radiat. Phys. Chem.* **1993**, *41* (6), 835–841. https://doi.org/10.1016/0969-806X(93)90029-T.
(116) Tomita, M.; Irie, M.; Ukita, T. Sensitized Photooxidation of Histidine and Its Derivatives. Products and Mechanism of the Reaction. *Biochemistry* **1969**, *8* (12), 5149–5160. https://doi.org/10.1021/bi00840a069.
(117) Mozziconacci, O.; Schöneich, C. Effect of Conformation on the Photodegradation of Trp- And Cystine-Containing Cyclic Peptides: Octreotide and Somatostatin. *Mol. Pharm.* **2014**, *11* (10), 3537–3546. https://doi.org/10.1021/mp5003174.
(118) Bellmaine, S.; Schnellbaecher, A.; Zimmer, A. Reactivity and Degradation Products of Tryptophan in Solution and Proteins. *Free Radic. Biol. Med.* **2020**, *160*, 696–718. https://doi.org/10.1016/j.freeradbiomed.2020.09.002.
(119) Zepp, R. G.; Cline, D. M. Rates of Direct Photolysis in Aquatic Environment. *Environ. Sci. Technol.* **1977**, *11* (4), 359–366. https://doi.org/10.1021/es60127a013.
(120) Leifer, A. *The Kinetics of Environmental Aquatic Photochemistry: Theory and Practice*; American Chemical Society, 1988.
(121) Kasson, T. M. D.; Barry, B. A. Reactive Oxygen and Oxidative Stress: N-Formyl Kynurenine in Photosystem II and Non-Photosynthetic Proteins. *Photosynth. Res.* **2012**, *114* (2), 97–110. https://doi.org/10.1007/s11120-012-9784-z.
(122) Anderson, L. B.; Maderia, M.; Ouellette, A. J. A.; Putnam-Evans, C.; Higgins, L.; Krick, T.; MacCoss, M. J.; Lim, H.; Yates, J. R.; Barry, B. A. Posttranslational Modifications in the CP43 Subunit of Photosystem II. *Proc. Natl. Acad. Sci.* **2002**, *99* (23), 14676–14681. https://doi.org/10.1073/pnas.232591599.
(123) Liu, Y.-H.; Yu, S.-B.; Peng, Y.-J.; Wang, C.-W.; Zhu, C.; Lin, S.-H. Excited-State Intramolecular Proton Transfer with and without the Assistance of Vibronic-Transition-Induced Skeletal Deformation in Phenol–Quinoline. *RSC Adv.* **2021**, *11* (59), 37299–37306. https://doi.org/10.1039/D1RA07042H.

(124) Demchenko, A. P. Proton Transfer Reactions: From Photochemistry to Biochemistry and Bioenergetics. *BBA Adv.* **2023**, *3*, 100085. https://doi.org/10.1016/j.bbadva.2023.100085.
(125) Hara, H. Photodecomposition of Amino Acids. *Nippon Nōgeikagaku Kaishi* **1960**, *34* (6), 493–498. https://doi.org/10.1271/nogeikagaku1924.34.6_493.
(126) Korshunov, S.; Imlay, K. R. C.; Imlay, J. A. Cystine Import Is a Valuable but Risky Process Whose Hazards Escherichia Coli Minimizes by Inducing a Cysteine Exporter. *Mol. Microbiol.* **2020**, *113* (1), 22–39. https://doi.org/10.1111/mmi.14403.
(127) Ochmann, M.; Hussain, A.; von Ahnen, I.; Cordones, A. A.; Hong, K.; Lee, J. H.; Ma, R.; Adamczyk, K.; Kim, T. K.; Schoenlein, R. W.; Vendrell, O.; Huse, N. UV-Photochemistry of the Disulfide Bond: Evolution of Early Photoproducts from Picosecond X-Ray Absorption Spectroscopy at the Sulfur K-Edge. *J. Am. Chem. Soc.* **2018**, *140* (21), 6554–6561. https://doi.org/10.1021/jacs.7b13455.
(128) Mopper, K.; Lindroth, P. Diel and Depth Variations in Dissolved Free Amino Acids and Ammonium in the Baltic Sea Determined by Shipboard HPLC Analysis1: Shipboard Amino Acid Analyses. *Limnol. Oceanogr.* **1982**, *27* (2), 336–347. https://doi.org/10.4319/lo.1982.27.2.0336.
(129) Nelson, M. L. Apparent Activation Energy of Hydrolysis of Some Cellulosic Materials. *J. Polym. Sci.* **1960**, *43* (142), 351–371. https://doi.org/10.1002/pol.1960.1204314207.
(130) Bender, M. L.; Ginger, R. D.; Unik, J. P. Activation Energies of the Hydrolysis of Esters and Amides Involving Carbonyl Oxygen Exchange1. *J. Am. Chem. Soc.* **1958**, *80* (5), 1044–1048. https://doi.org/10.1021/ja01538a006.
(131) Steen, H. B. Wavelength Dependence of the Quantum Yield of Fluorescence and Photoionization of Indoles. *J. Chem. Phys.* **2003**, *61* (10), 3997–4002. https://doi.org/10.1063/1.1681692.
(132) Grossweiner, L. I.; Brendzel, A. M.; Blum, A. Multiple Pathways of Tryptophan Photoionization. *Chem. Phys.* **1981**, *57* (1), 147–155. https://doi.org/10.1016/0301-0104(81)80029-8.
(133) Lao, K. Inverted Regions in the Curve of Photodestruction Quantum Yield versus Photon Energy. *J. Phys. Chem.* **1996**, *100* (12), 4693–4696. https://doi.org/10.1021/jp953305m.
(134) Zika, R. G.; Moffett, J. W.; Petasne, R. G.; Cooper, W. J.; Saltzman, E. S. Spatial and Temporal Variations of Hydrogen Peroxide in Gulf of Mexico Waters. *Geochim. Cosmochim. Acta* **1985**, *49* (5), 1173–1184. https://doi.org/10.1016/0016-7037(85)90008-0.
(135) Moore, C. A.; Farmer, C. T.; Zika, R. G. Influence of the Orinoco River on Hydrogen Peroxide Distribution and Production in the Eastern Caribbean. *J. Geophys. Res. Oceans* **1993**, *98* (C2), 2289–2298. https://doi.org/10.1029/92JC02767.
(136) Testa, A.; Dindo, M.; Rebane, A. A.; Nasouri, B.; Style, R. W.; Golestanian, R.; Dufresne, E. R.; Laurino, P. Sustained Enzymatic Activity and Flow in Crowded Protein Droplets. *Nat. Commun.* **2021**, *12* (1), 6293. https://doi.org/10.1038/s41467-021-26532-0.

(137) Haag, W. R.; Hoigne, Juerg. Singlet Oxygen in Surface Waters. 3. Photochemical Formation and Steady-State Concentrations in Various Types of Waters. *Environ. Sci. Technol.* **1986**, *20* (4), 341–348. https://doi.org/10.1021/es00146a005.
(138) Latch, D. E.; McNeill, K. Microheterogeneity of Singlet Oxygen Distributions in Irradiated Humic Acid Solutions. *Science* **2006**, *311* (5768), 1743–1747. https://doi.org/10.1126/science.1121636.
(139) Sohrin, Y.; Bruland, K. W. Global Status of Trace Elements in the Ocean. *TrAC Trends Anal. Chem.* **2011**, *30* (8), 1291–1307. https://doi.org/10.1016/j.trac.2011.03.006.
(140) Gledhill, M.; van den Berg, C. M. G. Determination of Complexation of Iron(III) with Natural Organic Complexing Ligands in Seawater Using Cathodic Stripping Voltammetry. *Mar. Chem.* **1994**, *47* (1), 41–54. https://doi.org/10.1016/0304-4203(94)90012-4.
(141) Tesmer, J. J. G.; Klem, T. J.; Deras, M. L.; Davisson, V. J.; Smith, J. L. The Crystal Structure of GMP Synthetase Reveals a Novel Catalytic Triad and Is a Structural Paradigm for Two Enzyme Families. *Nat. Struct. Biol.* **1996**, *3* (1), 74–86. https://doi.org/10.1038/nsb0196-74.
(142) Heinemann, K. J.; Yang, S.-Y.; Straube, H.; Medina-Escobar, N.; Varbanova-Herde, M.; Herde, M.; Rhee, S.; Witte, C.-P. Initiation of Cytosolic Plant Purine Nucleotide Catabolism Involves a Monospecific Xanthosine Monophosphate Phosphatase. *Nat. Commun.* **2021**, *12* (1), 1–9. https://doi.org/10.1038/s41467-021-27152-4.
(143) Neta, P.; Maruthamuthu, P.; Carton, P. M.; Fessenden, R. W. Formation and Reactivity of the Amino Radical. *J. Phys. Chem.* **1978**, *82* (17), 1875–1878. https://doi.org/10.1021/j100506a004.
(144) Kaleta, C.; Schäuble, S.; Rinas, U.; Schuster, S. Metabolic Costs of Amino Acid and Protein Production in Escherichia Coli. *Biotechnol. J.* **2013**, *8* (9), 1105–1114. https://doi.org/10.1002/biot.201200267.
(145) Zhu, X.; Miller, W. L.; Fichot, C. G. Simple Method to Determine the Apparent Quantum Yield Matrix of CDOM Photobleaching in Natural Waters. *Environ. Sci. Technol.* **2020**, *54* (21), 14096–14106. https://doi.org/10.1021/acs.est.0c03605.
(146) Ossola, R.; Jönsson, O. M.; Moor, K.; McNeill, K. Singlet Oxygen Quantum Yields in Environmental Waters. *Chem. Rev.* **2021**, *121* (7), 4100–4146. https://doi.org/10.1021/acs.chemrev.0c00781.
(147) Teague, B. Cytoflow: A Python Toolbox for Flow Cytometry. bioRxiv July 23, 2022, p 2022.07.22.501078. https://doi.org/10.1101/2022.07.22.501078.
(148) Gueymard, C. A. The SMARTS Spectral Irradiance Model after 25 years: New Developments and Validation of Reference Spectra. *Sol. Energy* **2019**, *187*, 233–253. https://doi.org/10.1016/j.solener.2019.05.048.
(149) Brown, G.; Singer, A.; Proudfoot, M.; Skarina, T.; Kim, Y.; Chang, C.; Dementieva, I.; Kuznetsova, E.; Gonzalez, C. F.; Joachimiak, A.; Savchenko, A.; Yakunin, A. F. Functional and Structural Characterization of Four Glutaminases from Escherichia Coli and Bacillus Subtilis. *Biochemistry* **2008**, *47* (21), 5724–5735. https://doi.org/10.1021/bi800097h.

(150) Fukuda, R.; Ogawa, H.; Nagata, T.; Koike, I. Direct Determination of Carbon and Nitrogen Contents of Natural Bacterial Assemblages in Marine Environments. *Appl. Environ. Microbiol.* **1998**, *64* (9), 3352–3358.
(151) Ploug, H.; Iversen, M. H.; Fischer, G. Ballast, Sinking Velocity, and Apparent Diffusivity within Marine Snow and Zooplankton Fecal Pellets: Implications for Substrate Turnover by Attached Bacteria. *Limnol. Oceanogr.* **2008**, *53* (5), 1878–1886. https://doi.org/10.4319/lo.2008.53.5.1878.
(152) Wilson, S. E.; Steinberg, D. K.; Buesseler, K. O. Changes in Fecal Pellet Characteristics with Depth as Indicators of Zooplankton Repackaging of Particles in the Mesopelagic Zone of the Subtropical and Subarctic North Pacific Ocean. *Deep Sea Res. Part II Top. Stud. Oceanogr.* **2008**, *55* (14–15), 1636–1647. https://doi.org/10.1016/j.dsr2.2008.04.019.
(153) Doherty, S. C.; Maas, A. E.; Steinberg, D. K.; Popp, B. N.; Close, H. G. Distinguishing Zooplankton Fecal Pellets as a Component of the Biological Pump Using Compound-Specific Isotope Analysis of Amino Acids. *Limnol. Oceanogr.* **2021**, *66* (7), 2827–2841. https://doi.org/10.1002/lno.11793.
(154) Shea, C. H.; Wojtal, P. K.; Close, H. G.; Maas, A. E.; Stamieszkin, K.; Cope, J. S.; Steinberg, D. K.; Wallsgrove, N.; Popp, B. N. Small Particles and Heterotrophic Protists Support the Mesopelagic Zooplankton Food Web in the Subarctic Northeast Pacific Ocean. *Limnol. Oceanogr.* **2023**, *68* (8), 1949–1963. https://doi.org/10.1002/lno.12397.
(155) Mitamura, O.; Saijo, Y. Urea Supply from Decomposition and Excretion of Zooplankton. *J. Oceanogr. Soc. Jpn.* **1980**, *36* (2), 121–125. https://doi.org/10.1007/BF02312097.
(156) Liu, S.; Parsons, R.; Opalk, K.; Baetge, N.; Giovannoni, S.; Bolaños, L. M.; Kujawinski, E. B.; Longnecker, K.; Lu, Y.; Halewood, E.; Carlson, C. A. Different Carboxyl-rich Alicyclic Molecules Proxy Compounds Select Distinct Bacterioplankton for Oxidation of Dissolved Organic Matter in the Mesopelagic Sargasso Sea. *Limnol. Oceanogr.* **2020**, *65* (7), 1532–1553. https://doi.org/10.1002/lno.11405.
(157) Repeta, D. J.; Ferrón, S.; Sosa, O. A.; Johnson, C. G.; Repeta, L. D.; Acker, M.; DeLong, E. F.; Karl, D. M. Marine Methane Paradox Explained by Bacterial Degradation of Dissolved Organic Matter. *Nat. Geosci.* **2016**, *9* (12), 884–887. https://doi.org/10.1038/ngeo2837.
(158) Sun, L.; Curson, A. R. J.; Todd, J. D.; Johnston, A. W. B. Diversity of DMSP Transport in Marine Bacteria, Revealed by Genetic Analyses. *Biogeochemistry* **2012**, *110* (1–3), 121–130. https://doi.org/10.1007/s10533-011-9666-z.
(159) De Corte, D.; Varela, M. M.; Louro, A. M.; Bercovici, S. K.; Valencia-Vila, J.; Sintes, E.; Baltar, F.; Rodríguez-Ramos, T.; Simon, M.; Bode, A.; Dittmar, T.; Niggemann, J. Zooplankton-derived Dissolved Organic Matter Composition and Its Bioavailability to Natural Prokaryotic Communities. *Limnol. Oceanogr.* **2023**, *68* (2), 336–347. https://doi.org/10.1002/lno.12272.
(160) Calleja, M. L.; Ansari, M. I.; Røstad, A.; Silva, L.; Kaartvedt, S.; Irigoien, X.; Morán, X. A. G. The Mesopelagic Scattering Layer: A Hotspot for Heterotrophic Prokaryotes in the Red Sea Twilight Zone. *Front. Mar. Sci.* **2018**, *5*.

(161) Valdés, V. P.; Fernandez, C.; Molina, V.; Escribano, R.; Joux, F. Dissolved Compounds Excreted by Copepods Reshape the Active Marine Bacterioplankton Community Composition. *Front. Mar. Sci.* **2017**, *4*.
(162) Porter, K. G.; Feig, Y. S. The Use of DAPI for Identifying and Counting Aquatic Microflora. *Limnol. Oceanogr.* **1980**, *25* (5), 943–948. https://doi.org/10.4319/lo.1980.25.5.0943.
(163) Jones, D. L. Fathom Toolbox for MATLAB: Software for Multivariate Ecological and Oceanographic Data Analysis., 2017. https://www.usf.edu/marine-science/research/matlab-resources/index.aspx/.
(164) Maas, A. E.; Miccoli, A.; Stamieszkin, K.; Carlson, C. A.; Steinberg, D. K. Allometry and the Calculation of Zooplankton Metabolism in the Subarctic Northeast Pacific Ocean. *J. Plankton Res.* **2021**, *43* (3), 413–427. https://doi.org/10.1093/plankt/fbab026.
(165) Maas, A. E.; Gossner, H.; Smith, M. J.; Blanco-Bercial, L. Use of Optical Imaging Datasets to Assess Biogeochemical Contributions of the Mesozooplankton. *J. Plankton Res.* **2021**, *43* (3), 475–491. https://doi.org/10.1093/plankt/fbab037.
(166) Henry, R. J. THE MODE OF ACTION OF SULFONAMIDES *. *Bacteriol. Rev.* **1943**, *7* (4), 175–262.
(167) Brown, G. M. The Biosynthesis of Folic Acid. *J. Biol. Chem.* **1962**, *237* (2), 536–540. https://doi.org/10.1016/S0021-9258(18)93957-8.
(168) Kanehisa, M.; Goto, S. KEGG: Kyoto Encyclopedia of Genes and Genomes. *Nucleic Acids Res.* **2000**, *28* (1), 27–30. https://doi.org/10.1093/nar/28.1.27.
(169) Kanehisa, M.; Furumichi, M.; Sato, Y.; Kawashima, M.; Ishiguro-Watanabe, M. KEGG for Taxonomy-Based Analysis of Pathways and Genomes. *Nucleic Acids Res.* **2023**, *51* (D1), D587–D592. https://doi.org/10.1093/nar/gkac963.
(170) Durham, B. P.; Boysen, A. K.; Carlson, L. T.; Groussman, R. D.; Heal, K. R.; Cain, K. R.; Morales, R. L.; Coesel, S. N.; Morris, R. M.; Ingalls, A. E.; Armbrust, E. V. Sulfonate-Based Networks between Eukaryotic Phytoplankton and Heterotrophic Bacteria in the Surface Ocean. *Nat. Microbiol.* **2019**, *4* (10), 1706–1715. https://doi.org/10.1038/s41564-019-0507-5.
(171) Tang, K.; Turk, V.; Grossart, H. Linkage between Crustacean Zooplankton and Aquatic Bacteria. *Aquat. Microb. Ecol.* **2010**, *61* (3), 261–277. https://doi.org/10.3354/ame01424.
(172) Bickel, S. L.; Tang, K. W.; Grossart, H.-P. Structure and Function of Zooplankton-Associated Bacterial Communities in a Temperate Estuary Change More with Time than with Zooplankton Species. *Aquat. Microb. Ecol.* **2014**, *72* (1), 1–15. https://doi.org/10.3354/ame01676.
(173) Chen, X.; Liu, L.; Gao, X.; Dai, X.; Han, Y.; Chen, Q.; Tang, K. Metabolism of Chiral Sulfonate Compound 2,3-Dihydroxypropane-1-Sulfonate (DHPS) by Roseobacter Bacteria in Marine Environment. *Environ. Int.* **2021**, *157*, 106829. https://doi.org/10.1016/j.envint.2021.106829.
(174) Tarrant, A. M.; McNamara-Bordewick, N.; Blanco-Bercial, L.; Miccoli, A.; Maas, A. E. Diel Metabolic Patterns in a Migratory Oceanic Copepod. *J. Exp. Mar. Biol. Ecol.* **2021**, *545*, 151643. https://doi.org/10.1016/j.jembe.2021.151643.

(175) Suttle, C.; Chan, A.; Fuhrman, J. Dissolved Free Amino Acids in the Sargasso Sea: Uptake and Respiration Rates, Turnover Times, and Concentrations. *Mar. Ecol. Prog. Ser.* **1991**, *70*, 189–199. https://doi.org/10.3354/meps070189.
(176) McDonnell, A. M. P.; Lam, P. J.; Lamborg, C. H.; Buesseler, K. O.; Sanders, R.; Riley, J. S.; Marsay, C.; Smith, H. E. K.; Sargent, E. C.; Lampitt, R. S.; Bishop, J. K. B. The Oceanographic Toolbox for the Collection of Sinking and Suspended Marine Particles. *Prog. Oceanogr.* **2015**, *133*, 17–31. https://doi.org/10.1016/j.pocean.2015.01.007.
(177) Redfield, A. C. On the Proportions of Organic Derivatives in Sea Water and Their Relation to Thecomposition of Plankton. In *James Johnstone memorial volume*; 1934; pp 176–192.
(178) Munk, W. H. Abyssal Recipes. *Deep Sea Res. Oceanogr. Abstr.* **1966**, *13* (4), 707–730. https://doi.org/10.1016/0011-7471(66)90602-4.
(179) Sarmiento, J. L.; Orr, J. C. Three-Dimensional Simulations of the Impact of Southern Ocean Nutrient Depletion on Atmospheric CO2 and Ocean Chemistry. *Limnol. Oceanogr.* **1991**, *36* (8), 1928–1950. https://doi.org/10.4319/lo.1991.36.8.1928.
(180) Garcia, B. M.; Becker, C. C.; Weber, L.; Swarr, G. J.; Soule, M. C. K.; Apprill, A.; Kujawinski, E. B. Advancing Reef Monitoring Techniques through Exometabolomics: Quantification of Labile Dissolved Organic Metabolites on Coral Reefs. bioRxiv December 21, 2023, p 2023.12.20.572630. https://doi.org/10.1101/2023.12.20.572630.
(181) Wienhausen, G.; Noriega-Ortega, B. E.; Niggemann, J.; Dittmar, T.; Simon, M. The Exometabolome of Two Model Strains of the Roseobacter Group: A Marketplace of Microbial Metabolites. *Front. Microbiol.* **2017**, *8*. https://doi.org/10.3389/fmicb.2017.01985.
(182) Wegley Kelly, L.; Nelson, C. E.; Aluwihare, L. I.; Arts, M. G. I.; Dorrestein, P. C.; Koester, I.; Matsuda, S. B.; Petras, D.; Quinlan, Z. A.; Haas, A. F. Molecular Commerce on Coral Reefs: Using Metabolomics to Reveal Biochemical Exchanges Underlying Holobiont Biology and the Ecology of Coastal Ecosystems. *Front. Mar. Sci.* **2021**, *8*.
(183) Petras, D.; Minich, J. J.; Cancelada, L. B.; Torres, R. R.; Kunselman, E.; Wang, M.; White, M. E.; Allen, E. E.; Prather, K. A.; Aluwihare, L. I.; Dorrestein, P. C. Non-Targeted Tandem Mass Spectrometry Enables the Visualization of Organic Matter Chemotype Shifts in Coastal Seawater. *Chemosphere* **2021**, *271*, 129450. https://doi.org/10.1016/j.chemosphere.2020.129450.
(184) Hellebust, J. A. Excretion of Some Organic Compounds by Marine Phytoplankton1. *Limnol. Oceanogr.* **1965**, *10* (2), 192–206. https://doi.org/10.4319/lo.1965.10.2.0192.
(185) Kujawinski, E. B. Electrospray Ionization Fourier Transform Ion Cyclotron Resonance Mass Spectrometry (ESI FT-ICR MS): Characterization of Complex Environmental Mixtures. *Environ. Forensics* **2002**, *3* (3–4), 207–216. https://doi.org/10.1080/713848382.
(186) Hertkorn, N.; Harir, M.; Koch, B. P.; Michalke, B.; Schmitt-Kopplin, P. High-Field NMR Spectroscopy and FTICR Mass Spectrometry: Powerful Discovery Tools for the Molecular Level Characterization of Marine Dissolved Organic Matter.

Biogeosciences **2013**, *10* (3), 1583–1624. https://doi.org/10.5194/bg-10-1583-2013.
(187) Suttle, C.; Chan, A.; Fuhrman, J. Dissolved Free Amino Acids in the Sargasso Sea: Uptake and Respiration Rates, Turnover Times, and Concentrations. *Mar. Ecol. Prog. Ser.* **1991**, *70*, 189–199. https://doi.org/10.3354/meps070189.
(188) Arrieta, J. M.; Mayol, E.; Hansman, R. L.; Herndl, G. J.; Dittmar, T.; Duarte, C. M. Dilution Limits Dissolved Organic Carbon Utilization in the Deep Ocean. *Science* **2015**, *348* (6232), 331–333. https://doi.org/10.1126/science.1258955.
(189) A. Bodar, P.; Singh Thakur, R.; V. Rajai, J.; Bhushan, S.; A. Mantri, V. A Metabolomic Snapshot through NMR Revealed Differences in Phase Transition during the Induction of Reproduction in Ulva Ohnoi (Chlorophyta). *Mol. Omics* **2024**, *20* (2), 86–102. https://doi.org/10.1039/D3MO00197K.
(190) Poulson-Ellestad, K. L.; Jones, C. M.; Roy, J.; Viant, M. R.; Fernández, F. M.; Kubanek, J.; Nunn, B. L. Metabolomics and Proteomics Reveal Impacts of Chemically Mediated Competition on Marine Plankton. *Proc. Natl. Acad. Sci.* **2014**, *111* (24), 9009–9014. https://doi.org/10.1073/pnas.1402130111.
(191) Mannochio-Russo, H.; Swift, S. O. I.; Nakayama, K. K.; Wall, C. B.; Gentry, E. C.; Panitchpakdi, M.; Caraballo-Rodriguez, A. M.; Aron, A. T.; Petras, D.; Dorrestein, K.; Dorrestein, T. K.; Williams, T. M.; Nalley, E. M.; Altman-Kurosaki, N. T.; Martinelli, M.; Kuwabara, J. Y.; Darcy, J. L.; Bolzani, V. S.; Wegley Kelly, L.; Mora, C.; Yew, J. Y.; Amend, A. S.; McFall-Ngai, M.; Hynson, N. A.; Dorrestein, P. C.; Nelson, C. E. Microbiomes and Metabolomes of Dominant Coral Reef Primary Producers Illustrate a Potential Role for Immunolipids in Marine Symbioses. *Commun. Biol.* **2023**, *6* (1), 1–19. https://doi.org/10.1038/s42003-023-05230-1.
(192) Popendorf, K. J.; Koblížek, M.; Van Mooy, B. A. S. Phospholipid Turnover Rates Suggest That Bacterial Community Growth Rates in the Open Ocean Are Systematically Underestimated. *Limnol. Oceanogr.* **2020**, *65* (8), 1876–1890. https://doi.org/10.1002/lno.11424.
(193) Bouillon, R.-C.; Miller, W. L. Photodegradation of Dimethyl Sulfide (DMS) in Natural Waters: Laboratory Assessment of the Nitrate-Photolysis-Induced DMS Oxidation. *Environ. Sci. Technol.* **2005**, *39* (24), 9471–9477. https://doi.org/10.1021/es048022z.
(194) Pailthorpe, M. T.; Bonjour, J. P.; Nicholls, C. H. The Photolysis of Tryptophan in the Presence of Oxygen. *Photochem. Photobiol.* **1973**, *17* (4), 209–223. https://doi.org/10.1111/j.1751-1097.1973.tb06350.x.
(195) Sherin, P. S.; Grilj, J.; Kopylova, L. V.; Yanshole, V. V.; Tsentalovich, Y. P.; Vauthey, E. Photophysics and Photochemistry of the UV Filter Kynurenine Covalently Attached to Amino Acids and to a Model Protein. *J. Phys. Chem. B* **2010**, *114* (36), 11909–11919. https://doi.org/10.1021/jp104485k.
(196) Voelker, A. L.; Taylor, L. S.; Mauer, L. J. Effect of pH and Concentration on the Chemical Stability and Reaction Kinetics of Thiamine Mononitrate and Thiamine Chloride Hydrochloride in Solution. *BMC Chem.* **2021**, *15* (1), 47. https://doi.org/10.1186/s13065-021-00773-y.
(197) Clifford, E. L.; Hansell, D. A.; Varela, M. M.; Nieto-Cid, M.; Herndl, G. J.; Sintes, E. Crustacean Zooplankton Release Copious Amounts of Dissolved Organic Matter

as Taurine in the Ocean: Dissolved Free Taurine in Oceanic Waters. *Limnol. Oceanogr.* **2017**, *62* (6), 2745–2758. https://doi.org/10.1002/lno.10603.
(198) Pileni, M.-P.; Santus, R.; Land, E. J. On the Photosensitizing Properties of N-Formylkynurenine and Related Compounds. *Photochem. Photobiol.* **1978**, *28* (4–5), 525–529. https://doi.org/10.1111/j.1751-1097.1978.tb06963.x.
(199) Heathcote, J.; Wills, B. A. Hydrolytic Destruction of Thiamine, Especially in the Presence of Cyanocobalamin. *J. Pharm. Pharmacol.* **1962**, *14* (1), 232–236. https://doi.org/10.1111/j.2042-7158.1962.tb11084.x.
(200) Gonsior, M.; Powers, L.; Lahm, M.; McCallister, S. L. New Perspectives on the Marine Carbon Cycle–The Marine Dissolved Organic Matter Reactivity Continuum. *Environ. Sci. Technol.* **2022**, *56* (9), 5371–5380. https://doi.org/10.1021/acs.est.1c08871.
(201) Cory, R. M.; Kling, G. W. Interactions between Sunlight and Microorganisms Influence Dissolved Organic Matter Degradation along the Aquatic Continuum. *Limnol. Oceanogr. Lett.* **2018**, *3* (3), 102–116. https://doi.org/10.1002/lol2.10060.
(202) Wienhausen, G.; Bruns, S.; Sultana, S.; Dlugosch, L.; Groon, L.-A.; Wilkes, H.; Simon, M. The Overlooked Role of a Biotin Precursor for Marine Bacteria - Desthiobiotin as an Escape Route for Biotin Auxotrophy. *ISME J.* **2022**, *16* (11), 2599–2609. https://doi.org/10.1038/s41396-022-01304-w.
(203) Phillips, H. E.; Joyce, T. M. Bermuda's Tale of Two Time Series: Hydrostation S and BATS*. *J. Phys. Oceanogr.* **2007**, *37* (3), 554–571. https://doi.org/10.1175/JPO2997.1.
(204) Bates, N. R.; Johnson, R. J. Acceleration of Ocean Warming, Salinification, Deoxygenation and Acidification in the Surface Subtropical North Atlantic Ocean. *Commun. Earth Environ.* **2020**, *1* (1), 1–12. https://doi.org/10.1038/s43247-020-00030-5.
(205) Validation of Analytical Procedures, 2022. https://www.ema.europa.eu/en/documents/scientific-guideline/ich-guideline-q2r2-validation-analytical-procedures-step-2b_en.pdf (accessed 2024-04-14).
(206) Akima, H. A New Method of Interpolation and Smooth Curve Fitting Based on Local Procedures. *J. ACM* **1970**, *17* (4), 589–602. https://doi.org/10.1145/321607.321609.
(207) Gilat, A.; Subramaniam, V. *Numerical Methods for Engineers and Scientists: An Introduction with Applications Using Matlab*, Third edition.; John Wiley & Sons, Inc: Hoboken, NJ, 2014.
(208) *Physical Optics of Ocean Water*.
(209) Lindroth, Peter.; Mopper, Kenneth. High Performance Liquid Chromatographic Determination of Subpicomole Amounts of Amino Acids by Precolumn Fluorescence Derivatization with O-Phthaldialdehyde. *Anal. Chem.* **1979**, *51* (11), 1667–1674. https://doi.org/10.1021/ac50047a019.
(210) Lu, K.; Liu, Z. The Formation of Refractory Dissolved Organic Nitrogen From Free Amino Acids in the Ocean. *Geophys. Res. Lett.* **2022**, *49* (18), e2022GL100041. https://doi.org/10.1029/2022GL100041.
(211) Popendorf, K. J.; Fredricks, H. F.; Van Mooy, B. A. S. Molecular Ion-Independent Quantification of Polar Glycerolipid Classes in Marine Plankton Using Triple

Quadrupole MS. *Lipids* **2013**, *48* (2), 185–195. https://doi.org/10.1007/s11745-012-3748-0.
(212) Van Mooy, B. A. S.; Rocap, G.; Fredricks, H. F.; Evans, C. T.; Devol, A. H. Sulfolipids Dramatically Decrease Phosphorus Demand by Picocyanobacteria in Oligotrophic Marine Environments. *Proc. Natl. Acad. Sci.* **2006**, *103* (23), 8607–8612. https://doi.org/10.1073/pnas.0600540103.
(213) Durham, B. P.; Sharma, S.; Luo, H.; Smith, C. B.; Amin, S. A.; Bender, S. J.; Dearth, S. P.; Van Mooy, B. A. S.; Campagna, S. R.; Kujawinski, E. B.; Armbrust, E. V.; Moran, M. A. Cryptic Carbon and Sulfur Cycling between Surface Ocean Plankton. *Proc. Natl. Acad. Sci.* **2015**, *112* (2), 453–457. https://doi.org/10.1073/pnas.1413137112.
(214) Landa, M.; Burns, A. S.; Durham, B. P.; Esson, K.; Nowinski, B.; Sharma, S.; Vorobev, A.; Nielsen, T.; Kiene, R. P.; Moran, M. A. Sulfur Metabolites That Facilitate Oceanic Phytoplankton–Bacteria Carbon Flux. *ISME J.* **2019**, *13* (10), 2536–2550. https://doi.org/10.1038/s41396-019-0455-3.
(215) Haimovich-Dayan, M.; Garfinkel, N.; Ewe, D.; Marcus, Y.; Gruber, A.; Wagner, H.; Kroth, P. G.; Kaplan, A. The Role of C4 Metabolism in the Marine Diatom Phaeodactylum Tricornutum. *New Phytol.* **2013**, *197* (1), 177–185. https://doi.org/10.1111/j.1469-8137.2012.04375.x.
(216) Kawamura, K.; Ono, K.; Tachibana, E.; Charriére, B.; Sempéré, R. Distributions of Low Molecular Weight Dicarboxylic Acids, Ketoacids and α-Dicarbonyls in the Marine Aerosols Collected over the Arctic Ocean during Late Summer. *Biogeosciences* **2012**, *9* (11), 4725–4737. https://doi.org/10.5194/bg-9-4725-2012.
(217) Sievering, H.; Boatman, J.; Luria, M.; Van Valin, C. C. Sulfur Dry Deposition over the Western North Atlantic: The Role of Coarse Aerosol Particles. *Tellus B* **1989**, *41B* (3), 338–343. https://doi.org/10.1111/j.1600-0889.1989.tb00312.x.
(218) Wurl, O.; Ekau, W.; Landing, W. M.; Zappa, C. J. Sea Surface Microlayer in a Changing Ocean – A Perspective. *Elem. Sci. Anthr.* **2017**, *5*, 31. https://doi.org/10.1525/elementa.228.
(219) Herbers, J.; Miller, R.; Walther, A.; Schindler, L.; Schmidt, K.; Gao, W.; Rupprecht, F. How to Deal with Non-Detectable and Outlying Values in Biomarker Research: Best Practices and Recommendations for Univariate Imputation Approaches. *Compr. Psychoneuroendocrinology* **2021**, *7*, 100052. https://doi.org/10.1016/j.cpnec.2021.100052.
(220) Keizer, R. J.; Jansen, R. S.; Rosing, H.; Thijssen, B.; Beijnen, J. H.; Schellens, J. H. M.; Huitema, A. D. R. Incorporation of Concentration Data below the Limit of Quantification in Population Pharmacokinetic Analyses. *Pharmacol. Res. Perspect.* **2015**, *3* (2), e00131. https://doi.org/10.1002/prp2.131.
(221) Werner, T.; Buchholz, F. Diel Vertical Migration Behaviour in Euphausiids of the Northern Benguela Current: Seasonal Adaptations to Food Availability and Strong Gradients of Temperature and Oxygen. *J. Plankton Res.* **2013**, *35* (4), 792–812. https://doi.org/10.1093/plankt/fbt030.
(222) Kujawinski, E. B.; Braakman, R.; Longnecker, K.; Chisholm, S. W.; Becker, J. W.; Dooley, K.; Soule, M. C. K.; Swarr, G. J.; Halloran, K. Metabolite Diversity among

Prochlorococcus Strains Belonging to Divergent Ecotypes. bioRxiv December 21, 2022, p 2022.12.20.521339. https://doi.org/10.1101/2022.12.20.521339.
(223) Hoarfrost, A.; Nayfach, S.; Ladau, J.; Yooseph, S.; Arnosti, C.; Dupont, C. L.; Pollard, K. S. Global Ecotypes in the Ubiquitous Marine Clade SAR86. *ISME J.* **2020**, *14* (1), 178–188. https://doi.org/10.1038/s41396-019-0516-7.
(224) Overmans, S.; Agustí, S. Latitudinal Gradient of UV Attenuation Along the Highly Transparent Red Sea Basin. *Photochem. Photobiol.* **2019**, *95* (5), 1267–1279. https://doi.org/10.1111/php.13112.
(225) Michaeli, A.; Feitelson, J. Reactivity of Singlet Oxygen Toward Amino Acids and Peptides. *Photochem. Photobiol.* **1994**, *59* (3), 284–289. https://doi.org/10.1111/j.1751-1097.1994.tb05035.x.
(226) Obernosterer, I.; Benner, R. Competition between Biological and Photochemical Processes in the Mineralization of Dissolved Organic Carbon. *Limnol. Oceanogr.* **2004**, *49* (1), 117–124. https://doi.org/10.4319/lo.2004.49.1.0117.
(227) Ward, C. P.; Cory, R. M. Complete and Partial Photo-Oxidation of Dissolved Organic Matter Draining Permafrost Soils. *Environ. Sci. Technol.* **2016**, *50* (7), 3545–3553. https://doi.org/10.1021/acs.est.5b05354.
(228) Haruki, H.; Hovius, R.; Pedersen, M. G.; Johnsson, K. Tetrahydrobiopterin Biosynthesis as a Potential Target of the Kynurenine Pathway Metabolite Xanthurenic Acid. *J. Biol. Chem.* **2016**, *291* (2), 652–657. https://doi.org/10.1074/jbc.C115.680488.
(229) Lombó, F.; Velasco, A.; Castro, A.; de la Calle, F.; Braña, A. F.; Sánchez-Puelles, J. M.; Méndez, C.; Salas, J. A. Deciphering the Biosynthesis Pathway of the Antitumor Thiocoraline from a Marine Actinomycete and Its Expression in Two Streptomyces Species. *ChemBioChem* **2006**, *7* (2), 366–376. https://doi.org/10.1002/cbic.200500325.
(230) Karimi, E.; Slaby, B. M.; Soares, A. R.; Blom, J.; Hentschel, U.; Costa, R. Metagenomic Binning Reveals Versatile Nutrient Cycling and Distinct Adaptive Features in Alphaproteobacterial Symbionts of Marine Sponges. *FEMS Microbiol. Ecol.* **2018**, *94* (6), fiy074. https://doi.org/10.1093/femsec/fiy074.
(231) Levitan, O.; Dinamarca, J.; Zelzion, E.; Lun, D. S.; Guerra, L. T.; Kim, M. K.; Kim, J.; Van Mooy, B. A. S.; Bhattacharya, D.; Falkowski, P. G. Remodeling of Intermediate Metabolism in the Diatom *Phaeodactylum Tricornutum* under Nitrogen Stress. *Proc. Natl. Acad. Sci.* **2015**, *112* (2), 412–417. https://doi.org/10.1073/pnas.1419818112.
(232) Noriega-Ortega, B. E.; Wienhausen, G.; Mentges, A.; Dittmar, T.; Simon, M.; Niggemann, J. Does the Chemodiversity of Bacterial Exometabolomes Sustain the Chemodiversity of Marine Dissolved Organic Matter? *Front. Microbiol.* **2019**, *10*.
(233) Pileni, M.-P.; Santus, R.; Land, E. J. On the Photosensitizing Properties of N-Formylkynurenine and Related Compounds. *Photochem. Photobiol.* **1978**, *28* (4–5), 525–529. https://doi.org/10.1111/j.1751-1097.1978.tb06963.x.
(234) Mackenzie, F. T.; Garrels, R. M. Chemical Mass Balance between Rivers and Oceans. *Am. J. Sci.* **1966**, *264* (7), 507–525. https://doi.org/10.2475/ajs.264.7.507.

(235) Hellweger, F. L. Combining Molecular Observations and Microbial Ecosystem Modeling: A Practical Guide. *Annu. Rev. Mar. Sci.* **2020**, *12* (1), 267–289. https://doi.org/10.1146/annurev-marine-010419-010829.
(236) Aumont, O.; Ethé, C.; Tagliabue, A.; Bopp, L.; Gehlen, M. PISCES-v2: An Ocean Biogeochemical Model for Carbon and Ecosystem Studies. *Geosci. Model Dev.* **2015**, *8* (8), 2465–2513. https://doi.org/10.5194/gmd-8-2465-2015.
(237) Catalá, T. S.; Shorte, S.; Dittmar, T. Marine Dissolved Organic Matter: A Vast and Unexplored Molecular Space. *Appl. Microbiol. Biotechnol.* **2021**, *105* (19), 7225–7239. https://doi.org/10.1007/s00253-021-11489-3.
(238) Inoue, R.; Kitamura, M.; Fujiki, T. Diel Vertical Migration of Zooplankton at the S1 Biogeochemical Mooring Revealed from Acoustic Backscattering Strength. *J. Geophys. Res. Oceans* **2016**, *121* (2), 1031–1050. https://doi.org/10.1002/2015JC011352.
(239) Fu, H.; Uchimiya, M.; Gore, J.; Moran, M. A. Ecological Drivers of Bacterial Community Assembly in Synthetic Phycospheres. *Proc. Natl. Acad. Sci.* **2020**, *117* (7), 3656–3662. https://doi.org/10.1073/pnas.1917265117.
(240) Stocker, R. Marine Microbes See a Sea of Gradients. *Science* **2012**, *338* (6107), 628–633. https://doi.org/10.1126/science.1208929.
(241) Paver, C. R.; Codispoti, L. A.; Coles, V. J.; Cooper, L. W. Sampling Errors Arising from Carousel Entrainment and Insufficient Flushing of Oceanographic Sampling Bottles. *Limnol. Oceanogr. Methods* **2020**, *18* (7), 311–326. https://doi.org/10.1002/lom3.10368.
(242) Johnson, W. M.; Kido Soule, M. C.; Longnecker, K.; Bhatia, M. P.; Hallam, S. J.; Lomas, M. W.; Kujawinski, E. B. Particulate and Dissolved Metabolite Distributions along a Latitudinal Transect of the Western Atlantic Ocean. *Limnol. Oceanogr.* **2023**, *68* (2), 377–393. https://doi.org/10.1002/lno.12275.
(243) McCune, B.; Grace, J. B. *Analysis of Ecological Communities*; MjM Software Design, 2002.
(244) Dudzik, D.; Barbas-Bernardos, C.; García, A.; Barbas, C. Quality Assurance Procedures for Mass Spectrometry Untargeted Metabolomics. a Review. *J. Pharm. Biomed. Anal.* **2018**, *147*, 149–173. https://doi.org/10.1016/j.jpba.2017.07.044.
(245) The Human Serum Metabolome (HUSERMET) Consortium; Dunn, W. B.; Broadhurst, D.; Begley, P.; Zelena, E.; Francis-McIntyre, S.; Anderson, N.; Brown, M.; Knowles, J. D.; Halsall, A.; Haselden, J. N.; Nicholls, A. W.; Wilson, I. D.; Kell, D. B.; Goodacre, R. Procedures for Large-Scale Metabolic Profiling of Serum and Plasma Using Gas Chromatography and Liquid Chromatography Coupled to Mass Spectrometry. *Nat. Protoc.* **2011**, *6* (7), 1060–1083. https://doi.org/10.1038/nprot.2011.335.
(246) Cohen, N. R.; McIlvin, M. R.; Moran, D. M.; Held, N. A.; Saunders, J. K.; Hawco, N. J.; Brosnahan, M.; DiTullio, G. R.; Lamborg, C.; McCrow, J. P.; Dupont, C. L.; Allen, A. E.; Saito, M. A. Dinoflagellates Alter Their Carbon and Nutrient Metabolic Strategies across Environmental Gradients in the Central Pacific Ocean. *Nat. Microbiol.* **2021**, *6* (2), 173–186. https://doi.org/10.1038/s41564-020-00814-7.
(247) Nicholson, D. P.; Stanley, R. H. R.; Doney, S. C. A Phytoplankton Model for the Allocation of Gross Photosynthetic Energy Including the Trade-Offs of

Diazotrophy. *J. Geophys. Res. Biogeosciences* **2018**, *123* (6), 1796–1816. https://doi.org/10.1029/2017JG004263.
(248) Amend, A.; Burgaud, G.; Cunliffe, M.; Edgcomb, V. P.; Ettinger, C. L.; Gutiérrez, M. H.; Heitman, J.; Hom, E. F. Y.; Ianiri, G.; Jones, A. C.; Kagami, M.; Picard, K. T.; Quandt, C. A.; Raghukumar, S.; Riquelme, M.; Stajich, J.; Vargas-Muñiz, J.; Walker, A. K.; Yarden, O.; Gladfelter, A. S. Fungi in the Marine Environment: Open Questions and Unsolved Problems. *mBio* **2019**, *10* (2), e01189-18. https://doi.org/10.1128/mBio.01189-18.
(249) McMonagle, H.; Llopiz, J. K.; Hilborn, R.; Essington, T. E. High Uncertainty in Fish Bioenergetics Impedes Precision of Fish-Mediated Carbon Transport Estimates into the Ocean's Twilight Zone. *Prog. Oceanogr.* **2023**, *217*, 103078. https://doi.org/10.1016/j.pocean.2023.103078.
(250) Irigoien, X.; Klevjer, T. A.; Røstad, A.; Martinez, U.; Boyra, G.; Acuña, J. L.; Bode, A.; Echevarria, F.; Gonzalez-Gordillo, J. I.; Hernandez-Leon, S.; Agusti, S.; Aksnes, D. L.; Duarte, C. M.; Kaartvedt, S. Large Mesopelagic Fishes Biomass and Trophic Efficiency in the Open Ocean. *Nat. Commun.* **2014**, *5* (1), 3271. https://doi.org/10.1038/ncomms4271.
(251) Drago, L.; Panaïotis, T.; Irisson, J.-O.; Babin, M.; Biard, T.; Carlotti, F.; Coppola, L.; Guidi, L.; Hauss, H.; Karp-Boss, L.; Lombard, F.; McDonnell, A. M. P.; Picheral, M.; Rogge, A.; Waite, A. M.; Stemmann, L.; Kiko, R. Global Distribution of Zooplankton Biomass Estimated by In Situ Imaging and Machine Learning. *Front. Mar. Sci.* **2022**, *9*. https://doi.org/10.3389/fmars.2022.894372.
(252) Bar-On, Y. M.; Milo, R. The Biomass Composition of the Oceans: A Blueprint of Our Blue Planet. *Cell* **2019**, *179* (7), 1451–1454. https://doi.org/10.1016/j.cell.2019.11.018.
(253) Hernández-León, S.; Ikeda, T. A Global Assessment of Mesozooplankton Respiration in the Ocean. *J. Plankton Res.* **2005**, *27* (2), 153–158. https://doi.org/10.1093/plankt/fbh166.
(254) Vincent, F.; Gralka, M.; Schleyer, G.; Schatz, D.; Cabrera-Brufau, M.; Kuhlisch, C.; Sichert, A.; Vidal-Melgosa, S.; Mayers, K.; Barak-Gavish, N.; Flores, J. M.; Masdeu-Navarro, M.; Egge, J. K.; Larsen, A.; Hehemann, J.-H.; Marrasé, C.; Simó, R.; Cordero, O. X.; Vardi, A. Viral Infection Switches the Balance between Bacterial and Eukaryotic Recyclers of Organic Matter during Coccolithophore Blooms. *Nat. Commun.* **2023**, *14* (1), 510. https://doi.org/10.1038/s41467-023-36049-3.
(255) Wan, B.; Huang, R.; Diaz, J. M.; Tang, Y. Rethinking the Biotic and Abiotic Remineralization of Complex Phosphate Molecules in Soils and Sediments. *Sci. Total Environ.* **2022**, *833*, 155187. https://doi.org/10.1016/j.scitotenv.2022.155187.
(256) Knowles, A. F. The GDA1_CD39 Superfamily: NTPDases with Diverse Functions. *Purinergic Signal.* **2011**, *7* (1), 21–45. https://doi.org/10.1007/s11302-010-9214-7.
(257) Riewe, D.; Grosman, L.; Fernie, A. R.; Zauber, H.; Wucke, C.; Geigenberger, P. A Cell Wall-Bound Adenosine Nucleosidase Is Involved in the Salvage of Extracellular ATP in Solanum Tuberosum. *Plant Cell Physiol.* **2008**, *49* (10), 1572–1579. https://doi.org/10.1093/pcp/pcn127.

(258) Forte, G. M.; Davie, E.; Lie, S.; Franz-Wachtel, M.; Ovens, A. J.; Wang, T.; Oakhill, J. S.; Maček, B.; Hagan, I. M.; Petersen, J. Import of Extracellular ATP in Yeast and Man Modulates AMPK and TORC1 Signalling. *J. Cell Sci.* **2019**, *132* (7), jcs223925. https://doi.org/10.1242/jcs.223925.
(259) Sutherland, K. M.; Wankel, S. D.; Hansel, C. M. Dark Biological Superoxide Production as a Significant Flux and Sink of Marine Dissolved Oxygen. *Proc. Natl. Acad. Sci.* **2020**, *117* (7), 3433–3439. https://doi.org/10.1073/pnas.1912313117.
(260) Liu, S.; Liu, Z. Free Extracellular Enzymes Dominate Initial Peptide Hydrolysis in Coastal Seawater. *Mar. Chem.* **2018**, *199*, 37–43. https://doi.org/10.1016/j.marchem.2018.01.005.
(261) Labatut, M.; Lacan, F.; Pradoux, C.; Chmeleff, J.; Radic, A.; Murray, J. W.; Poitrasson, F.; Johansen, A. M.; Thil, F. Iron Sources and Dissolved-Particulate Interactions in the Seawater of the Western Equatorial Pacific, Iron Isotope Perspectives. *Glob. Biogeochem. Cycles* **2014**, *28* (10), 1044–1065. https://doi.org/10.1002/2014GB004928.
(262) Faust, B. C.; Zepp, R. G. Photochemistry of Aqueous Iron(III)-Polycarboxylate Complexes: Roles in the Chemistry of Atmospheric and Surface Waters. *Environ. Sci. Technol.* **1993**, *27* (12), 2517–2522. https://doi.org/10.1021/es00048a032.
(263) Meng, X.; Pang, H.; Sun, F.; Jin, X.; Wang, B.; Yao, K.; Yao, L.; Wang, L.; Hu, Z. Simultaneous 3-Nitrophenylhydrazine Derivatization Strategy of Carbonyl, Carboxyl and Phosphoryl Submetabolome for LC-MS/MS-Based Targeted Metabolomics with Improved Sensitivity and Coverage. *Anal. Chem.* **2021**, *93* (29), 10075–10083. https://doi.org/10.1021/acs.analchem.1c00767.
(264) Halloran, K. H.; Kido Soule, M. C.; Anderson, H.; Zhu, Y.; McParland, E. L.; Haley, S. T.; Dyhrman, S. T.; Kujawinski, E. B. Expanded Quantification of Marine Metabolites via Aniline Derivatization with Liquid Chromatography-Mass Spectrometry [in Prep], 2024.
(265) Halloran, K. H.; Kido Soule, M. C.; Braakman, R.; Coe, A.; Swarr, G. J.; Chisholm, S. W.; Kujawinski, E. B. Variable Uptake of Prochlorococcus-Derived Metabolites by Alteromonas Macleodii MIT1002 Shows High Levels of Substrate Specificity [in Prep], 2024.